Aspects of the chemistry of dimolybdenum acetylide, vinylidene and allenylidene complexes

Clare, Philip M.

Award date:
1994

Awarding institution:
University of Bath

ASPECTS OF THE CHEMISTRY OF DIMOLYBDENUM ACETYLIDE, VINYLIDENE AND ALLENYLIDENE COMPLEXES

submitted by Philip M. Clare

for the degree of PhD

of the University of Bath

1994

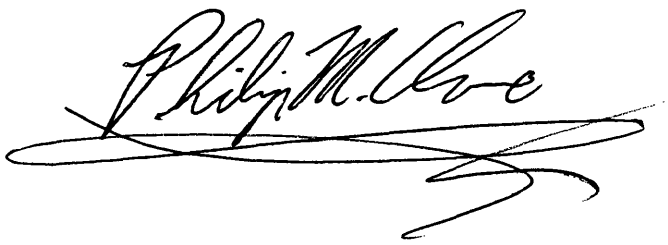

ProQuest LLC
789 East Eisenhower Parkway
P.O. Box 1346
Ann Arbor, MI 48106-1346

Summary

The work described in this thesis is centred around the chemistry of dimolybdenum acetylide complexes and their derivatives, with an additional section describing work involving functionalised η^3-allyl complexes of iron.

The introduction contains a review of acetylide, vinylidene and allenylidene complexes followed by a discussion of η^4-*trans*-diene complexes as precursors to η^3-allyl complexes.

The results and discussion section begins with a discussion of the X-ray crystal structure of $[Mo_2(\mu\text{-}HCCCMe_2)(CO)_4(\eta\text{-}C_5Me_5)_2]BF_4$ (3), generated by protonation of the allenylidene $[Mo_2(\mu\text{-}\sigma,\eta^2\text{-}CCCMe_2)(CO)_4(\eta\text{-}C_5Me_5)_2]$, and of its reactivity towards nucleophiles which is restricted by steric factors. Also detailed is the attempt to prepare $[Mo_2(\mu\text{-}\sigma,\eta^2\text{-}CCCH_2)(CO)_4(\eta\text{-}C_5H_5)_2]$ and the X-ray crystal structure of $[Mo_2(\mu\text{-}HCCCH_2OCH_2CH_3)(CO)_4(\eta\text{-}C_5H_5)_2]$ (8) which arose from this.

Following this is a discussion of the preparation of trinuclear acetylide complexes $[Mo_2M(\mu\text{-}C{\equiv}CR)(CO)_4(L)(\eta^5\text{-}L')_2]$ where R = Ph, ^{t}Bu; M = Ir, L = $(CO)_2$, (COD), L' = (C_5H_5); M = Rh, L = $(CO)_2$, (nbd), L' = (C_5H_5), (C_5Me_5); M = Mn, L = $(CO)_3$, L' = (C_5H_5); M = Ru, L = (C_5H_5); L' = (C_5H_5). These complexes are found to have an extremely unusual open structure. The X-ray crystal structures and variable temperature n.m.r. characteristics of $[Mo_2Rh(\mu\text{-}C{\equiv}CPh)(CO)_6(\eta\text{-}C_5H_5)_2]$ (12) and $[Mo_2Mn(\mu\text{-}C{\equiv}C^tBu)(CO)_7(\eta\text{-}C_5H_5)_2]$ (24) are presented. Preceding this the serendipitous discovery of the unusual 14-electron complex $[Rh(NCMe)(norbornadiene)]BF_4$ (7) is reported. The protonation of two trinuclear acetylide complexes to give the cationic complexes $[Mo_2Rh(CCH^tBu)(CO)_6(\eta\text{-}C_5H_5)_2]BF_4$ (26) and $[Mo_2Ir(\mu\text{-}CCHPh)(CO)_6(\eta\text{-}C_5H_5)_2]BF_4$ (27) is also discussed. The question of whether they can be regarded as vinylidene complexes or stabilised carbonium ions is addressed.

In the following section the preparation and reactivity of the "oxoallyl" complex *exo-anti*-[Fe(η-C_5H_5)(CO)(η^3-$CH_2CHCHCHO$)] (30) is presented, concluding with further work proposed in this area.

Finally there follows an experimental section and appendices containing crystallographic data.

Acknowledgements

Most of all, I would like to express my gratitude to Professor Michael Green. Our many conversations over the years I have worked for him have greatly broadened my understanding of chemistry and my thirst for knowledge of all kinds, as well as providing encouragement and inspiration at the times I have needed them most. I am also deeply indebted to Dr Mary Mahon for four crystallographic studies which have made a crucial contribution to this work.

Many other people have made contributions in many ways including fellow students, postdoctoral workers and technicians. I am grateful for preliminary experiments conducted by Dr R.J. Mercer and Monika Kursawe. I am particularly indebted to Robert and Ahmed who worked many miracles in trying times.

I would also like to thank the SERC for a grant and especially the Masonic Trust for Girls and Boys whose financial contributions, not only during my postgraduate studies but throughout my whole education, have made my studies possible.

Finally I should like to thank my family and friends too numerous to name for their continuous support and encouragement.

Dedication

To my Father, in loving memory

To my Mother, with love and gratitude beyond the power of words to express

To Howard and Bryan

To Chris, with love, for love and support from the depths to the heights

To God, for the splendour of his creation and the gift of curiosity

Memorandum

The work described in this thesis was carried out by the author between October 1989 and June 1990 within the Department of Chemistry of King's College London and between June 1990 and November 1992 within the School of Chemistry of the University of Bath under the supervision of Professor Michael Green. Unless otherwise acknowledged, it is the individual, original work of the author and has not been submitted for any other degree.

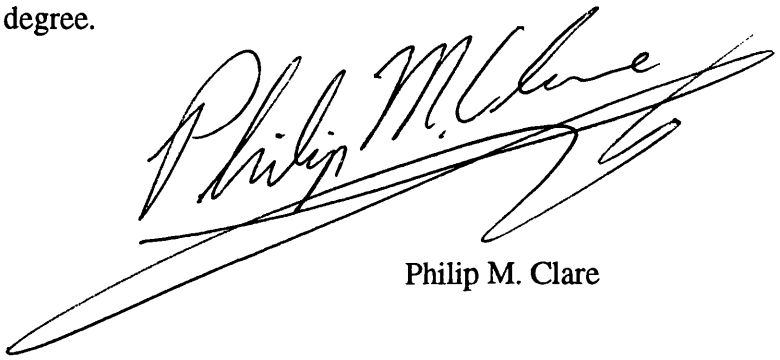

Philip M. Clare

Abbreviations

R	:	an alkyl or aryl group
Me	:	methyl
Et	:	ethyl
Pr	:	propyl
Bu	:	butyl
Ph	:	phenyl
L	:	ligand
M	:	metal
X	:	halide
n	:	normal
i	:	iso
s	:	secondary
t	:	tertiary
Cp	:	η^5-cyclopentadienyl
Cp*	:	η^5-pentamethylcyclopentadienyl
COD	:	cyclo-octa-1,5-diene
nbd	:	norbornadiene
py	:	pyridine
TMS	:	tetramethylsilane
THF	:	tetrahydrofuran
HOMO	:	highest occupied molecular orbital
LUMO	:	lowest unoccupied molecular orbital
MO	:	molecular orbital
r.t.	:	room temperature
Δ	:	heat

hr	:	hour
min	:	minute
hν	:	photolysis
uv	:	ultra-violet
ir	:	infra-red
Nuc^-	:	nucleophile
E^+	:	electrophile
n.m.r.	:	nuclear magnetic resonance
mol	:	mole
mmol	:	milli-mole
FT	:	Fourier Transform
oxoallyl	:	complex containing an oxygen-substituted allyl ligand

relating to ir data

ν_{CO}	:	wavenumber of carbonyl stretch (cm^{-1})
s	:	strong
m	:	medium
w	:	weak
vs	:	very strong
sh	:	shoulder
b	:	broad

relating to n.m.r. data

J	:	scalar coupling constant

δ	:	chemical shift (positive to high frequency of TMS)
s	:	singlet
d	:	doublet
t	:	triplet
q	:	quartet
m	:	multiplet
dd	:	doublet of doublets
ddd	:	doublet of doublet of doublets
b	:	broad

Contents Page No.

1. Introduction

... to comprehend the works of God
And God himself, and all God's intercourse
With human mind.

Paracelsus

1.1. Transition Metal Acetylide Complexes.

The acetylide anion is a versatile ligand giving rise to an extremely wide area of chemistry. $HC{\equiv}C^-$ is isolobal with CO, also having a polarised triple bond,[1] and similarly is capable of both σ- and π-donation leading to a wide variety of bonding modes. This diversity is apparent in figure 1, which shows some possible co-ordination geometries of the alkynyl ligand.

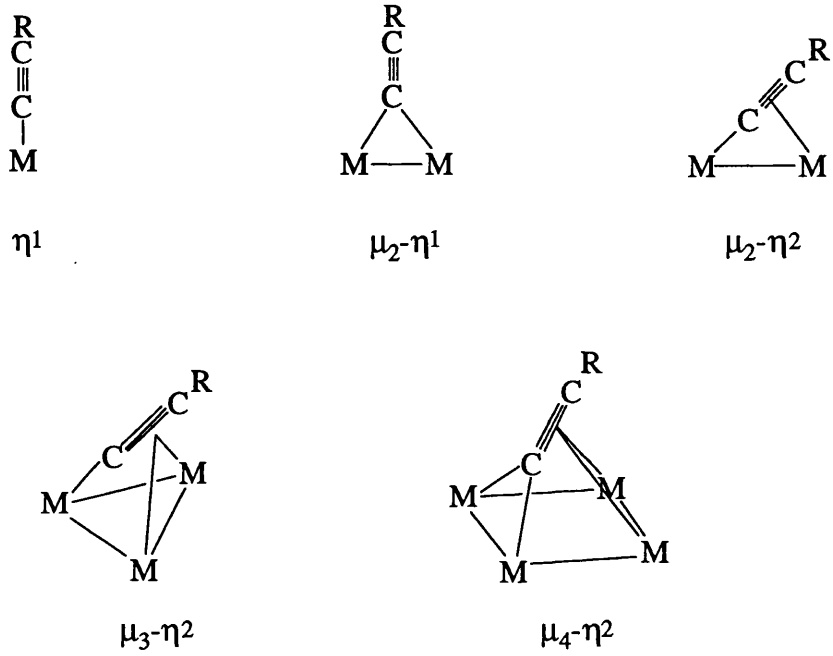

figure 1

The η^1-bonding mode of this ligand has been investigated[2] in a theoretical study for the complex $[Fe(\eta^1\text{-}C{\equiv}CPh)(CO)_2(\eta\text{-}C_5H_5)]$ and it was shown that in this case the acetylide ligand functions only as a σ-donor as the π^*-orbitals have a much higher energy than the filled d-orbitals on the iron atom, precluding any significant back-bonding. The relevant metal orbitals would interact with the acetylide fragment's filled π-orbitals producing only a destabilising effect. The HOMO is 30% localised on the β-carbon of the acetylide, whereas the LUMO is confined to the metal fragment.

Based on these observations it is expected that electrophilic attack would occur at the β-carbon of the acetylide ligand, while nucleophilic attack on the ligand would

occur at the α-carbon. Obviously, nucleophiles may also attack the other metal ligands or the metal α-bound to the acetylide. Phosphines, for example may be expected to attack the metal, leading to ligand exchange reactions.

1.2 Mononuclear Alkynyl Complexes

The range of η^1-alkynyl adducts that have been prepared is enormous, either with acetylide ligands alone, or in which the acetylide ligand is one of several. The usual method of preparation of these complexes is by reaction of the relevant metal halide with an alkynating agent, for example alkynyl compounds of the alkali metals, or by HX elimination between metal halides and activated acetylenes with an electron withdrawing substituent.[3]

When the alkynyl group was originally being investigated as a ligand, it was assumed that, being isoelectronic with $N{\equiv}C^-$, $RC{\equiv}C^-$ should have similar properties. In fact this correlation is manifest in many examples of acetylide complexes which have similar stereochemistry, magnetic properties and colour to their analogous cyanide counterparts, for example; $K_3[M(C_2H)_6]$, (M = Cr, Mn, Fe); $K_2[M(C_2H)_4]$, (M = Ni, Pt).[4] These species are sensitive to protolysis and are often explosive in the solid state. The truth of this assumption can also be seen in low oxidation state complexes stabilised by acetylide anion such as the zero-valent complexes $K_4[Ni(C_2H)_4]$, $K_2[M(C_2H)_2]$, (M = Pt, Pd).[4] These species are very unstable and tend to be pyrophoric.

Most σ-alkynyl complexes, however, contain other ligands, are neutral and are much less reactive. For example the bis-alkynyl species, $[M(\eta\text{-}C_5H_5)_2(C{\equiv}CPh)_2]$ (I), are readily formed from the titanium and zirconium dihalides (figure 2).[5,6]

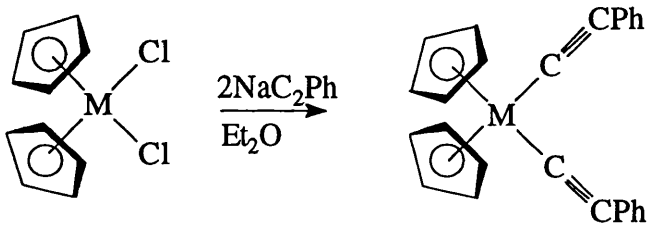

(I)

M = Ti, Zr

figure 2

The heavier lanthanides (figure 3) form similar complexes [(II) and (III)] although the earlier, larger metals seem reluctant to form metal carbon σ-bonds.[7,8]

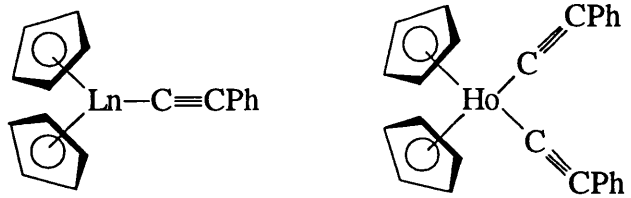

(II) (III)

Ln = Gd, Er, Yb, Ho

figure 3

Figure 4 shows a uranium σ-acetylide complex (IV) in which structural characterisation showed a pseudo-tetrahedral geometry, with an almost linear phenylacetylide ligand.[9]

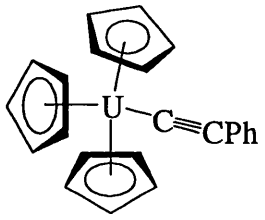

(IV)

figure 4

Molybdenum η^1-alkynyl complexes are readily accessible, for example $[Mo(CO)_3(\eta\text{-}C_5H_5)(C{\equiv}CR)]$ (V) is easily prepared by treatment of $[MoCl(CO)_3(\eta\text{-}C_5H_5)]$ with $RC{\equiv}CMgBr$ (figure 5).[10]

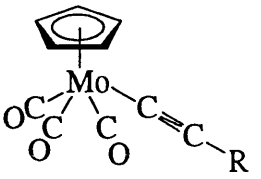

(V) R = Ph, ^{n}Bu

figure 5

An example of the reactivity of acetylide β-carbons toward electrophilic attack was demonstrated in 1984 [11] using anionic tungsten acetylide complexes (figure 6).

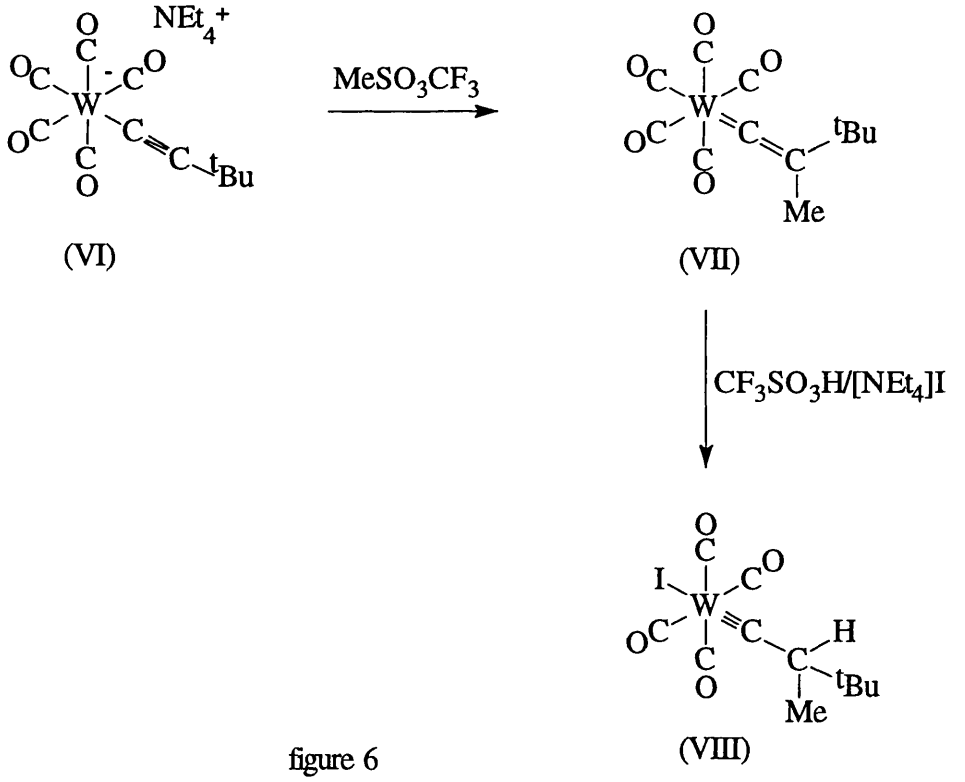

figure 6

Methylation of (VI) yields a neutral vinylidene (VII). Protonation of this product in the presence of iodide gives the carbyne (VIII). From this observation it

follows that the β-carbon of both the acetylide and the vinylidene are susceptible to electrophilic attack as predicted by theory.[2]

Complex (IX), an anionic tungsten complex with a bidentate ligand, reacts in a similar fashion with protonating and methylating agents to give vinylidenes (X) (figure 7). Notably, in this reaction the carbonyls switch from being *fac* to *mer*. Intramolecular carbonyl rearrangement is known to be facile, and labelling studies have shown that this mechanism is indeed operative.[12]

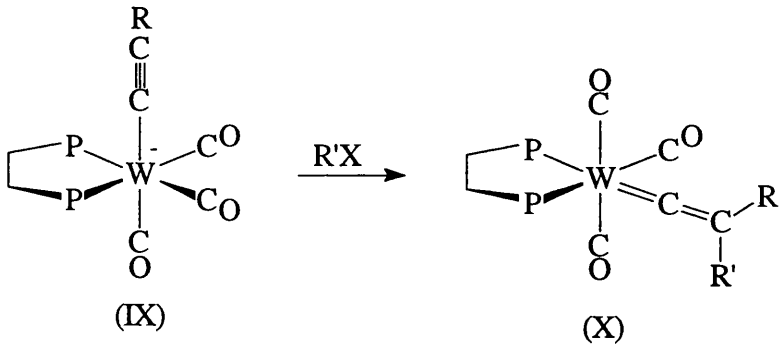

(IX) (X)

R = H, Ph; R' = H; X = BF_4

R = H, Ph; R' = Me; X = I

figure 7

Gladysz [13] *et al* also made a cationic vinylidene (XII) in a similar fashion, by the reaction of [Re(η^1-C≡CMe)(NO)(PPh_3)(η-C_5H_5)] (XI) with CH_3SO_3F at 0 °C (figure 8).

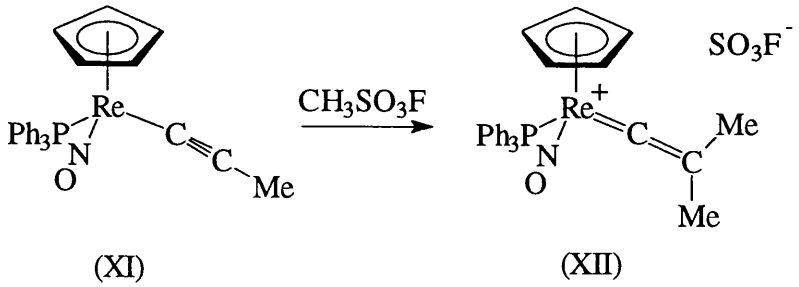

(XI) (XII)

figure 8

Gladysz also found that treatment of the acetylide with CD_3SO_3F gave only one of the two possible isomers at 0 °C, although at 25 °C a slow isomerisation process occurs, giving a 1:1 mixture. This shows that despite the fact that the acetylide ligand is formally cylindrically symmetric, the chirality of the rhenium is transmitted through it.

A similar strategy has been used to prepare many such complexes of the general formula $[M(\eta^1\text{-}C{\equiv}CR)(L)(L')(\eta\text{-}C_5H_5)]$, where M = Fe, Ru, Os, and L, L' = CO, PR_3, *etc.* [4,10]

Werner *et al*, in 1983, observed [14,15] that the square planar rhodium acetylene adduct (XIII) undergoes an intramolecular rearrangement involving oxidative addition of a C-H bond to form an alkynyl hydrido complex (XIV). The equilibrium can be driven to the right by addition of pyridine to form an isolable octahedral complex (XV) which, when heated in benzene, loses pyridine and rearranges to form a vinylidene (XVI), illustrated in figure 9. This can be rationalised, as in previous cases, by deprotonation followed by protonation at the β-alkynyl carbon.

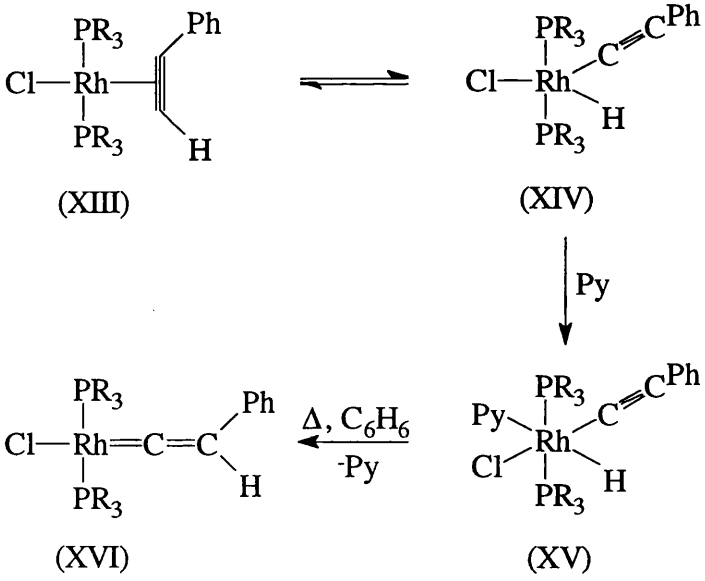

figure 9

Among the earliest transition metal σ-acetylide complexes discovered are those of the nickel triad. In 1959 Chatt and Shaw reported the formation of the complex

trans-[Pt(C≡CR)$_2$(PEt$_3$)$_2$].[16] The *trans*-isomer of these complexes is generally the product of such experiments irrespective of the stereochemistry of the starting materials,[3] as it is thermodynamically more stable. A similar inclination is observed in the analogous complexes where one acetylide is replaced by a halide.[4] Many compounds of the general formulae *trans*-[M(C≡CR)$_2$(L)$_2$] and *trans*-[M(C≡CR)(X)(L)$_2$] have been prepared where M = Ni, Pt, Pd; R = H, Alkyl, Aryl; L = PR$_3$, AsR$_3$, SbR$_3$ and X = Halide.[4] Some of the thermodynamically less stable *cis*-adducts have been prepared, such as *cis*-[Pt(C≡CR)$_2$(PEt$_3$)$_2$][3] and *cis*-[Pt(C≡CPh)$_2$(PPh$_3$)$_2$].[17]

Extensive studies have been made of the protonation of the platinum *trans-bis*-acetylide complexes (XVII).[18-20] Reaction with one molar equivalent of HPF$_6$ or HSbF$_6$ in alcoholic solvents gives a cationic alkynylalkoxycarbene (XVIII) as shown in figure 10. The proposed mechanism again begins with protonation at the acetylide β-carbon to give a cationic vinylidene. Various studies suggest that this reacts with the solvent and proceeds *via* the neutral intermediate shown.

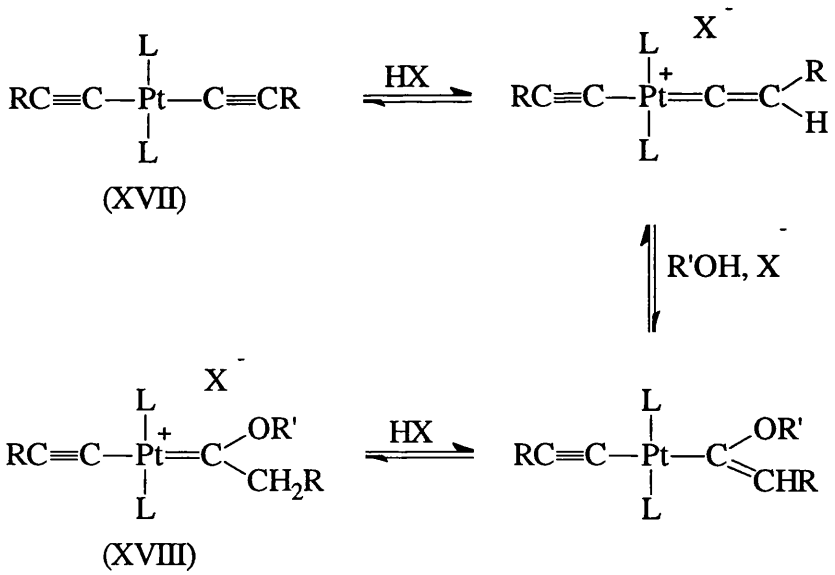

R = H, Me, Ph R' = Me, Et, ^{i}Pr, ^{n}Pr
X = PF$_6$, SbF$_6$ L = PMe$_2$Ph

figure 10

In 1984 it was shown[21] that the η^1-acetylide (XIX) reacts with a Pt-H bond, in the form of $[Pt(H)(acetone)(PEt_3)_2]BF_4$ to form a symmetrically bonded $\mu^2\eta^1$-vinylidene (XX). Only the *cis*-product is observed (figure 11). M-H bonds are known to add across free acetylenes in this way[21], and so this reaction is consonant with the theoretical proposal[2] that σ-acetylides have relatively little effect on the C≡C bond.

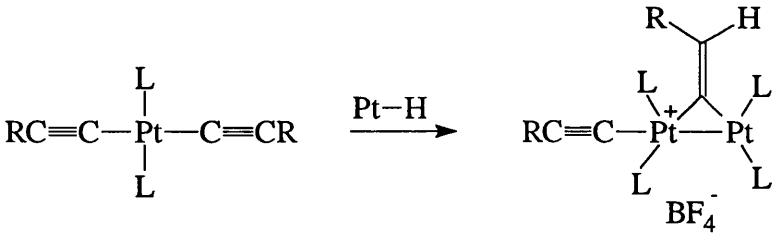

(XIX) (XX)

Pt—H = $[Pt(H)(acetone)(PEt_3)_2BF_4$ L = PEt_3; R = Ph

figure 11

1.3 Dinuclear Alkynyl Complexes

In contrast to the case described above, η^2-alkynyls would be expected to exhibit a greater perturbation of the C≡C triple bond than the η^1-complexes, particularly in the μ_2 case as the ligand is involved in both π- and σ-donation. The electron richness of the β-carbon, however, is expected to continue to be a characteristic. A feature of η^2-acetylides is the existence of facile fluxional processes, which are commonly found in complexes comprising acetylides bonded to more than one metal.

An example of this behaviour can be observed in the product of the reaction between $[Rh_2(\mu\text{-}O_2CR')(CO)_2(\mu\text{-dppm})_2]ClO_4$ with acetylenes R(C≡CH).[22] The acetylene displaces the carboxylate ligand to afford a fluxional cationic acetylide complex with a μ_2-η^2-bonding mode (XXI). This has been characterised (R = ^{t}Bu) by X-ray crystallography (figure 12).[23]

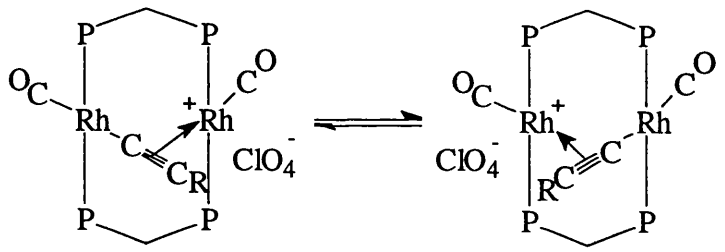

(XXI)

R = ^{t}Bu , Ph, H R' = CH_3, CF_3 P^P = dppm

figure 12

The acetylide moves back and forth between the metals, alternating its σ and π bonding. This process is extremely facile and is rapid even at -80 °C.

More relevant to this thesis, however, are examples of acetylide bridges supported by metal-metal bonds, for instance the dirhenium μ_2-η^2-acetylide (XXII) prepared by Brown (figure 13).[24]

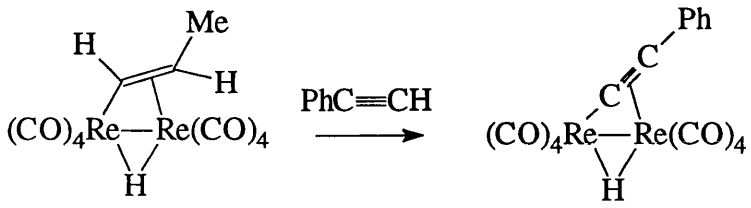

(XXII)

figure 13

This complex also displays facile fluxionality as shown in figure 14.

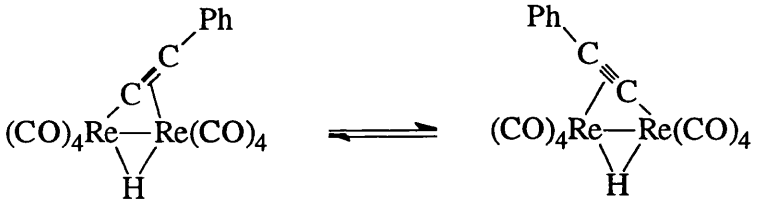

figure 14

The carbonyl ligands of this complex are very labile with respect to substitution by phosphines, thus an excess of PPh_3 induces replacement of one CO from each metal to give (XXIV), $[Re_2(CO)_6(PPh_3)_2(H)(C{\equiv}CPh)]$, *via* the monosubstituted complex (XXIII) (figure 15). The reaction kinetics suggest a CO dissociative mechanism and the acetylides of both substituted complexes remain fluxional.

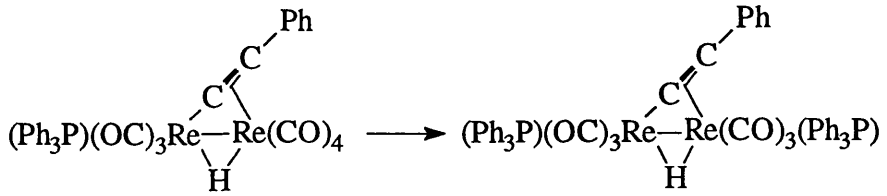

(XXIII) (XXIV)

figure 15

When PMe_3 is used as a ligand, however, CO substitution does not occur. Instead, a 1:1 adduct is formed *via* attack at the acetylide ligand.[24] In view of the nucleophilic nature of the β-carbon, the initial attack site is likely to be at the metal or at Cα.

Generation of the dirhenium acetylide (XXII) (figure 13) occurs *via* cleavage at the C-H σ-bond of phenyl acetylene. This results in the Re-Re bond being bridged by hydride and acetylide ligands. A similar procedure has been used to instigate P-C σ-bond cleavage in order to incorporate phosphide and acetylide ligands into a dimetal organometallic fragment.[1,25] Thus $[Fe_2(CO)_9]$ reacts with Ph_2P-C≡CPh to produce a diiron complex (XXV) with bridging phosphide and acetylide ligands (figure 16).[26]

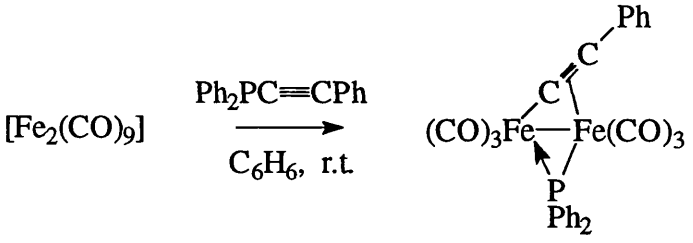

(XXV)

figure 16

Similar ruthenium complexes have been prepared from $[Ru_3(CO)_{12}]$.[25]

The mechanism by which the reaction shown in figure 16 proceeds has been reasonably well elucidated[2] (figure 17). Initially a molecule of $Ph_2PC{\equiv}CR$ coordinates to a $[Fe(CO)_4]$ moiety to produce a σ-bonded acetylide complex. This coordinates to

a further molecule of $[Fe(CO)_4]$ which has been shown[27] by crystallography (R = ^{t}Bu) to give complex (XXVI). The reaction proceeds *via* oxidative insertion of $[Fe(CO)_4]$ into the P-C bond and loss of two molecules of CO to give (XXV).

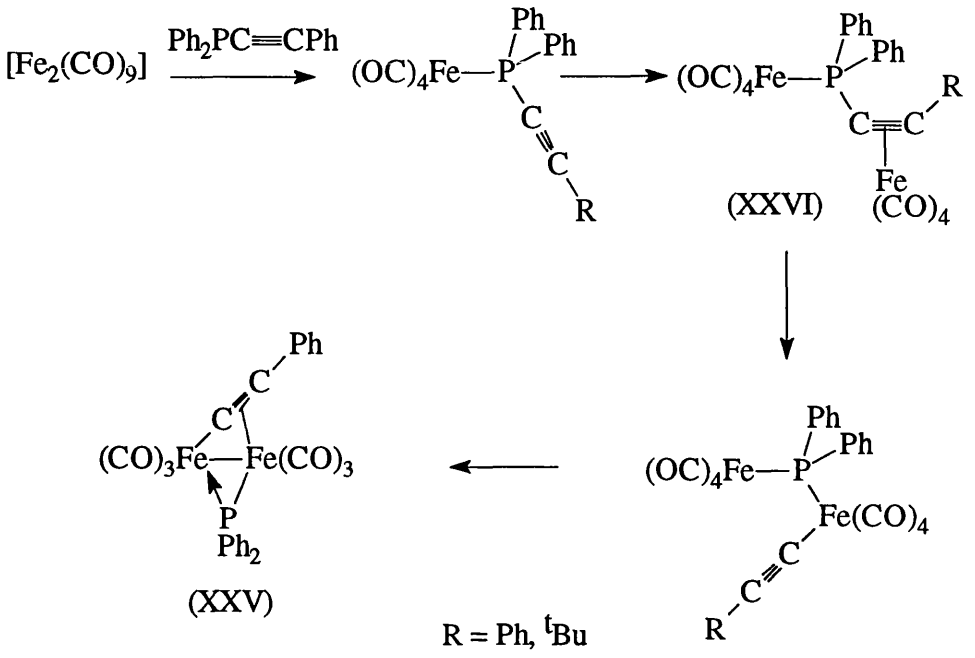

figure 17

The chemistry of (XXV), with respect to nucleophilic attack, is similar to that of the dirhenium hydride acetylide discussed earlier. Reaction with an excess of ^{t}BuNC for two hours at room temperature[28] affords two products. One results from substitution of two carbonyls as before (XXVII), the other from isocyanide attack at the α-carbon of the acetylide ligand (XXVIII). Both products have been structurally characterised (figure 18).

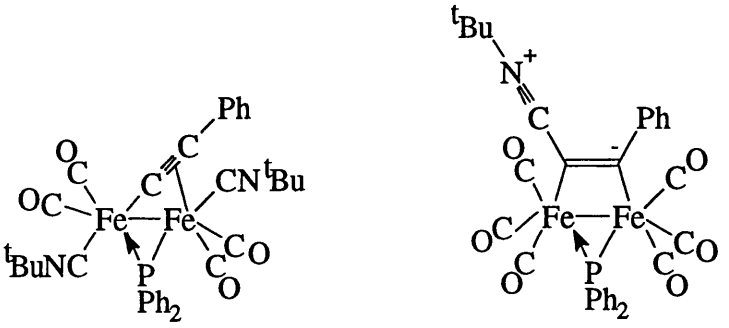

(XXVII) (XXVIII)

figure 18

CO substitution and nucleophilic attack at the α-carbon can thus be seen to be in competition, and lower temperature favours the latter. Nucleophilic attack at the metal and α-carbon is what would be expected of a metal/C_α-based LUMO,[2] and thus dinuclear acetylide complexes share characteristics of mononuclear acetylides, namely that the alkynyl α-carbon is electron deficient and the β-carbon electron rich.

1.4 Cluster Alkynyl Complexes

Trinuclear acetylide complexes, of which there are many involving the Fe triad, generally exhibit the μ_3-η^2-bonding mode (figure 1) in which the acetylide ligand donates five electrons to one side of a metal triangle. They are easily accessible, for instance, $[Ru_3(CO)_{12}]$ reacts with 3,3-dimethylbut-1-yne to give the triruthenium complex (XXIX) (figure 19).[29]

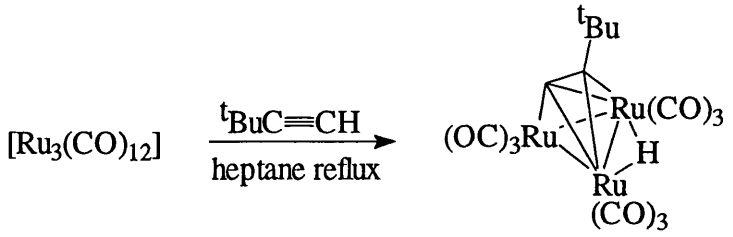

(XXIX)

figure 19

A similar reaction starting with $[Os_3H_2(CO)_{10}]$ has been shown to give an analogous product. [30]

Complex (XXIX) has been extensively investigated, including X-ray[31] and neutron diffraction[32] studies. This shows that the distortion of the acetylide ligand in this μ_3-η^2-complex is much larger than in the μ_2-η^2-mode. The α-carbon is significantly exposed, and the C-C angle at the β-carbon is much larger. The ruthenium atoms form an equilateral triangle within experimental error, one side of which is bridged by a symmetrical Ru-H-Ru bond. Each ruthenium atom has three carbonyl ligands, one is axial and two are equatorial, and these are shown by ^{13}C n.m.r. to be exchanging on the n.m.r. time scale[33] (the analogous osmium cluster is also fluxional). At -62 °C (XXIX) is seen to have five carbonyl resonances in the ratio 1:2:2:2:2, assigned as shown in figure 20.

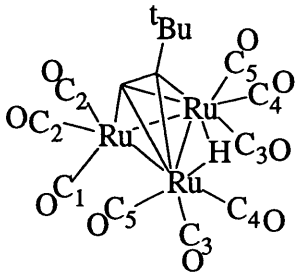

(XXIX) -62 °C

figure 20

Carbonyls 1 and 3 are axial, 2, 4, and 5 are equatorial, CO(5) showing a *trans*-coupling to the hydride. As the sample is warmed, a localised axial-equatorial site exchange occurs at the ruthenium σ-bound to the acetylide Cα. This results in equivalence of carbonyls (1) and (2) ($\Delta G = 55$ KJ mol^{-1}). As the temperature rises further axial-equatorial exchange is observed at the other two ruthenium atoms ($\Delta G =$ 65 KJ mol^{-1}), overlapping with the onset of total carbonyl scrambling at 153 °C ($\Delta G >$ 75 KJ mol^{-1}). Whether this final exchange process can be explained by movement of carbonyls around the ring *via* CO bridged intermediates, or by rotation of the acetylide coupled with axial-equatorial exchange cannot be determined from this set of data.[34]

The reaction of this complex with phosphines, phosphites and isonitriles yields carbonyl substitution products; for example, reaction with PR_3 affords both monosubstituted (XXX) and disubstituted (XXXI) products[34] (figure 21).

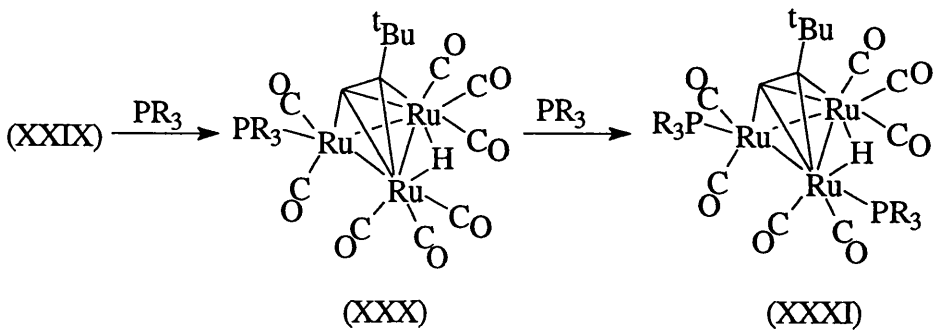

(XXX) (XXXI)

R = Ph, OMe

figure 21

In the monosubstituted complex (XXX) the new ligand takes up an equatorial position at the σ-bound ruthenium atom and the molecule again shows axial-equatorial exchange. This could be facilitated either by successive pairwise exchange of two of the three ligands or by rotation of the three ligands as a unit. A later study[35] showed that the latter is the case. In the disubstituted product (XXXI), n.m.r. data suggests that the second PR_3 ligand also occupies an equatorial position, *syn* to the bridging hydride.

In contrast, when the analogous cluster is prepared using phenylacetylene, similar nucleophiles do not displace CO, but attack the α-carbon.[1,36] So, reaction with ^{t}BuNC affords a zwitterionic compound (XXXII) (figure 22).

The osmium analogue displays similar behaviour.[37]

Obviously the R group of the acetylide has great importance in determining the reactivity of the complexes $[M_3(\mu_3\text{-}\eta^2\text{-}C{\equiv}CR)(H)(CO)_9]$ (M = Ru, Os). A possible explanation is that the zwitterionic species cannot be formed if the acetylide has an electron releasing substituent such as ^{t}Bu because of the ensuing destabilisation of the formal negative charge on the β-carbon.

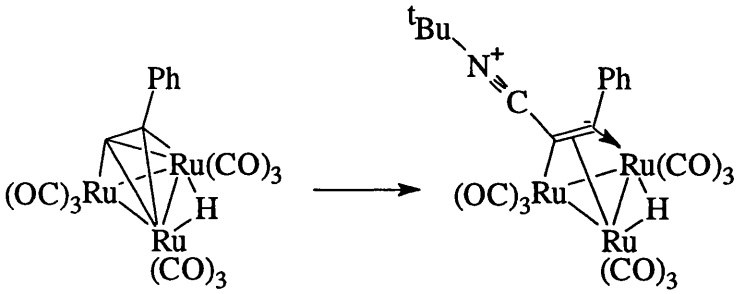

(XXXII)

figure 22

Once again, however, the common theme throughout the reactivity of metal acetylides becomes apparent, namely that again nucleophiles either substitute carbonyl ligands or attack the acetylide α-carbon.

In view of these observations, an anomalous result observed by Henrick *et al*[37] is of interest (figure 23). The treatment of the triosmium cluster (XXXIII) with PMe_2Ph results in the addition of the nucleophile to the β-carbon to give (XXXIV).

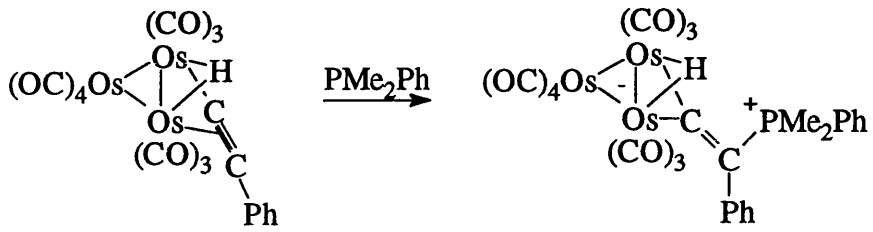

(XXXIII) (XXXIV)

figure 23

The mechanism of this reaction is unclear as to whether this is a kinetic product or whether (XXXIV) results from attack at a metal atom or at Cα.

A variety of intramolecular reactions of these cluster acetylides illustrate the electron deficiency of the α-carbon. An example of this can be found in figure 24. In this isomerisation the NMe_2 moiety of (XXXV) undergoes a 1,3-shift to the α-carbon.[38]

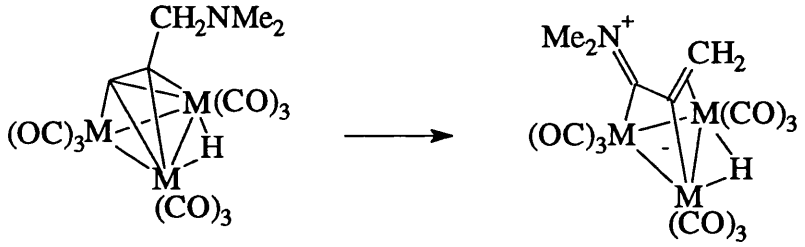

(XXXV) (XXXVI)

M = Ru, Os

figure 24

A crystal structure obtained of the ruthenium complex suggests that the molecule is best formulated as shown.

Figure 25 also shows an intramolecular reaction initiated by nucleophilic attack upon the α-carbon.[39] On this occasion OH attack at the Cα of (XXXVII) is followed by transfer of a hydrogen from oxygen to the osmium triangle to give (XXXVIII).

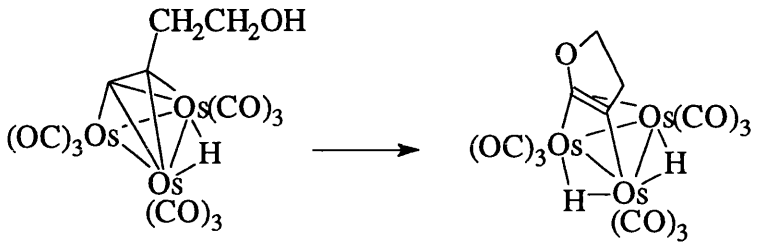

(XXXVII) (XXXVIII)

figure 25

These examples of the electrophilic nature of the α-carbon are concordant with theoretical predictions.[40]

Since bridging hydrides can be regarded as protonated metal-metal bonds, it would seem to follow that trinuclear acetylide complexes with such a bridge should be susceptible to deprotonation which would form an anion. This has been shown to be the case,[41] with the triruthenium *tert*-butylacetylide complex (XXIX) shown in figure 20 readily being deprotonated in THF at room temperature (figure 26) to give (XXXIX).

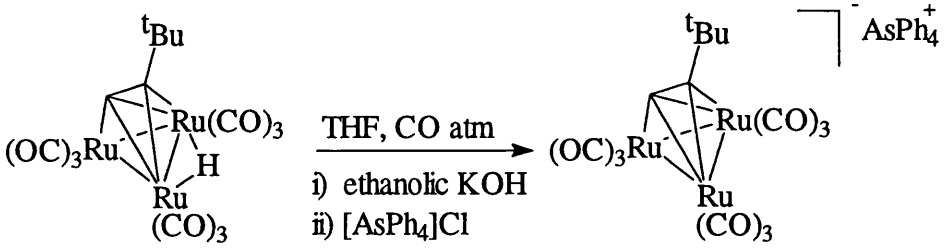

(XXIX) (XXXIX)

figure 26

Protonation of the anionic cluster complex (XXXIX) affords the original neutral cluster (XXIX), showing that the HOMO of this molecule lies within the metal triangle, not at the acetylide ligand. (XXXIX) has been structurally characterised, the only significant change being the shortening of the previously bridged Ru-Ru bond. ^{13}C n.m.r. experiments again show fluxionality of the carbonyl ligands, although it is considerably more facile. It reacts readily with mercury(II) salts to form bridged dimers with Hg occupying the bridging position previously containing the hydride.[42]

As is the case with dinuclear acetylide complexes, P-C bond cleavage can be used to form clusters containing both μ_3-η^2-acetylide and phosphide ligands. Thus treatment of $[Ru_3(CO)_{12}]$ with $Ph_2PC{\equiv}CR$ has been used to produce (XL)[25] as shown in figure 27.

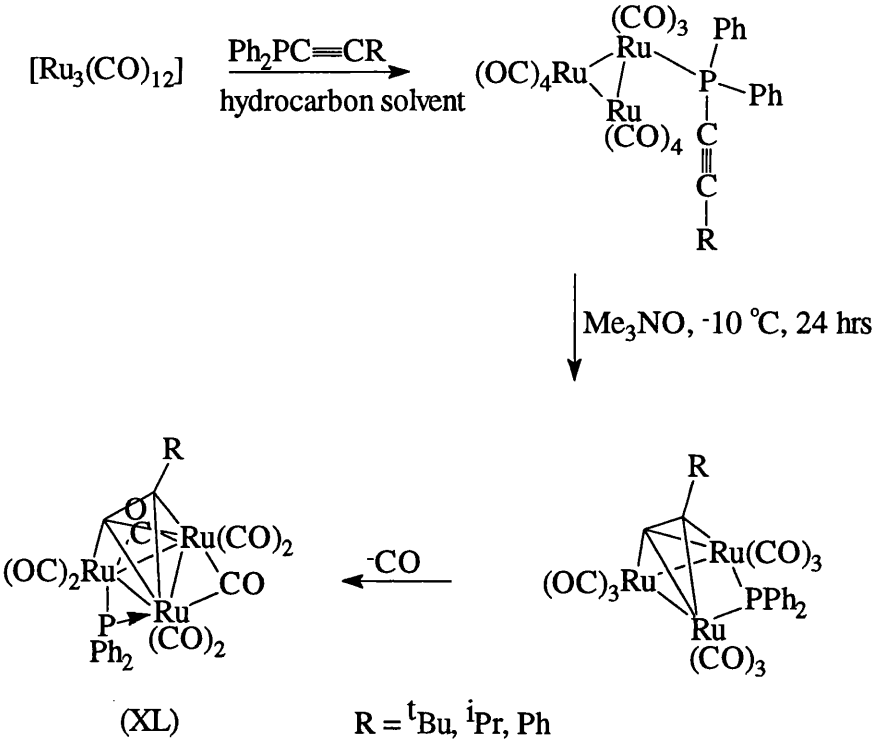

(XL) R = ^{t}Bu, ^{i}Pr, Ph

figure 27

Initially, a carbonyl is replaced by a $Ph_2PC{\equiv}CR$ ligand in which the phosphorus atom is σ-bonded to a metal leaving a dangling acetylene. Treatment with Me_3NO

removes CO allowing the acetylene to coordinate, and P-C σ-bond cleavage results in formation of a μ_3-η^2-acetylide complex (XL). This product is similar to the previously mentioned acetylide clusters except that the bridging phosphide ligand replaces both the bridging hydride and the Ru-Ru bond, showing a significant influence of phosphide ligands on cluster geometry. In solution this compound is labile, losing CO to generate a new cluster in which the Ru_3 triangle has closed, the phosphide group moves to bridge to the ruthenium atom α-bound to the acetylide ligand and the other edges of the triangle are bridged by carbonyls. This final decarbonylation reaction is reversible under CO pressure. The whole reaction sequence has been duplicated with osmium as the metal.[25]

This technique of P-C bond cleavage can be used to form many acetylide clusters not all of which comprise μ_3-η^2-acetylide ligands. Figure 28 shows an unusual cluster isolated by Carty *et al* by refluxing $[Ru_3(CO)_9(Ph_2PC{\equiv}CR)_3]$ in acetonitrile. (XLI) contains two acetylide ligands, one bonded μ_2-η^2 and one μ_2-η^1, together with a dangling acetylene. Thus both bonding modes possible for a μ_2-bridging acetylide ligand are extant in one molecule.

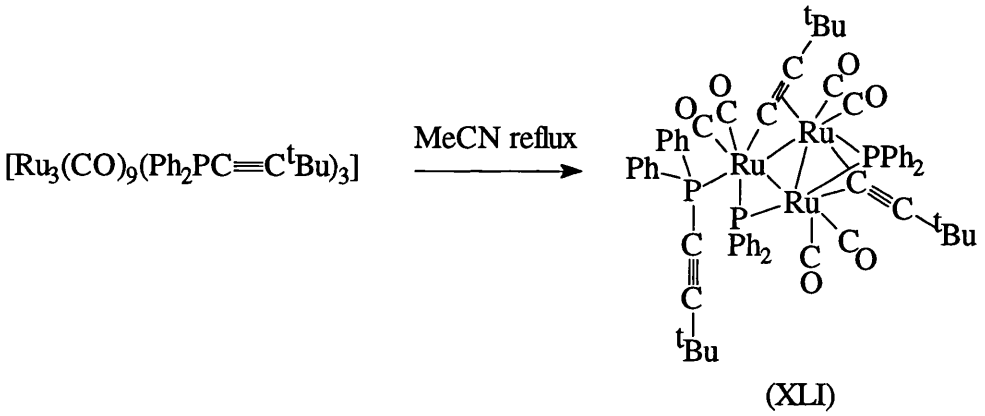

(XLI)

figure 28

It is possible, as shown by Bruce *et al*[44], to obtain μ_3-η^2-alkynyl clusters beginning with mononuclear acetylide complexes. Reaction of the mononuclear iron complex, $[Fe(\eta^1\text{-}C{\equiv}CPh)(CO)_2(\eta\text{-}C_5H_5)]$ (XLII) with $[Fe_2(CO)_9]$ affords such a

species, (XLIII), the structure of which was originally proposed to be as shown in figure 29, with the acetylide α-carbon remaining σ-bound to the iron atom attached to the η^5-cyclopentadienyl ligand.

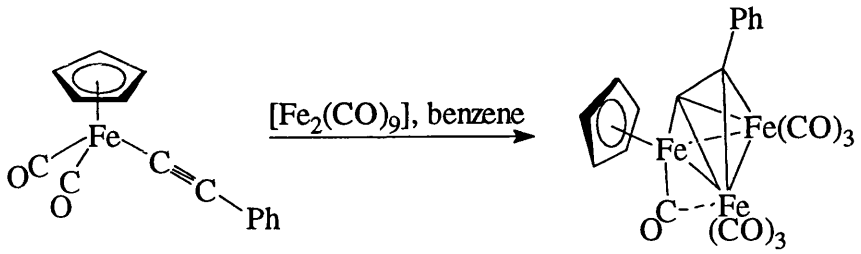

(XLII) (XLIII)

figure 29

At a later date[45], a crystal structure of (XLIII) was obtained which contradicted the original proposed formulation. In the solid state the acetylide proved to be bound to an $[Fe(CO)_3]$ fragment (figure 30).

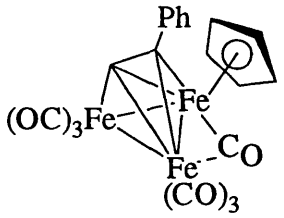

(XLIII)

figure 30

The implications of these observations are that in a trinuclear cluster, a μ_3-η^2-alkynyl ligand can change the metal to which it is σ-bound.

The extraordinary thermodynamic stability of the μ_3-η^2-acetylide bond is illustrated by the reaction shown in figure 31, in which heating the mononuclear carbyne complex $[W{\equiv}CR(CO)_2(\eta\text{-}C_5H_5)]$ (XLIV) with $[Et_3NH][Fe_3(\mu\text{-}H)(CO)_{11}]$ produces another trinuclear acetylide (XLV).[46] Fission of the C-R σ-bond gives a

carbide which apparently picks up a CR fragment to generate a C≡CR moiety. Under forcing conditions the fragments combine to form the stable product. N.m.r. studies of (XLV) have demonstrated fluxionality, with the carbonyls attached to the tungsten atom rendered equivalent by rotation of the $[W(CO)_2(\eta\text{-}C_5H_5)]$ moiety and CO exchange also occurring at the $[Fe(CO)_3]$ centres.

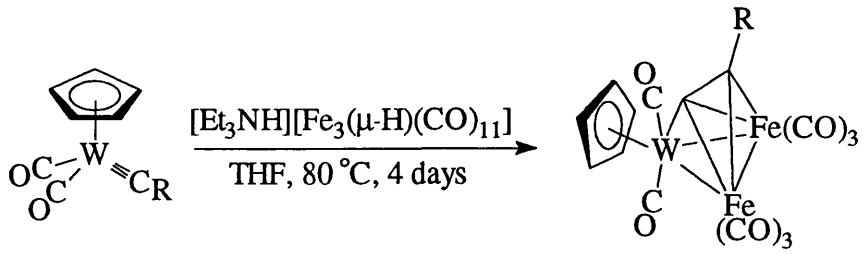

(XLIV) (XLV)

R = Me, p-tolyl

figure 31

This type of reaction, in which a carbide generates a $\mu_3\text{-}\eta^2$-acetylide *via* capture of a CR fragment, has also been demonstrated at a triiron centre.[47] Reaction of $[Fe_3(CO)_9(\mu_3\text{-}CCH_3)(\mu_3\text{-}COC_2H_5)]$ with two molar equivalents of $[Mn(CO)_5]^-$ yields $[Mn_2(CO)_{10}]$ and the anionic acetylide cluster (XLVI) shown in figure 32.

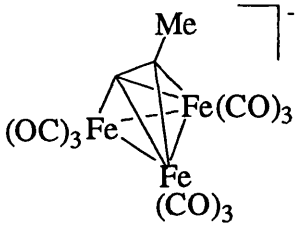

(XLVI)

figure 32

It is suggested that initially the triiron complex is reduced followed by loss of $[C_2H_5O]^-$ to form a carbide. This then couples with the μ_3-ethylidyne ligand still attached to the cluster to form the $\mu_3\text{-}\eta^2$-alkynyl complex (XLVI).

Figure 33 shows an unusual reaction in which the product appears to result from α-addition to the acetylide ligand.[48] In the first step acetyl chloride attacks the oxygen of the ketenyl ligand of (XLVII) to produce an anionic cluster (XLVIII) which reacts with HSO_3F to form the neutral product (XLIX).

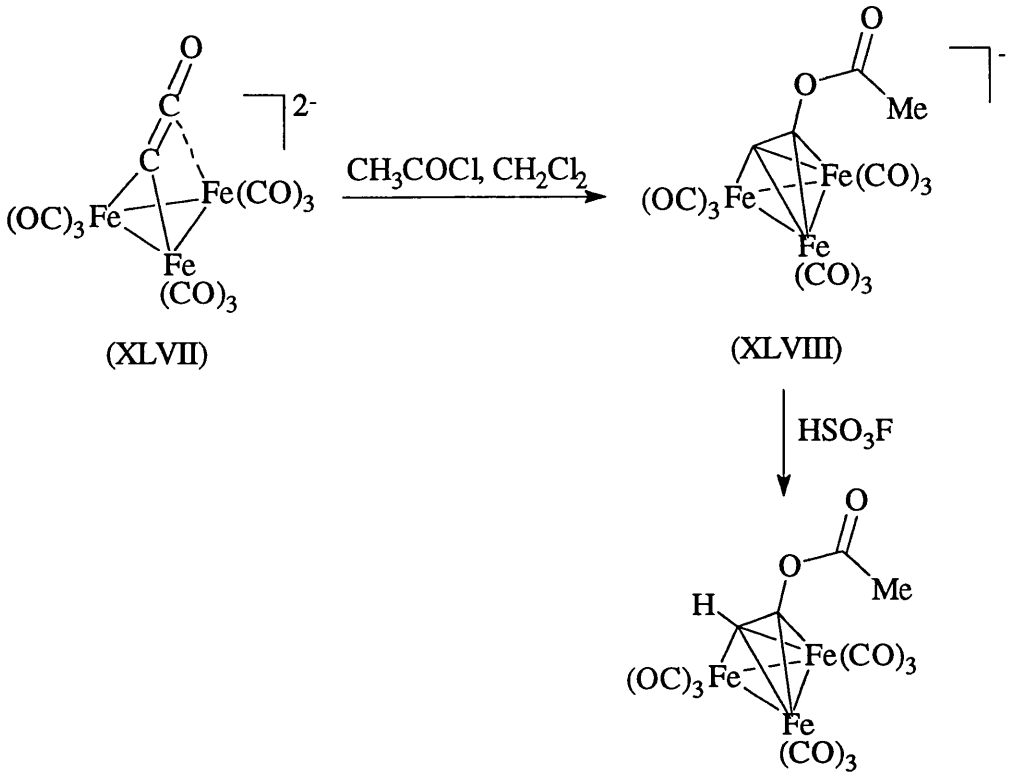

(XLVII) (XLVIII) (XLIX)

figure 33

It would not be expected, given earlier observations that the HOMOs of such anions appear to lie within the metal triangle[41], that attack by H^+ would occur at the α-carbon. Thus it is probable that initial attack does, in fact, occur at the metal triangle, with subsequent H-migration to the α-carbon producing the observed product.

The μ_3-η^2-bonded acetylide occurs in more clusters than just the trinuclear species heretofore discussed. An example of this is the tetraruthenium complex (L) shown in figure 34. This contains two acetylide ligands, one μ_3-η^2 and one μ_2-η^2, a dangling acetylene and two bridging phosphide ligands.[1] The carbonyl groups have been omitted for clarity.

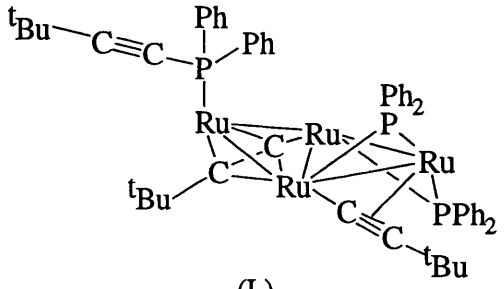

(L)

figure 34

Another of these tetraruthenium 'butterfly complexes' (LI) has been prepared containing only one μ_2-η^2-acetylide and one bridging phosphide (figure 35).[1]

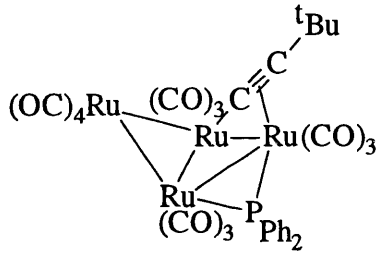

(LI)

figure 35

Acetylide ligands can adopt even more complex bonding modes in larger clusters (figure 36). If $[Ru_5(CO)_{11}(Ph_2PC{\equiv}CPh)]$ (LII) is refluxed in n-heptane a pentaruthenium complex containing a μ_4-η^2-acetylide ligand (LIII) is formed.[49] CO addition, which is reversible, results in an opening in the square pyramidal framework and the α-carbon of the acetylide is drawn within the cluster, producing a most unusual bonding mode.

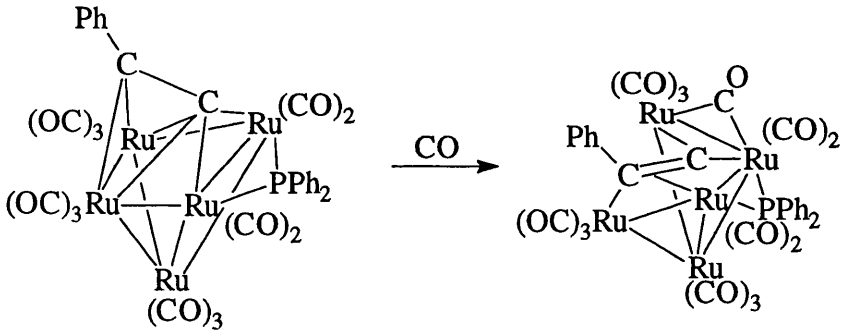

(LII) (LIII)

figure 36

Some extraordinary molecules involving a hexanuclear cluster bonded to a large number of acetylide ligands have been prepared by Bruce. Treatment of Vaska's compound, *trans*-[IrCl(CO)(PPh_3)$_2$], with [Cu(C≡CR)] yields a cluster comprising six metal atoms (two iridium, four copper) arranged in a slightly irregular octahedron (LIV), which is illustrated in figure 37.[50,51] Each phosphine ligand is apically bonded to an iridium atom which is also σ-bonded to four acetylide ligands. Each of these is π -bonded to a copper atom, such that each Cu is attached to one ligand bonded to each Ir in an unsymmetrical manner.

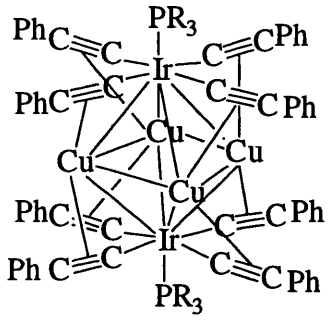

(LIV)

figure 37

Analogues of this complex have been prepared in which Ir is replaced by Rh, Cu by Ag and Ph by C_6F_5.[50,52]

Several other unusual clusters have emerged from Bruce's work, two of which are illustrated in figure 38. The first, (LV), contains four μ_2-η^2-alkynyl and one μ_3-η^2-alkynyl ligands and in the second, (LVI), two acetylides are σ-bonded and two are π-bonded to an [$Ag(PPh_3)$] moiety.[53]

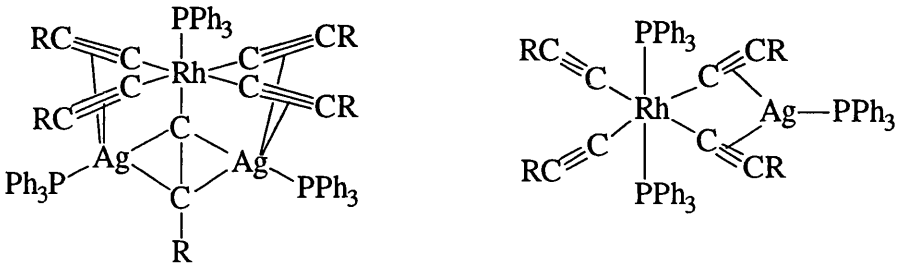

(LV) (LVI)

$R = C_6F_5$

figure 38

In conclusion, acetylide ligands display a multiplicity of bonding modes. This diversity ranges from the simple σ-donor ligand to complexes in which the ligand is coordinated to the face of a cluster. In clusters with a large number of acetylide ligands it appears that donation of three electrons is preferred to donating five, although the two possible 3-electron coordination geometries, μ_2-η^2 and μ_2-η^1, are similar in energy. The chemistry of alkynyl complexes is dominated by an electrophilic α-carbon and a nucleophilic β-carbon, although in systems where more electrons are donated by the acetylide π-system the β-carbon becomes less electron rich. Thus reactivity towards nucleophiles is the predominant aspect of the chemistry of cluster complexes containing μ_3-η^2-(5e)-acetylide ligands. The variety of available bonding modes leads to fluxionality in these ligands, a factor in their extensive chemistry. All these aspects combine to make this an interesting and rewarding field of study.

1.5 Vinylidene Complexes

The formation and investigation of carbon-bridged di- and poly-nuclear transition-metal complexes, have been of interest for some time[54, 55], as a means of attempting to understand metal surface promoted organic transformations, such as the Fischer-Tropsch reaction. Vinylidene[56] and allenylidene[57] complexes form a significant part of this field of research.

The free vinylidene fragment, CCH_2, is highly unstable and rearranges to give acetylene (figure 39), although evidence for its existence has been reported[58, 59].

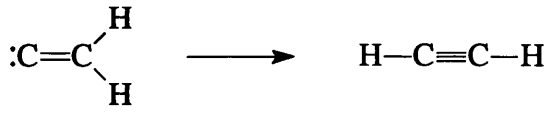

figure 39

There is evidence for the intermediacy of metal bound vinylidene species in reactions occurring at metal surfaces. In particular, there is evidence for the process illustrated in figure 40 leading to an adsorbed vinylidene fragment.

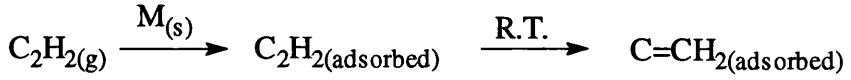

$M_{(s)}$ = Pt(111), references: 60, 61

$M_{(s)}$ = Pd(111), reference: 62

$M_{(s)}$ = Ni(111), references: 63-67

figure 40

Adsorption of ethylene onto a Ni(111) surface below 200 K and subsequently allowing it to warm to room temperature results in the formation of an organic layer, originally believed to be an acetylene layer resulting from dehydrogenation[63-65]. Direct

adsorption of acetylene also produces such a layer, but a closer investigation of the vibrational frequencies obtained using High Resolution Electron Energy Loss Spectroscopy[66] led to the suggestion that the layer may consist of chemisorbed vinylidene[67].

The evidence for chemisorbed vinylidenes is often inconclusive and thus the details of the bonding mode are uncertain. Nevertheless, a theoretical treatment of the question was conducted by Hoffmann[68] using the extended Hückel method, investigating the four bonding modes to an idealised Pt(111) surface illustrated in figure 41.

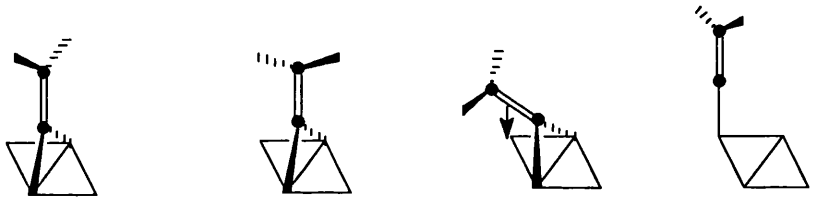

2-fold parallel	2-fold perpendicular	2-fold bent	2-fold linear
I	II	III	IV

figure 41

The calculations predicted that bonding modes I and III are the most energetically favourable, but have little difference between them. In Hoffmann's opinion, the 2-fold bent configuration (III), a μ_3-σ,σ,η^2-bonding mode, is the more favourable. The experimental evidence supports this in the case of C_2H_2 adsorbed onto Ni(111)[67] and to a lesser degree for C_2H_2 on Pt(111)[60].

Many programmes of research into the preparation and reactions of organic species adsorbed onto metal surfaces have been undertaken, but the associated experimental problems are considerable[69]. The effective concentration of these species is extremely low, necessitating the use of very sensitive spectroscopic techniques. Conditions of ultra-high vacuum are also required, both for the operation of the

analytical techniques and in order to minimise the rate of surface contamination. Thus the development of the chemistry of related organometallic complexes has been pursued as a means of modelling the behaviour of surface species in order to better understand the many catalytic processes which are widely used but little understood. It may be argued that such low oxidation state complexes, containing small numbers of metal atoms, are inadequate representations of systems which essentially possess an infinite array of metal atoms, nevertheless the cluster-surface analogy often seems to hold true[68]. This concurs with the observations of Hoffmann *et al*[70], whose calculations predict that the perturbations caused by the interaction of an organic fragment with a metal surface have a short range and that bonding is effectively localised to those metal atoms directly connected to the organic fragment.

As the transformation of terminal acetylenes to vinylidenes is promoted by a metal surface, so the use of terminal acetylenes is involved in an important method for the preparation of vinylidene complexes, *via* a 1,2 hydrogen shift (figure 42).

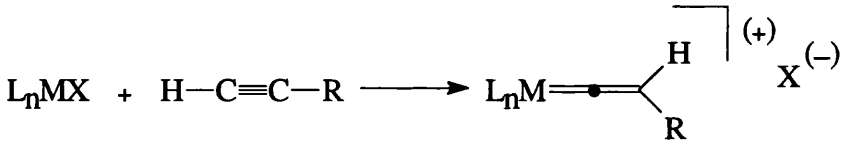

(LVII)	$L_nM = FeCl(depe)_2$	reference 71
(LVIII)	$L_nM = Ru(PPh_3)_2(\eta\text{-}C_5H_5)$	reference 72
(LIX)	$L_nM = Re(CO)_2(\eta\text{-}C_5H_5)$	reference 73
(LX)	$L_nM = Os(PPh_3)(CO)(\eta\text{-}C_5Me_5)$	reference 74
(LXI)	$L_nM = Mo(dppe)(\eta 7\text{-}C_7H_7)$	reference 75
(LXII)	$L_nM = ReCl(dppe)_2$	reference 76

$X = CO, N_2$, solvent or halogen

figure 42

These reactions probably proceed *via* an intermediate η^2-alkyne complex. Evidence for this can be seen in the reaction of $[Mn(CO)_3(\eta\text{-}C_5H_5)]$ with phenylacetylene[77], illustrated in figure 43, where both the isomers (LXIII) and (LXIV) can be isolated.

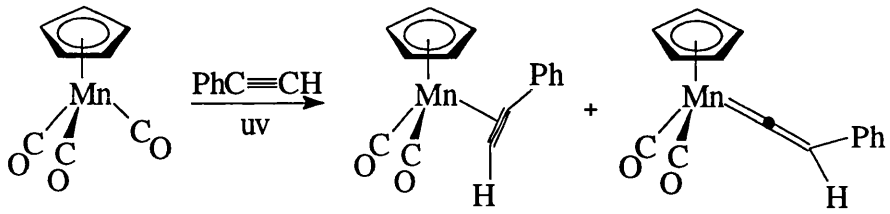

(LXIII) (LXIV)

figure 43

Complex (LXIII) is unstable with respect to (LXIV), and the yield ratio is dependant on the basicity of the alumina used in the chromatography column during workup. It is suggested that this is evidence for the formation of (LXIII) initially, followed by subsequent rearrangement to (LXIV) *via* a deprotonation/protonation process.

Similar behaviour has been reported[78] for ruthenium complexes. Reaction of $[RuCl(PMe_3)_2(\eta\text{-}C_5H_5)]$ with either ethyne or propyne in methanol led to the formation of the η^2-alkyne complexes $[Ru(\eta^2\text{-}HCCR)(PMe_3)_2(\eta\text{-}C_5H_5)]^+$ (R = H, Me). Gentle heating of these complexes in a solution of methanol or acetonitrile induced rearrangement to the vinylidene complexes $[Ru(CCHR)(PMe_3)_2(\eta\text{-}C_5H_5)]^+$, the propyne derivative undergoing this transformation more rapidly.

This acetylene to vinylidene rearrangement has also been reported as occurring at a dinuclear centre[79] (figure 44).

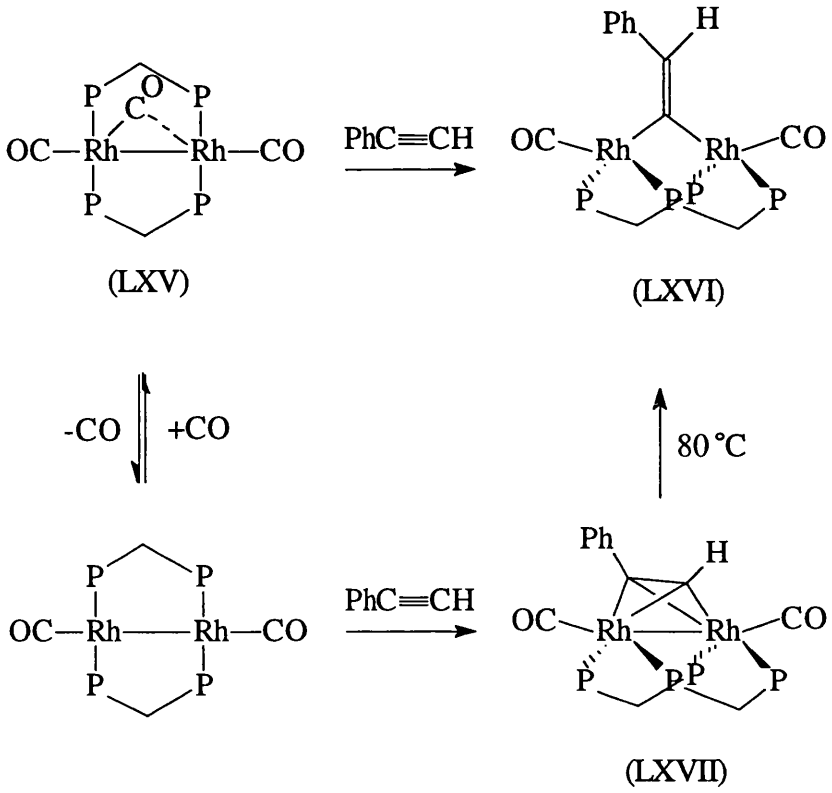

figure 44

Reaction of (LXV) with phenylacetylene gives a mixture of (LXVI) and (LXVII) *via* two different routes. The kinetically favoured μ-acetylene complex, (LXVII), rearranges on heating to the thermodynamically favoured product, the vinylidene complex (LXVI). Interestingly this rearrangement results in a decrease in the number of electrons formally attributed to each rhodium atom from 18 to 16, as the μ-alkyne ligand acts as a 4-electron donor, whereas the bridging μ-vinylidene ligand only contributes two. The breaking of the Rh-Rh bond accounts for the remainder of the decrease.

The upright symmetrical configuration of the vinylidene ligand of (LXVI) is representative of most dinuclear vinylidene complexes. More recently though, examples of molecules containing μ-σ, η^2-vinylidene ligands have been reported, in which the vinylidene ligand asymmetrically bridges two metals and acts as a four electron donor. A good example of this is the synthesis of [Mo_2(μ-σ, η^2-

$CCH_2)(CO)_4(\eta\text{-}C_5Me_5)]$[80], (LXVIII), by reaction of the triply bonded molybdenum dimer $[Mo_2(CO)_4(\eta\text{-}C_5Me_5)]$ with acetylene, as shown in figure 45.

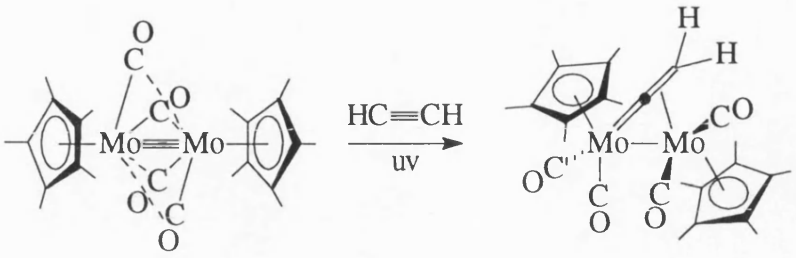

(LXVIII)

figure 45

If this reaction is performed in the absence of uv radiation, the thermodynamic product, (LXIX), is formed, shown in figure 46. Heating the vinylidene complex (LXVIII) also causes rearrangement to the μ-alkyne complex (LXIX).

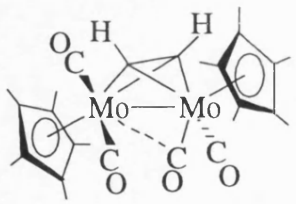

(LXIX)

figure 46

Another bonding mode of the vinylidene ligand is illustrated by complex (LXXI), shown in figure 47. Its precursor (LXX) is isolable from the products of the facile reaction between $RuCo_2(CO)_{11}$ and a terminal alkyne[81, 82].

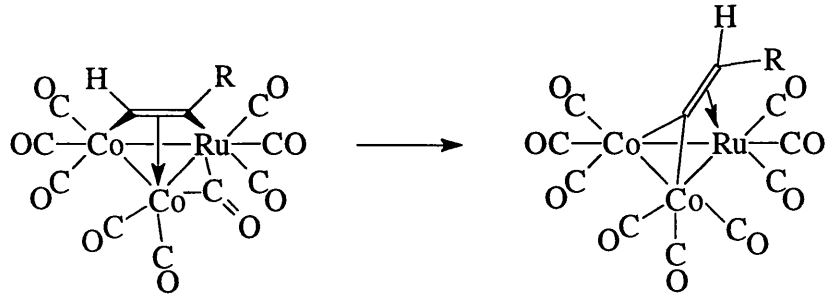

(LXX) (LXXI)

R = H, Me, ^{t}Bu, Ph

figure 47

In contrast to the example shown in figure 44, in this case both the μ-alkyne and the μ-vinylidene ligands act as 4-electron donors. The triangular metal base for complexes (LXX) and (LXXI) provides a convenient model for the infinite array of triangular units presented by a hexagonal close packed metal surface.

The maximum number of metal atoms that a vinylidene has been observed to bond to is four[83]. The complex shown in figure 48, (LXXIII), is again prepared by addition of a terminal alkyne to a cluster and is an example of a tetranuclear cluster containing a μ_4-vinylidene ligand.

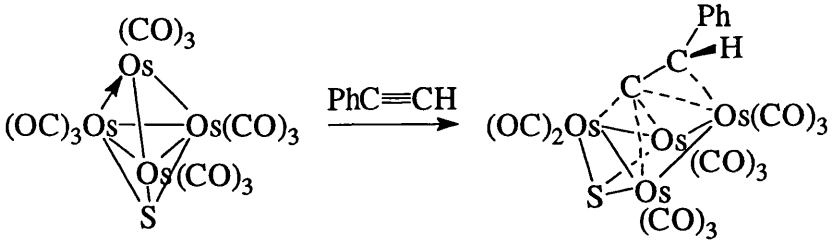

(LXXII) (LXXIII)

figure 48

Another useful method for the preparation of vinylidene complexes is *via* the use of acetylide complexes as a precursor. Among the methods used to prepare these complexes are deprotonation of terminal η^2-alkyne complexes and oxidative addition of an acetylinic C-H bond and so the formation of vinylidene complexes by this route

does not necessarily proceed *via* a distinct mechanism from terminal alkyne isomerisation. As has been previously discussed, the β-carbon of an acetylide is generally susceptible to nucleophilic attack and therefore protonation often generates a vinylidene[84], as will migration of hydride to Cβ in a hydrido-acetylide complex. Figures 49 and 50 show how these points are illustrated by the work of Werner *et al*[85].

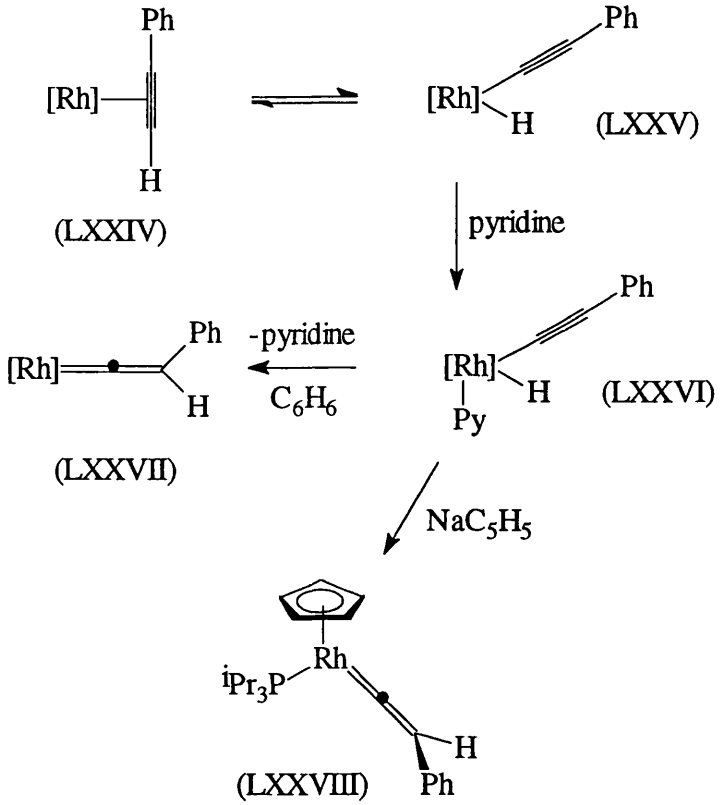

[Rh] = $RhCl(P^iPr_3)_2$

figure 49

The equilibrium between the η^2-alkyne complex (LXXIV) and the hydrido-acetylide complex (LXXV) proved to be driven completely to the right by the addition of pyridine to generate (LXXVI). Stirring of a benzene solution of (LXXVI) at room temperature afforded (LXXVII), which can also be obtained quantitatively from (LXXIV), probably *via* (LXXV). In contrast, the reaction of (LXXVI) with NaC_5H_5 was shown to give (LXXVIII) *via* the intermediate (LXXIX), shown in figure 50, and thus the hydrogen shift is probably intramolecular.

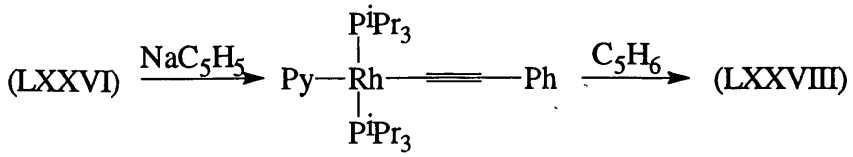

(LXXIX)

figure 50

Slightly different behaviour is reported in the chemistry of the iridium analogue of (LXXIV), *trans*-[IrCl(HC≡CR)(P^iPr_3)$_2$]. The rearrangement to the vinylidene complex [IrCl(=C=CHPh)(P^iPr_3)$_2$], analogous to (LXXVII), which in the rhodium case (figure 49) proceeds at room temperature, requires much more forcing conditions and it is possible to isolate the hydrido-acetylide intermediate. This observation was claimed to provide proof [76] that the general reaction , M(η^2-HC≡CR) → M(=C=CHR), proceeds *via* an intermediate M(σ-C≡CH)H. Doubt was cast on this hypothesis, however, by Hoffmann[86] whose calculations suggested that this intramolecular route is not the most energetically favourable. Hoffmann favoured a concerted process in which the alkyne ligand slips to an η^1-configuration, illustrated in figure 51.

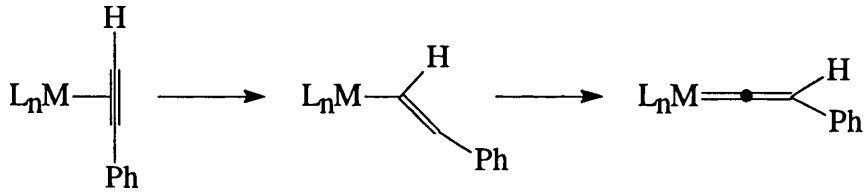

figure 51

The susceptibility of the β-carbon of an acetylide ligand to attack by electrophiles, therefore, usually leads to protonation resulting in the formation of a vinylidene complex and use of other electrophiles in these reactions also produces similar results. An instance of this is shown in figure 52 where the electrophile used is a methylating agent[13, 87].

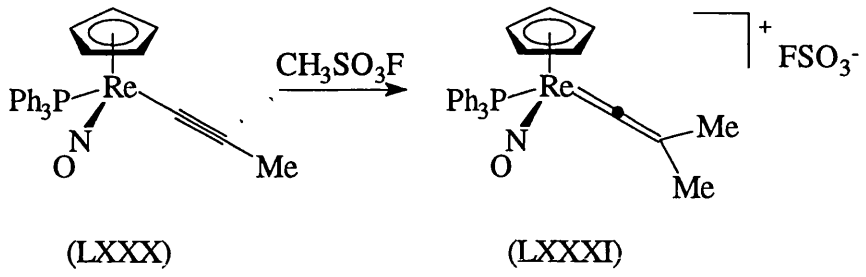

(LXXX) (LXXXI)

figure 52

Similar reactions of polynuclear acetylides have been reported, in particular by Green *et al*[56], who prepared the μ-σ,η^2-vinylidene complexes illustrated in figure 53.

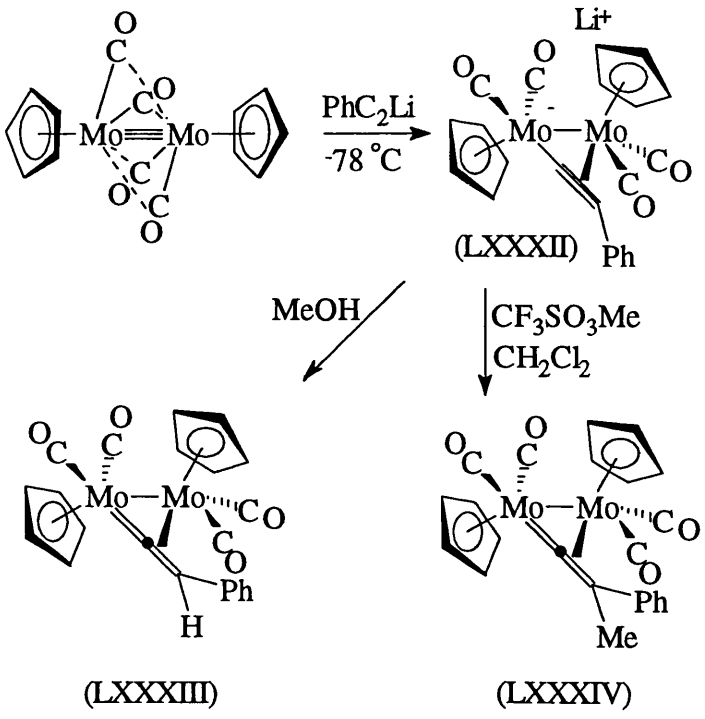

figure 53

The anionic μ-acetylide complex (LXXXII) was prepared by the addition of lithium phenylacetylide to the dimer shown. (LXXXII) is also accessible *via* the deprotonation of the μ-alkyne complex formed by the reaction of the dimer with phenylacetylene, but the yield is lower. Protonation or reaction with the methylating agent methyl trifluoromethane sulphonate yielded the μ-σ,η^2-vinylidene complexes

(LXXXIII) and (LXXXIV) respectively. (LXXXIII) is relatively unstable and rearranges within 12 hours in benzene to the isomeric μ-alkyne complex. In contrast, (LXXXIV) is stable at room temperature and heating in toluene at 50 °C resulted in a transformation to the μ-allylidene complex (LXXXV) as illustrated in figure 54.

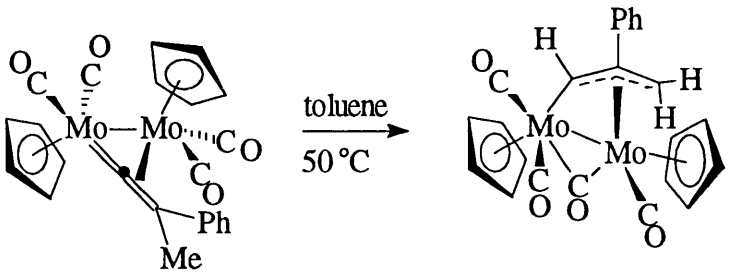

(LXXXIV) (LXXXV)

figure 54

A similar strategy was used[88] to prepare the two analogous vinylidene complexes $[M_2(\mu\text{-}\sigma,\eta^2\text{-}C{=}CMe_2(CO)_4(\eta\text{-}C_5H_5)_2]$, (LXXXVI), (M = Mo, W). The n.m.r. data obtained in the analysis of these complexes demonstrated that fluxional processes occur in these molecules and the evidence suggests that site exchange occurs *via* a higher energy σ,σ(2e)-bonded vinylidene (LXXXVII) as illustrated in figure 55 for the case M = Mo.

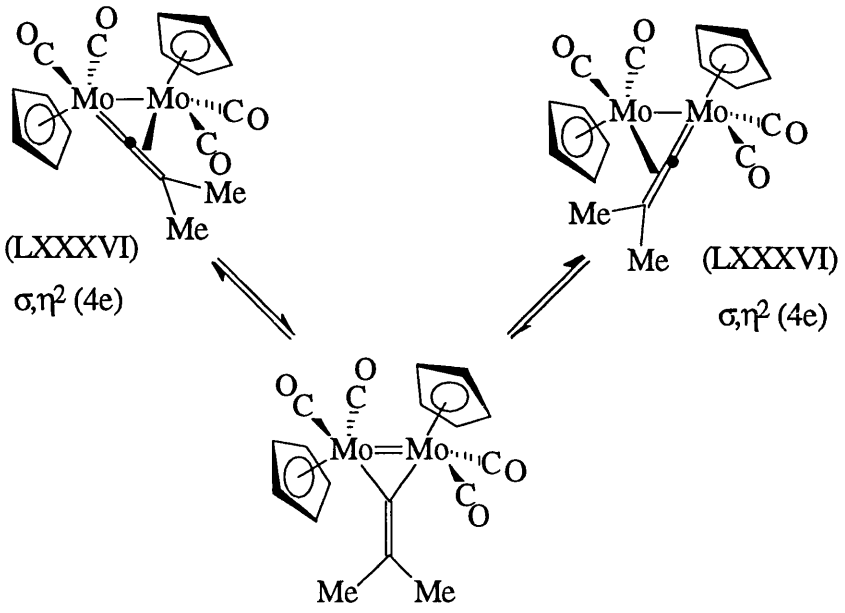

(LXXXVI)
σ,η² (4e)

(LXXXVI)
σ,η² (4e)

(LXXXVII)
σ,σ (2e)

figure 55

An asymmetrical μ_3-η^2-vinylidene (LXXXVIII) which has been the subject of much investigation[89], has been synthesised from neutral μ_3-alkylidynes as shown in figure 56. This was achieved either by elimination of OH^- from the β-carbon or by protonation of a vinyl group attached to the α-carbon.

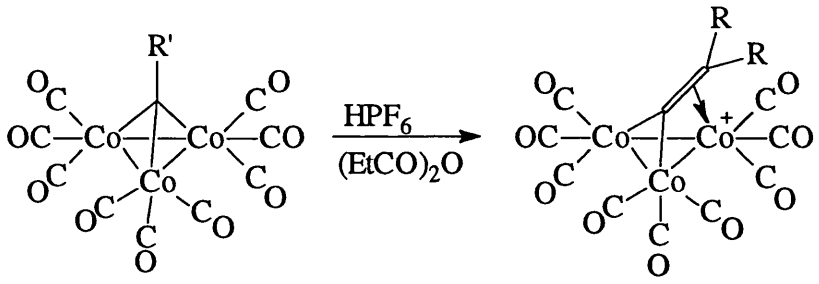

R' = CR_2OH or $CR{=}CH_2$

(LXXXVIII)

figure 56

The β-carbon of (LXXXVIII) has been shown to be extremely electrophilic in nature and perhaps can be more properly viewed as a stabilised carbonium ion (figure 57). There has been considerable debate over the structure and stabilisation of this

molecule[90, 91], but the description of (LXXXVIII) as a vinylidene is certainly acceptable.

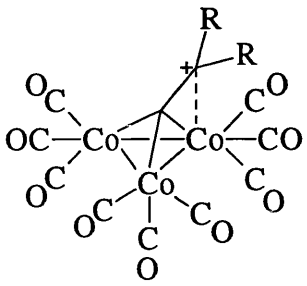

(LXXXVIII)

figure 57

1.6 Allenylidene Complexes

A number of studies have been made of free propadienylidene (XC)(the parent allenylidene)[93]. It has been detected using ir spectroscopy following irradiation of (LXXXIX) within a matrix. Irradiation with light of a different frequency reverses the process.

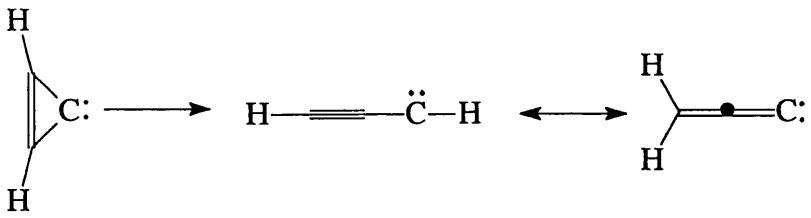

(LXXXIX) (XC)

figure 58

There are obvious similarities with vinylidene, the most notable difference being the absence of a stable isomer to which can rearrange as vinylidene can to acetylene. Mononuclear allenylidene complexes contain an approximately linear MCCC unit similar to the MCC unit of vinylidene complexes, but the γ-carbon substituents take up positions orthogonal to the analogous terminal groups of vinylidene complexes[94].

The area of the chemistry of allenylidene complexes has been explored relatively little[84, 94]. The first allenylidene complex to be described was prepared in 1976 by E.O. Fischer *et al*[95] by inducing the loss of ethanol from a Fischer-carbene complex (XCI) to give (XCII) as illustrated in figure 59.

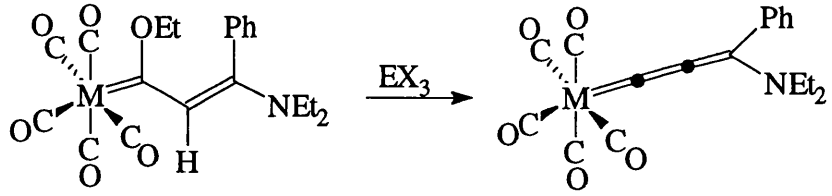

(XCI) (XCII)

M = Cr, EX_3 = BF_3

M = W, EX_3 = $AlEt_3$

figure 59

The ruthenium allenylidene complex (XCIV) was synthesised by base catalysed dehydration of the vinylidene complex (XCIII)[96] as shown in figure 60.

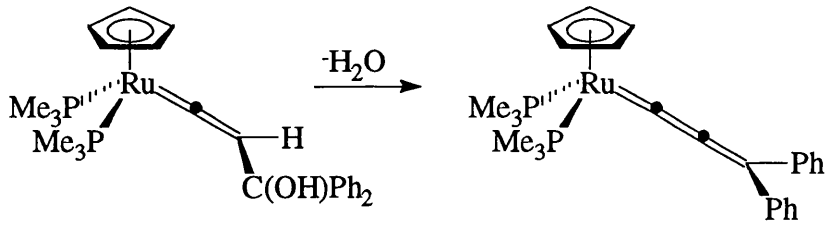

(XCIII) (XCIV)

figure 60

Whereas mononuclear allenylidene complexes obviously only have one possible configuration (linear), dinuclear μ_2-allenylidene complexes are capable of bridging the metal atoms in two bonding modes, illustrated in figure 61. Structure (A), the symmetrical μ-σ,σ (2e) bonding mode and the side-on bonded structure (B), described asμ-σ,η^2 (4e), both have obvious analogies with vinylidene systems.

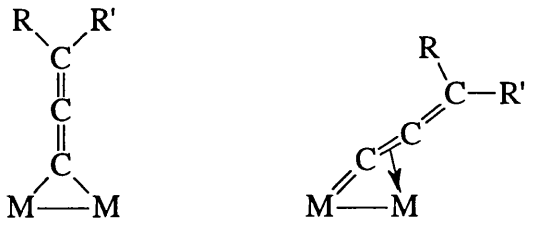

(A) (B)

figure 61

A convenient method of preparation of dinuclear allenylidene species by the reaction of mononuclear allenylidene complexes with a metal fragment has been described[97, 98]. This approach was used[99] to prepare the dinuclear allenylidene complexes illustrated in figures 62 and 63.

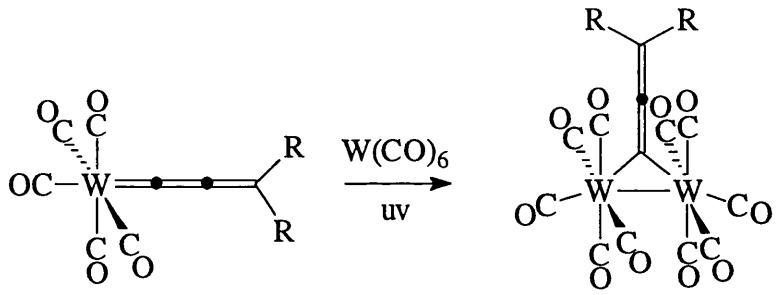

(XCV) (XCVI)

figure 62

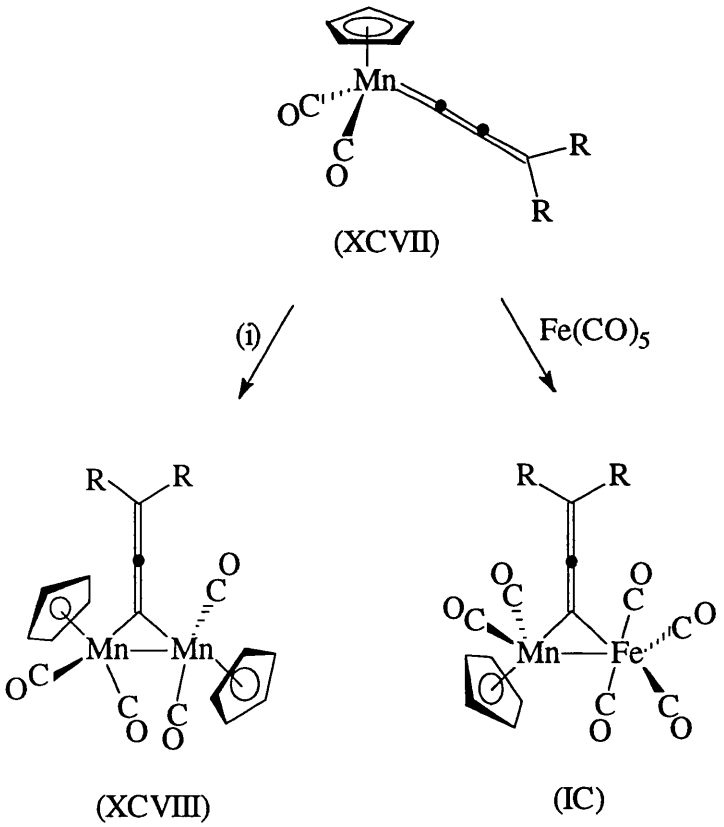

(i) = $[Mn(CO)_2(OEt_2)(\eta\text{-}C_5H_5)]$

figure 63

It is noteworthy that in all these cases the allenylidene ligand adopts the symmetrical $\mu\text{-}\sigma,\sigma$ (2e) bonding mode and this is the case for the majority of allenylidene complexes that have been isolated.

S.F.T. Froom *et al* prepared the first example of a "side-on" bonded ($\mu\text{-}\sigma,\eta^2$ (4e)) allenylidene complex[57] by protonation of the acetylide complex (C) to give (CI) as shown in figure 64.

MO calculations on (XCVII) where R = Ph have predicted that Cα and Cγ are electrophilic and Cβ is nucleophilic[100]. Experimental results confirm this, with hard bases (such as MeO^- and Me_2N^-) adding to Cα and soft bases (such as PR_3) to Cγ, although the former produces a more stable product[101, 102]. The side-bonded allenylidene ligand, however, undergoes nucleophilic attack at Cγ and electrophilic attack at Cα. The preparation and reactivity of side-bonded allenylidene complexes will be discussed in greater detail at a later stage.

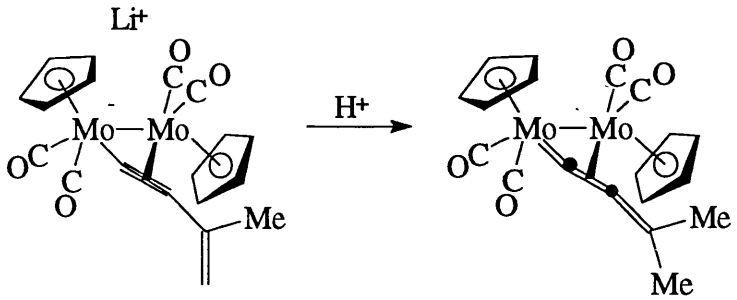

(C) (CI)

figure 64

Very few examples of trinuclear allenylidene complexes are extant and no such complexes of higher nuclearity appear to have been reported. The complex (CII), illustrated in figure 65, was prepared[103] by acid-induced migration of a hydroxy group from a μ_3-σ,η^2-acetylide ligand to the metal frame.

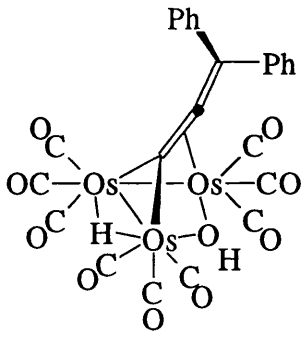

(CII)

figure 65

Reaction of the mononuclear allenylidene complex [Fe(CCC^{t}Bu$_2$)(CO)$_4$] (CIII) with successive Fe(CO)$_4$ moieties yielded both a symmetrical dinuclear μ-allenylidene species (CIV) and a trinuclear allenylidene complex (CV) (figure 66)[104].

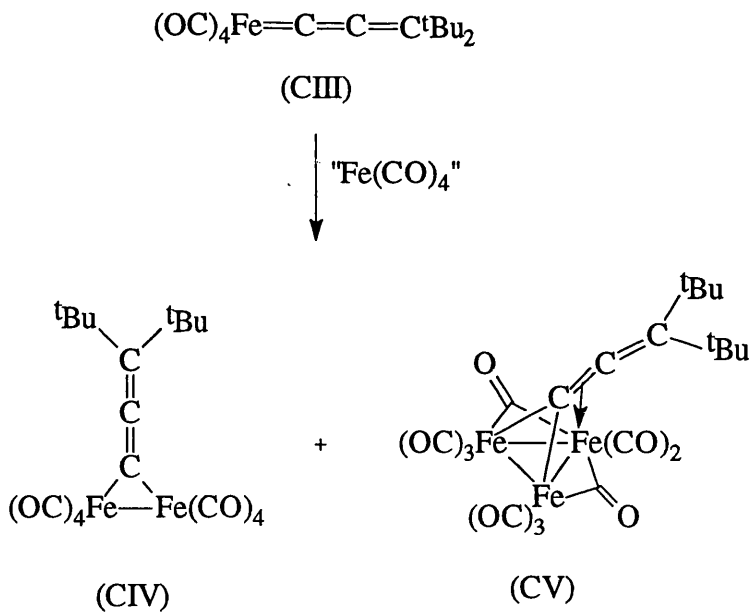

(CIV) (CV)

figure 66

The allenylidene ligand of the trinuclear complex (CV) shows an interesting equilibrium between μ_3- and μ_2-bonding modes, with concomitant change of a bridging carbonyl ligand to a terminal position.

1.7 Transition Metal η^4-*trans*-1,3-Diene Complexes

In numerous cases it has been demonstrated that transition metal complexes of η^4-bound acyclic conjugated dienes prefer to adopt *s-cis* geometry rather than the *s-trans* arrangement, irrespective of the preferred conformation of the free ligand[105, 106]. While the first report of a coordinated conjugated diene complex, [Fe(η^4-C_4H_6)$(CO)_3$], appeared in 1930[107], systems containing an *s-trans*-conjugated diene, in which the diene bridged a metal-metal bond, were not described until the 1970's[108, 109] and it was not until 1980 that Erker *et al* reported the preparation of a mononuclear *s-trans*-η^4-diene complex[110]. Low temperature photolysis of diphenyl zirconocene in the presence of 1,3-butadiene followed by reaction workup at ambient temperature and fractional crystallisation from toluene yielded a mixture of the *s-cis* and *s-trans* [Zr(η-$C_5H_5)_2$(η^4-C_4H_6)] complexes, (CVI) and (CVII), respectively. Complete conversion of (CVI) to (CVII) was achieved by photolysis at low temperature, while at room temperature the reverse rearrangement of (CVII) to (CVI) occurred slowly (figure 67).

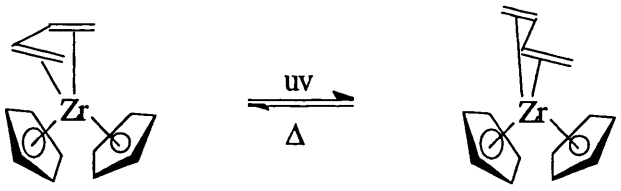

(CVI) (CVII)

figure 67

During the next decade this chemistry was extended further through the periodic table to include compounds of hafnium[111]and niobium[112], and these complexes proved to be useful in stereoselective preparations of a variety of organic products[113]. In 1988 the preparation of several complexes of the form Cp'Mo(NO)(η^4-diene) where Cp' = (η-C_5H_5) or (η-C_5Me_5) was reported[114] in which the thermodynamically most stable forms were *trans*-diene complexes.

The next progression in this chemistry came at the end of the decade when Green *et al* reported the preparation of cationic η^4-*s-trans*-1,3-diene complexes of molybdenum and ruthenium[115, 116]. In the case of the ruthenium chemistry illustrated in figure 68, the configuration of the product proved to be dependant on the degree of steric hindrance present in the diene used in the reaction.

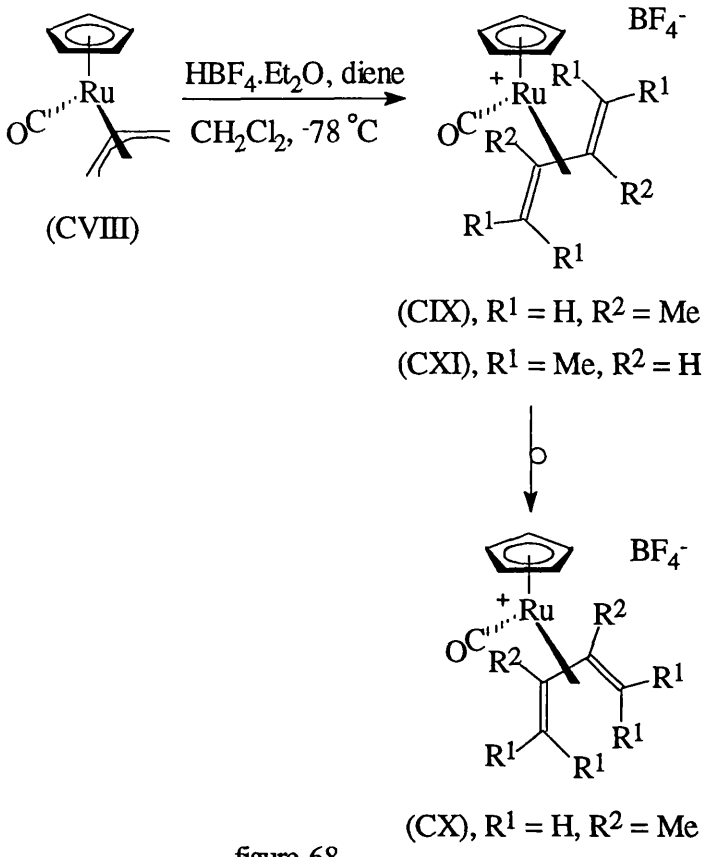

(CVIII)

(CIX), R^1 = H, R^2 = Me

(CXI), R^1 = Me, R^2 = H

(CX), R^1 = H, R^2 = Me

figure 68

Protonation of the allyl complex (CVIII) in the presence of 2,3-dimethylbuta-1,3-diene yielded a mixture of the *s-cis* and *s-trans* cations (CIX) and (CX). At room temperature, (CIX) proved to be unstable in solution and slowly rearranged to (CX). If the more sterically demanding 2,5-dimethylhexa-2,4-diene is used, the *s-trans* cation (CXI) is the only product. Complex (CXI) is completely stable in solution at room temperature, the first example of a stable cationic η^4-*s-trans*-1,3-diene complex[116].

Similarly the *s-trans*-diene complex (CXIII) was prepared by protonating the *syn*-η^3-pentadienyl species *syn*-(CXII) as illustrated in figure 69 [116]. Again this

complex slowly rearranged over 48 hours at room temperature to give a *cis*-diene complex (CXIV). Reaction of (CXIII) with a base regenerated *syn*-(CXII), whereas similar treatment of (CXIV) gave the *anti*-η^3-pentadienyl isomer *anti*-(CXII).

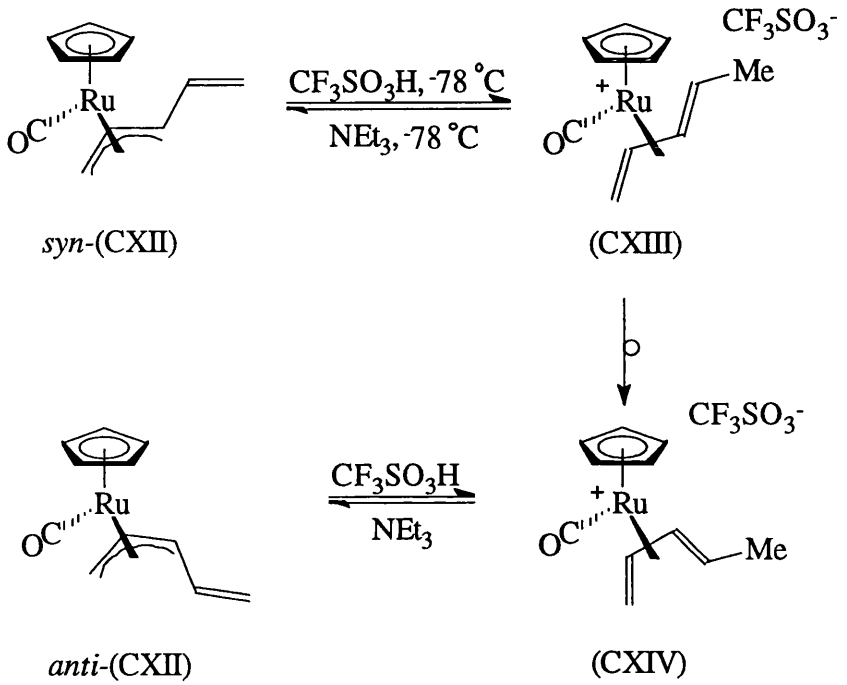

syn-(CXII) (CXIII)

anti-(CXII) (CXIV)

figure 69

In the case of analogous molybdenum systems[115] the rearrangement of the *s-trans*-diene complexes *exo*- and *endo-s-trans*-[Mo(η-C_5Me_5)$(CO)_2(CH_2CHCHCHMe)$] to the respective *s-cis*-dienes was substantially more facile and occurred rapidly at temperatures in excess of -20 °C.

The preparative route used to gain access to these η^4-penta-1,3-diene complexes is illustrated in figure 70. Reaction of the cationic complexes [M'$(NCMe)_2$]BF_4 (CXV) where M' = Ru(CO)(η-C_5H_5), Mo$(CO)_2$(η-C_5Me_5) with 1-trimethylsilyloxybuta-1,3-diene yielded the oxoallyl species [M'(η-L)(η^3-$CH_2CHCHCHO$)] (CXVI) *via* a fluoride-anion-induced desilylation of the initially formed diene cation. Further reaction of this complex with the Wittig reagent $Ph_3P{=}CH_2$ gave the η^3-pentadienyl complexes (CXVII) (equivalent to complex (CXII) when M = Ru). Figure 70 illustrates this series of reactions for the *exo-s-trans*- and *exo-syn* isomers.

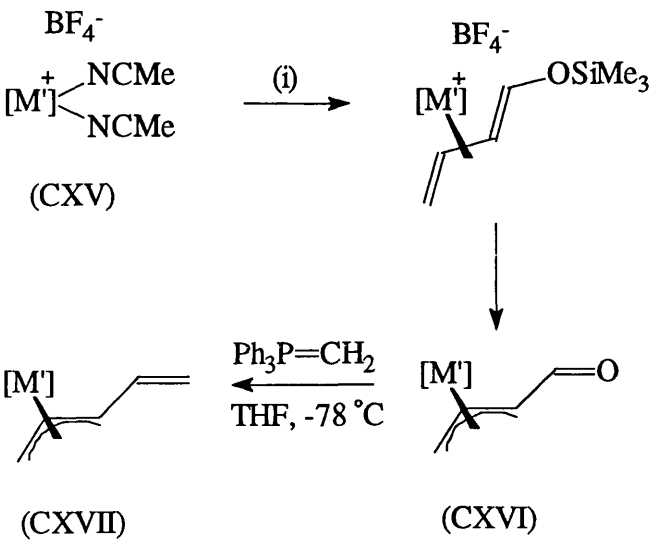

(i) 1-Trimethysilyloxybuta-1,3-diene

[M'] = $Ru(\eta\text{-}C_5H_5)(CO)$, $Mo(\eta\text{-}C_5Me_5)(CO)_2$

figure 70

The reactions shown in figure 70, however, do not constitute the whole story. The initial reaction produced a mixture of isomers of (CXVI); when M = Ru a 4:1 mixture of *exo-syn : endo-syn* isomers was observed and for M = Mo a mixture of three isomers was identified - *exo-syn* (39 %), *endo-syn* (24 %) and *exo-anti* (37 %). No *endo-anti* isomer was identified. It is not clear whether these four complexes, illustrated in figure 71 are interconvertible in solution *via* $\eta^3\text{-}\sigma\text{-}\eta^3$ rearrangement and thus no conclusions can be drawn from this distribution.

(CXVI)

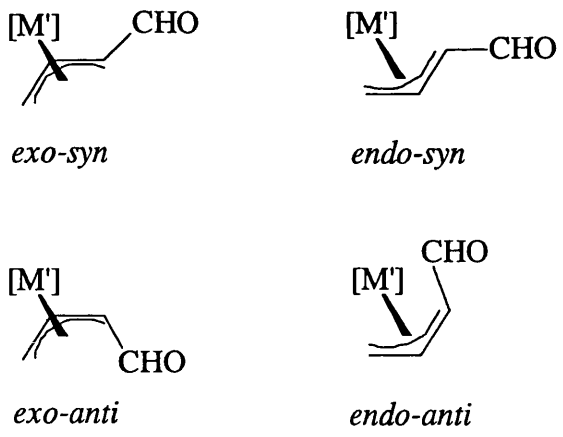

exo-syn *endo-syn*

exo-anti *endo-anti*

figure 71

Further reaction of these complexes (CXVI) with $Ph_3P{=}CH_2$ gave an η^3-pentadienyl complex with the same orientation. Investigation of the reactivity of the molybdenum oxoallyl complexes showed that it is possible to engineer some isomeric interconversion by making use of the previously noted facile rearrangement of η^4-1,3-diene complexes from the *trans-* to the *cis-* isomers (figure 72)[115]. Protonation of the *exo-syn*-oxoallyl complex (CXVI) with trifluoromethanesulphonic acid generated the *exo-s-trans*-isomer of the cationic η^4-1,3-diene complex (CXVIII), with the hydroxyl substituent observed to assume *trans* geometry. Warming of the reaction mixture to room temperature effected a transformation to the *endo-s-cis* isomer which could be used to generate the *endo-anti*-oxoallyl complex by treatment with triethylamine. In a similar manner, protonation of *endo-syn*-(CXVI) yielded the *endo-s-trans*-diene complex which in turn rearranged to the *exo-s-cis*-diene complex. Treatment with triethylamine generated *exo-anti*-(CXVI).

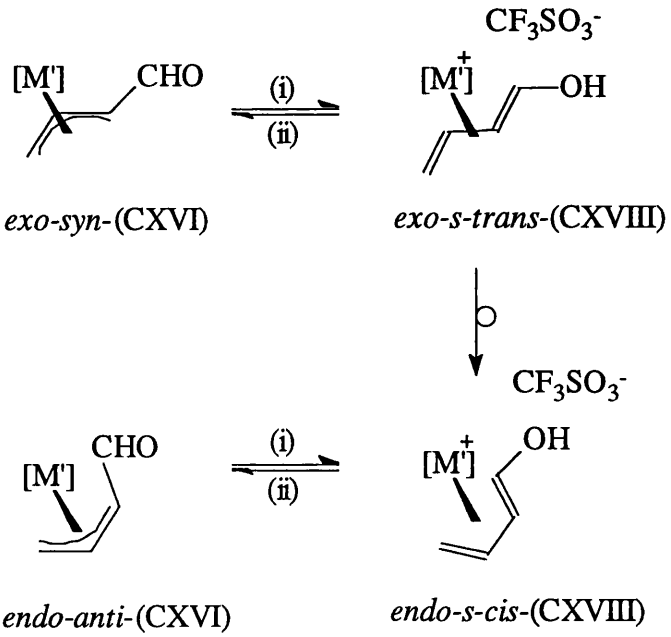

(i) CF_3SO_3H, CH_2Cl_2, -78 °C

(ii) NEt_3, CH_2Cl_2, -78 °C

[M'] = $Mo(CO)_2(\eta\text{-}C_5Me_5)$

figure 72

Subsequently this chemistry has been extended to complexes of iron[117]. The iron η^3-oxoallyl complex (CXX) was generated by protonation of $[Fe(\eta\text{-}C_5H_5)(CO)(\eta^3\text{-}C_3H_5)]$ (CXIX) in the presence of 1-trimethylsilyloxybuta-1,3-diene (figure 73). Surprisingly (CXX) was found to have exclusively the *exo-syn* geometry.

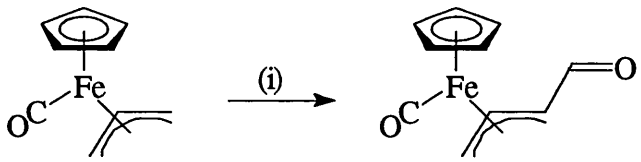

(CXIX) *exo-syn*-(CXX)

(i) $HBF_4.Et_2O$, 1-trimethylsilyloxybuta-1,3-diene

figure 73

The isolation of only the *exo-syn* isomer of (CXX) does not rule out the possibility of other isomers also being formed, it merely suggests that this isomer is the

most thermodynamically stable. Indeed, the transient cationic 1-trimethylsilyloxybuta-1,3-diene complex formed prior to desilylation must adopt a *trans* geometry in order to generate the observed isomer.

Complex (CXX) has been shown to possess reactivity similar to the molybdenum oxoallyl complexes referred to earlier[117]. For example, treatment of (CXX) with $Ph_3P{=}CH_2$ affords the *exo-syn* η^3-pentadienyl complex (CXXI) illustrated in figure 74.

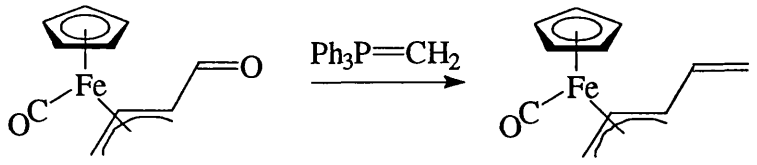

exo-syn-(CXX) *exo-syn*-(CXXI)

figure 74

Further developments of this iron chemistry are discussed in chapter 2.3.

2. Results and Discussion

The only existing things are atoms and empty space;
all else is mere opinion.

Democritus of Abdera
d *c* 370 BC

2.1 Synthesis and Reactivity of Allenylidene Complexes

In 1991 [57], S.F.T. Froom *et al* synthesised the dinuclear side bonded allenylidene complexes $[M_2\{\mu\text{-}\sigma,\eta^2\text{-}(4e)\text{-}C{=}C{=}CMe_2\}(CO)_4(L)_2]$ where L = cyclopentadienyl or pentamethylcyclopentadienyl, M = Mo or W. This was achieved by the preparation of a THF solution of $CH_2{=}C(Me)C_2Li$ by treatment of 2-methylbut-1-ene-3-yne with ^tBuLi. This was subsequently reacted with the dimers $[M_2(CO)_4(L)_2]$ to yield the lithium salts $[M_2\{\mu\text{-}\sigma,\eta^2\text{-}(3e)\text{-}C_2C(Me){=}CH_2\}(CO)_4(L)_2]Li$ from which the allenylidene complexes were then generated by protonation on addition of alumina. A study was made of the reactions of the complex containing cyclopentadienyl but not in the C_5Me_5 case.

Protonation of the cyclopentadienyl allenylidenes gave a cationic complex characterised as $[M_2(\mu\text{-}HCCCMe_2)(CO)_4(\eta\text{-}C_5H_5)_2]BF_4$ (1) for M = Mo, W, and a crystal structure was obtained for the tungsten complex. The structure showed great similarities with that of μ-alkyne complexes, with regard to both the pseudo-tetrahedral W_2C_2 core and the disposition of the other ligands about it (figure 75).

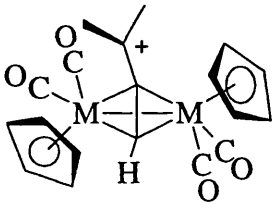

(1)

figure 75

The carbon nominally bearing the positive charge ($\underline{C}Me_2$), proved to be electrophilic in nature, as evinced by reaction with nucleophiles. Reaction of complex (1) with $K[^sBu_3BH]$ gave a mixture of the addition and elimination products $[M_2(\mu\text{-}HCC^iPr)(CO)_4(\eta\text{-}C_5H_5)_2]$ and $[M_2(\mu\text{-}HCCC(Me)CH_2)(CO)_4(\eta\text{-}C_5H_5)_2]$ respectively (figure 76).[120]

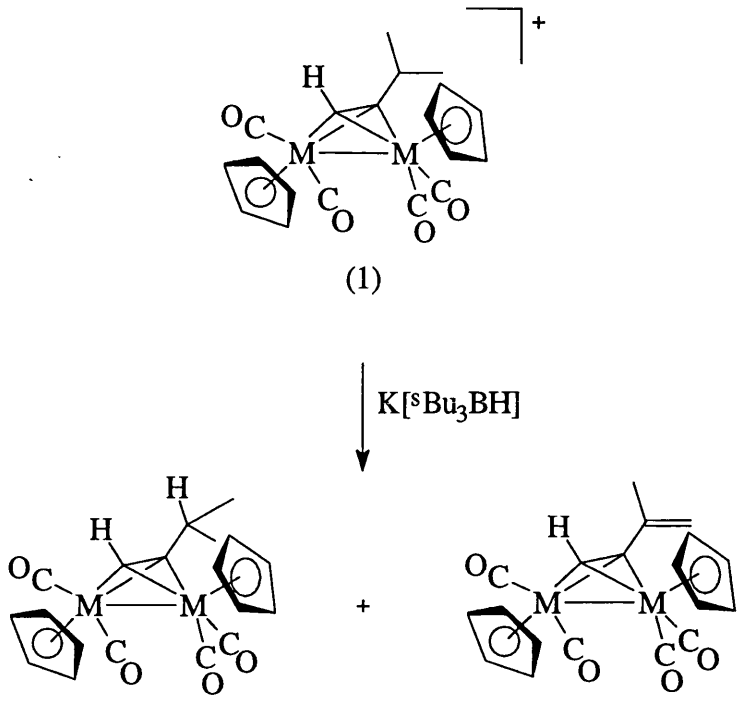

figure 76

The γ-carbon, however, despite being reactive to nucleophiles, was shown not to be particularly electron deficient by the ^{13}C n.m.r. data, in which the chemical shift for this carbon atom was 147.7 ppm for M = Mo. The C_3 plane is in fact rotated with respect to the metal-metal bond which has the effect of bringing this carbon closer to one metal than the other, although the proximity is not sufficient to suggest any significant interaction between the two. In addition the planar geometry about this atom is not disturbed as would be expected if donation from the metal was the source of the observed stabilisation. It seems, and this is supported by the X-ray data, that the positive charge is stabilised by delocalisation of electron density from the M_2C_2 core into the vacant p-orbital on the carbon. Hence in figure 77, the structure is more adequately represented by a structure which is an intermediate between the two canonical forms, I and II.

I II

figure 77

A crystal structure of a compound of similar formula but with different solid state characteristics has been synthesised by Curtis *et al* [118]. $[Mo_2(\mu\text{-}HC_2CH_2)(CO)_4(\eta\text{-}C_5H_4Me)_2][BF_4]$ (2) is significantly different only in the replacement of methyl groups for protons, yet the X-ray structure suggests that the positive charge is stabilised by a direct metal-carbon electron donation (figure 78).

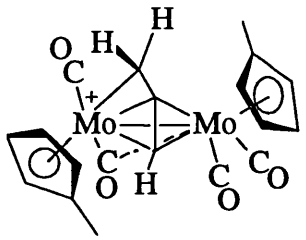

(2)

figure 78

This data shows that all three carbon atoms of the ligand are bound to Mo(1), the other metal atom being attached only to C(1) and C(2).

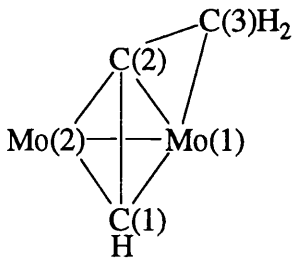

figure 78a

The ^{13}C n.m.r. data of the C_3H_3 fragment proved useful in seeking to describe the bonding mode of this complex. The chemical shifts of carbon atoms of unsubstituted π-allyl complexes generally fall in the range of δ 90-115 ppm for the central carbon and δ 40-55 ppm for the terminal carbons.[119] The chemical shifts of C(1), C(2) and C(3) are 81, 118 and 76 ppm respectively and thus bear comparison with those of π-allyl complexes. This complex, then, can be regarded as a μ-η^2,η^3-allenyl complex, in which the bonding of the fragment to Mo(1) resembles that of a π-allyl complex and the C(1)-C(2) bond is π-bonded orthogonally to Mo(2).

Both of these compounds experience exchange processes wherein the η^5-rings exchange environments as the ligand changes its orientation towards the other metal atom, although whereas the methyl groups of figure 75 exchange, the hydrogens of figure 78 do not. In both cases the high energy intermediate is symmetrical on a plane bisecting the metal-metal bond (except for the Cp' rings) with the positive charge formally centred on the β-carbon.

The difference between these two compounds can be rationalised in terms of the greater ability of the methyl groups to stabilise the positive charge on the carbon, and this theory is supported by the fact that the energy barrier for the exchange process of the structure illustrated in figure 75 ($\Delta G = 44$ kJmol^{-1}) is considerably higher than for that in figure 78 ($\Delta G = 71$ kJmol^{-1}).

In view of the numerous points of interest raised by the comparison of these two compounds, it was the logical consequence to investigate another, similar, complex in

order to extend the understanding of the electronic properties of these interesting species. $[Mo_2(\mu\text{-}HCCCMe_2)(CO)_4(\eta\text{-}C_5Me_5)_2]BF_4$ (3) was prepared by treatment of the allenylidene $[Mo_2(\mu\text{-}\sigma,\eta^2\text{-}CCCMe_2)(CO)_4(\eta\text{-}C_5Me_5)_2]$, which was generated using the same method as Froom[57], with $HBF_4.Et_2O$. The red solid was easily precipitated from dichloromethane with diethyl ether in high yield. A comparison of the three compounds under discussion here is presented in Table 1. Please refer to figure 78a and figure 79 in which C(1), (2) and (3) represent C(25), (26) and (27) respectively.

Table 1

Parameter	Compound (1)	Compound (2)	Compound (3)
^{13}C C(1) ppm	76	81	77
^{13}C C(2) ppm	105	118	104
^{13}C C(3) ppm	148	76	160
^{1}H C<u>H</u> ppm	6.29	6.76	4.63
M(1)-C(3) Å	2.84*	2.47	3.04

* The X-ray data for complex (1) is taken from the tungsten analogue[57] as the only data set available.

In the case of (3) the major difference initially observed from (1) was that the HC proton occurs at δ 4.63 ppm (as opposed to 6.29 ppm in the Cp case) and a crystal structure was obtained in order to ascertain the source of this apparent anomaly. The X-ray data (figure 79) showed that the structure is consistent with what would be expected from the earlier experiments, in terms of a Mo-Mo single bond and the pseudo-tetrahedral Mo_2C_2 core characteristic of μ-alkyne complexes. The C(3)-Mo distances, at 3.42 Å and 3.04 Å, show conclusively that there is no metal-carbon interaction as is the case in compound (2) and indicate an even smaller degree of metal-carbon interaction than in the cyclopentadienyl-tungsten complex. This is confirmed by the observation that a planar geometry is maintained about C(3), showing an absence of the "bend-back" distortion

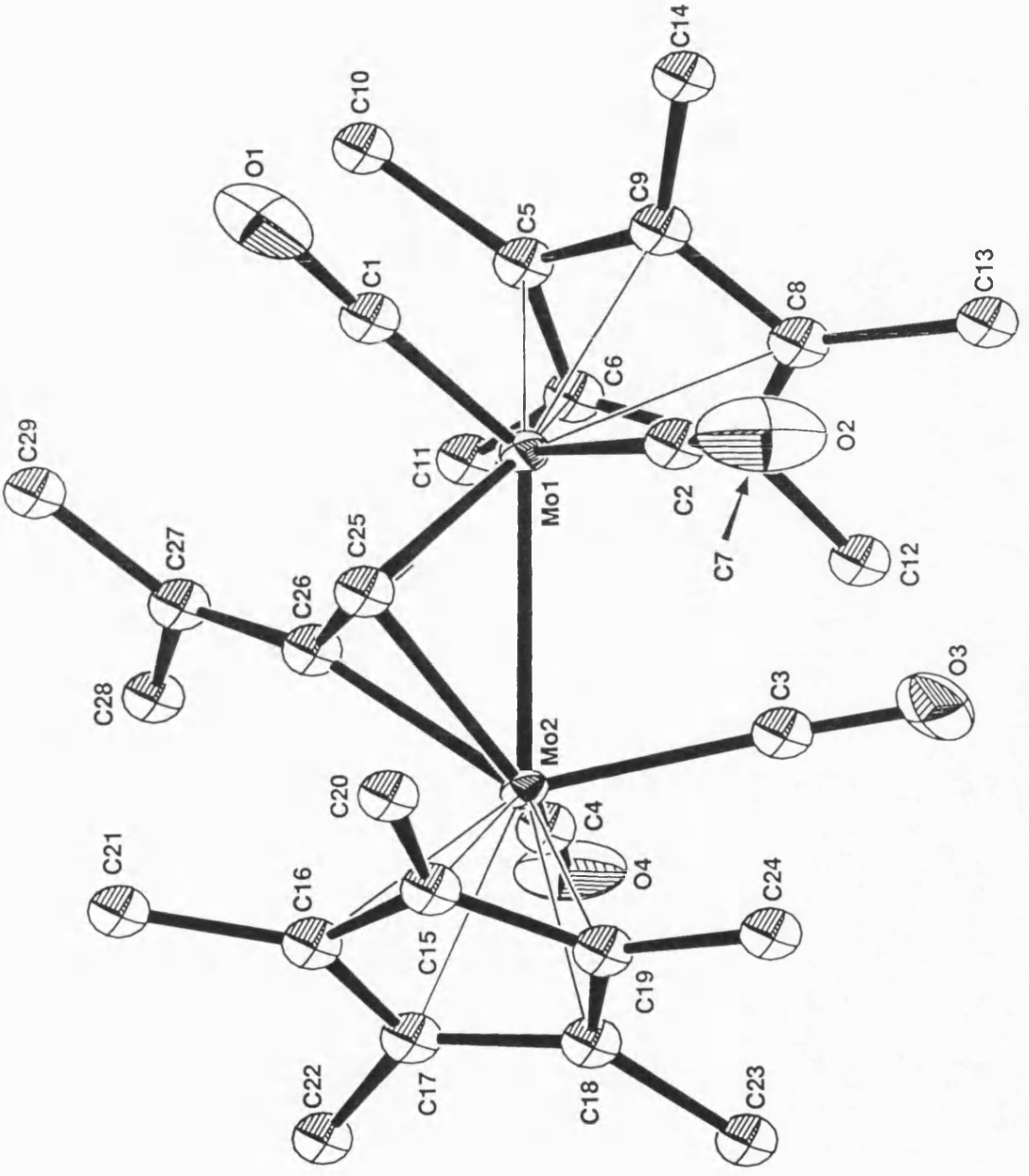

X-ray cystal structure of $[Mo_2\{\mu_2\text{-}C(H)CCMe_2\}(CO)_4(\eta\text{-}C_5Me_5)_2]BF_4$ (3)

figure 79

characteristic of such an interaction. The ^{13}C n.m.r. data for C(3) shows a chemical shift of 160.0 ppm as compared to 147.7 ppm for the complex (1). This shows again that the carbon is not particularly electron deficient, indeed that the positive charge is stabilised more than in the Cp case. The explanation for this further increase of stabilisation would seem to lie in the presence of the pentamethylcyclopentadienyl ring which has a greatly increased capacity for electron donation to the metal, enabling a further delocalisation to shift the equilibrium shown in figure 77 more to the right. The upfield shift of about 1.6 ppm exhibited by the CH proton is explained by the increased anisotropic shielding provided by the Cp* ring.

As has been previously discussed, reaction of (1) with $K[Bu^s_3BH]$ showed[120] that the γ-carbon is reactive towards nucleophiles, giving an inseparable mixture of products arising from competing deprotonation and nucleophilic addition reactions (figure 76).

It proved possible to prepare the Cp* analogues of these compounds from (3) selectively by use of a reagent which exclusively delivers a hydride ion ($[(CH_3)_2CHCH_2]_2AlH$) to give $Mo_2\{\mu_2\text{-}HCCC(H)Me_2\}(CO)_4(\eta\text{-}C_5Me_5)_2$ (4) or abstracts a proton ($(Me_3Si)_2NLi$ or 1,8-*bis*-(dimethylamino)naphthalene) to give $Mo_2\{\mu_2\text{-}HCCCH_2Me\}(CO)_4(\eta\text{-}C_5Me_5)_2$ (5) as described in figure 80. Reaction of (3) with sodium dimethyl malonate also gave the elimination product (5).

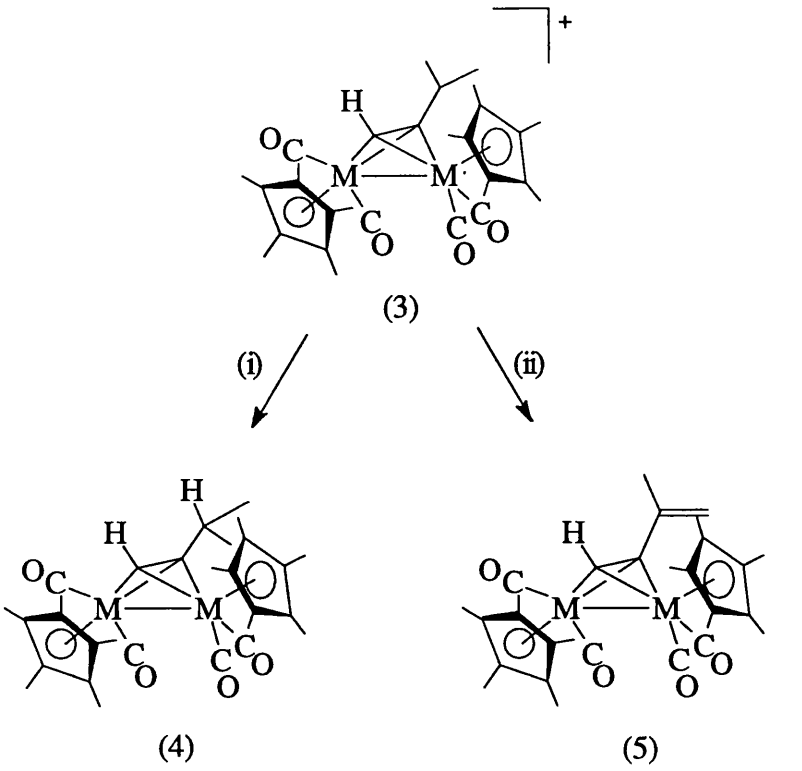

(i) $[(CH_3)_2CHCH_2]_2AlH$

(ii) $(Me_3Si)_2NLi$, proton sponge or $NaCH(CO_2Me)_2$

figure 80

Froom also treated his Cp_2Mo_2 cation (1) with EtMgBr, resulting in a mixture of three products, the two shown in figure 76 and the major product formed by addition of the ethyl group at $C\gamma$ (figure 81), the second most prominent being the elimination product.

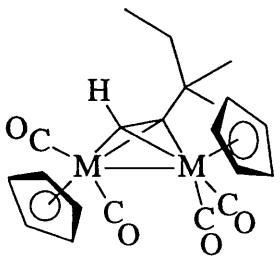

figure 81

A similar treatment of the tungsten complex resulted in the addition product of figure 81 with the addition product of figure 76 occurring only in a low proportion.

Treatment of (3) with MeMgBr did not result in a clean reaction, but on workup the only product to be isolated was the elimination product (5). No addition product was detected. Complex (3) also proved to be unreactive when stirred with the phosphines diphenylmethylphosphine or trimethylphosphine for several days. The explanation for the reluctance of (3) to react with any nucleophile larger than hydride anion seems to rest in the extreme degree of steric constraint provided by the pentamethylcyclopentadienyl ligands of the complex.

As has already been indicated, molybdenum allenylidene complexes are accessible *via* protonation of the complex $[Mo_2\{\mu\text{-}\sigma,\eta^2\text{-}(3e)\text{-}C_2C(Me)=CH_2\}(CO)_4(L)_2]Li$ where L = cyclopentadienyl or pentamethylcyclopentadienyl[57]. This reaction occurs[120] initially *via* the attack of a proton at Cβ of the acetylide complex, followed by rapid migration of the proton to the $\underline{C}H_2$ Cδ to form the allenylidene complex (figure 82).

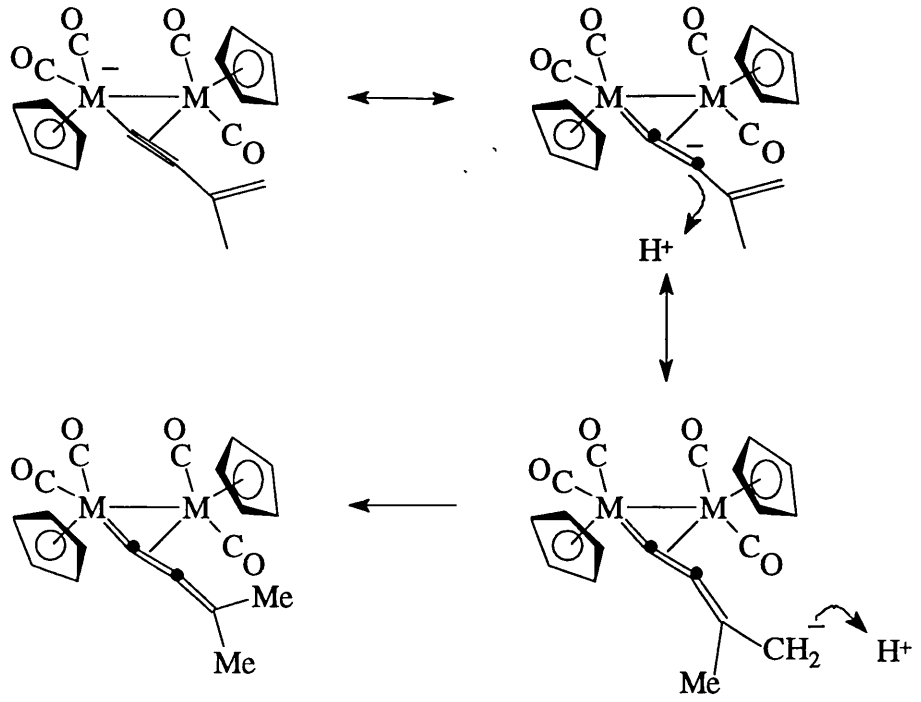

figure 82

Unfortunately, this method is not usable for preparing allenylidene complexes of the form $[M_2\{\mu\text{-}\sigma,\eta^2\text{-}(4e)\text{-}C{=}C{=}CH_2\}(CO)_4(L)_2]$, and an attempt was made to prepare them using a different method. To this end, an analogue of complex (2) was prepared, with the aim of deprotonating it in order to force rearrangement to the allenylidene (figure 83).

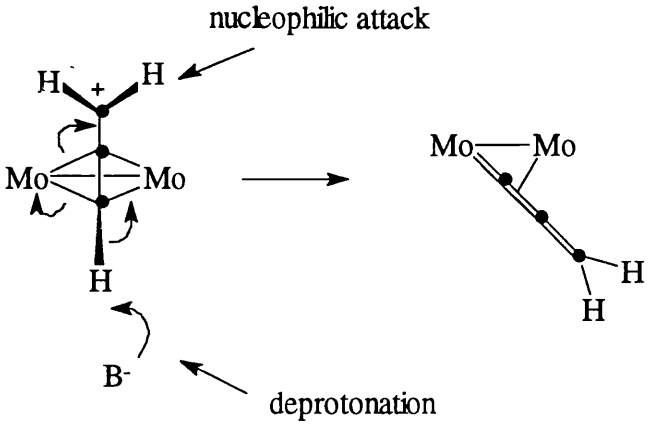

figure 83

The strategy was to use a proton selective base such as proton sponge which is able to deprotonate the complex but is unable to attack as a nucleophile, thereby avoiding a competing nucleophilic addition reaction. Removal of the acidic terminal acetylene proton would force the complex to rearrange into a allenylidene.

Two methods were used for the generation of $[Mo_2(\mu\text{-}HC_2CH_2)(CO)_4(\eta\text{-}C_5H_5)_2][BF_4]$ (7). Method A used Curtis' strategy[118] of preparing the μ-alkyne complex $[Mo_2(\mu\text{-}HCCCH_2OCH_3)(CO)_4(\eta\text{-}C_5H_5)_2]$ (6) by the reaction of propargyl methyl ether with $[Mo_2(CO)_4(\eta\text{-}C_5H_5)_2]$ and subsequently protonating it with $HBF_4.Et_2O$ in dichloromethane. Complex (7) is also accessible *via* the reaction of $[Mo_2(CO)_4(\eta\text{-}C_5H_5)_2]$ with propargyl alcohol in a similar fashion. This generated a red oil which was again protonated with $HBF_4.Et_2O$ to afford (7).

Reaction of a yellow solution of (7) in THF at -78 °C with $(Me_3Si)_2NLi$ produced an immediate colour change to dark green, a colour characteristic of all allenylidenes of the type $[M_2\{\mu\text{-}\sigma,\eta^2\text{-}(4e)\text{-}C{=}C{=}CR_2\}(CO)_4(L)_2]$ hitherto prepared. On warming above -50 °C, however, the solution changed to a dark purple colour and all attempts to isolate a product failed. A successful analysis of the green product was not obtained.

Use of the base 1,8-*bis*-(dimethylamino)naphthalene (proton sponge), which is more specific to deprotonation, gave a red oil. Protracted extraction with diethyl ether yielded a red solid which appeared to be a mixture of products. Crystallisation from CH_2Cl_2 / Et_2O yielded red crystals of the μ-alkyne complex $[Mo_2(\mu\text{-}HCCCH_2OCH_2CH_3)(CO)_4(\eta\text{-}C_5H_5)_2]$. The solid state structure of (8) was established by X-ray crystallography (figure 84).

Complex (8) is shown to a symmetrically bridged μ-acetylene complex with a pseudo-tetrahedral Mo_2C_2 core. The Mo2-C15 bond is marginally shorter than the Mo1-C15 bond, but only by 0.085 Å, which is not very significant. The Mo1-Mo2 bond length of 2.98 Å is characteristic of a Mo-Mo single bond. The cyclopentadienyl ligands occupy positions as far removed from each other as possible. The Mo1-C4 distance of 2.90 Å suggests that there is a small degree of semi-bridging character about this carbonyl ligand. The bond angles of the CH_2OEt terminal acetylide group indicate no unusual conformation about it and thus no hindrance from the rest of the molecule.

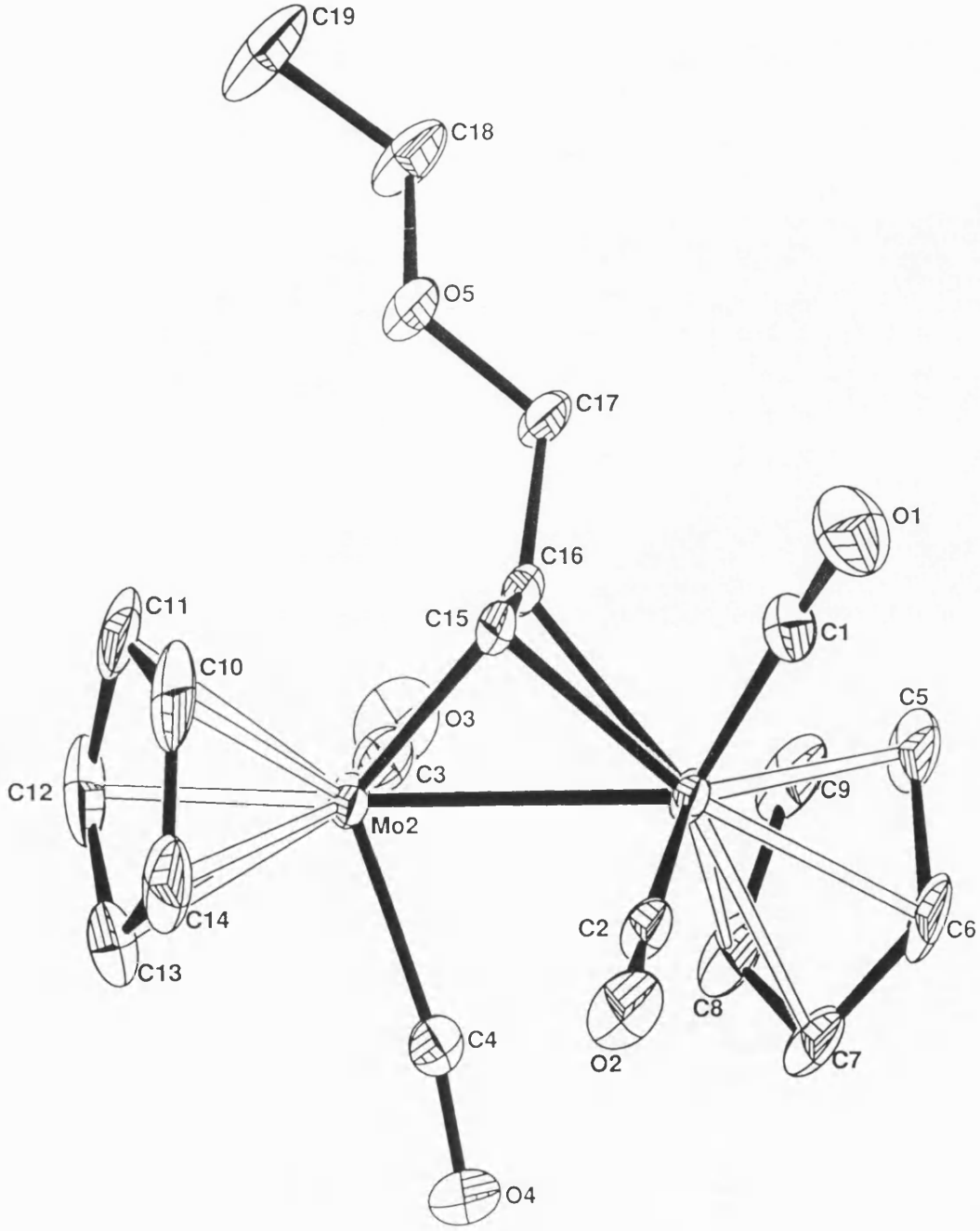

X-ray crystal structure of $[Mo_2(\mu\text{-}HCCCH_2OCH_2CH_3)\ (CO)_4(\eta\text{-}C_5H_5)_2]$ (8)

figure 84

2.2 Trimetal alkynyl complexes

The synthesis of metal cluster bound organic moieties, including acetylides[1], is well established and is pursued in the hope of gaining insight into reactions occurring at metal surfaces. The large variety of chemistry arising from the reactivity of η^2-acetylide complexes to electrophiles has already been alluded to and the use of a selection of cationic metal complexes in these reactions provides a synthetic route to trimetal alkynyl complexes containing different metal atoms.

The initial work in this area was done by A.W. Al-Saadoon *et. al.* in 1990[121], beginning with the preparation of the trimolybdenum μ-acetylide complex $[Mo_3(\mu\text{-}C{\equiv}CPh)(CO)_5(\eta\text{-}C_5H_5)_3]$. This was achieved by the treatment of a dichloromethane solution of $Li[Mo_2(\mu\text{-}C{\equiv}CPh)(CO)_4(\eta\text{-}C_5H_5)_2]$ with $[Mo(NCMe)_2(CO)_2(\eta\text{-}C_5H_5)]BF_4$ at room temperature (figure 85) and the solid state structure was obtained by X-ray crystallography.

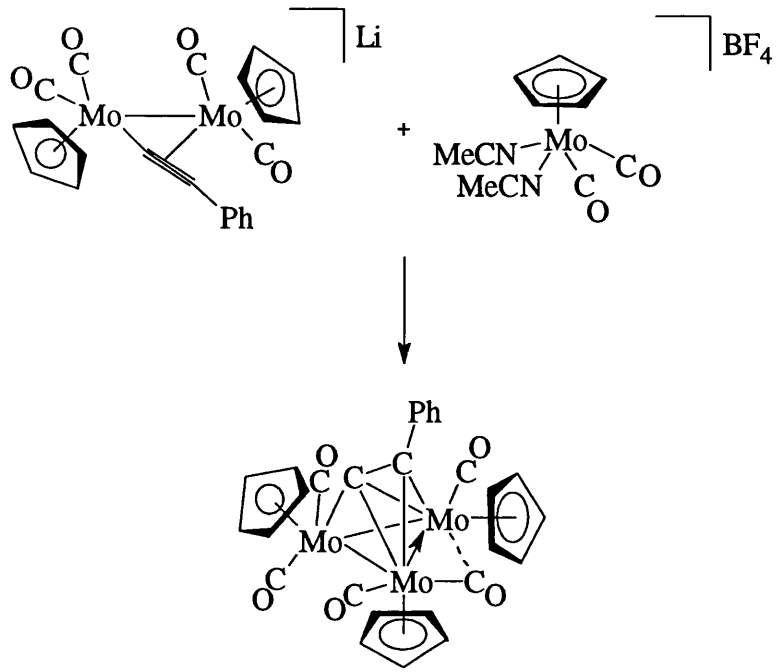

figure 85

The molecule is a 48 electron cluster, with three cyclopentadienyl ligands and five carbonyl ligands, one of which is semi-bridging. Electron counting at the three molybdenum atoms reveals that one is electron deficient, one is coordinatively saturated and one has one electron too many, hence the formal donor bond shown between two Mo atoms in figure 85. The α-carbon of the acetylide ligand, which resonates at δ 178.5 ppm in the ^{13}C n.m.r. spectrum, symmetrically bridges the metal triangle, whereas the β-carbon, which bridges the two formally non-saturated metal atoms and occurs at δ 116.9 ppm, is tilted slightly towards the formally electron deficient molybdenum (bond length 2.165 Å as opposed to 2.343 Å). As the α-carbon adopts a symmetrical bridging mode, the structure can be considered as a Mo_3C tetrahedron face-capped by CPh. In solution this complex shows dynamic behaviour at room temperature and the variable temperature n.m.r. data suggests that there is a synchronous rotation of the acetylide fragment, carbonyls and metal-metal donor bond around the Mo_3 triangle, leading to equivalence of all three Mo atoms.

In the same paper, Al-Saadoon *et al* also briefly reported the preparation of the Mo_2Rh and Mo_2Ru clusters $[Mo_2Rh(\mu\text{-}C{\equiv}CPh)(CO)_4(\eta\text{-}C_5H_5)_2L_2]$ where L = CO or L_2 = norbornadiene and $[Mo_2Ru(\mu\text{-}C{\equiv}C^tBu)(CO)_4(\eta\text{-}C_5H_5)_3]$ which were believed to adopt a similar configuration to the trimolybdenum cluster. The properties of these complexes and their analogues are discussed later in this section.

In the light of these results it was decided to expand this area into complexes involving other metals and undertake a deeper study into the properties of these heterometallic acetylide cluster complexes.

As an aside to this discussion, an interesting discovery was made during preparation of starting materials for this series of investigations. While preparing the rhodium complex $[Rh(NCMe)_2(norbornadiene)]BF_4$ (6) by using a method based on that in the literature[122], it was observed that a subtle difference in the method of preparation

resulted in the wholly unexpected formation of the monoacetonitrile rhodium cation [Rh(NCMe)(norbornadiene)]BF_4 (7). Reaction of [Rh(norbornadiene)Cl]$_2$ with $AgBF_4$ in acetonitrile afforded a yellow solution and a precipitate of AgCl. The silver chloride was filtered off and the product obtained thereafter was dependant on the final workup. Reduction of the solution to minimum volume *in vacuo* followed by addition of diethyl ether resulted in the precipitation of the intended product, the *bis*-acetonitrile rhodium cation [Rh(NCMe)$_2$(norbornadiene)]BF_4. If all the acetonitrile solvent was removed before washing with diethyl ether, however, the product, a yellow solid identical in appearance to (6), was shown by n.m.r. spectroscopy to contain only one acetonitrile ligand. Microanalysis confirmed the product as [Rh(NCMe)(norbornadiene)]BF_4 (7). This result presented two intriguing possibilities, either that the acetonitrile ligand is η^2-bonded and donates four electrons, or that it donates two electrons and is either η^1- or η^2-bonding, which results in an unusual formally 14-electron rhodium system.

Very few η^2-nitrile complexes have been characterised and of these in even fewer can the ligand be considered as a four electron donor.[123, 138] An example of this is the preparation by Harman *et al* of the 16 electron species [W(bpy)(PMe_3)$_2$Cl(η^2-NCMe)]PF_6.[124] This complex was identified as containing a 4-electron donating acetonitrile ligand on the basis of a ^{13}C chemical shift of 235 ppm. This is consistent with the conclusions of Templeton *et al*[125] regarding ^{13}C chemical shifts in η^2-coordinated alkyne complexes. They reported a correlation between the alkyne ^{13}C chemical shift and the effective number of electrons donated by the alkyne to the metal, in that four-electron donors show ^{13}C shifts generally in the region of 190-250 ppm whereas the resonances for two-electron donors occur from 100-120 ppm. Comparison with the chemical shifts for uncoordinated nitriles (~110 ppm) and alkynes (70-90 ppm) supports Harman's analysis that a shift of 235 ppm is indicative of a four-electron donating ligand.

In the case of [Rh(NCMe)(norbornadiene)]BF_4 (7) the ^{13}C chemical shift of the nitrile carbon occurs at 124.0 ppm, which rules out the possibility of a four-electron

donating acetonitrile ligand. Indeed, a further comparison with η^2-4e-alkyne metal complexes shows that the presence of a similar ligand in a rhodium complex is extremely unlikely, as known examples of such ligands are confined almost exclusively to d^4 metal complexes.[126] There is no reason to suppose that the acetonitrile ligand has adopted an η^2-bonding mode, which is not usually preferred, leading to the conclusion that, assuming that the tetrafluoroborate counterion is innocent, complex (7) is a 14-electron rhodium cation with a very open configuration (figure 86).

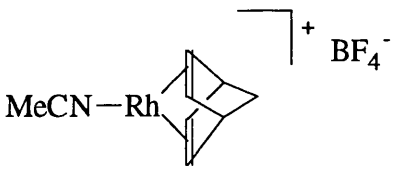

(7)

figure 86

An electron deficient complex with such an open configuration, however, would not be expected to be particularly stable, but (7) is stable for an hour in air and at least a year under nitrogen. This suggests that the anion is not merely a spectator but is bound in some way to the rhodium centre. A weakly bound BF_4 ligand could account for the observation that addition of ether allows a second acetonitrile to bind to the metal, by displacing the counterion. Many coordinating complexes of so-called non-coordinating anions and, in particular of BF_4^-, have been known for several years[127, 128], and an investigation was pursued into fluorine-bridged SbF_4^-, PF_6^- and BF_4^- adducts of tungsten in 1989 [129] which included X-ray crystal structures of all of these. Of particular interest are the ^{19}F n.m.r. data that they obtained for the BF_4^- adduct $[W(CO)_3(PMe_3)(NO)(FBF_3)]$. At low temperature (185 K) the BF_3 fluorine atoms appeared at -153 ppm and the W-F-B fluorine at -240 ppm with attendant couplings due to fluorine and boron. The ^{19}F n.m.r. data for complex (7) in CD_2Cl_2, however, shows

only two peaks at 153.07 and 153.12 ppm in a 1:4 ratio. This is indicative of a free BF_4^- ion, the two peaks reflecting the proportion of the two naturally occurring isotopes of boron in the isotopomers $^{10}BF_4^-$ and $^{11}BF_4^-$. If there is any interaction here it is so weak that it is disrupted by dissolution in CH_2Cl_2 and as the complex does not dissolve in non-donor solvents this is a moot point. The conclusion to be drawn from these data, therefore, is that complex (7) is indeed a very unusual example of a stable 14-electron rhodium complex.

The Mo_2Rh complex prepared by A.W. Al-Saadoon *et al*[121] was taken as a starting point for the extension of this chemistry. The *tert*-butyl acetylide analogue $[Mo_2Rh(\mu\text{-}C{\equiv}C^tBu)(CO)_4(\eta\text{-}C_5H_5)_2(nbd)]$ where nbd = norbornadiene was prepared by a similar method and the investigation was extended down the triad by the preparation of the Mo_2Ir complexes $[Mo_2(\mu\text{-}C{\equiv}CR)(CO)_4(\eta\text{-}C_5H_5)_2(COD)]$ where R = ^{t}Bu, Ph and COD = cyclo-octa-1,5-diene. All of these complexes were prepared using a similar method. The acetylides $LiC{\equiv}CR$ were prepared by the addition of ^{t}BuLi to $HC{\equiv}CR$ in THF at -78 °C. These were treated with the triply bonded molybdenum dimer $[Mo_2(CO)_4(\eta\text{-}C_5H_5)_2]$ and the solution was allowed to warm to ambient temperature to generate the appropriate lithium acetylide complex $Li[Mo_2(\mu\text{-}C{\equiv}CR)(CO)_4(\eta\text{-}C_5H_5)_2]$. To this complex was added a cationic metal complex $[M(NCMe)_2(L)]BF_4$ ((9) M = Rh, L = nbd; (15) M = Ir, L = COD) and the solution darkened to brown. Use of $[Rh(NCMe)(norbornadiene)]BF_4$ (10) results in the same product as (9). After several hours of reaction, chromatography afforded dark red or brown micro-crystals of $[Mo_2M(\mu\text{-}C{\equiv}CR)(CO)_4(L)(\eta\text{-}C_5H_5)_2]$ (11, 13, 16, 18). Complexes (11) and (13), $[Mo_2Rh(\mu\text{-}C{\equiv}CR)(CO)_4(\eta\text{-}C_5H_5)_2(nbd)]$, reacted readily with carbon monoxide in dichloromethane in one hour to induce a facile replacement of the norbornadiene ligand with two carbonyls, yielding complexes (12) and (14) $[Mo_2Rh(\mu\text{-}C{\equiv}CR)(CO)_6(\eta\text{-}C_5H_5)_2]$. A similar replacement of the cyclo-octadiene ligand for two carbonyls is possible for the Mo_2Ir

complexes (16) and (18) to produce complexes (17) and (19), $[Mo_2Ir(\mu\text{-}C{\equiv}CR)(CO)_6(\eta\text{-}C_5H_5)_2]$. These complexes (12, 14, 17, 19) all have a dark red or brown colour and the reactions leading to their formation are summarised in figure 87.

In addition the Mo_2Ru cluster $[Mo_2Ru(\mu\text{-}C{\equiv}CPh)(CO)_4(\eta\text{-}C_5H_5)_3]$ (25) was prepared by treatment of $Li[Mo_2(\mu\text{-}C{\equiv}CPh)(CO)_4(\eta\text{-}C_5H_5)_2]$ with $[Ru(CO)(NCMe)_2(\eta\text{-}C_5H_5)]BF_4$ in a similar manner and the Mo_2Mn clusters $[Mo_2Mn(\mu\text{-}C{\equiv}CR)(CO)_7(\eta\text{-}C_5H_5)_2]$ ((23) R = Ph, (24) R = ^{t}Bu) by reaction of $Li[Mo_2(\mu\text{-}C{\equiv}CR)(CO)_4(\eta\text{-}C_5H_5)_2]$ with the cationic complexes $[Mn(CO)_3(NCMe)_3]BF_4$ and $[Mn(CO)_3(NCMe)_3]ClO_4$ respectively.

Finally the pentamethylcyclopentadienyl analogues of complexes (11) and (13), $[Mo_2Rh(\mu\text{-}C{\equiv}CR)(CO)_4(\eta\text{-}C_5Me_5)_2(nbd)]$ (complex (20) R = Ph, complex (21) R = ^{t}Bu) were prepared by the reaction of $[Rh(NCMe)_2(nbd)]BF_4$] (9) with $Li[Mo_2(\mu\text{-}C{\equiv}CR)(CO)_4(\eta\text{-}C_5Me_5)_2]$, which was in turn prepared by the reaction of the triply-bonded molybdenum dimer $[Mo_2(CO)_4(\eta\text{-}C_5Me_5)_2]$ with the acetylides $LiC{\equiv}CR$.

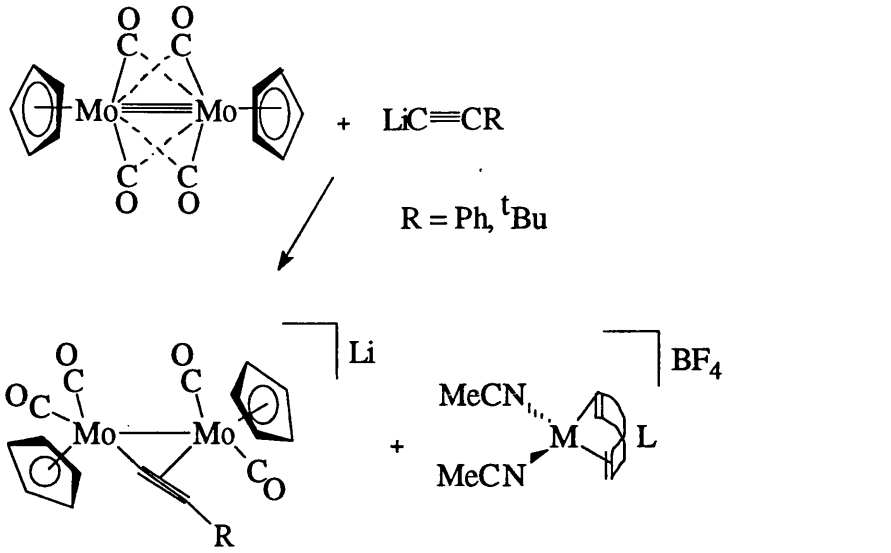

(9), M = Rh, L = norbornadiene
(15), M = Ir, L = cyclo-octa-1,5-diene

$[MoM(\mu\text{-}CCR)(CO)_4(\eta\text{-}C_5H_5)_2L]$

(11), M = Rh, L = norbornadiene, R = Ph
(13), M = Rh, L = norbornadiene, R = ^{t}Bu
(16), M = Ir, L = cyclo-octa-1,5-diene, R = Ph
(18), M = Ir, L = cyclo-octa-1,5-diene, R = ^{t}Bu

$[MoM(\mu\text{-}CCR)(CO)_6(\eta\text{-}C_5H_5)_2]$

(12), M = Rh, R = Ph
(14), M = Rh, R = ^{t}Bu
(17), M = Ir, R = Ph
(19), M = Ir, R = ^{t}Bu

figure 87

A preliminary examination of the n.m.r. data of this range of complexes revealed that they undergo a range of dynamic processes. Most of the data obtained was consistent with the assumption that these complexes adopt a similar structure to $[Mo_3(\mu\text{-}C{\equiv}CPh)(CO)_5(\eta\text{-}C_5H_5)_3]$ (figure 85), but one apparent anomaly was noted (figure 88).

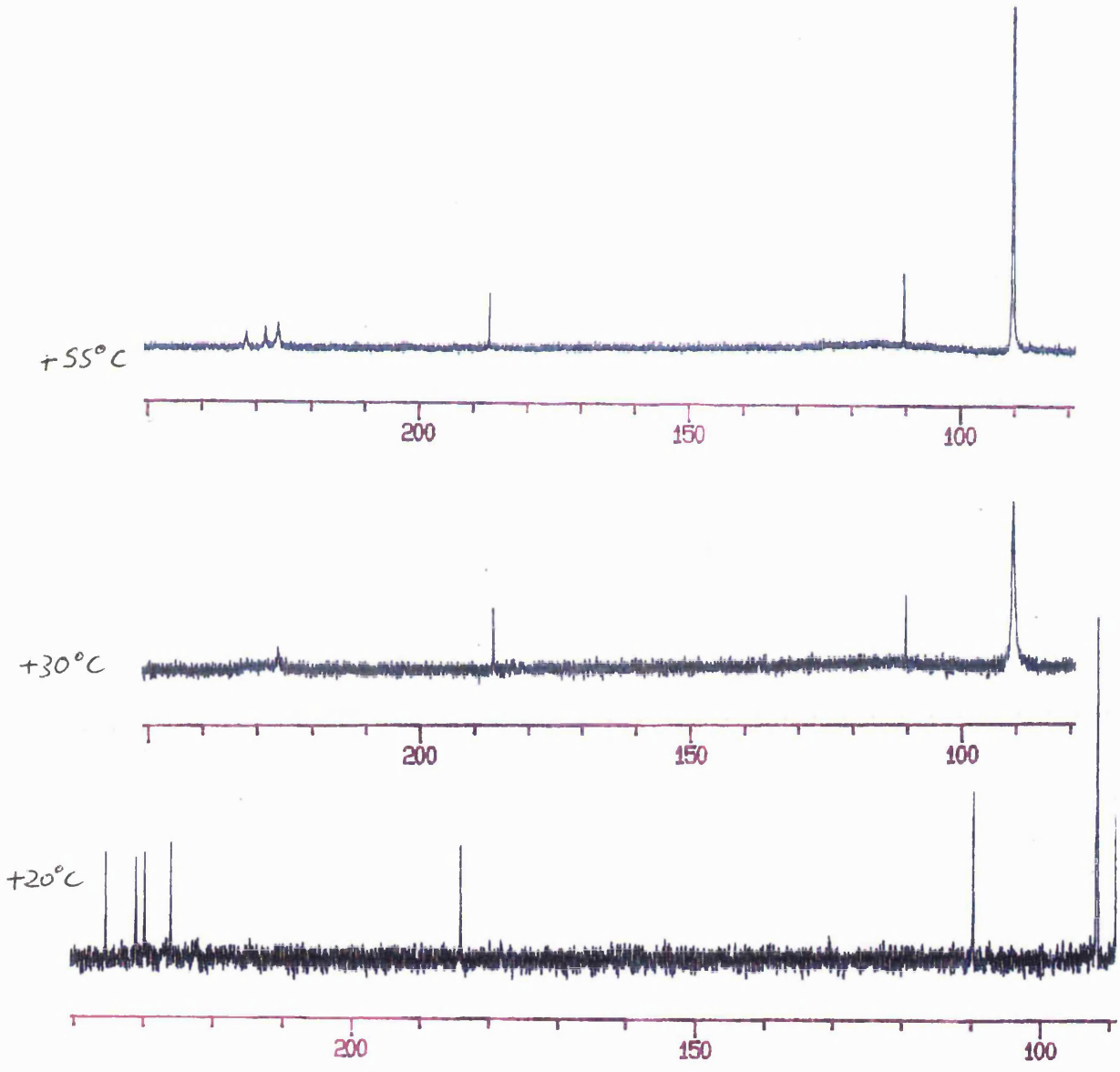

^{13}C n.m.r. spectrum of $[Mo_2Mn(\mu\text{-}C{\equiv}C^tBu)(CO)_7(\eta\text{-}C_5H_5)_2]$ (24)

figure 88

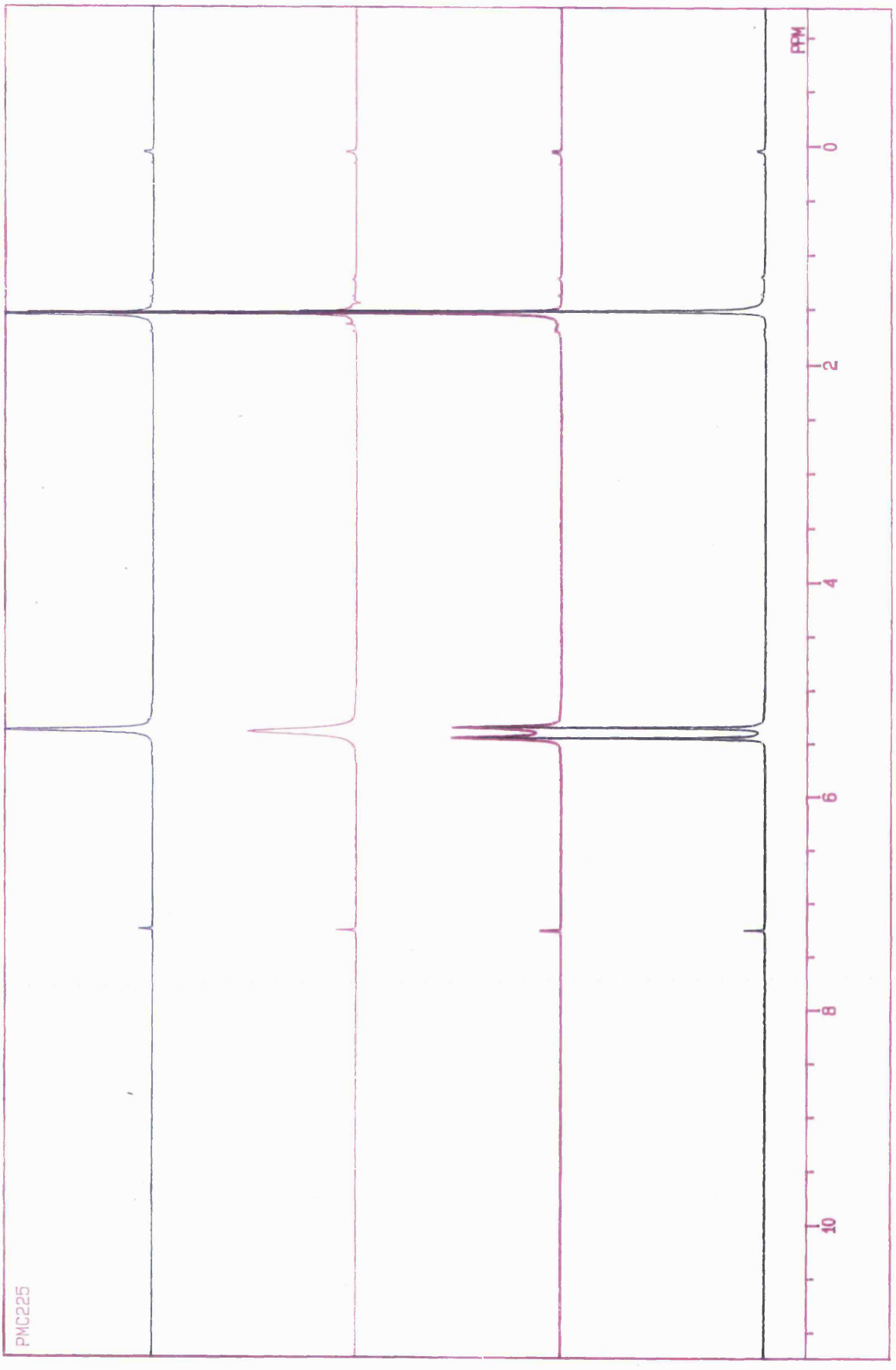

^{1}H n.m.r. spectrum of $[Mo_2Mn(\mu\text{-}C{\equiv}C^tBu)(CO)_7(\eta\text{-}C_5H_5)_2]$ (24)

figure 88a

A variable temperature ^{13}C n.m.r. study of complex (24) revealed details of the exchange processes involving the cyclopentadienyl and carbonyl ligands. At 20 °C the ^{13}C n.m.r. spectrum showed four carbonyl signals and two Cp signals. If the temperature is increased to 30 °C only one carbonyl peak and one Cp peak, both broad singlets, can be seen. On further warming to 55 °C, the Cp signal becomes a sharp singlet and three sharp carbonyl peaks can be observed.

At 20 °C, therefore, the exchanges taking place are such that four CO environments can be observed and no Cp exchange takes place. At 55 °C further processes occur in which the Cp ligands become equivalent and three CO environments are observed. The coalescence of signals for both Cp and CO occurs at 30 °C and so the two processes are synchronous. This information is very difficult to reconcile with the concept of a closed structure based around a metal triangle similar to the one established for $[Mo_3(\mu\text{-}C{\equiv}CPh)(CO)_5(\eta\text{-}C_5H_5)_3]$. Figure 89 shows such a structure for complex (24), with three possible CO environments labelled.

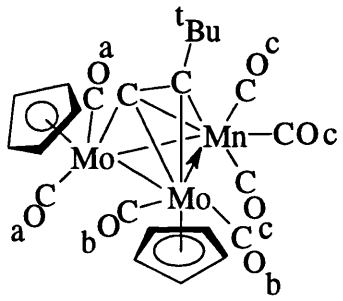

figure 89

The high temperature n.m.r. data, in which three CO environments are observed and the cyclopentadienyl rings are equivalent, is consistent with the structure shown above. At low temperature, however, there is no Cp exchange and four carbonyl environments are extant. It is extremely unlikely that both CO_a ligands are equivalent and the CO_b ligands are not, or vice versa, so the CO_c ligands would have to have two

environments. One would expect the exchange of carbonyl ligands about the Mn atom to be relatively facile, and there is no reason why this process would have to be synchronous with equivalence of the C_5 rings. While the closed structure shown in figure 89 is possible, therefore, the evidence for it is not compelling and the data suggests that a different structure is likely.

In the light of this information a study was undertaken to establish the solid state structures of $[Mo_2Mn(\mu\text{-}C{\equiv}C^tBu)(CO)_7(\eta\text{-}C_5H_5)_2]$ (24) and $[Mo_2Rh(\mu\text{-}C{\equiv}CPh)(CO)_6(\eta\text{-}C_5H_5)_2]$ (12). The crystal structures proved that the complexes were not based around a metal triangle, but possessed an open structure in which only two of the metals, Mo-Rh or Mo-Mn, are bonded together (figures 90 and 94 respectively). Both complexes adopt a μ-acetylene-type structure, with a $MoMC_2$ pseudo-tetrahedral core, in which one end of the acetylene is occupied by the R group (Ph or ^{t}Bu) and the other by a $Mo(CO)_2(\eta\text{-}C_5H_5)_2$ fragment. Comparison of the n.m.r. data of these two complexes suggested that the major dynamic exchange processes operate at a higher rate for complex (24) than for complex (12).

In the case of complex (12) the Mo2-Mo1 (3.214 Å) and Mo2-Rh1 (3.237 Å) distances are greater than would be expected for a metal-metal single bond, proving that there is no interaction between them. By comparison the Mo1-Rh1 bond length is 2.687 Å. The phenyl terminal acetylene group is "bent back" away from the Mo1-Rh1 axis (C17-C18-C19 = 138.3 °) and the $Mo(CO)_2(\eta\text{-}C_5H_5)_2$ moiety (C18-C17-Mo2 = 165.4 °) deviates only 15 ° from the C17-C18 axis and is tilted towards the Mo1-Rh1 axis. The C17 atom of the acetylide ligand is almost equidistant from Mo1 and Rh1 (Mo1-C17 = 2.235 Å, Rh1-C17 = 2.281 Å) with a slight inclination towards the rhodium atom, although the fact that Rh-C single bonds are generally shorter than Rh-Mo bonds reduces further the significance of this C-Rh proximity, and the β-carbon, C18, is significantly closer to the rhodium atom (Mo1-C18 = 2.306 Å, Rh1-18 = 2.132 Å), thus the acetylide ligand is inclined towards Rh1.

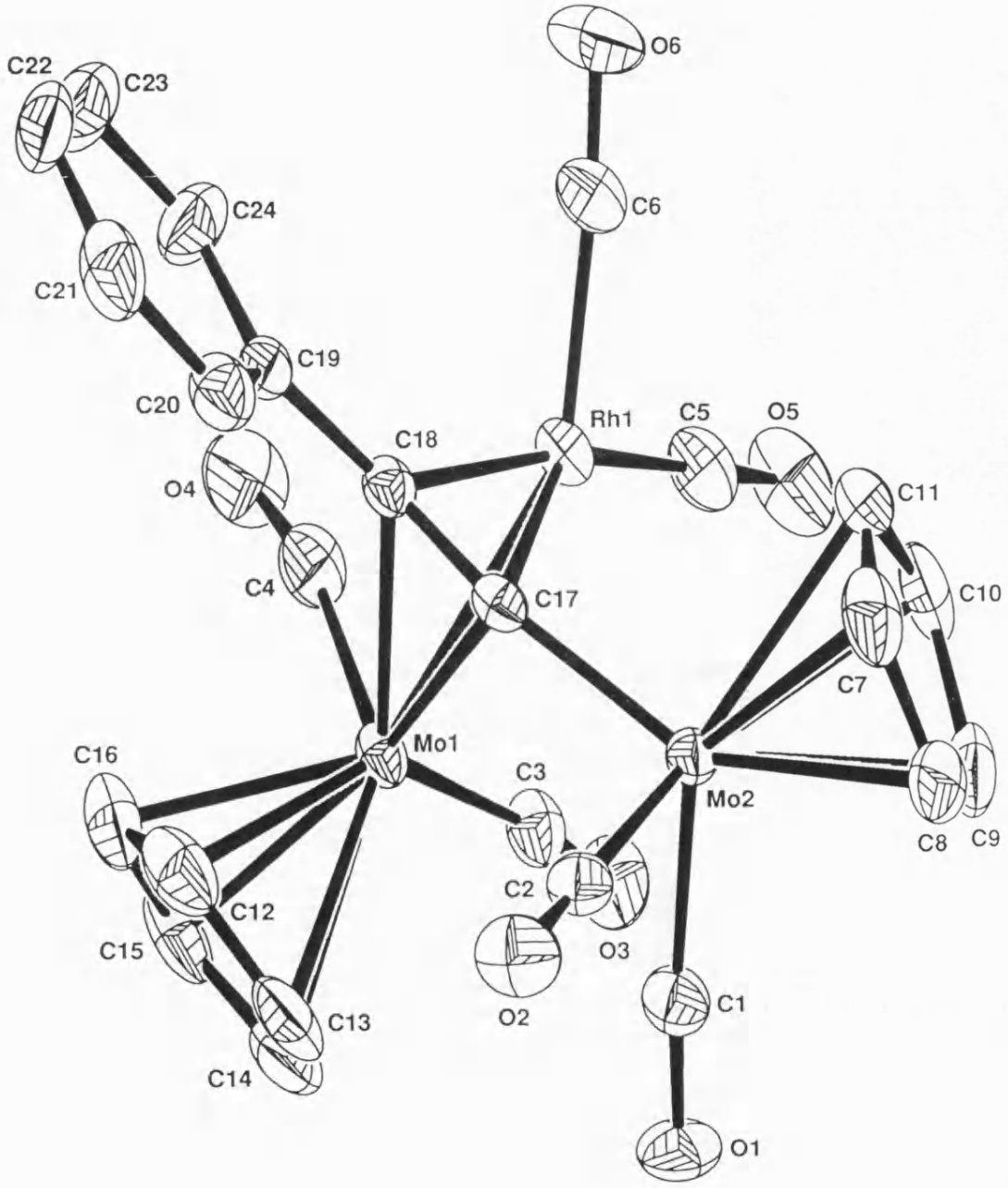

X-ray crystal structure of $[Mo_2Rh(\mu\text{-}C{\equiv}CPh)(CO)_6(\eta\text{-}C_5H_5)_2]$ (12)

figure 90

The Mo1-C_5H_5 axis is almost parallel to the Mo1-Rh1 bond and is inclined away from the Mo2 fragment and toward the Ph group by approximately 10 °. A smaller deviation away from the C_2 acetylene moiety can also be observed. The C_5 ring bonded to Mo_2 is directed towards Rh1 and away from Mo1 as evinced by the intramolecular distance C5...H101 (2.76 Å). Correspondingly the less bulky Mo2 carbonyls are closer to Mo1 than Rh1. This is clearly a consequence of the more sterically demanding cyclopentadienyl ligands settling as far apart as possible.

Electron counting reveals that Rh1 formally has 16 electrons, the molybdenum atom bonded to it, Mo1, has 18 electrons and Mo2 has 16 electrons. This is a remarkable observation. Adoption of the closed structure similar to that shown for [Mo_3(μ-C≡CPh)$(CO)_5$(η-C_5H_5)$_3$] in figure 85 would enable all three metal atoms to exist as 18 electron centres, instead, the open structure is preferred in spite of the fact that two of the three metal atoms are electron deficient.

Examination of the molecular structure of (12) reveals no planes or axes of symmetry and thus it is chiral, existing as a racemic mixture of the two enantiomers illustrated in figure 91 (in which the carbonyl groups are omitted for greater clarity).

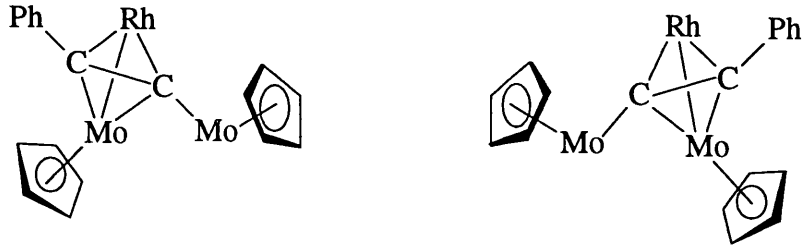

figure 91

The n.m.r. data suggest the existence of an exchange process in which the two cyclopentadienyl ligands and thus also the two molybdenum atoms become equivalent. An intermediate for this process must be equally likely to rearrange into either enantiomer, so, even if a means were devised to selectively prepare one enantiomer of this complex, a

racemic mixture would result unless the temperature were to be kept below the threshold at which the exchange process occurs. For this intermediate to exist the molecule must assume a conformation which possesses a plane of symmetry which also enables the electronic environments of the Mo atoms to be identical. The structure previously obtained for $[Mo_3(\mu\text{-}C{\equiv}CPh)(CO)_5(\eta\text{-}C_5H_5)_3]$ serves as an example for a possible closed structure for this intermediate. This implies that the exchange process which equivalences the cyclopentadienyl environments of (12) is accompanied by an opening and closing of the metal triangle and this is illustrated for both enantiomers in figure 92.

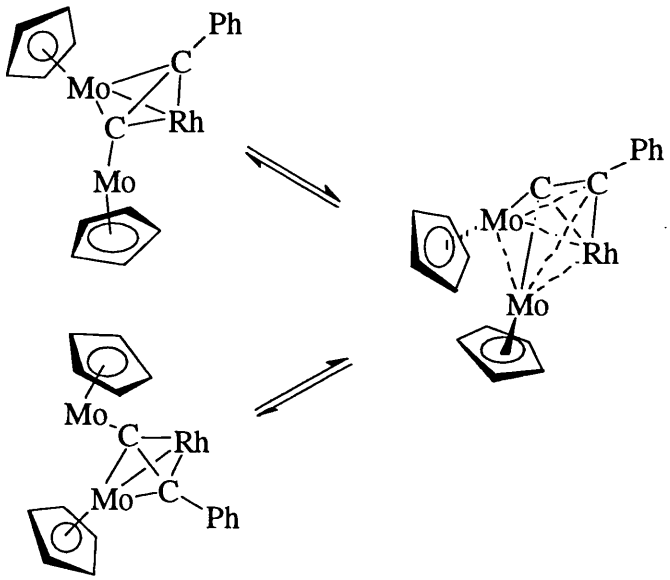

figure 92

During the process in which the two enantiomers interchange the Rh1-C18 bond can be said to be making a "windscreen wiper" type motion in which the bond moves from side to side across the molecule, with C18 describing a longer arc than Rh1. This is likely to be accompanied by an inward movement of the molybdenum atoms resulting in increased closure of the structure to a metal triangle based intermediate, which reduces hindrance to the movement of the Rh-Cβ bond. The intermediate formed at the mid-point of this movement possesses a plane of symmetry and fulfils the conditions set out above

for the equivalence of the Mo-Cp moieties. Figure 93 shows a plan view of this structure which illustrates the point.

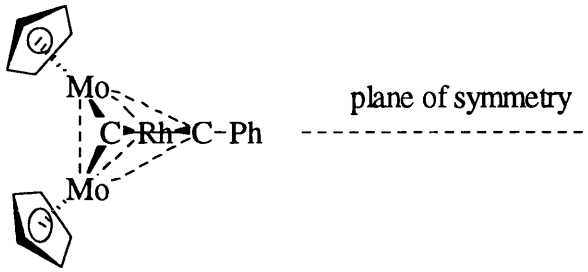

figure 93

Viewed from this perspective, the rhodium atom is directly beneath the C-C bond. The inward movement of the Mo atoms to facilitate the transfer of the C-C-R moiety to the other side of the rhodium atom is accompanied by synchronous movement of the cyclopentadienyl ligands to adopt the conformation shown. The inclination of Mo2 downwards rather than "bending back" in the solid state structure also supports the supposition of a tendency to the formation of a metal triangle.

The diagrams in figures 91-93 have had the carbonyl ligands omitted for clarity and to investigate the fluxional processes in which they are involved, it is necessary to refer to the solid state structure and variable temperature n.m.r. studies of complex (24), $[Mo_2Mn(\mu\text{-}C{\equiv}C^tBu)(CO)_7(\eta\text{-}C_5H_5)_2]$ (figures 94 and 88).

The structure of complex (24) (figure 94) is similar to that of complex (12) in that it has an open configuration. The Mo2-Mo1 distance is 3.113 Å and the Mo2-Mn1 distance is 2.940 Å as compared to 2.795 Å for Mo1-Mn1. While there is thus no Mo-Mo bond, the disparity in Mn-Mo distances is much lower than in the $RhMo_2$ complex, indicating that the $MnMo_2$ complex is much closer to having a closed configuration than the $RhMo_2$ complex. Assuming a closed intermediate, this is consistent with the greater ease of exchange at room temperature exhibited by this complex in the ^1H n.m.r. data comparison with complex (12).

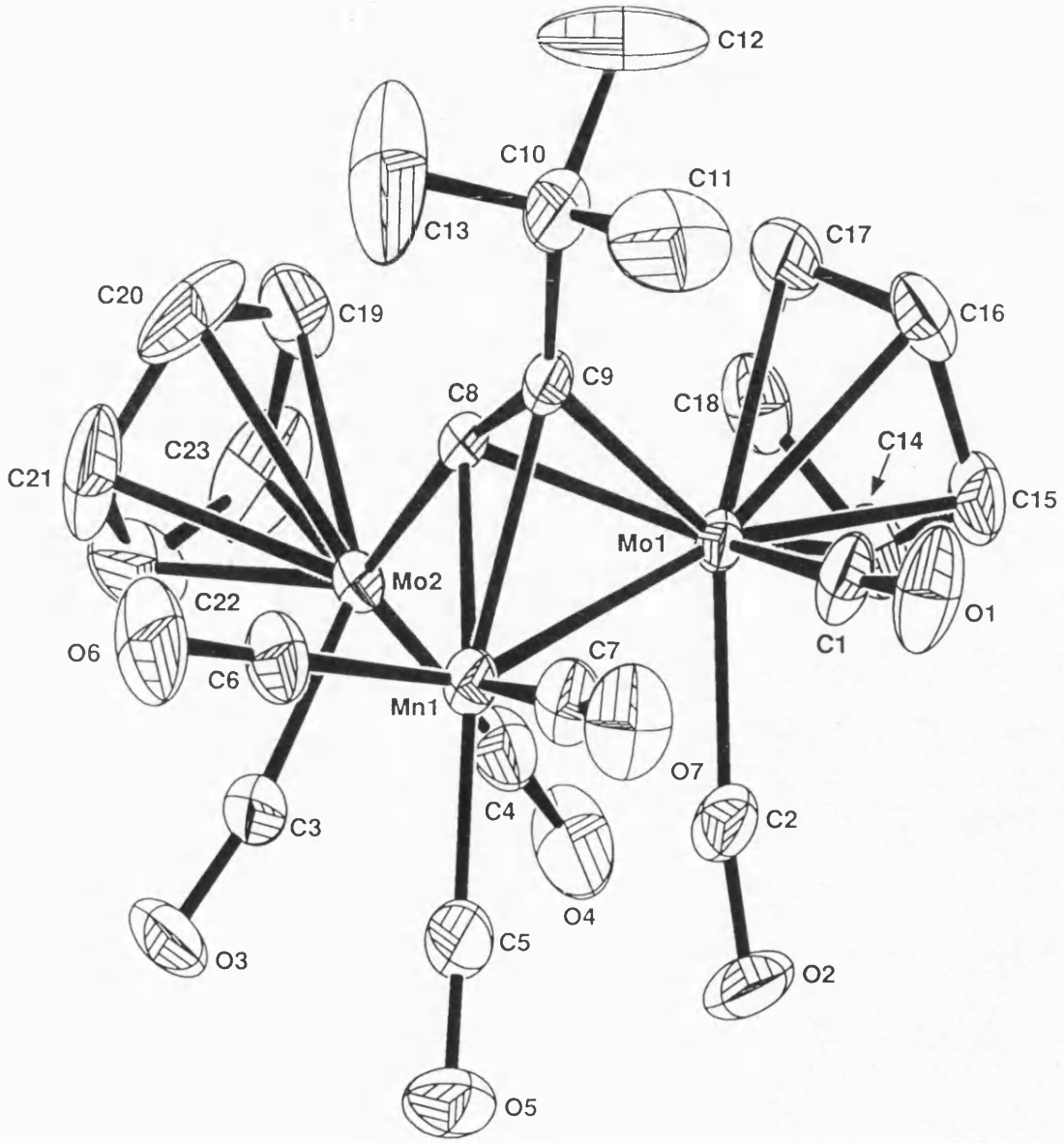

X-ray crystal structure of $[Mo_2Mn(\mu\text{-}C{\equiv}C^tBu)(CO)_7(\eta\text{-}C_5H_5)_2]$ (24)

figure 94

Again as in complex (12), the *tert*-butyl acetylide ligand is "bent back" away from the Mo1-Mn1 axis, the bond angle C8-C9-C10 being 139.4 °, similar to the corresponding effect in complex (12). The $Mo(CO)_2(\eta\text{-}C_5H_5)_2$ moiety is again bent in the opposite direction towards the other metal atoms, in this case by 12 ° from the C8-C9 axis (C9-C8-Mo2 = 168.4 °). In this case both the α-carbon and the β-carbon of the acetylide ligand are closer to the manganese atom than the molybdenum (Mn1-C8 = 2.054 Å, Mo1-C8 = 2.233 Å, Mn1-C9 = 2.175 Å, Mo1-C9 = 2.330 Å) and so the acetylide ligand is more skewed towards the "third metal" than in complex (12). Again this is consistent with a closer resemblance to the closed intermediate for the $MnMo_2$ complex than for the $RhMo_2$ complex.

As in complex (12), the cyclopentadienyl ring attached to Mo1 is almost opposite the Mn1-Mo1 bond, but in contrast the cyclopentadienyl ring on Mo2 is inclined away from Mn1 rather than towards it. This is shown by the proximity of the Mo2 carbonyls to the Mn1 carbonyls (C3...C5 = 2.70 Å) and the Mo1 CO ligands (C2...C4 = 2.81 Å). This configuration reduces the amount of movement required by the C_5 rings during the exchange process, which provides further evidence that complex (24) is closer to the structure of the intermediate than complex (12).

An electron count reveals that Mo1 formally has 18 electrons whereas Mo2 and Mn1 have 16 electrons each, again showing a preference for an open, electron deficient structure. The exchange process, as is the case in complex (12), thus involves the breaking of bonds Mo1-C9 and Mo1-Mn1 and the formation of bonds between Mo2 and the same atoms, C9 and Mn1. All the evidence, therefore, supports the theory of a similar intermediate in the exchange process to that of complex (12) (figure 95), but that in the case of complex (24) the process is more facile.

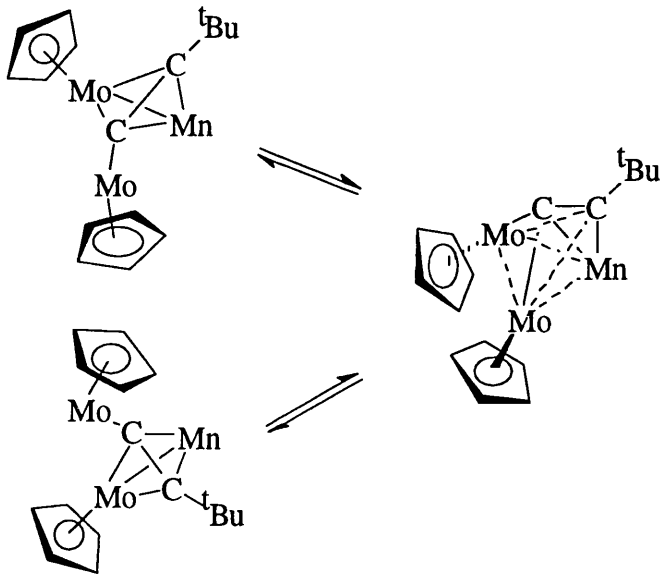

figure 95

The revelation of the open structure of complex (24) allowed a more consistent interpretation of the ^{13}C n.m.r. data discussed above. The observation that three carbonyl environments and one cyclopentadienyl environment are observed at higher temperatures is consistent with the structure of the intermediate closed structure, but the great dissimilarity between the environments of the molybdenum atoms in the two enantiomers of (24) allows the interpretation of the four environments observed at lower temperature when the Cp rings are inequivalent, shown in figure 96.

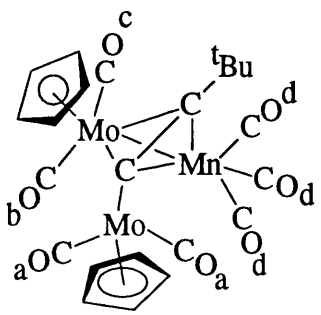

figure 96

The carbonyl atoms around Mo1 are in quite different environments and Mo1 is more sterically hindered than Mo2. If this hindrance is sufficient to prevent facile carbonyl exchange, then exchange can only be accomplished by the equivalence of the molybdenum atoms. Rotation of Mo2 about the Mo2-C8 bond, however is likely to be much easier. This, then explains the existence of two synchronous fluxional processes, one of carbonyl ligands and one of cyclopentadienyl ligands.

Elucidation of the solid state structures of (12) and (24) permitted a fuller investigation of the n.m.r. data and comparisons of the rates of dynamic behaviour.

Taking first the complexes $[Mo_2Rh(\mu\text{-}C{\equiv}CR)(CO)_4(\eta\text{-}C_5H_5)_2(nbd)]$ (11 and 13), their probable structures can now be assigned as shown in figure 97.

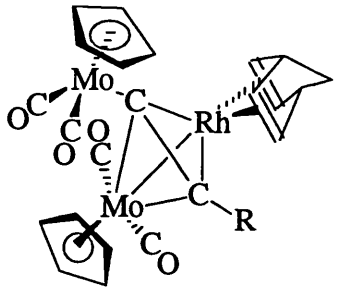

(11), R = Ph
(13), R = ^{t}Bu

figure 97

Both show a simple infra-red spectrum containing three major signals in the carbonyl region. The ^1H n.m.r. spectrum in the case of complex (11) (R = Ph) shows three peaks attributable to the norbornadiene ligand, shown in figure 98, whereas complex (13) shows four.

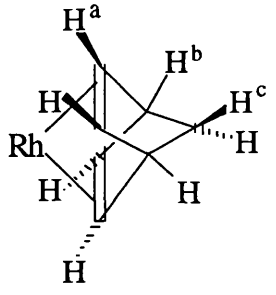

figure 98

The H^a protons appear as a broad singlet at δ 3.02 ppm (R = Ph) or as two very broad singlets at δ 4.13 and 3.41 ppm (R = ^{t}Bu). The conclusion to be drawn from this is that at room temperature the norbornadiene ligand of complex (11) is able to rotate about an axis through the rhodium atom and the γ-carbon whereas that of complex (13) cannot. The bulky *tert*-butyl ligand, therefore, causes more steric interference than the planar phenyl ligand and the energy barrier for rotation of the norbornadiene ligand is higher for R = ^{t}Bu than for R = Ph. Both signals are extremely broad, however, indicating that room temperature is close to the coalescence temperature for both complexes and the difference in the size of the energy barrier is correspondingly slight. In the attempt to establish the structure of these complexes the results demonstrate the proximity of the acetylide γ-carbon to the rhodium atom.

The orientation of the norbornadiene ligand cannot be accurately determined, but it is likely that it adopts the configuration in which the C=C double bonds lie approximately parallel to the C-C acetylide bond (figure 97), which appears to offer the least steric hindrance from the terminal acetylide group and the C_5 ring bonded to Mo2, assuming that the configuration adopted by the rest of the molecule is broadly similar to that proven for complex (12).

By contrast, the peaks attributable to the cyclopentadienyl ligands show a fluxional process which is slower for R = Ph than for R = ^{t}Bu. Complex (11) shows two sharp peaks at δ 5.51 and 5.23 ppm whereas complex (13) shows two very broad peaks, almost

at the point of coalescence at 5.47 and 5.30 ppm. This process, therefore, involves at least the two molybdenum atoms and its rate is not dictated by the steric influence of the acetylide ligand. This data is consistent with the exchange process described above. Variable temperature n.m.r. studies were undertaken of complex (13), $[Mo_2Rh(\mu\text{-}C\equiv C^tBu)(CO)_4(\eta\text{-}C_5H_5)_2(nbd)]$, in order to examine further the fluxional processes exhibited. At 40 °C the $\eta\text{-}C_5H_5$ signals have coalesced into a single broad peak at δ 5.23 ppm. Similarly the olefinic protons of the norbornadiene ligand exhibit only one broad resonance: at δ 3.69 ppm and thus at 40 °C both exchange processes take place fairly rapidly. At the lower temperature of -40 °C, the $\eta\text{-}C_5H_5$ signals occur as two sharp signals at δ 5.62, 5.47 ppm and the four olefinic protons can be seen as four distinct, although still broad, peaks occurring at δ 4.38, 3.99, 3.79, 3.16 ppm. Clearly interchange of the Cp environments does not occur and the rotation of the norbornadiene ligand has slowed down markedly.

The ^{13}C n.m.r. data for complex (11) show resonances at δ 181.0 and 96.8 ppm for Cα and Cβ respectively and for complex (13) Cα occurs at δ 192.5 ppm and Cβ at 110.0 ppm.

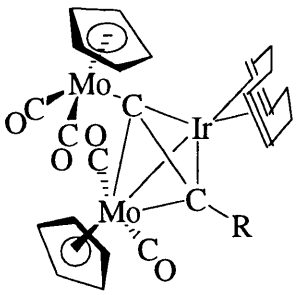

(16), R = Ph
(18), R = ^{t}Bu

figure 99

For the complexes $[Mo_2Ir(\mu\text{-}C\equiv CR)(CO)_4(\eta\text{-}C_5H_5)_2(COD)]$ (16 and 18) shown in figure 99, similar information can be gleaned from a study of the spectra. In both cases

the ^1H n.m.r. spectra of the cyclo-octa-1,5-diene ligand (figure 100) show a high degree of complexity.

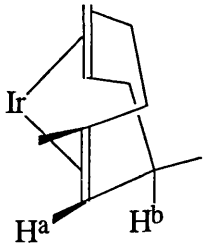

figure 100

In complex (16), where R = Ph, the H^a protons occur as broad singlets at δ 4.20 and 2.80 ppm and the H^b protons as multiplets at δ 2.34 and 1.12 ppm. Complex (18) shows the H^a resonances at δ 4.25, 2.91 and 2.75 ppm and the H^b at 2.31 and 0.89 ppm. Clearly the cyclo-octadiene ligand is unable to rotate freely even at room temperature in both cases. As the cyclo-octadiene ligand is bulkier than the norbornadiene ligand used in the rhodium complexes this obviously results in a further increase in the steric factors which hinder rotation. The definition of the peaks is noticeably more pronounced in the case of complex (18), again showing that the bulkier *tert*-butyl ligand provides more resistance to rotation than the phenyl and supporting further the theory that it is the terminal acetylide group which controls the ease of rotation of the bidentate ligand.

It is likely that the configuration adopted by the cyclo-octadiene ligand is similar to that of the norbornadiene ligand in complexes (11) and (13), in which the C=C double bonds lie approximately parallel to the C-C acetylide bond (figure 99), thus minimising the steric hindrance from the terminal acetylide group and the C_5 ring bonded to Mo2, again assuming that the configuration adopted by the rest of the molecule is broadly similar to that proven for complex (12).

In both (16) and (18) two sharp peaks are observed for the cyclopentadienyl ligands indicating that exchange does not occur at ambient temperature.

The preparation of complexes (12) and (14), $[Mo_2Rh(\mu\text{-}C{\equiv}CR)(CO)_6(\eta\text{-}C_5H_5)_2]$, by replacing the norbornadiene ligands of (11) and (13), respectively, with carbonyl groups (figure 101) is accompanied by a corresponding increase in the complexity of the infra-red spectrum in the carbonyl region with five peaks extant.

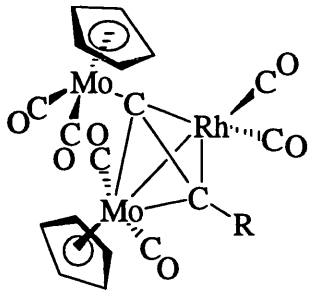

(12), R = Ph
(14), R = ^{t}Bu

figure 101

The ^{1}H n.m.r. data again show two sharp peaks for $\eta\text{-}C_5H_5$ when R = Ph at δ 5.10 and 4.70 ppm and two very broad peaks when R = ^{t}Bu at δ 5.52 and 5.48 ppm. This again suggests a fluxional process rendering the cyclopentadienyl ligands equivalent which is faster for complex (14) (R = ^{t}Bu) than for complex (12) (R = Ph). The Cp signals are shifted slightly upfield from the analogous values for complexes (11) and (13). In the ^{13}C n.m.r. both the Cα and Cβ values are higher than for the corresponding norbornadiene complexes indicating a greater degree of deshielding from the carbonyl ligands than from the norbornadiene. The Rh-C splitting is visible for the carbonyl ligands, and for both Cα and Cβ.

The ^{1}H n.m.r. data for complexes (17) and (19), $[Mo_2Ir(\mu\text{-}C{\equiv}CR)(CO)_6(\eta\text{-}C_5H_5)_2]$ (figure 102) show only one broad resonance for the cyclopentadienyl ligands, indicating that equivalence occurs at room temperature for both R = Ph and ^{t}Bu, and so this occurs more readily for the iridium system than for the rhodium.

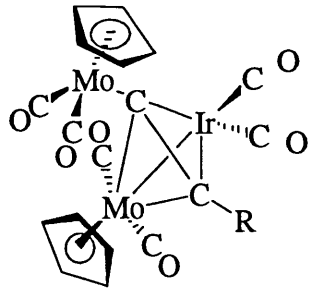

(17), R = Ph
(19), R = ^{t}Bu

figure 102

The ^{13}C n.m.r data for complex (17) show Cα at δ 187.3 and Cβ at δ 95.6 ppm and for complex (18), Cα is at δ 173.3 and Cβ occurs at δ 96.2 ppm. In this case the Cβ values are lower than is exhibited for the one value obtained from the corresponding cyclo-octadiene complexes.

Complexes (20) and (21), $[Mo_2Rh(\mu\text{-}C{\equiv}CR)(CO)_4(\eta\text{-}C_5Me_5)_2(nbd)]$ (figure 103), show interesting differences in their n.m.r. spectra when compared to complexes (11) and (13) (figure 97).

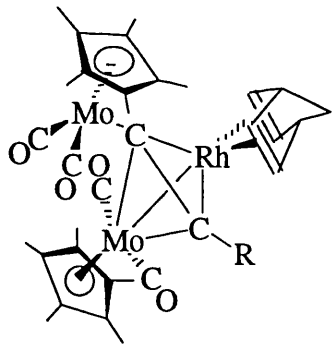

(20), R = Ph
(21), R = ^{t}Bu

figure 103

The ^{1}H n.m.r. spectra show two peaks for the olefinic norbornadiene protons for both complexes, indicating that there is no facile rotation of the norbornadiene ligand about an axis through the rhodium atom and the γ-carbon. This indicates an increase in

the steric factors influencing rotation due to the presence of the pentamethylcyclopentadienyl ligands as the norbornadiene ligand is unable to rotate even in the case of complex (20) (R = Ph). In both ^{1}H and ^{13}C n.m.r. spectra the $\underline{C}_5Me_5$ and $C_5\underline{Me}_5$ resonances appear as a single peak, implying that exchange occurs much faster than is the case with C_5H_5 ligands. The ^{13}C n.m.r. spectra for complexes (20) and (21) show resonances for Cα at δ 198.0 and 200.4 ppm respectively and for Cβ at δ 136.2 and 143.2 ppm respectively. The values for Cβ are significantly higher than for the series of complexes where the molybdenum atoms carry cyclopentadienyl ligands, presumably because of the increased deshielding effect of the proximity of the methyl groups of the C_5 ring.

The Mo_2Mn complexes (23) R = Ph and (24) R = ^{t}Bu [$Mo_2Mn(\mu\text{-}C{\equiv}CR)(CO)_7(\eta\text{-}C_5H_5)_2$] (figure 104) show strong absorption in the carbonyl region of their infra-red spectra as would be expected.

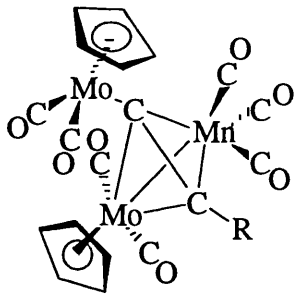

(23), R = Ph
(24), R = ^{t}Bu

figure 104

At room temperature, the ^{1}H n.m.r. spectra show one singlet for the two cyclopentadienyl ligands, although in the case of complex (23) (R = Ph) the peak is broad. Clearly interconversion of the Cp environments is rapid at room temperature in the case of the Mo_2Mn clusters and again the process is faster for a *tert*-butyl acetylide fragment than for a phenyl.

The ^{13}C n.m.r. data again show resonances for Cα (R = Ph, δ 188.9 ppm and R = ^{t}Bu, δ 184.4 ppm) and Cβ (R = Ph, δ 97.9 ppm and R = ^{t}Bu, δ 109.9 ppm) which are consistent with the other results reported for this class of compounds. In the case of both complexes the Cp ligands appear as separate peaks on the ^{13}C n.m.r. time scale at 20 °C. The variable temperature n.m.r. characteristics of complex (24) have already been discussed elsewhere.

Complex (25), $[Mo_2Ru(\mu\text{-}C{\equiv}CPh)(CO)_4(\eta\text{-}C_5H_5)_3]$ (figure 105) and the previously prepared analogue $[Mo_2Ru(\mu\text{-}C{\equiv}C^{t}Bu)(CO)_4(\eta\text{-}C_5H_5)_3]$ both show three discrete resonances for the $\eta\text{-}C_5H_5$ ligand in the ^1H n.m.r. spectrum at δ 5.65 (assigned to Ru-Cp), 5.06 and 4.97 ppm for R = Ph (25) and at δ 5.57, 5.03 and 4.98 ppm for R = ^{t}Bu. The cyclopentadienyl ligands, therefore are not exchanging rapidly at room temperature. Cα appears at δ 203.1 ppm for R = Ph and at δ 203.2 ppm for R = ^{t}Bu, a little higher than is usual for these compounds, and Cβ at 93.2 for R = Ph, a little lower.

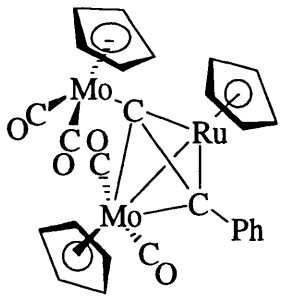

(25)

figure 105

In the absence of any evidence to the contrary, the structure of (25) is presented as open, although in this case neither is there structural evidence to support this assertion. In terms of the 18 electron rule, it should be noted that in the case of the structure for (25) presented in figure 105 the ruthenium formally has 16 electrons, analogous to the clusters already discussed, as has the molybdenum which is not bound to it. It is possible that this

complex adopts the closed position originally conceived[121] for its analogue [$Mo_2Ru(\mu\text{-}C{\equiv}C^tBu)(CO)_4(\eta\text{-}C_5H_5)_3$] and this possible structure, in which all three metal atoms formally possess 18 electrons, is illustrated in figure 106.

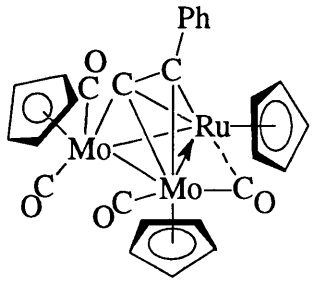

(25)

figure 106

Without an X-ray study of a crystal of complex (25), it's solid state structure cannot be determined beyond doubt, but the relatively downfield shift of the α-carbon ^{13}C n.m.r. signal (δ 203 ppm) lends credence to the open structure of figure 105. The variations in quaternary carbon atom n.m.r. signals are discussed more fully below.

A summary of the ^{13}C n.m.r. data for Cα and Cβ for these complexes is presented in Table 2 and a summary of room temperature exchange processes for the cyclopentadienyl, pentamethylcyclopentadienyl, norbornadiene and cyclo-octadiene ligands is given in Table 3.

Table 2 ^{13}C data for complexes [{$Mo_2(L)_2(CO)_4$}{ML"}{μ-CCR}]

L"	M	L	R	Cα	Cβ
(η-C_5H_5)	Mo	(η-C_5H_5)(CO)	Ph	178.5	116.9
(η-C_5H_5)	Rh	nbd	Ph	181.0	96.8
(η-C_5H_5)	Rh	nbd	^{t}Bu	192.5	110.0
(η-C_5H_5)	Rh	$(CO)_2$	Ph	199.1	105.8
(η-C_5H_5)	Rh	$(CO)_2$	^{t}Bu	194.0	126.5
(η-C_5Me_5)	Rh	nbd	Ph	198.0	136.2
(η-C_5Me_5)	Rh	nbd	^{t}Bu	200.4	143.2
(η-C_5H_5)	Ir	COD	Ph	172.2	
(η-C_5H_5)	Ir	COD	^{t}Bu	198.5	133.0
(η-C_5H_5)	Ir	$(CO)_2$	Ph	187.3	95.6
(η-C_5H_5)	Ir	$(CO)_2$	^{t}Bu	173.3	96.2
(η-C_5H_5)	Mn	$(CO)_3$	Ph	188.9	97.9
(η-C_5H_5)	Mn	$(CO)_3$	^{t}Bu	184.4	109.9
(η-C_5H_5)	Ru	(η-C_5H_5)	Ph	203.1	93.2
(η-C_5H_5)	Ru	(η-C_5H_5)	^{t}Bu	203.2	

Table 2 shows a broad consistency in these chemical shift values, and there are few features of note. The higher values of Cβ when L" = C_5Me_5 are the only significant deviations from the norm. The chemical shift values of Cα broadly reflect the degree of closure of the structure. The Cα of open structures with a more rapid rate of exchange, namely the Mn and Ir complexes, mostly occur in the range δ 172-189 ppm, whereas the more slowly exchanging rhodium complexes exhibit Cα chemical shifts at δ 181-201 ppm.

The most closed structure of all, the Mo_3 system, has a relatively low Cα chemical shift of δ 178.5 ppm. This variation can be attributed to the higher electron density of carbon atoms in a closed structure. As the structure closes, Cα rises above the metal triangle, rather than being at the centre of it, and the metal-metal interactions increase. This reduces the electron-withdrawing effect of the metals resulting in an upfield shift of the ^{13}C n.m.r. signal. The ruthenium complexes have the highest Cα resonances of all at δ 203 ppm and, in the context of these observations, this lends support for the theory that it adopts the open structure illustrated in figure 105.

Table 3 Some exchange processes in complexes [{$Mo_2(L)_2(CO)_4$}{ML''}{μ-CCR}]

L''	M	L	R	L'' exchange?	L rotation ?
(η-C_5H_5)	Mo	(η-C_5H_5)(CO)	Ph	No	
(η-C_5H_5)	Rh	nbd	Ph	No	Yes
(η-C_5H_5)	Rh	nbd	^{t}Bu	Yes	No
(η-C_5H_5)	Rh	$(CO)_2$	Ph	No	
(η-C_5H_5)	Rh	$(CO)_2$	^{t}Bu	Yes	
(η-C_5Me_5)	Rh	nbd	Ph	Yes	No
(η-C_5Me_5)	Rh	nbd	^{t}Bu	Yes	No
(η-C_5H_5)	Ir	COD	Ph	No	No
(η-C_5H_5)	Ir	COD	^{t}Bu	No	No
(η-C_5H_5)	Ir	$(CO)_2$	Ph	Yes	
(η-C_5H_5)	Ir	$(CO)_2$	^{t}Bu	Yes	
(η-C_5H_5)	Mn	$(CO)_3$	Ph	Yes	
(η-C_5H_5)	Mn	$(CO)_3$	^{t}Bu	Yes	
(η-C_5H_5)	Ru	(η-C_5H_5)	Ph	No	

(η-C_5H_5) Ru (η-C_5H_5) ^tBu No

A summary of the effects of the various differing atoms and groups on the rate of fluxionality is as follows: The ease of rotation of the nbd and COD ligands on some of the complexes is dictated by the relative steric effects of both the terminal acetylide group and the η^5-ring attached to the molybdenum atoms. The rate of equivalence of the Cp ligands on the Mo atoms is affected by several factors. The rate is higher for R = ^tBu than for R = Ph, and higher for L = C_5Me_5 than for L = C_5H_5. The rate is reduced by the addition of a bulky bidentate ligand to the "third metal", M, and COD has a greater effect than nbd. The rate of exchange therefore varies according to the nature of M in the manner Ir>Mn> Rh>(Mo, Ru). There is insufficient data to make a comparison between Mo and Ru, and the difference between Mn and Ir is relatively small. No judgement can be made with available data on the degree of influence of the Cp ligands on M when M = Mo, Ru, and the explanation for the slow rate of exchange may lie chiefly here.

In conclusion, across a range of analogous Mo_2M μ-acetylide cluster complexes, the previously published solid state crystal structure of [Mo_3(μ-C≡CPh)(CO)$_5$(η-C_5H_5)$_3$], which exhibited a closed configuration, has proved to be the exception rather than the rule. Examination by X-ray diffraction of a selection of heterogeneous tri-metal acetylide clusters has demonstrated a tendency towards the adoption of an open configuration, which is obviously chiral. These complexes show evidence that the exchange process which renders the environments of the η^5-ring equivalent occurs *via* a closed intermediate resembling the solid state structure of the Mo_3 system. The relative rate of this process in different complexes is higher when the structure bears a closer resemblance to the closed structure (*c.f.* complex (24)) than to the open structure (*c.f.* complex (12)). While superficially the rate of exchange is influenced by many factors, such as the nature of the metal, metal ligands and acetylide ligand, perhaps the significant

factor can be best expressed as the influence that these things have on the opening or closing of the lowest energy conformation. Evidence for this is provided by the pentamethylcyclopentadienyl complexes (20 and (21), $[Mo_2Rh(\mu\text{-}C{\equiv}CR)(CO)_4(\eta\text{-}C_5Me_5)_2(nbd)]$. Despite the presence of sterically bulky ligands, the exchange process is faster than for complex (12), $[Mo_2Rh(\mu\text{-}C{\equiv}CPh)(CO)_6(\eta\text{-}C_5H_5)_2]$, and probably for complex (14), $[Mo_2Rh(\mu\text{-}C{\equiv}C^tBu)(CO)_6(\eta\text{-}C_5H_5)_2]$. While a first approximation suggests that these ligands would slow the process down, the opposition of the bulky ligands influencing a more closed structure, in which they are required to oscillate less, provides an explanation for the increased rate of this process. The closed structure, then, can perhaps be regarded as a good expression of the basic form of these tri-metal acetylides from which the open conformation proceeds, but the introduction of a heterogeneous organometallic fragment strains the structure sufficiently for the lowest energy conformation to be that of the open structure. Electron counting reveals a common result in all the open-structured complexes discussed above. The molybdenum atom bonded to the third metal formally has 18 electrons, while the third metal itself and the other molybdenum atoms both have 16 electrons, a most unusual occurrence.

2.21 A study of the protonation of complexes (14) and (17)

In the preliminary stages of this work[121], a complex containing an Mo_3 triangle, $[Mo_3(\mu\text{-}C{\equiv}C^tBu)(CO)_5(\eta\text{-}C_5H_5)_2(\eta^5\text{-}C_9H_7)]$, was treated with $HBF_4.Et_2O$ to form the stable cation $[Mo_3(\mu\text{-}CCH^tBu)(CO)_5(\eta\text{-}C_5H_5)_2(\eta^5\text{-}C_9H_7)]BF_4$ (28) shown in figure 107.

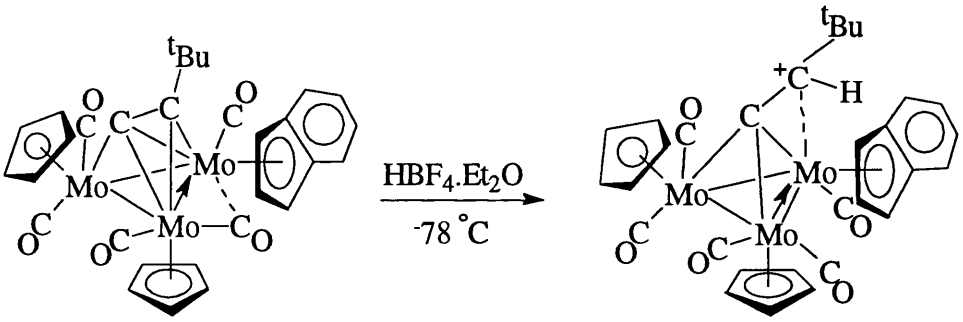

(28)

figure 107

At the same time, however, protonation of the vinyl-substituted cluster $[Mo_3(\mu_3\text{-}CCH{=}CMe_2)(CO)_6(\eta\text{-}C_5H_5)_2(\eta^5\text{-}C_9H_7)]$ gave the superficially similar complex $[Mo_3(\mu_3\text{-}CCH^iPr)(CO)_6(\eta\text{-}C_5H_5)_2(\eta^5\text{-}C_9H_7)]BF_4$ (29) shown in figure 108.

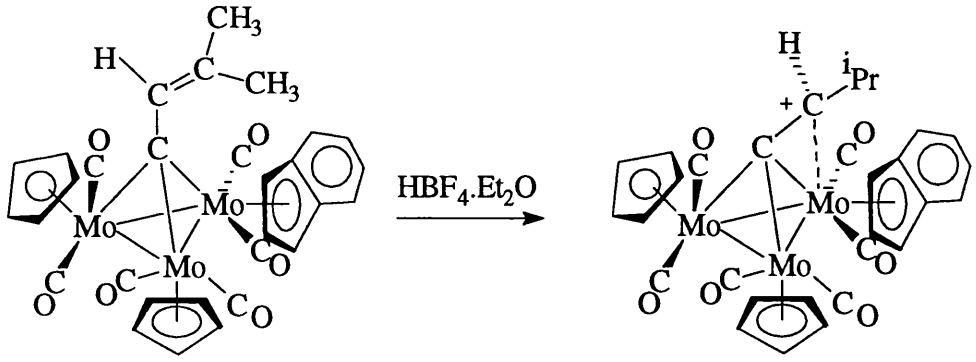

(29)

figure 108

The existence of an extra carbonyl ligand in (29) enables this complex to adopt a less complex bonding mode than is required in complex (28). In the ^1H n.m.r. analysis of these complexes the most significant piece of information is the chemical shift of the lone proton attached to the β-carbon. In the case of complex (28) this signal appears at δ 2.85 ppm, whereas in (29) the proton resonates at δ 5.99 ppm, a chemical shift more typical of those previously observed for tricobalt nonacarbonyl-bound carbonium ions by Seyferth[89]. This may be indicative of a different bonding mode for complex (28) and it has been suggested that this complex may have more vinylidene character than complex (29), a phenomenon discussed later in this chapter.

It was decided to investigate the protonation of some of the open complexes described above. Complex (14), $[Mo_2Rh(\mu\text{-}C{\equiv}C^tBu)(CO)_6(\eta\text{-}C_5H_5)_2]$, was treated with $HBF_4.Et_2O$ at -78 °C in dichloromethane to give a light brown complex, (26), which analysis proved had the empirical formula $C_{22}H_{20}O_6Mo_2RhBF_4$. This is consistent with the formation of $[Mo_2Rh(CCH^tBu)(CO)_6(\eta\text{-}C_5H_5)_2]BF_4$.

The ^1H n.m.r. spectrum revealed two broad cyclopentadienyl peaks at δ 5.93 and 5.76 ppm, which almost obscured a singlet proton at δ 5.78 ppm. This suggests that complex (26) adopts a similar bonding mode to complex (29), despite the fact that the fragment $[M(CO)_2]$ (M = Rh, Ir) is isolobal with $[Mo(CO)(\eta\text{-}C_7H_9)]$ (as in (28)) rather than $[Mo(CO)_2(\eta\text{-}C_7H_9)]$ or $[Co(CO)_3]$. Indeed the bonding system thus constructed for complex (26) is equally simple (figure 109).

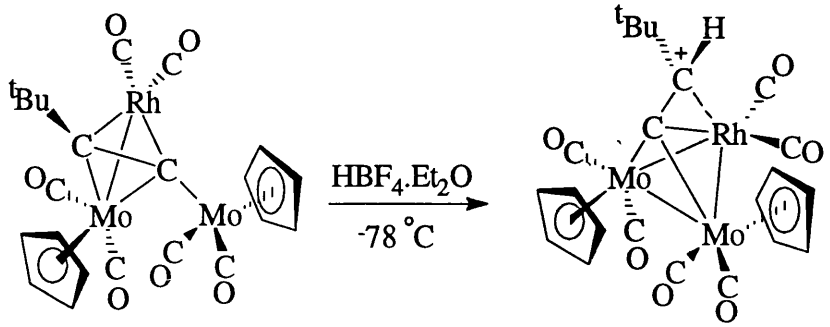

(14) (26)

figure 109

The two cyclopentadienyl signals indicate dynamic behaviour, implying that Cβ is associated with one of the metal atoms. The ^{13}C n.m.r. data reveals two quaternary carbon atoms that show splitting due to rhodium coupling, at δ 185.0 and 149.1 ppm, assigned to Cα and Cβ. This implies that Cβ is associated with the rhodium atom, rather than one of the molybdenum atoms. The molecule does not have a plane of symmetry as, even if the C-C bond is parallel to a line bisecting the metal triangle, the different terminal groups are unlikely to lie in the Rh-C-C plane in the lowest energy conformation. It is more likely, given previous results, that the C-C bond lies to one side of the rhodium atom resulting in a chiral complex and the cyclopentadienyl rings are rendered equivalent at higher temperatures *via* a similar windscreen wiper motion to that described earlier for the starting material.

Protonation of complex (17), $[Mo_2Ir(\mu\text{-}C{\equiv}CPh)(CO)_6(\eta\text{-}C_5H_5)_2]$, in a similar manner resulted in the formation of a pale brown solid identified as $[Mo_2Ir(\mu\text{-}CCHPh)(CO)_6(\eta\text{-}C_5H_5)_2]BF_4$ (27). The ^1H n.m.r. spectrum showed a singlet at δ 5.55 ppm for the cyclopentadienyl rings, indicating that any dynamic behaviour is faster for complex (27) than for (26). The single proton resonates at δ 5.67 ppm suggesting that a similar structure to that of (26) is adopted (figure 110).

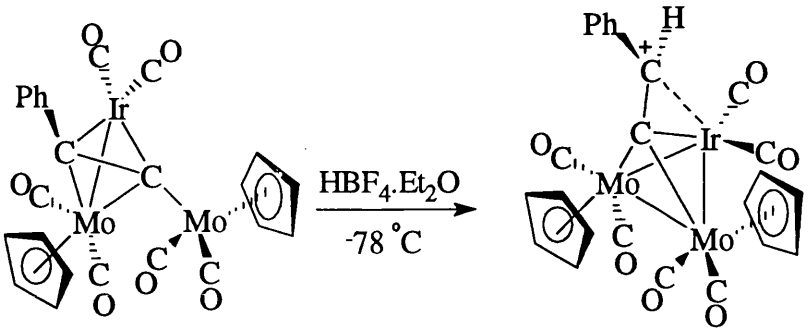

(17) (27)

figure 110

The ^{13}C n.m.r. data has been assigned on a similar basis to complex (26), namely that Cα = δ 168.1 ppm and Cβ = δ 139.9 ppm. No further evidence can be offered for the orientation of the ligand as iridium is not spin-active but it is likely that complex (27) is closely analogous to (26).

In both complexes (26) and (27) the rhodium still has formally 16 electrons, while the molybdenum atoms both possess 18 electrons as the closure of the structure allows the formation of further metal-metal bonds and thus increased electronic saturation of the second molybdenum atom. The β-carbon is no longer able to bind to two metal centres and so it is extremely unlikely that these complexes adopt an open structure similar to their precursors without supposing the existence of at least one 17 electron metal centre. Attempts to speculate on possible open structures for these cations have not yielded a feasible solution.

The principle of stabilisation of the positively-charged β-carbon by donation of electron density from the metal has been established in the literature[89, 118] and this effect is mentioned in the introduction and in chapter 2.1 with reference to the cationic μ-acetylene complex $[Mo_2(\mu\text{-}HC_2CH_2)(CO)_4(\eta\text{-}C_5H_4Me)_2][BF_4]$ (2). It is equally valid to describe complexes (26) and (27) in terms of the vinylidene ligand being η^2-bound to the rhodium atom and these two canonical forms are illustrated in figure 111.

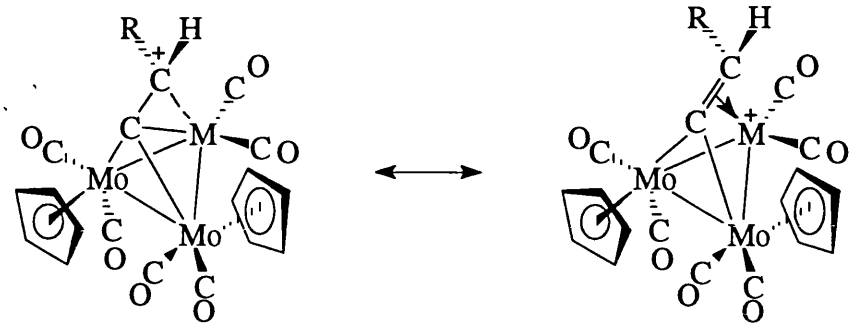

figure 111

The rhodium-carbon coupling of Cβ (δ 5.2 Hz) is much smaller than for Cα (δ 34.0 Hz) and the interaction is therefore very much weaker, thus the true description of the bonding in this molecule probably lies somewhere between these two canonical forms.

A comparison of the ^{13}C chemical shifts of the carbon atoms with the n.m.r. data previously reported by Green[121] for trimolybdenum systems and by Seyferth[89] for tricobalt nonacarbonyl-bound carbonium ions reveals more of this matter. The data, summarised in Table 4, shows that for (26) and (27) the α-carbon is shifted upfield and the β-carbon is shifted significantly downfield when compared with these results. This is consistent with an increase in vinylidene-type behaviour for the organic moiety, Cα being less closely associated with the metal triangle and the positive charge on Cβ being reduced by closer association with the metal atom.

Table 4

Metal triangle	Cα	Cβ
Co_3	255-275	90-125
Mo_3	191, 190	74, ?
Mo_2Rh	185	149
Mo_2Ir	168	140

These complexes show that Mo_2Rh and Mo_2Ir complexes do form closed, triangular structures if the correct conditions prevail, and support the theory that dynamic behaviour in the open-structured complexes proceeds *via* a closed intermediate.

2.3 Functionalised η^3-allyl complexes of iron

The work discussed in this chapter was undertaken at the end of the laboratory time allotted for this thesis and thus the proposed experimental programme was not brought to completion. An outline of some suggested further work in this area is presented at the end of the section.

A proposed route to Mo_2Fe acetylide complexes analogous to those described in the preceding section involved reaction of dimolybdenum acetylide anions with the cationic iron propene complex $[Fe(\eta\text{-}C_5H_5)(CO)(\eta^2\text{-}C_3H_6)]BF_4$ accessible *via* the protonation of $[Fe(\eta\text{-}C_5H_5)(CO)(\eta^3\text{-}C_3H_5)]$ (28) with $HBF_4.Et_2O$. This experimental programme was not initiated but an investigation into some of the chemistry arising from the reactivity of this cation is presented below.

It has been mentioned earlier in this thesis that the iron η^3-oxoallyl complex (29) was generated by protonation of $[Fe(\eta\text{-}C_5H_5)(CO)(\eta^3\text{-}C_3H_5)]$ (28) in the presence of 1-trimethylsilyloxybuta-1,3-diene (figure 112)[117]. Notably the sole product was the *exo-syn*-isomer.

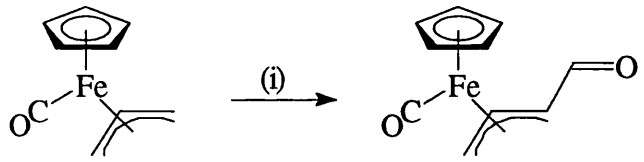

(28) (29)

(i) $HBF_4.Et_2O$, 1-trimethylsilyloxybuta-1,3-diene

figure 112

In the case of molybdenum chemistry a mixture of *syn-* and *anti*-isomers of the oxoallyl complex were obtained which is explained by the presence of a transient diene cation (figure 112a).

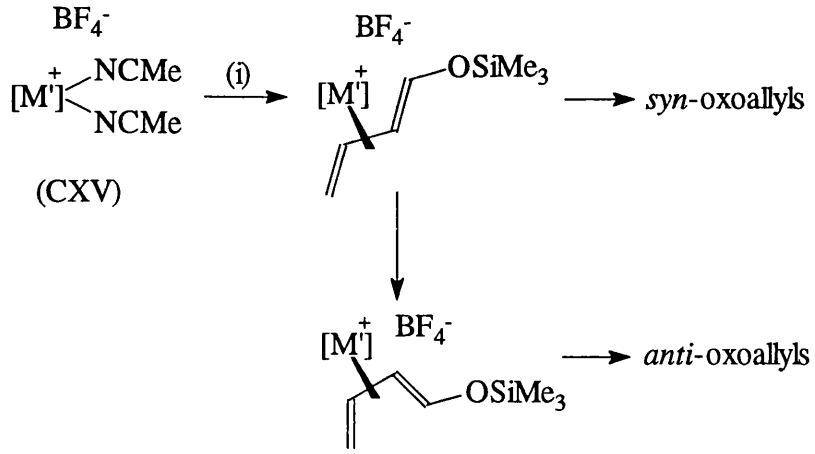

(i) 1-Trimethysilyloxybuta-1,3-diene

[M'] = $Ru(\eta\text{-}C_5H_5)(CO)$, $Mo(\eta\text{-}C_5Me_5)(CO)_2$

figure 112a

Upon coordination of the siloxydiene moiety, activation towards nucleophilic attack is such that the tetrafluoroborate anion is sufficient to effect desilylation and the conflict between the rate of this reaction and the rate of formation of the *cis*-diene cation is responsible for the ratio of the isomers observed. This proposed mechanism is further substantiated by observation of the analogous reaction with a BPh_4^- counterion, in which the ratio of *syn* : *anti* isomers is lower. This is consistent with the presence of the less nucleophilic BPh_4^- anion resulting in an increase in longevity for the intermediate siloxydiene cation, thereby allowing a greater degree of *trans* → *cis* isomerisation prior to desilylation.

In the case of the reaction illustrated in figure 112 the exclusive formation of the *syn*-isomer suggests that the rate of desilylation is much higher than the rate of isomerisation.

In order to investigate the full range of possibilities with regard to preparative organic chemistry, it was necessary to devise a method of preparation for the *anti*-isomer of complex (29). The first step was the protonation of (29) to give a more stable diene complex in order to allow more complete isomerisation to the *cis*-isomer. Complex (29) was protonated with either trifluoromethane sulphonic acid or hydrofluoroboric acid in dichloromethane at -78 °C to give a cationic *trans*-1-hydroxybuta-1,3-diene complex. Upon warming to room temperature this complex rearranged to give a higher proportion of the *cis*-diene complex. Further treatment with triethylamine at room temperature generated a mixture of (29) and the *exo-anti*-oxoallyl complex (30) as illustrated in figure 113.

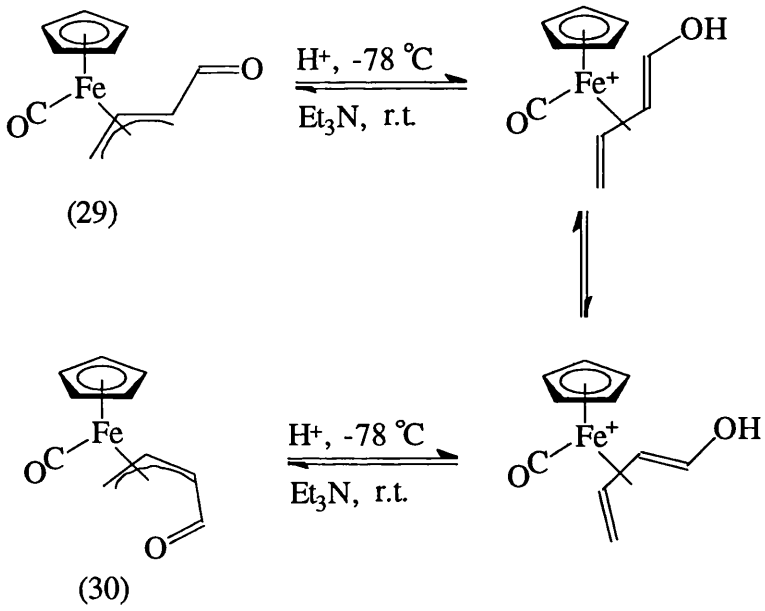

figure 113

A preliminary variable temperature n.m.r. experiment was performed in order to elucidate the pathway of this transformation. A sample of (29) was dissolved in CD_2Cl_2 in an n.m.r. tube and cooled to -78 °C, $HBF_4.Et_2O$ was added and the ^1H n.m.r. spectrum monitored as the sample was warmed to room temperature. While the data obtained were

not clear enough to publish, they were suggestive of a transformation from *trans*- to *cis*-diene complexes occurring between -10 and +10 °C. Treatment with Et_3N yielded the oxoallyl complex as an orange solid. The *syn*- and *anti*-isomers of the oxoallyl complex (29) and (30) proved amenable to separation by column chromatography and were isolated in the ratio of approximately 5:11. Either the *trans*-diene complex is sufficiently stable to be present in solution to a significant degree or, more probably, a longer reaction time is required.

Complex (30) is assigned the structure shown in figure 113 on the basis of the coupling constants exhibited in the ^1H n.m.r. spectrum (figure 114).

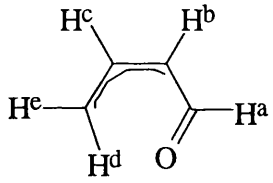

figure 114

J_{ab}, J_{bc} and J_{ce} are all small (6.69, 7.33 and 7.88 Hz respectively) and so these relationships are assigned as *cis*. J_{cd} is 11.91 Hz, indicative of a *trans* relationship.

A more selective preparative method for complex (30) was desirable and so it was felt, based on molybdenum chemistry currently being pursued in the same laboratory, that protonation of (28) in the presence of 1-acetoxybuta-1,3-diene would generate exclusively the cationic *cis*-η^4-acetoxybutadiene complex *cis*-$[Fe(\eta\text{-}C_5H_5)(CO)(\eta^4\text{-}CH_2CHCHCHOCMeO)]BF_4$ (31) (figure 115). This approach arose in the case of molybdenum chemistry from a systematic variation of the size and nature of the leaving group. Reaction of this complex with a base (figure 115a) should then result in the formation of complex (30) with no detectable presence of the *syn*-isomer (29).

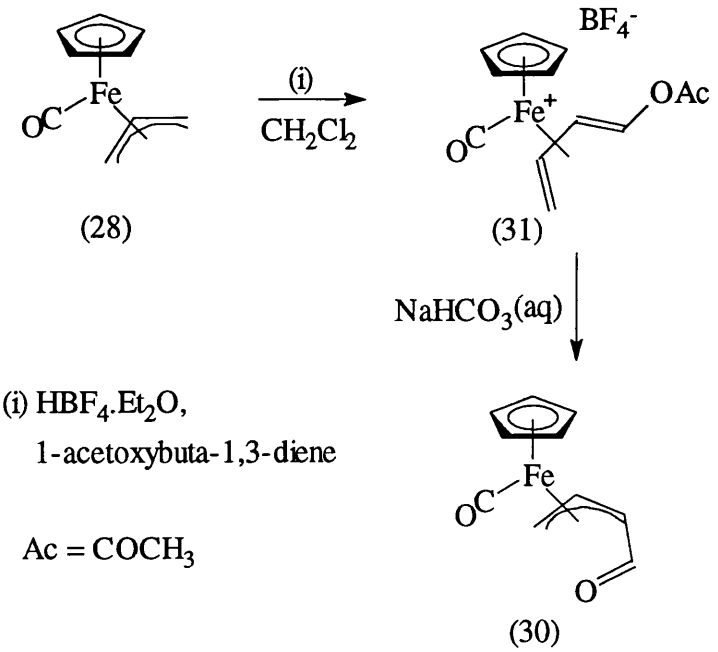

figure 115

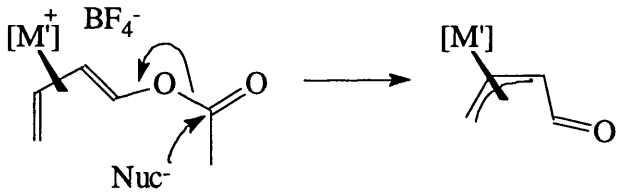

figure 115a

In practice this method proved successful, although in practice the coupling constants revealed in the ^1H n.m.r. data indicate that the structure illustrated in figure 116 is more representative for the *cis*-diene complex (31), which is perhaps not what would be expected. This is consistent with the orientation proven for the *exo-anti*-oxoallyl complex (30).

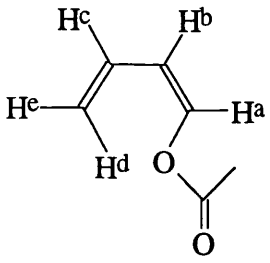

figure 116

The J_{cd} value of 10.26 Hz indicates a transoid coupling and thus H^c and H^e are *cis* to each other (J_{ce} 5.13 Hz). J_{ab} is 7.50 Hz, a value usually taken to indicate a *cis* relationship. An element of doubt is cast on this conclusion by the observation that J_{ab} is mid-way between the values obtained for *cis* and *trans* geometries elsewhere in the same ligand, but a comparison with data obtained for similar molybdenum complexes[115] supports this deduction.

Further experiments were concerned with the reactivity of complex (30). Treatment of complex (30) with the Wittig reagent $Ph_3P{=}CH_2$ gave the allyl complex *exo-anti*-[Fe(η-C_5H_5)(CO)(η^3-$CH_2CHCHCH{=}CH_2$)] (32) as illustrated in figure 117.

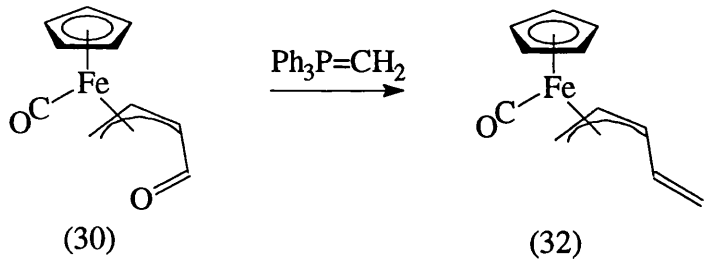

(30) (32)

figure 117

Again the orientation of the organic ligand can be ascertained by recourse to the proton-proton coupling values revealed in the ^1H n.m.r. spectrum (figure 118).

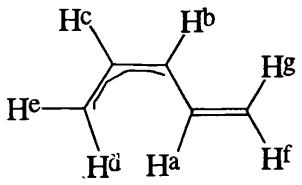

figure 118

As expected, H^c and H^d show a transoid coupling (J_{cd} 10.08 Hz) and H^c and H^e are *cis* (J_{ce} 6.59 Hz). H^b and H^c are again *cis* (J_{bc} 6.42) and H^f and H^g are assigned on the basis of their couplings with H^a (J_{af} 6.96 Hz - *cis* and J_{ag} 9.53 Hz - *trans*). J_{ab} is 15.75 Hz unequivocally indicating a *trans* relationship and thus the $C=CH_2$ double bond is seen to adopt a different orientation than the C=O bond of complex (30).

Reaction of complex (30) with $NaBH_4$ followed by an aqueous workup generated *anti*-[Fe(η-C_5H_5)(CO)(η^3-$CH_2CHCHCH_2OH$)] (33) as a yellow powder.

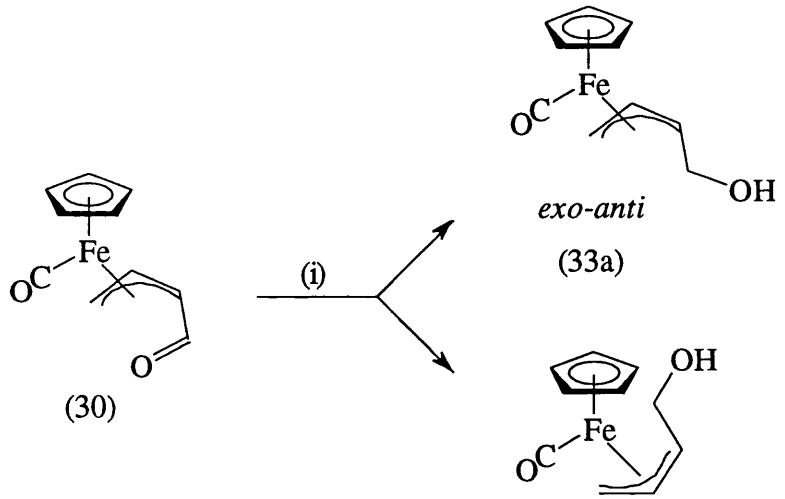

(i) $NaBH_4$ then hydrolysis

figure 119

Examination of the ^1H and ^{13}C n.m.r. data revealed that two isomers were present in a ratio of approximately 3:2 which are assigned as the *exo-* and *endo-anti*-isomers, (33a) and (33b), illustrated in figure 119. Determination of the values for the proton-

proton couplings is difficult as the signals for all the protons except H^c and H^d, as shown in figure 120 are superimposed. A ^{13}C n.m.r. investigation of the mixture reveals two signals for C^2, C^3 and C^4, and a superimposed signal for C^1.

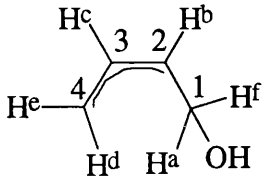

figure 120

The values for the coupling of H^b with H^a and H^f are approximately 10 Hz and H^d and H^e are assigned on the basis of the values J_{cd} 9.67 Hz and J_{ce} 5.91 Hz. Unfortunately the crucial J_{bc} value is unclear but comparison with previously published data[117] for the *exo-syn*-isomer rules out a *syn* configuration for (33). On this basis complex (33) is presented as a mixture of *exo-anti-* and *endo-anti*-isomers. With the evidence currently available it is impossible to establish which of the complexes (33a) and (33b) is *exo* or *endo*. Previous evidence suggests[115] that the *exo-anti*-isomer is thermodynamically preferred to the *endo-anti-* and it could be argued that the more prevalent isomer (33a) is *exo-anti-*, but this is at best a tenuous argument. Interestingly, this reaction differs from the similar reaction of the *exo-syn*-oxoallyl complex with $NaBH_4$[117] in which only the *exo-syn-* product is isolated.

Proposed future investigations

Further investigation is desirable into the η^4-diene cations involved in the preparation of (30) from (29), and their interconversion. An attempt should be made to separate (33a) and (33b) and further n.m.r. studies are needed to establish the finer details of the analytical data. Pilot studies have suggested that reaction of (30) with MeMgI

results in the formation of a secondary alcohol complex analogous to (33). This investigation should be pursued, especially in view of the formation of isomers of (33) noted above. Finally protonation of (28) followed by reaction with dimolybdenum acetylide complexes, or their reaction with (31), should provide a means of preparing trinuclear acetylide complexes and thus of expanding the area discussed in the previous chapter.

3. Experimental

General Practical Details.

All experiments were performed in an atmosphere of dry nitrogen using standard Schlenk tube techniques unless otherwise stated. Solvents were freshly distilled in a nitrogen atmosphere from potassium metal (toluene), sodium/potassium alloy (hexane, pentane), Na/K benzophenone ketyl (diethyl ether, THF) and calcium hydride (dichloromethane, acetonitrile). All chemicals used were reagent grade and were used as received, unless otherwise stated. Chromatography columns were packed with BDH aluminium oxide for chromatography, Brockman Activity II, unless otherwise stated. Deuterated n.m.r. solvents were dried and distilled as necessary and were always degassed (using the freeze, pump, thaw method) before use.

^{1}H and ^{13}C n.m.r. spectra were recorded on JEOL JNM-GX270 or JNM-EX400 Fourier Transform spectrometers. All temperatures were recorded at ambient temperatures unless otherwise recorded. Chemical shifts were referenced internally to the protio impurity in the deuterated solvent.

Infra-red spectra were recorded on a Nicolet 510P FT-IR spectrophotometer as solutions using sodium chloride cells.

Microanalyses were performed within the School of Chemistry of the University of Bath on a CARLO ERBA 1106 Elemental Analyser.

Preparation of $[Mo_2\{\mu\text{-}\sigma,\eta^2\text{-}(4e)\text{-}C{=}C{=}CMe_2\}(CO)_4(\eta\text{-}C_5Me_5)_2]$ (1) [57]

A solution of 2-methylbut-1-ene-3-yne (185 µl, 1.94 mmol) in 20 cm^3 THF was cooled to -78 °C and 1 equivalent of ^{t}BuLi solution was added. An immediate colour change to purple was observed. $[Mo_2(CO)_4(\eta\text{-}C_5Me_5)_2]$ (1.114g, 1.94 mmol) was added and the solution was allowed to return to room temperature and stir for 24 hours. The resultant dark purple solution was protonated by the addition of Al_2O_3 at -78 °C, and warming to room temperature resulted in a change of colour to green. The solvent

was completely removed *in vacuo* and the dry alumina with adsorbed product was placed on top of a chromatography column packed with alumina and washed with hexane to remove the small amount of red isomeric μ-alkyne product generated. A further elution with 1:1 hexane: diethyl ether yielded a green band. The solvent was removed *in vacuo* to yield a green powder (1) in 65% yield.

Microanalysis

$C_{29}H_{36}Mo_2O_4$ requires: C, 54.4%, H, 5.7%.

found: C, 54.1%, H, 5.6%.

Infra-red (CH_2Cl_2)

ν_{CO} 1952m, 1980s, 1829w cm^{-1}

^{1}H n.m.r. ($CDCl_3$)

δ 2.41 (q, 3H, Me, ^4J(MeH) 0.7 Hz), 2.14 (q, 3H, Me, ^4J(MeH) 0.7 Hz), 1.87 (s, 15H, C_5Me_5), 1.81 (s, 15H, C_5Me_5) ppm.

^{13}C n.m.r. ($CDCl_3$)

δ 302.5 (C_α), 243.0, 240.0, 235.1, 233.8 (CO),156.5, 141.9 (C), 105.5 (C_5Me_5), 105.1 (C_5Me_5), 34.5 (Me), 24.9 (Me), 10.8, (C_5Me_5), 10.7 (C_5Me_5) ppm.

Preparation of $[Mo_2\{\mu_2\text{-}C(H)CCMe_2\}(CO)_4(\eta\text{-}C_5Me_5)_2]BF_4$ (3).

A solution of $[Mo_2\{\mu\text{-}\sigma,\eta^2\text{-}(4e)\text{-}C{=}C{=}CMe_2\}(CO)_4(\eta\text{-}C_5Me_5)_2]$ (200 mg, 0.312 mmol) in 20 cm^3 of CH_2Cl_2 was prepared and cooled to -78 °C. Tetrafluoroboric acid etherate (1.1 equivalents, 81 µl, 0.343 mmol) was added with stirring and the solution was allowed to return to room temperature. The colour changed rapidly to bright red. The solvent was reduced *in vacuo* to minimum volume and addition of diethyl ether caused the product to precipitate as a dark red solid which was washed repeatedly with diethyl ether. Crystallisation from dichloromethane/diethyl ether/hexane afforded dark red crystals of (3) in a yield of 84% (191 mg). An X-ray crystal structure of (3) was obtained.

Microanalysis

$C_{29}H_{37}Mo_2O_4BF_4$ requires: C, 47.7 %, H, 5.1 %.

found: C, 47.9 %, H, 5.2 %.

Infra-Red (CH_2Cl_2)

ν_{CO} 2018vs, 1977m, 1954m, 1892w, 1856w cm^{-1}.

^{1}H n.m.r. (CD_2Cl_2)

δ 4.63 (s, 1H, C<u>H</u>), 2.01 (s, 30H, $C_5\underline{Me}_5$), 1.92 (bs, 6H, $C\underline{Me}_2$) ppm.

^{13}C n.m.r. (CD_2Cl_2)

211.3, 205.8 (s, <u>C</u>O), 160.0 (s, <u>C</u>Me$_2$), 106.9 (s, <u>C</u>$_5$Me$_5$), 103.9 (s, C<u>C</u>C), 77.4 (s, <u>C</u>H), 31.2 (s, <u>Me</u>), 10.8 (s, $C_5\underline{Me}_5$) ppm.

Reaction of $[Mo_2\{\mu_2\text{-}C(H)CCMe_2\}(CO)_4(\eta\text{-}C_5Me_5)_2]^+BF_4^-$ (3) with hydride source.

A sample of the complex (3) (65 mg, 0.097 mmol) was dissolved in 10 cm^3 of CH_2Cl_2 and cooled to -78 °C. One equivalent (97 µl) of $[(CH_3)_2CHCH_2]_2AlH$ (DIBAL-H, 1.0M solution) was added dropwise with stirring and the orange red solution was allowed to return to room temperature and stir overnight. The solution was reduced to minimum volume *in vacuo* and placed on a Florasil packed chromatography column. Washing with hexane removed any excess starting material and elution with diethyl ether afforded a red band. The ether was removed *in vacuo* leaving a red powder shown to be $Mo_2\{\mu_2\text{-}HCCC(H)Me_2\}(CO)_4(\eta\text{-}C_5Me_5)_2$ (4) (50 mg, 80% yield).

Microanalysis

$C_{29}H_{38}Mo_2O_4$ requires: C, 54.2 %, H, 6.0 %.
found: C, 53.9 %, H, 5.9 %.

Infra-red (CH_2Cl_2)

ν_{CO} 1964(m), 1889(s), 1806(m) cm^{-1}

^1H n.m.r. (CD_2Cl_2)

δ 4.80 (s, CC<u>H</u>), 2.71 (septet, C<u>Me</u>$_2$H, $^3J_{HH}$ 6.59 Hz), 1.93 (s, C_5<u>Me</u>$_5$), 1.90 (s, C_5<u>Me</u>$_5$), 1.10 (d, C<u>Me</u>$_2$H, $^3J_{HH}$ 6.59 Hz), 0.84 (d, C<u>Me</u>$_2$H, $^3J_{HH}$ 6.59 Hz) ppm.

^{13}C n.m.r. (CD_2Cl_2)

δ 242.1, 237.12, 237.06, 225.1 (s, $\underline{C}O$), 113.7, 90.8 (s, $H\underline{C}_2Pr^i$), 103.4, 102.7 ($\underline{C}_5Me_5$), 27.4, 26.6 (s, $CH\underline{Me}_2$), 24.6 (s, $\underline{C}HMe_2$), 10.9, 10.5 ($C_5\underline{Me}_5$) ppm.

Reaction of $[Mo_2\{\mu_2\text{-}C(H)CCMe_2\}(CO)_4(\eta\text{-}C_5Me_5)_2]^+BF_4^-$ (3) with $(Me_3Si)_2NLi$

The complex (3) (60 mg, 0.082 mmol) was suspended in 10 cm^3 THF and cooled to -78 °C. An excess (0.1 mmol) of $(Me_3Si)_2NLi$ solution was added and the reaction allowed to return to room temperature. The red solution was observed to darken. The solvent was removed *in vacuo* and the product was redissolved in the minimum volume of dichloromethane. Elution on a Florasil packed chromatography column with diethyl ether yielded a dark red solid which was characterised as $Mo_2\{\mu_2\text{-}HCCCH_2Me\}(CO)_4(\eta\text{-}C_5Me_5)_2$ (5) in 64% yield (34 mg).

Microanalysis

$C_{29}H_{36}Mo_2O_4$ requires:	C, 54.4 %, H, 5.7 %.
found:	C, 54.6 %, H, 5.5 %.

Infra-red (CH_2Cl_2)

ν_{CO} 1968m, 1900s, 1817m cm^{-1}

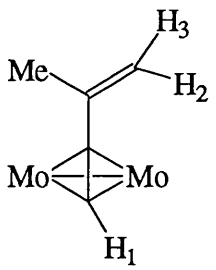

^{1}H n.m.r. (CD_2Cl_2)

δ 4.98 (dq, 1H, H_3, $^{2}J_{HH}$ 1.5 Hz, $^{4}J_{MeH}$ <1.0 Hz), 4.83 (s, 1H, H_1), 4.80 (dq, 1H, H_2, $^{2}J_{HH}$ 1.5 Hz, $^{4}J_{MeH}$ <1.0 Hz), 1.89 (s, 30H, C_5Me_5), 1.81 (dd, 3H, CH_3, $^{4}J_{MeH}$ <1.0 Hz) ppm.

^{13}C n.m.r. (CD_2Cl_2)

δ 238.5, 229.0 (s, CO), 143.4 (s, CMe), 113.6 (s CH_2), 102.4 (s, C_5Me_5), 95.3 (s, CH), 76.6 (s, HCC), 25.2 (s, Me), 10.3 (s, C_5Me_5) ppm.

Reaction of $[Mo_2\{\mu_2\text{-}C(H)CCMe_2\}(CO)_4(\eta\text{-}C_5Me_5)_2]^+BF_4^-$ (3) with Proton Sponge (1,8-*bis*-(dimethylamino)naphthalene).

The complex (3) (120 mg, 0.16 mmol) was dissolved in 10 cm^3 of THF and an excess (42 mg, 0.20 mmol) of proton sponge was added. On stirring the colour darkened to a deep red within a few minutes. The solvent was removed *in vacuo* and the product was redissolved in the minimum volume of dichloromethane. Elution on a Florasil packed chromatography column with diethyl ether yielded a dark red solid which was identified as (5) by infra-red and ^{1}H n.m.r. comparisons. Yield was 76% (78 mg).

Data for (5) are presented above.

Reaction of $[Mo_2\{\mu_2\text{-}C(H)CCMe_2\}(CO)_4(\eta\text{-}C_5Me_5)_2]^+BF_4^-$ (3) with sodium dimethyl malonate.

The complex (3) (100 mg, 0.14 mmol) was dissolved in 10 cm^3 of dichloromethane. One equivalent (21 mg) of $NaCH(CO_2Me)_2$ was added and the solution was allowed to stir for 1 hour during which time the colour darkened to deep red. Elution with diethyl ether on a Florasil packed chromatography column gave a dark red powder shown to be (5).

Data for (5) are presented above.

Reaction of $[Mo_2\{\mu_2\text{-}C(H)CCMe_2\}(CO)_4(\eta\text{-}C_5Me_5)_2]^+BF_4^-$ (3) with MeMgBr.

50 mg (0.07 mmol) of (3) were dissolved in 15 cm^3 of dichloromethane and cooled to -78 °C. 1 equivalent (69 µl of 1.0M solution) of methylmagnesium bromide was added and left to stir overnight by which time the solution had turned yellow-green. Elution with diethyl ether on a Florasil packed chromatography column yielded only a small amount of a dark red powder which seemed to be a mixture of products, the most prevalent of which was characterised by n.m.r. as (5) in low yield. No product formed by an addition reaction was isolated.

Data for (5) are presented above.

Preparation of $[Mo_2(\mu\text{-}HCCCH_2OCH_3)(CO)_4(\eta\text{-}C_5H_5)_2]$ (6)

A solution of $[Mo_2(CO)_4(\eta\text{-}C_5H_5)_2]$ (250 mg, 0.58 mmol) in 20 cm^3 CH_2Cl_2 was prepared. One equivalent (40 mg, 49 µl) propargyl methyl ether was added and the reaction was stirred for 30 minutes. The solvent was removed *in vacuo* to give a dark red solid (6) which was recrystallised from hexane at -78 °C (155 mg, 53% yield).

Microanalysis

$C_{18}H_{16}Mo_2O_5$ requires: C, 42.9 %, H, 3.2 %.

found: C, 42.4 %, H, 3.3 %.

Infra-red (CH_2Cl_2)

ν_{CO} 1991m, 1957w, 1916s, 1836m cm^{-1}.

^{1}H n.m.r. (CD_2Cl_2)

δ 5.86 (s, 1H, C<u>H</u>), 5.32 (s, 10H, $C_5\underline{H}_5$), 4.44 (s, 2H, $C\underline{H}_2$), 3.32 (s, 3H, $C\underline{H}_3$) ppm.

^{13}C n.m.r. (CD_2Cl_2)

δ 231.91, 227.74 (<u>C</u>O), 90.90 ($\underline{C}_5H_5$), 82.43 (<u>C</u>H), 75.92 ($\underline{C}H_2$), 58.47 ($\underline{C}H_3$), 55.76 (<u>C</u>CH) ppm.

Preparation of $[Mo_2(\mu\text{-}HCCCH_2)(CO)_4(\eta\text{-}C_5H_5)_2]BF_4$ (7)

Method A

Complex (6) (155 mg, 0.31 mmol) was dissolved in CH_2Cl_2 and 1.1 equivalents (0.34 mmol, 55 mg, 47 μl) of $HBF_4.Et_2O$ were added. The mixture was stirred for 15 minutes. The solvent was reduced to minimum volume *in vacuo* and the product precipitated by addition of diethyl ether. The resultant bright yellow solid (7) was washed with diethyl ether (164 mg, 95% yield).

Microanalysis

$C_{17}H_{13}Mo_2O_4BF_4$ requires: C, 36.5%, H, 2.3%.

found: C, 36.0%, H, 2.4%.

Infra-red (CH_2Cl_2)

ν_{CO} 2058s, 2008vs, 1910m cm^{-1}.

^{1}H n.m.r. (CD_3CN)

δ 6.54 (s, 1H, CC<u>H</u>), 5.71 (s, 5H, $C_5\underline{H}_5$), 5.64 (s, 5H, $C_5\underline{H}_5$), 5.39 (s, 1H, $C\underline{H}_2$), 4.75 (s, 1H, $C\underline{H}_2$) ppm.

^{13}C n.m.r. (CD_3CN)

δ 227.70, 227.17, 220.38, 217.79 (<u>C</u>O), 118.38 (<u>C</u>CH), 95.02, 93.76 ($\underline{C}_5H_5$), 79.97 (<u>C</u>H), 75.39 ($\underline{C}H_2$) ppm.

Method B

The dimeric molybdenum complex $[Mo_2(CO)_4(\eta\text{-}C_5H_5)_2]$ (440 mg, 1.01 mmol) was dissolved in 20 cm^3 CH_2Cl_2 and 1 equivalent (56.8 mg, 59 µl) of propargyl alcohol was added. The solution was left to stir for 12 hours. The dark purple solution turned dark red and was reduced to minimum volume *in vacuo*. A dark red product was precipitated by addition of pentane at -78 °C. The product (100 mg) was dissolved in 20 cm^3 CH_2Cl_2, cooled to -78 °C and 31 µl (0.22 mmol) of $HBF_4.Et_2O$ was added. The solution was allowed to return to room temperature, reduced to

minimum volume *in vacuo* and the yellow product (7) was precipitated by addition of diethyl ether.

Data for (7) is presented above.

Reaction of (7) with 1,8-*bis*-(dimethylamino)naphthalene

A solution of $[Mo_2(\mu\text{-}HCCCH_2)(CO)_4(\eta\text{-}C_5H_5)_2]BF_4$ (5) (53 mg, 0.095 mmol) in 20 cm^3 THF was prepared and cooled to -78 °C. One equivalent (20 mg) of proton sponge was added - no immediate colour change was observed. The solution was allowed to return to room temperature and a gradual colour change to red was observed. The solvent was removed *in vacuo* and the resultant solid redissolved in the minimum volume of CH_2Cl_2 and placed on a florasil column. The column was washed with hexane to remove excess reagent and a red band was eluted with a 1:1 mixture of diethyl ether: hexane. The solvent was removed *in vacuo* to give a red oil. Crystallisation from diethyl ether / dichloromethane / pentane yielded only one product which could be fully characterised, (8), identified as $[Mo_2(\mu\text{-}HCCCH_2OCH_2CH_3)(CO)_4(\eta\text{-}C_5H_5)_2]$ (21 mg 42% yield). An X-ray crystal structure of complex (8) was obtained.

Microanalysis

$C_{19}H_{18}Mo_2O_5$ requires: C, 44.0%, H, 3.5%.

found: C, 43.7%, H, 3.4%.

Infra-red (THF), before workup

ν_{CO} 1989s, 1917vs, 1838m cm^{-1}.

Infra-red (CH_2Cl_2)

ν_{CO} 1991s, 1919vs, 1835m cm^{-1}.

^{1}H n.m.r. (CD_2Cl_2)

δ 5.84 (s, 1H, C$\underline{H}$), 5.32 (s, 10H, $C_5\underline{H}_5$), 4.47 (s, 2H, CC$\underline{H}_2$), 3.47 (q, 2H, C$\underline{H}_2CH_3$), 1.13 (t, 3H, $CH_2C\underline{H}_3$) ppm.

^{13}C n.m.r. (CD_2Cl_2)

δ 231.9, 227.9 (s, $\underline{C}O$), 90.9 (s, $\underline{C}_5H_5$), 81.6 (s, $\underline{C}H$), 74.2 (s, C$\underline{C}H_2$), 66.5 (s, O$\underline{C}H_2$), 57.3 (s, $\underline{C}CH_2$), 22.2 (s, $\underline{C}H_3$) ppm.

Reaction of (7) with $(Me_3Si)_2NLi$

A solution of complex (7) in THF at -78 °C was treated with a small excess of lithium *bis*-trimethylsilylamide solution. As the solutions were mixed an immediate colour change from yellow to green was observed. The solution was allowed to warm up and an almost immediately the colour changed to dark purple. The solvent was removed *in vacuo* and no attempts to purify the resulting dark oil yielded a complex which could be characterised.

Preparation of $[Rh(NCMe)_2(norbornadiene)]BF_4$ (9)

Norbornadienerhodium(I) chloride was prepared, according to the literature method[130], by the reaction of rhodium(III) chloride with norbornadiene in ethanol for two days. $[Rh(NBD)Cl]_2$ (500 mg, 1.09 mmol) was dissolved in 20 cm^3 MeCN and 1 molar equivalent (213 mg) $AgBF_4$ was added at room temperature. The mixture was

stirred for 15 minutes and a white precipitate of AgCl was observed. The yellow solution was filtered through Celite and was reduced to minimum volume *in vacuo*. Addition of diethyl ether resulted in the precipitation of the product which was washed with diethyl ether and was isolated as a bright yellow powder (750 mg, 95% yield). The observed data concurred with previously recorded observations regarding an alternative preparative method[131].

Microanalysis

$C_{11}H_{14}N_2RhBF_4$ requires: C, 36.3 %; H, 3.9 %; N, 7.7 %

found: C, 35.7 %; H, 3.9 %; N, 7.1 %

^{1}H n.m.r. ($CDCl_3$)

4.28 (q, 4H, C<u>H</u>=CH), 3.88 (m, 2H, C<u>H</u>), 2.33 (s, 6H, C<u>H</u>$_3$CN), 1.26 (t, 2H, C<u>H</u>$_2$) ppm.

Preparation of [Rh(NCMe)(norbornadiene)]BF_4 (10)

This complex was prepared using an identical method to that given above for the preparation of [Rh(NCMe)$_2$(norbornadiene)]BF_4 with the following exception. When the solution had been filtered, all the solvent was removed *in vacuo* and the resulting solid was kept under vacuum for a further two hours to remove all traces of free acetonitrile before being washed with a little diethyl ether. The dark yellow solid was similar in appearance to [Rh(NCMe)$_2$(norbornadiene)]BF_4 and again was prepared in high yield (644 mg, 92% yield).

Microanalysis

$C_9H_{11}NRhBF_4$ requires: C, 33.5 %; H, 3.4 %; N, 4.3 %

found: C, 33.4 %; H, 3.7 %; N, 4.9 %

^{1}H n.m.r. ($CDCl_3$)

4.09 (dd, 4H, CH=CH), 3.84 (m, 2H, CH), 2.33 (s, 3H, CH_3CN), 1.21 (t, 2H, CH_2) ppm.

^{13}C n.m.r. ($CDCl_3$)

124.0 (s, NCMe), 61.4 (s, CH, C_7H_8), 55.5 (bs, CH, C_7H_8), 50.5 (s, CH_2, C_7H_8), 2.85 (s, NCMe) ppm.

^{19}F n.m.r. (CD_2CL_2), 21 °C

δ -153.07, -153.12 (d, ratio 1:4, 4F, BF_4) ppm.

Preparation of $[Rh(NCMe)_2(norbornadiene)]BF_4$ (9) from (10)

The monoacetonitrile complex (10) (100 mg, 0.31 mmol) was dissolved in the minimum volume of acetonitrile and stirred for 15 minutes. Diethyl ether was added and a yellow precipitate was observed which was washed with diethyl ether. Analysis demonstrated it to be $[Rh(NCMe)_2(norbornadiene)]BF_4$ (9) (110 mg, 98% yield).

Data for (9) are presented above.

Preparation of $[Mo_2Rh(\mu\text{-}C{\equiv}CPh)(CO)_4(nbd)(\eta\text{-}C_5H_5)_2]$ (11)

A solution of $Li[Mo_2(\mu\text{-}C{\equiv}CPh)(CO)_4(\eta\text{-}C_5H_5)_2]$ was prepared by the following method. A solution of phenylacetylene (196 mg, 211 µl, 1.92 mmol)in 20 cm^3 THF was cooled to -78 °C and 1 equivalent of ^{t}BuLi solution was added. When the ^{t}BuLi entered the THF solution there was an instantaneous yellow colouration which dispersed as it reacted with the acetylene, hence the end-point of this reaction is denoted by a slight yellow tinge and any excess ^{t}BuLi can be destroyed by the addition of a few µl of HCCPh. $[Mo_2(CO)_4(\eta\text{-}C_5H_5)_2]$ (1.103 g, 1.92 mmol) was added and the solution was allowed to return to room temperature and stir for 2 hours.

To this red-brown $Li[Mo_2(\mu\text{-}C{\equiv}CPh)(CO)_4(\eta\text{-}C_5H_5)_2]$ solution was added 1 equivalent of $[Rh(NCMe)_2(norbornadiene)]BF_4$ (9) (700 mg, 1.92 mmol) and the resulting dark brown solution was stirred for a further 24 hours before the solvent was removed *in vacuo*. The residue was taken up in a large volume of diethyl ether, filtered through a Celite pad and recrystallised from CH_2Cl_2/hexane to give $[Mo_2Rh(\mu\text{-}C{\equiv}CPh)(CO)_4(nbd)(\eta\text{-}C_5H_5)_2]$ (11) as a brown powder in 75 % yield (625 mg).

Microanalysis

$C_{29}H_{23}Mo_2O_4Rh$ requires: C, 47.7 %; H, 3.2 %.
found: C, 47.7 %; H, 2.9 %.

Infra-red (CH_2Cl_2)

ν_{CO} 1935s, 1911s, 1863s cm^{-1}.

^{1}H n.m.r. (CD_2Cl_2)

δ 7.52, 7.33 (m, 2H, $C_6\underline{H}_5$), 7.21 (m, 1H, $C_6\underline{H}_5$), 5.51, 5.23 (s, 5H, $C_5\underline{H}_5$), 3.44 (m, 2H, $C_7\underline{H}_8$), 3.02 (m, 4H, $C_7\underline{H}_8$), 1.12 (t, 2H, $C_7\underline{H}_8$) ppm.

^{13}C n.m.r. (CD_2Cl_2)

δ 237.5, 232.8, 231.6 (s, $\underline{C}O$), 181.0 (d, $\underline{C}$, Cα, $^1J_{RhC}$ 9.2 Hz), 135.6 (s, $\underline{C}$, C_6H_5), 130.0, 127.7, 125.7 (s, $\underline{C}H$, C_6H_5), 96.8 (d, $\underline{C}$, Cβ, $^1J_{RhC}$ 9.2 Hz), 91.7, 88.8 (s, $\underline{C}_5H_5$), 59.9, 58.9 (d, $\underline{C}H$, C_7H_8, $^1J_{RhC}$ 6.1 Hz), 55.1, 53.7 (d, $\underline{C}H$, C_7H_8, $^1J_{RhC}$ 9.2 Hz), 46.0 (s, $\underline{C}H$, C_7H_8), 29.0 (s, $\underline{C}H_2$, C_7H_8) ppm.

Preparation of $[Mo_2Rh(\mu\text{-}C{\equiv}CPh)(CO)_6(\eta\text{-}C_5H_5)_2]$ (12)

The complex (11) (100 mg, 0.14 mmol) was dissolved in 30 cm^3 of CH_2Cl_2 and CO was bubbled through the solution for one hour at room temperature. The reaction was monitored by infra-red spectrophotometry. When the reaction was complete the solvent was reduced to minimum volume *in vacuo* and loaded onto a column packed with alumina. Elution with diethyl ether elicited a red/brown band which was recrystallised from diethyl ether/hexane to give brown micro-crystals of complex (12) (90 mg, 95% yield). An X-ray crystal structure of (12) was obtained.

Microanalysis

$C_{24}H_{15}Mo_2O_6Rh$ requires: C, 41.5 %, H, 2.2%.

found: C, 41.6 %, H, 2.2%.

Infra-red (CH_2Cl_2)

ν_{CO} 2019s, 1965s, 1949m, 1923m, 1859m cm^{-1}.

^{1}H n.m.r. (CD_2Cl_2)

δ 7.73 (m, 2H, C_6H_5), 6.96 (m, 3H, C_6H_5), 5.10, 4.70 (s, 5H, C_5H_5) ppm.

^{13}C n.m.r. (CD_2Cl_2), -60 °C.

δ 237.2, 235.4 (s, CO), 227.1 (d, CO, $^1J_{RhC}$ 36.7 Hz), 199.1 (bs, C, Cα), 137.7, (s, C, C_6H_5), 130.5, 129.1, 128.1 (s, CH, C_6H_5), 105.8 (d, C, Cβ, $^1J_{RhC}$ 12.2 Hz), 94.5, 89.4 (s, C_5H_5) ppm.

Preparation of $[Mo_2Rh(\mu\text{-}C{\equiv}C^tBu)(CO)_4(nbd)(\eta\text{-}C_5H_5)_2]$ (13)

A solution of $Li[Mo_2(\mu\text{-}C{\equiv}C^tBu)(CO)_4(\eta\text{-}C_5H_5)_2]$ was prepared by the method described above using *tert*-butyl acetylene instead of phenylacetylene and was reacted with one equivalent of $[Rh(NCMe)_2(norbornadiene)]BF_4$ (9) for 24 hours at room temperature in THF. The solvent was removed *in vacuo* and the residue was taken up in a large volume of diethyl ether, filtered through a Celite pad and recrystallised from CH_2Cl_2/hexane to give $[Mo_2Rh(\mu\text{-}C{\equiv}C^tBu)(CO)_4(nbd)(\eta\text{-}C_5H_5)_2]$ (13) as a brown powder in 78% yield (115 mg).

Microanalysis

$C_{27}H_{27}O_4Mo_2Rh$ requires: C, 45.7 %, H, 3.8 %.

found: C, 45.3 %, H, 3.8 %.

Infra-red (CH_2Cl_2)

ν_{CO} 1931s, 1872s, 1862s, 1825w, sh cm^{-1}.

^{1}H n.m.r. (CD_2Cl_2) 25 °C.

δ 5.47, 5.30 (bs, 5H, $C_5\underline{H}_5$), 4.13 (bs, 2H, C$\underline{H}$=CH, C_7H_8), 3.66 (bm, 2H, C$\underline{H}$, C_7H_8), 3.41 (bs, C$\underline{H}$=CH, 2H, C_7H_8), 1.34 (bt, 2H, C$\underline{H}_2$, C_7H_8), 1.22 (s, 9H, $C(C\underline{H}_3)_3$) ppm.

^{1}H n.m.r. (CD_2Cl_2) 40 °C, Cp and nbd H_a and H_b regions

δ 5.23 (bs, 10H, $C_5\underline{H}_5$), 3.69 (bs, 4H, C$\underline{H}$=CH, C_7H_8), 3.61 (bm, 2H, C$\underline{H}$, C_7H_8) ppm.

^{1}H n.m.r. (CD_2Cl_2) -40 °C, Cp and nbd Ha and Hb regions

δ 5.62, 5.47 (s, 5H, $C_5\underline{H}_5$), 4.38, 3.99, 3.79 (bs, 1H, C$\underline{H}$=CH, C_7H_8), 3.63 (bm, 2H, C$\underline{H}$, C_7H_8), 3.16 (bs, 1H, C$\underline{H}$=CH, C_7H_8) ppm.

^{13}C n.m.r. (CD_2Cl_2)

δ 209.3, 203.0 (s, $\underline{C}$O), 192.5 (s, C$\underline{\alpha}$), 110.0 (s, C$\underline{\beta}$), 93.7, 87.2 (s, $\underline{C}_5H_5$), 62.3, 62.23, 62.19, 60.2, 53.9, 47.7 (s, $\underline{C}$H, C_7H_8), 37.2 (s, $\underline{C}Me_3$), 32.7 (s, C$\underline{Me}_3$), 31.5 (s, $\underline{C}H_2$, C_7H_8) ppm.

Preparation of $[Mo_2Rh(\mu\text{-}C{\equiv}C^tBu)(CO)_6(\eta\text{-}C_5H_5)_2]$ (14)

The complex (14) was prepared in identical fashion to (12) by bubbling CO through a solution of (13). A similar workup produced brown micro-crystals of (14) in 93% yield.

Microanalysis

$C_{22}H_{19}O_6Mo_2Rh$ requires: C, 39.2 %, H, 2.8 %.

found: C, 39.1 %, H, 3.1 %.

Infra-red (CH_2Cl_2)

ν_{CO} 2031s, 1975s, 1946m, 1923s, 1862s cm^{-1}.

^1H n.m.r. (CD_2Cl_2)

δ 5.52, 5.48 (bs, 5H, C_5H_5), 1.42 (s, 9H, CMe_3) ppm.

^{13}C n.m.r. (CD_2Cl_2)

δ 236.5, 236.3, 227.7, 226.3 (s, Mo-CO), 203.0, 202.6 (d, Rh-CO, $^1J_{RhC}$ 5.4 Hz), 194.0 (d, Cα, $^1J_{RhC}$ 77.3 Hz), 126.5 (d, Cβ, $^1J_{RhC}$ 12.2 Hz), 93.1, 87.7 (s, C_5H_5), 37.6 (s, CMe_3), 34.0 (s, CMe_3) ppm.

Preparation of $[Ir(\text{cyclo-octa-1,5-diene})(NCMe)_2]BF_4$ (15)

A sample of $[Ir(C_8H_{12})Cl]_2$ was prepared, according to the literature method[131], by the reaction of iridium(III) chloride with cyclo-octa-1,5-diene in ethanol for two days. A

solution of $[Ir(C_8H_{12})Cl]_2$ (1.00 g, 1.49 mmol) in MeCN was prepared and 2.1 molecular equivalents (6.9 mg) of $AgBF_4$ were added. The solution was left to stir for 15 minutes and a white precipitate of AgCl was observed to form. The yellow solution was filtered through Celite and was reduced to minimum volume *in vacuo*. Addition of diethyl ether resulted in the precipitation of the product which was washed with diethyl ether and was isolated as a bright yellow powder (1.19 g, 85% yield). The observed data concurred with previously recorded observations regarding an alternative preparative method for (15)[132].

Microanalysis

$C_{12}H_{18}BF_4N_2Ir$ requires: C, 30.7 %, H, 3.8 %.

found: C, 31.0 %, H, 3.9 %.

^{1}H n.m.r. ($CDCl_3$)

δ 4.17 (s, 4H, C<u>H</u>=CH), 2.39 (s, 6H, NCC<u>H</u>$_3$), 2.20, 1.70 (m, 8H, C<u>H</u>$_2$CH$_2$) ppm.

Preparation of $[Mo_2Ir(\mu\text{-}C{\equiv}CPh)(CO)_4(COD)(\eta\text{-}C_5H_5)_2]$ (16)

To a solution of $Li[Mo_2(\mu\text{-}C{\equiv}CPh)(CO)_4(\eta\text{-}C_5H_5)_2]$ in THF at ambient temperature, prepared in the manner outlined above, was added one equivalent (324 mg, 0.69 mmol) of $[Ir(COD)(NCMe)_2]BF_4$ (15). A colour change to brown was observed and the solution was stirred for a further 24 hours. The solvent was removed *in vacuo* and the residue was taken up in a large volume of diethyl ether, filtered through a Celite pad and recrystallised from CH_2Cl_2/hexane to give $[Mo_2Ir(\mu\text{-}C{\equiv}CPh)(CO)_4(COD)(\eta\text{-}C_5H_5)_2]$ (16) as a brown powder in 61% yield (351 mg).

Microanalysis

$C_{30}H_{27}O_4IrMo_2$ requires: C, 43.1 %, H, 3.3 %.

found: C, 43.3 %, H, 3.1 %.

Infra-red (CH_2Cl_2)

ν_{CO} 2034s, 2008s, 1975s cm^{-1}.

^{1}H n.m.r. (CD_2Cl_2)

δ 7.33 (m, 5H, $C_6\underline{H}_5$), 5.49, 5.30 (s, 5H, $C_5\underline{H}_5$), 4.20 (bs, 2H, C$\underline{H}$=CH, C_8H_{12}), 2.80 (bs, 2H, C$\underline{H}$=CH, C_8H_{12}), 2.34, 1.12 (m, 4H, C$\underline{H}_2$, C_8H_{12}) ppm.

^{13}C n.m.r. (CD_2Cl_2)

δ 228.6, 224.9 (s, $\underline{C}$O), 172.2 (s, $\underline{C}\alpha$), 129.3, 129.0, 128.7, 128.5, 128.2 (s, $\underline{C}_6H_5$), 101.1 (s, $\underline{C}\beta$), 98.2 (s, $\underline{C}_5H_5$), 95.1, 90.7 (s, $\underline{C}$H=CH, C_8H_{12}), 53.3, 47.3 (s, CH$\underline{C}H_2$, C_8H_{12}), 18.7, 16.7 (s, CHCH$_2\underline{C}H_2$, C_8H_{12}) ppm.

Preparation of $[Mo_2Ir(\mu\text{-}C{\equiv}CPh)(CO)_6(\eta\text{-}C_5H_5)_2]$ (17)

The complex (17) was prepared in identical fashion to (12) by bubbling CO through a solution of (16). A similar workup produced brown micro-crystals of (17) in 87% yield.

Microanalysis

$C_{24}H_{15}O_6Mo_2Ir$ requires: C, 36.8 %, H, 1.9 %.

found: C, 36.3 %, H, 1.8 %.

^{1}H n.m.r. (CD_2Cl_2)

δ {7.72, 7.38, 7.27} (m, 5H, $C_6\underline{H}_5$), 5.22 (s, 10H, $C_5\underline{H}_5$) ppm.

^{13}C n.m.r. (CD_2Cl_2)

δ 231.6, 227.1, 205.2, (s, $\underline{C}O$), 187.3 (s, $\underline{C}\alpha$), 131.4, 130.6, 129.4, 129.0, 128.4, 127.1 (s, $\underline{C}_6H_5$), 95.6 (s, $\underline{C}\beta$), 92.2, 91.5 (s, $\underline{C}_5H_5$) ppm.

Preparation of $[Mo_2Ir(\mu\text{-}C{\equiv}C^tBu)(CO)_4(COD)(\eta\text{-}C_5H_5)_2]$ (18)

To a solution of $Li[Mo_2(\mu\text{-}C{\equiv}C^tBu)(CO)_4(\eta\text{-}C_5H_5)_2]$ in THF at ambient temperature, prepared in the manner outlined above, was added one equivalent (80 mg, 0.17 mmol) of $[Ir(COD)(NCMe)_2]BF_4$ (15). A colour change to brown was observed and the solution was stirred for a further 24 hours. The solvent was removed *in vacuo* and the residue was taken up in a large volume of diethyl ether, filtered through a Celite pad and recrystallised from CH_2Cl_2/hexane to give $[Mo_2Ir(\mu\text{-}C{\equiv}C^tBu)(CO)_4(COD)(\eta\text{-}C_5H_5)_2]$ (18) as a brown powder in 65 % yield.

Microanalysis

$C_{28}H_{31}O_4Mo_2O_4$ requires: C, 41.2 %, H, 3.8 %.

found: C, 41.1 %, H, 3.8 %.

Infra-red (CH_2Cl_2)

ν_{CO} 1958m, 1933m, 1902s, 1842s cm^{-1}.

^{1}H n.m.r. (CD_2Cl_2)

δ 6.05, 5.56 (s, 5H, $C_5\underline{H}_5$), 4.25 (bs, 2H, C<u>H</u>=CH, C_8H_{12}), 2.91, 2.75 (bs, 1H, C<u>H</u>=CH, C_8H_{12}), 2.31 (m, 4H, $C\underline{H}_2$, C_8H_{12}), 1.27 (s, 9H, C<u>Me</u>$_3$), 0.89 (m, 4H, $C\underline{H}_2$, C_8H_{12}) ppm.

^{13}C n.m.r. (CD_2Cl_2)

δ 237.5, 218.7, 217.7 (s, <u>C</u>O), 198.5 (s, <u>C</u>α), 133.0 (s, <u>C</u>β), 101.3 (s, $\underline{C}_5H_5$), 98.9, 97.8 (s, <u>C</u>H=CH, C_8H_{12}), 41.5 (s, <u>C</u>Me$_3$), 38.7 (s, $\underline{C}_8H_{12}$), 36.5 (s, C<u>Me</u>$_3$), 36.1, 34.8, 29.5, 20.6 (s, $CHCH_2\underline{C}H_2$, C_8H_{12}) ppm.

Preparation of $[Mo_2Ir(\mu\text{-}C{\equiv}C^tBu)(CO)_6(\eta\text{-}C_5H_5)_2]$ (19)

The complex (19) was prepared in identical fashion to (12) by bubbling CO through a solution of (18). A similar workup produced brown crystals of (19) in 88% yield.

Microanalysis

$C_{22}H_{19}O_6Mo_2Ir$ requires: C, 34.6 %, H, 2.5 %.

found: C, 34.2 %, H, 2.3 %.

Infra-red (CH_2Cl_2)

ν_{CO} 1985m, 1916s, 1831w cm^{-1}.

^{1}H n.m.r. (CD_2Cl_2)

δ 5.41 (bs, 10H, C_5H_5), 1.28 (s, 9H, CMe_3) ppm.

^{13}C n.m.r. (CD_2Cl_2)

δ 233.5, 234.0, 218.7 (s, CO), 173.3 (s, Cα), 96.2 (s, Cβ), 91.2 (s, C_5H_5), 34.1 (s, CMe_3), 29.9 (s, CMe_3) ppm.

Preparation of $[Mo_2Rh(\mu\text{-}C{\equiv}CPh)(CO)_4(nbd)(\eta\text{-}C_5Me_5)_2]$ (20)

A solution of $Li[Mo_2(\mu\text{-}C{\equiv}CPh)(CO)_4(\eta\text{-}C_5Me_5)_2]$ was prepared by the following method. A solution of phenylacetylene (102 mg, 110 µl, 1.00 mmol) in 20 cm^3 THF was cooled to -78 °C and 1 equivalent of ^{t}BuLi solution was added. $[Mo_2(CO)_4(\eta\text{-}C_5Me_5)_2]$ (573 mg, 1.00 mmol) was added and the solution was allowed to return to room temperature and stir for 16 hours. A subtle colour change to a darker red was observed, the progress of the reaction being monitored by i.r. spectroscopy.

To this $Li[Mo_2(\mu\text{-}C{\equiv}CPh)(CO)_4(\eta\text{-}C_5Me_5)_2]$ solution was added 1 equivalent of $[Rh(NCMe)_2(norbornadiene)]BF_4$ (9) (323 mg, 1.00 mmol) and the resulting brown solution was stirred for a further 24 hours before the solvent was removed *in vacuo*. The residue was taken up in a large volume of diethyl ether, filtered through a Celite pad and recrystallised from CH_2Cl_2/hexane to give $[Mo_2Rh(\mu\text{-}C{\equiv}CPh)(CO)_4(nbd)(\eta\text{-}C_5Me_5)_2]$ (20) as a brown powder in 70 % yield (609 mg).

Microanalysis

$C_{39}H_{43}O_4Mo_2Rh$ requires: C, 53.8 %, 5.0 %.

found: C, 53.6 %, 4.7 %.

Infra-red (CH_2Cl_2)

ν_{CO} 1956s, 1929s, 1850w, 1813m cm^{-1}.

^{1}H n.m.r. (CD_2Cl_2)

δ 7.05 (m, 5H, $C_6\underline{H}_5$), 4.87 (bs, 2H, C<u>H</u>=CH, C_7H_8), 3.92 (bs, 2H, C<u>H</u>=CH, C_7H_8), 3.08 (bm, 2H, C<u>H</u>CH_2, C_7H_8), 2.02 (s, 30H, $C_5\underline{Me}_5$), 1.59 (bt, 2H, CH$C\underline{H}_2$, C_7H_8) ppm.

^{13}C n.m.r. (CD_2Cl_2)

δ 244.4, 244.2, 230.54, 230.50 (s, <u>C</u>O), 198.0 (s, <u>C</u>α), 136.2 (s, <u>C</u>β), 128.6, 126.0, 125.6 (s, $\underline{C}_6H_5$), 108.8 (s, $\underline{C}_5Me_5$), 62.25, 62.19, 46.6 (s, <u>C</u>H, C_7H_8), 10.9 (s, $C_5\underline{Me}_5$) ppm.

Preparation of $[Mo_2Rh(\mu\text{-}C{\equiv}C^tBu)(CO)_4(nbd)(\eta\text{-}C_5Me_5)_2]$ (21)

A solution of $Li[Mo_2(\mu\text{-}C{\equiv}C^tBu)(CO)_4(\eta\text{-}C_5Me_5)_2]$ was prepared by the following method. A solution of *tert*-butyl acetylene (107 mg, 161 μl, 1.31 mmol) in 20 cm^3 THF was cooled to -78 °C and 1 equivalent of ^{t}BuLi solution was added. $[Mo_2(CO)_4(\eta\text{-}C_5Me_5)_2]$ (750 mg, 1.31 mmol) was added and the solution was allowed to return to room temperature and stir for 16 hours. A gradual colour change to purple was observed.

To this $Li[Mo_2(\mu\text{-}C{\equiv}C^tBu)(CO)_4(\eta\text{-}C_5Me_5)_2]$ solution was added 1 equivalent of $[Rh(NCMe)_2(norbornadiene)]BF_4$ (9) (422 mg, 1.31 mmol) and the resulting brown solution was stirred for a further 24 hours before the solvent was removed *in vacuo*. The residue was taken up in a large volume of diethyl ether, filtered through a Celite pad and recrystallised from CH_2Cl_2/hexane to give $[Mo_2Rh(\mu\text{-}C{\equiv}C^tBu)(CO)_4(nbd)(\eta\text{-}C_5Me_5)_2]$ (21) as a brown powder in 73 % yield (810 mg).

Microanalysis

$C_{37}H_{47}O_4Mo_2Rh$ requires: C, 52.3 %, H, 5.6 %.

found: C, 52.0 %, H, 5.6 %.

Infra-red (CH_2Cl_2)

ν_{CO} 1958m, 1923m, 1867s, 1833m cm^{-1}.

^1H n.m.r. (CD_2Cl_2)

δ 4.06 (bs, 2H, C<u>H</u>=CH, C_7H_8), 3.84 (bs, 2H, C<u>H</u>=CH, C_7H_8), 3.74 (bm, 2H, C<u>H</u>CH_2, C_7H_8), 1.94 (bt, 2H, CHC<u>H</u>$_2$, C_7H_8), 1.90 (s, 30H, C_5<u>Me</u>$_5$), 1.21 (s, 9H, $C(C\underline{H}_3)_3$) ppm.

^{13}C n.m.r. (CD_2Cl_2)

δ 242.0, 238.7 (s, <u>C</u>O), 200.4 (s, <u>C</u>α), 143.2 (s, <u>C</u>β), 103.0 (s, <u>C</u>$_5$Me$_5$), 67.5, 67.3, 53.3, 50.1, 39.8 (s, <u>C</u>H, C_7H_8), 37.3 (s, <u>C</u>Me_3), 32.2 (s, <u>C</u>H_2, C_7H_8), 31.9 (s, C<u>Me</u>$_3$), 9.7 (s, C_5<u>Me</u>$_5$) ppm.

Preparation of $[Mn(CO)_3(NCMe)_3]BF_4$ (22)

To a solution of $Mn(CO)_5Br$ (2.75 g, 10.0 mmol) in 20 cm^3 acetonitrile was added slightly more than one equivalent (2.00 g, 10.3 mmol) of $AgBF_4$. Light was excluded from the reaction vessel and the solution was refluxed for 16 hours. The precipitated silver bromide was filtered off using a Celite pad and the resulting solution was evaporated to dryness *in vacuo* yielding a yellow powder which was recrystallised from $MeCN/Et_2O$ to give (22) in a 67% yield. The analysis is compatible with that given in the literature[133] for $[Mn(CO)_3(NCMe)_3]ClO_4$.

Microanalysis

$C_9ClH_9N_3O_7Mn$ requires: C, 29.9 %, H, 2.5 %, N, 11.6 %.

found: C, 29.3 %, H, 2.6 %, N, 10.9 %.

Infra-red (MeCN)

ν_{CO} 2066s, 2026s, 1975m cm^{-1}

^{1}H n.m.r. (CD_2Cl_2)

δ 2.27 (s, 9H, NCMe) ppm.

Preparation of $[Mo_2Mn(\mu\text{-}C{\equiv}CPh)(CO)_7(\eta\text{-}C_5H_5)_2]$ (23)

A solution of $Li[Mo_2(\mu\text{-}C{\equiv}CPh)(CO)_4(\eta\text{-}C_5H_5)_2]$ (1.00 mmol) in 25 cm^3 THF was prepared as described above and 1.1 equivalents (384 mg) of $[Mn(CO)_3(NCMe)_3]BF_4$ (22) were added. The solution darkened and was left to stir for 16 hours, whereupon the solvent was removed *in vacuo*, the residue redissolved in CH_2Cl_2 and filtered

through a Celite pad. The solvent was again removed *in vacuo*, and the residue placed on a Florasil column. Elution with 10:1 hexane/Et_2O removed a narrow red band. Subsequent elution with diethyl ether produced a narrow orange band followed by a broad brown band which was collected and recrystallised from diethyl ether/hexane to give (23) as dark red micro-crystals (420 mg, 62 % yield).

Microanalysis

$C_{25}H_{15}O_7MnMo_2$ requires: C, 44.5 %, H, 2.2 %.
found: C, 43.9 %, H, 2.4 %.

Infra-red (CH_2Cl_2)

ν_{CO} 2017s, 1986w, 1959m, 1945s, 1917w cm^{-1}

^{1}H n.m.r. (CD_2Cl_2)

δ 7.73 (m, 2H, C_6H_5), 7.44 (m, 3H, C_6H_5), 5.37 (bs, 10H, C_5H_5) ppm.

^{13}C n.m.r. (CD_2Cl_2)

δ 232.2, 230.1, 226.0 (s, CO), 188.9 (s, Cα), 139.1 (s, C, C_6H_5), 130.7, 130.1, 129.0, 128.1, 127.8 (s, CH, C_6H_5), 97.9 (s, Cβ), 92.3, 92.0 (s, C_5H_5) ppm.

Preparation of $[Mo_2Mn(\mu\text{-}C{\equiv}C^tBu)(CO)_7(\eta\text{-}C_5H_5)_2]$ (24)

A solution of $Li[Mo_2(\mu\text{-}C{\equiv}C^tBu)(CO)_4(\eta\text{-}C_5H_5)_2]$ (0.50 mmol) in 25 cm^3 THF was prepared as described above and 1.1 equivalents (192 mg) of the manganese complex $[Mn(CO)_3(NCMe)_3]ClO_4$ prepared according to the literature method[133] were added.

The solution darkened and was left to stir for 16 hours, whereupon the solvent was removed *in vacuo*, the residue redissolved in CH_2Cl_2 and filtered through a Celite pad. The solvent was again removed *in vacuo*, and the residue placed on a Florasil column. Elution with 10:1 hexane/Et_2O removed a narrow red band. Subsequent elution with diethyl ether produced a narrow orange band followed by a broad brown band which was collected and recrystallised from diethyl ether/hexane to give (24) as dark red micro-crystals (230 mg, 70 % yield).

Microanalysis

$C_{23}H_{19}O_7MnMo_2$ requires: C, 42.2 %, H, 2.9 %.

found: C, 41.9 %, H, 2.9 %.

Infra-red (CH_2Cl_2)

ν_{CO} 2016s, 2008w, 1983m, 1950s, 1921m cm^{-1}

^{1}H n.m.r. ($CDCl_3$) 20 °C

δ 5.39 (s, 10H, C_5H_5), 1.56 (s, 9H, CMe_3) ppm.

^{1}H n.m.r. ($CDCl_3$) -40 °C

δ 5.46, 5.36 (s, 5H, C_5H_5), 1.52 (s, 9H, CMe_3) ppm.

^{13}C n.m.r. ($CDCl_3$) 20 °C

δ 235.6, 231.2, 230.0, 226.3 (s, CO), 184.4 (s, Cα), 109.9 (s, Cβ), 92.1, 89.1 (s, C_5H_5), 38.7 (s, CMe_3), 34.0 (s, CMe_3) ppm.

^{13}C n.m.r. ($CDCl_3$) 30 °C {CO and C_5H_5 region}

δ 226.4 (bs, CO), 110.4 (bs, C_5H_5) ppm.

^{13}C n.m.r. ($CDCl_3$) 55 °C {CO and C_5H_5 region}

δ 232.1, 228.6, 226.3 (bs, CO), 90.6 (s, C_5H_5) ppm.

Preparation of $[Mo_2Ru(\mu\text{-}C{\equiv}CPh)(CO)_4(\eta\text{-}C_5H_5)_3]$ (25)

A solution of $Li[Mo_2(\mu\text{-}C{\equiv}CPh)(CO)_4(\eta\text{-}C_5H_5)_2]$ (0.23 mmol) in 15 cm^3 THF was prepared as described above and 1 equivalent (84 mg) of $[Ru(CO)(NCMe)_2(\eta\text{-}C_5H_5)]BF_4$ was added. The solution darkened and a gas was evolved. It was left to stir for 16 hours, whereupon the solvent was removed *in vacuo*, the residue redissolved in CH_2Cl_2 and filtered through a Florasil pad. The solvent was again removed *in vacuo*, and the residue recrystallised from CH_2Cl_2/hexane to give complex (25) as a dark brown powder (55 mg, 34 % yield).

Microanalysis

$C_{27}H_{20}O_4Mo_2Ru$ requires: C, 46.2 %, H, 2.9 %.

found: C, 45.7 %, H, 2.9 %.

Infra-red (CH_2Cl_2)

ν_{CO} 1964m, 1929s, 1872m, 1748m cm^{-1}

^{1}H n.m.r. ($CDCl_3$)

δ 7.34 (m, 5H, $C_6\underline{H}_5$), 5.65 (s, 5H, $RuC_5\underline{H}_5$), 5.06, 4.97 (s, 5H, $MoC_5\underline{H}_5$) ppm.

^{13}C n.m.r. ($CDCl_3$)

δ 241.6, 239.0, 228.2, 223.8 (s, $\underline{C}O$), 203.1 (s, $\underline{C}\alpha$), 128.2, 128.0, 127.5, 126.8 (s, $\underline{C}_6H_5$), 99.6 (s, $Ru\underline{C}_5H_5$), 93.2 (s, $\underline{C}\beta$), 91.0 (s, $Mo\underline{C}_5H_5$) ppm.

Protonation of $[Mo_2Rh(\mu\text{-}C{\equiv}C^tBu)(CO)_6(\eta\text{-}C_5H_5)_2]$ (14)

A sample of complex (14) (150 mg, 0.022 mmol) was dissolved in 20 cm^3 CH_2Cl_2 and cooled to -78 °C. 1.1 equivalents of $HBF_4.Et_2O$ were added and the solution was allowed to return to ambient temperature. The colour of the solution changed rapidly to dark green. The solution was reduced to minimum volume *in vacuo* and diethyl ether was added and a brown precipitate was observed. The supernatant liquid was removed and the product was washed with diethyl ether and recrystallised from CH_2Cl_2 to yield light brown crystals of (26) identified as $[Mo_2Rh(CCH^tBu)(CO)_6(\eta\text{-}C_5H_5)_2]BF_4$ in 87 % yield (147 mg).

Microanalysis

$C_{22}H_{20}O_6Mo_2RhBF_4$ requires:		C, 34.7 %, H, 2.7 %
	found:	C, 34.8 %, H, 2.8 %.

Infra-red (CH_2Cl_2)

ν_{CO} 2083s, 2047m, 2018m, 1956w, 1913w cm^{-1}.

^{1}H n.m.r. (CD_2Cl_2)

δ 5.93 (bs, 5H, C_5H_5), 5.78 (s, 1H, CH^tBu), 5.76 (bs, 5H, C_5H_5), 1.25 (s, 9H, CMe_3) ppm.

^{13}C n.m.r. (CD_2Cl_2)

δ 225.9, 223.0 (s, MoCO), 185.0 (s, Cα, $^1J_{RhC}$ 34.0 Hz), 149.1 (d, Cβ, $^1J_{RhC}$ 5.2 Hz), 95.4 (s, C_5H_5), 35.3 (s, CMe_3), 31.8 (s, CMe_3) ppm.

Protonation of $[Mo_2Ir(\mu\text{-}C{\equiv}CPh)(CO)_6(\eta\text{-}C_5H_5)_2]$ (17)

A sample of complex (17) (100 mg, 0.013 mmol) was dissolved in 10 cm^3 CH_2Cl_2 and cooled to -78 °C. 1.1 equivalents of $HBF_4.Et_2O$ were added and the solution was allowed to return to ambient temperature. The colour of the solution remained dark brown. The solution was reduced to minimum volume *in vacuo*, diethyl ether was added and a brown precipitate was observed. The supernatant liquid was removed and the product was washed with diethyl ether and recrystallised from CH_2Cl_2 to yield light brown crystals of (27) identified as $[Mo_2Ir(CCHPh)(CO)_6(\eta\text{-}C_5H_5)_2]BF_4$ in 89 % yield (101 mg).

Microanalysis

$C_{24}H_{16}O_6Mo_2IrBF_4$ requires: C, 33.1 %, H, 1.9 %.

found: C, 33.0 %, H, 2.0 %.

Infra-red (CH_2Cl_2)

ν_{CO} 2094w, 2045s, 2020m, 2003m, 1979m cm^{-1}.

ν_{BF} 1080s, 1034s cm^{-1}.

^{1}H n.m.r. (CD_2Cl_2)

δ 7.47 (m, 5H, C_6H_5), 5.67 (s, 1H, CHPh), 5.55 (s, 10H, C_5H_5) ppm.

^{13}C n.m.r. (CD_2Cl_2)

δ 240.1, 221.3, 219.5 (s, CO), 168.1 (s, Cα), 139.9 (s, Cβ), 130.9, 130.6, 130.5, 130.1, 129.8, 129.3 (s, C_6H_5), 93.0 (s, C_5H_5) ppm.

Preparation of [Fe(η-C_5H_5)(CO)(η^3-C_3H_5)] (28)

Complex (28) was prepared using a variation of the literature method[134]. Benzyltriethylammonium chloride (27g, 120 mmol) and allyl bromide (16.3 cm^3, 200 mmol) were dissolved in 75 cm^3 toluene in a flask fitted with a mechanical stirrer and 200 cm^3 5N NaOH were added, followed by 10g (40 mmol) of [Fe(η-C_5H_5)$(CO)_2$Br] prepared according to the literature method[135]. The reaction mixture was stirred rapidly for 16 hours and the organic layer was transferred directly onto a large chromatography column (50x6 cm) packed with alumina. The column was washed repeatedly with pentane until all the product had been removed. The solvent was removed *in vacuo* and the resultant orange oil was taken up in pentane and cooled to give orange crystals of (28) in 42 % yield (3.2g).

Preparation of *exo-syn*-[Fe(η-C_5H_5)(CO)(η^3-$CH_2CHCHCHO$)] (29)

A solution of complex (28) (1.74 g, 9.09 mmol) in 40 cm^3 of CH_2Cl_2 was cooled to -78 °C and treated with 1.1 equivalents (1.49 cm^3, 9.90 mmol) of $HBF_4.Et_2O$. The solution was stirred for 15 minutes and an excess of 1-trimethylsilyloxybuta-1,3-diene

(4.0 cm^3, 22.8 mmol) was added. The orange solution deepened in colour and was allowed to return to ambient temperature whereupon the colour changed to dark red. The solution was allowed to stir further for one hour and reduced to a volume of 10 cm^3 *in vacuo*. The concentrate was transferred to a column packed with alumina and eluted with a 1:1 mixture of hexane/dichloromethane. The product moved as an orange band and the solvent was removed *in vacuo* to give (29) as an orange powder in 74 % yield (1.47g).

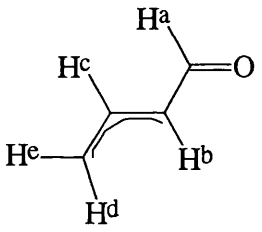

figure 121

Microanalysis

$C_{10}H_{10}O_2Fe$ requires: C, 55.1 %, H, 4.6 %.

found: C, 55.0 %, H, 4.6 %.

Infra-red (CH_2Cl_2)

ν_{CO} 1964s, 1667s cm^{-1}.

^{1}H n.m.r. (CD_2Cl_2)

δ 9.37 (d, 1H, H^a, $J(H^aH^b)$ 6.08 Hz), 5.33 (ddd, 1H, H^c, $J(H^bH^c)$ 9.78 Hz, $J(H^cH^d)$ 11.23 Hz, $J(H^cH^e)$ 7.24 Hz), 4.64 (s, 5H, C_5H_5), 3.08 (dd, 1H, H^e, $J(H^cH^e)$ 7.17 Hz, $J(H^dH^e)$ 1.15 Hz), 1.44 (dd, 1H, H^b, $J(H^aH^b)$ 6.20 Hz, $J(H^bH^c)$ 9.71 Hz), 1.19 (d, 1H, H^d, $J(H^cH^d)$ 11.45 Hz ppm.

^{13}C n.m.r. (CD_2Cl_2)

δ 220.9 (s. CO), 197.6 (s, CHO), 79.5 (s, C_5H_5), 77.5 (s, CH_2CH), 51.4 (s, CHCHO), 37.4 (s, CH_2) ppm.

Preparation of *exo-anti*-[Fe(η-C_5H_5)(CO)(η^3-$CH_2CHCHCHO$)] (30)

A solution of complex (29) (186 mg, 0.85 mmol) was dissolved in 20 cm^3 dichloromethane and cooled to -78 °C. 1.05 equivalents (79 μl, 0.89 mmol) of CF_3SO_3H were added, the solution darkened to red, and it was allowed to return to room temperature and to stir for 12 hours. 1.1 equivalents (131 μl, 0.94 mmol) of triethylamine were added and the solution was stirred for one hour during which time the colour lightened to yellow. The solution was reduced in volume *in vacuo* and chromatographed on a column packed with alumina. Elution with hexane developed two bands. The first, narrower, orange band was identified as *exo-syn*-[Fe(η-C_5H_5)(η^3-$CH_2CHCHCHO$)] (29) in 20 % yield. The second band was lighter in colour and the solvent was removed *in vacuo* affording a yellow powder characterised as *exo-anti*-[Fe(η-C_5H_5)(η^3-$CH_2CHCHCHO$)] (30) (77 mg, 42 % yield).
Protonation with $HBF_4.Et_2O$ gave the same result within experimental error, (29) in 19 % yield, (30) in 44 % yield.

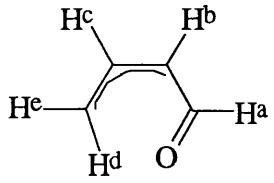

figure 122

Microanalysis

$C_{10}H_{10}O_2Fe$ requires: C, 55.1 %, H, 4.6 %.

found: C, 55.6 %, H, 4.9 %.

Infra-red (CH_2Cl_2)

ν_{CO} 1960s, 1655s cm^{-1}

^1H n.m.r. ($CDCl_3$)

δ 7.25 (d, 1H, H^a, $J(H^aH^b)$ 6.69 Hz), 5.25 (ddd, 1H, H^c, $J(H^bH^c)$ 7.33 Hz, $J(H^cH^e)$ 7.88 Hz, $J(H^cH^d)$ 11.91 Hz), 4.71 (s, 5H, C_5H_5), 4.30 (dd, 1H, H^b, $J(H^aH^b)$ 6.69 Hz, $J(H^bH^c)$ 7.33 Hz), 3.07 (dd, 1H, H^e, $J(H^cH^e)$ 7.88 Hz, $J(H^dH^e)$ 2.38 Hz), 1.33 (dd, 1H, H^d, $J(H^cH^d)$ 11.91 Hz, $J(H^dH^e)$ 2.38 Hz) ppm.

^{13}C n.m.r. ($CDCl_3$)

δ 221.4 (s, CO), 191.0 (s, CHO), 79.9 (s, C_5H_5), 77.6 (s, CH_2CH), 56.0 (s, CHCHO), 36.3 (s, CH_2) ppm.

Preparation of *cis*-[Fe(η-C_5H_5)(CO)(η^4-$CH_2CHCHCHOCMeO$)]BF_4 (31)

A solution of complex (28) (500 mg, 2.63 mmol) in 20 cm^3 of CH_2Cl_2 was cooled to -78 °C and treated with 1.1 equivalents (404 μl, 2.89 mmol) of $HBF_4.Et_2O$. The solution was stirred for 15 minutes and an excess of 1-acetoxybuta-1,3-diene (1.0 cm^3, 8.4 mmol) was added. The solution was allowed to return to room temperature and stirred for one hour. The solution was reduced to minimum volume *in vacuo* and the product was precipitated by addition of diethyl ether. The product was washed with

diethyl ether and dried under nitrogen to afford complex (31) as an orange powder (448 mg, 49 % yield).

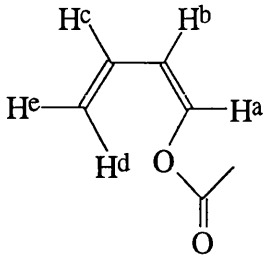

figure 123

Microanalysis

$C_{12}H_{13}FeO_3BF_4$ requires: C, 41.4 %, H, 3.8 %.

found: C, 41.1 %, H, 3.8 %.

^{1}H n.m.r. (CD_2Cl_2)

δ 6.70 (d, 1H, H^a, $J(H^aH^b)$ 7.50 Hz), 5.42 (s, 5H, C_5H_5), 5.16 (ddd, 1H, H^c, J values unclear), 4.26 (dd, H^b, $J(H^aH^b)$ 7.50 Hz), 3.39 (dd, H^e, $J(H^cH^e)$ 5.13 Hz), 2.17 (s, 3H, CH_3), 0.60 (dd, H^d, $J(H^cH^d)$ 10.26 Hz) ppm.

^{13}C n.m.r. (CD_2Cl_2)

δ 216.4 (s, CO), 96.3 (s, CHOC), 86.1 (s, C_5H_5), 83.4 (s, CH), 75.9 (s, CH), 50.5 (s, CH_2), 31.3 (s, CH_3) ppm.

Reaction of *cis*-[Fe(η-C_5H_5)(CO)(η^3-$CH_2CHCHCHOAc$)]BF_4 (31) with $NaHCO_3$

A solution of complex (31) (100 mg, 0.29 mmol) in 20 cm^3 dichloromethane was prepared and to this was added an excess of $NaHCO_3$ (500 mg, 6.0 mmol) dissolved in 5 cm^3 of distilled water. The mixture was stirred rapidly for 4 hours and the organic layer separated and reduced to minimum volume *in vacuo*. This was then chromatographed on a column packed with alumina and eluted with hexane. A yellow band was collected and the solvent removed *in vacuo* to leave a yellow powder characterised as *exo-anti*-[Fe(η-C_5H_5)(η^3-$CH_2CHCHCHO$)] (30) (47 mg, 75 % yield).

Data for complex (30) is presented above.

Preparation of *exo-anti*-[Fe(η-C_5H_5)(CO)(η^3-$CH_2CHCHCH{=}CH_2$)] (32)

The Wittig reagent $Ph_3P{=}CH_2$ was prepared by the addition of *n*-butyllithium (1.6 M solution in hexane) (344 µl, 0.55 mmol) to a suspension of Ph_3PMeBr (196 mg, 0.55 mmol) in 10 cm^3 of THF at -78 °C. With the yellow solution still at -78 °C, complex (30) (100 mg, 0.46 mmol) was added and the solution was allowed to return to room temperature. After two hours of stirring the solvent was removed *in vacuo*, the oily residue extracted with hexane (2x10 cm^3) and the extracts chromatographed on alumina. Elution with hexane developed an orange band which was collected and the solvent removed *in vacuo* to afford (32) as an orange oil (67 mg, 68 % yield).

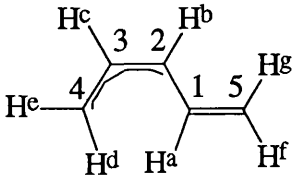

figure 124

Infra-red (CH_2Cl_2)

ν_{CO} 1934s, 1610w (alkene) cm^{-1}.

^1H n.m.r. (CD_2Cl_2)

δ 5.07 (ddd, 1H, H^a, $J(H^aH^b)$ 15.75 Hz, $J(H^aH^f)$ 6.96 Hz, $J(H^aH^g)$ 9.53 Hz), 4.63 (d, 1H, H^g, $J(H^aH^g)$ 9.53 Hz), 4.55 (s, 5H, C_5H_5), 4.50 (d, 1H, H^f, $J(H^aH^f)$ 6.96 Hz), 3.05 (ddd, 1H, H^c, $J(H^bH^c)$ 6.42 Hz, $J(H^cH^d)$ 10.08 Hz, $J(H^cH^e)$ 6.59 Hz), 1.27 (dd, 1H, H^e, $J(H^cH^e)$ 6.59 Hz), 1.17 (dd, 1H, H^d, $J(H^cH^d)$ 10.08 Hz), 0.88 (dd, 1H, H^b, $J(H^aH^b)$ 15.75 Hz, $J(H^bH^c)$ 6.42 Hz) ppm.

^{13}C n.m.r. (CD_2Cl_2)

δ 222.2 (s, CO), 140.5 (s, C^1), 107.7 (s, C^5), 79.1 (s, C_5H_5), 72.2 (s, C^3), 56.1 (s, C^2), 32.6 (s, C^4) ppm.

Preparation of *anti*-[Fe(η-C_5H_5)(CO)(η^3-$CH_2CHCHCH_2OH$)] (33)

A solution of complex (30) (50 mg, 0.23 mmol) in 5 cm^3 of methanol was prepared to which was added an excess of sodium borohydride was added (20 mg, 0.53 mmol) and the reaction mixture was allowed to stir for two hours during which time the colour of the solution changed from orange to bright yellow. The product was isolated by removing the solvent *in vacuo*, partially dissolving the yellow residue in 10 cm^3 diethyl ether and adding 0.5 cm^3 of distilled water whilst stirring rapidly. The yellow ethereal layer was separated, concentrated to 1 cm^3 *in vacuo* and chromatographed on alumina. Elution with a 3:1 mixture of diethyl ether/dichloromethane developed a yellow band which was collected and the solvent removed *in vacuo* to give a mixture of two

isomers (33a) and (33b) in a ratio of 60:40 as a yellow powder which was recrystallised from pentane (33 mg, 65 % yield).

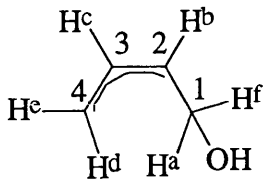

figure 125

Microanalysis

$C_{10}H_{12}O_2Fe$ requires: C, 54.6 %, H, 5.5 %.

found: C, 54.8 %, H, 5.3 %.

Infra-red (pentane)

ν_{CO} 1952 cm^{-1}.

^{1}H n.m.r. (CD_2Cl_2) (33a)

δ 4.51 (s, 5H, $C_5\underline{H}_5$), 4.43, 3.83 (m, 1H, $\underline{H}^a$, $\underline{H}^f$, J(H^aH^b) *circa* 10 Hz, J(H^bH^f) *circa* 10 Hz), 3.20, (dd, 1H, $\underline{H}^d$, J(H^cH^d) 9.67 Hz), 2.95 (dd, 1H, $\underline{H}^e$, J(H^cH^e) 5.91 Hz), 1.98 (bs, 1H, O$\underline{H}$), 1.66 (ddd, 1H, $\underline{H}^c$, J(H^cH^e) 5.91 Hz, J(H^cH^d) 9.67 Hz), 0.91 (ddd, 1H, $\underline{H}^b$, J(H^aH^b) *circa* 10 Hz, J(H^bH^f) *circa* 10 Hz) ppm.

^{13}C n.m.r. (CD_2Cl_2) (33a)

δ 222.2 (s, $\underline{C}O$), 79.9 (s, $\underline{C}_5H_5$), 72.7 (s, $\underline{C}^1$), 69.8 (s, $\underline{C}^3$), 52.2 (s, $\underline{C}^2$), 34.8 (s, $\underline{C}^4$) ppm.

^{1}H n.m.r. (CD_2Cl_2) (33b)

δ 4.51 (s, 5H, $C_5\underline{H}_5$), 4.43, 3.83 (m, 1H, $\underline{H}^a$, $\underline{H}^f$, J(H^aH^b) *circa* 10 Hz, J(H^bH^f) *circa* 10 Hz), 3.11, (dd, 1H, $\underline{H}^d$, J(H^cH^d) 9.67 Hz), 2.95 (dd, 1H, $\underline{H}^e$, J(H^cH^e) 5.91 Hz), 1.98 (bs, 1H, O$\underline{H}$), 1.78 (ddd, 1H, $\underline{H}^c$, J(H^cH^e) 5.91 Hz, J(H^cH^d) 9.67 Hz), 0.91 (ddd, 1H, $\underline{H}^b$, J(H^aH^b) *circa* 10 Hz, J(H^bH^f) *circa* 10 Hz) ppm.

^{13}C n.m.r. (CD_2Cl_2) (33b)

δ 222.2 (s, $\underline{C}O$), 79.9 (s, $\underline{C}_5H_5$), 72.7 (s, $\underline{C}^1$), 70.2 (s, $\underline{C}^3$), 52.1 (s, $\underline{C}^2$), 34.7 (s, $\underline{C}^4$) ppm.

4. References

1. A.J. Carty, *Pure Appl. Chem.*, **1982**, *54*, 113.
2. N.M. Kostic and R.F. Fenske, *Organometallics*, **1982**, *1*, 974.
3. S. Sonogashira, Y. Fujikara, T. Yakate, N. Toyoshima, S. Takahashi and N. Hagihara, *J. Organomet. Chem.*, **1978**, *145*, 101.
4. R. Nast, *Coord. Chem. Rev.*, **1982**, *47*, 89.
5. R. Jiminez, M.C. Barral, V. Moreno and A. Santos, *J. Organomet. Chem.*, **1979**, *174*, 281.
6. R. Jiminez, M.C. Barral, V. Moreno and A. Santos, *J. Organomet. Chem.*, **1979**, *182*, 353.
7. M. Tsutsui and N. Ely, *J. Am. Chem. Soc.*, **1974**, *96*, 4042.
8. N. Ely and M. Tsutsui, *Inorg. Chem.*, **1975**, *14*, 2680.
9. J.L. Attwood and C.F. Hains, *J. Chem. Soc., Chem. Commun.*, **1973**, 452.
10. M.L.H. Green and T. Mole, *J. Organomet. Chem.*, **1968**, *12*, 404.
11. A. Mayr, K.C. Schaefer and E.Y. Huang, *J. Am. Chem. Soc.*, **1984**, *106*, 1517.
12. W.A. Schenk and H. Muller, *Chem. Ber.*, **1982**, *115*, 3618.
13. W.A. Mong and J.H. Gladysz, *J. Am. Chem. Soc.*, **1982**, *104*, 4948.
14. J. Wolf, H. Werner, O. Serhadli and M.L. Ziegler, *Angew. Chem., Int. Ed. Engl.*, **1983**, *22*, 414.
15. F.J.G. Alonso, A. Hohn, J. Wolf, H. Otto and H. Werner, *Angew. Chem., Int. Ed. Engl.*, **1985**, *24*, 406.
16. J. Chatt and B.L. Shaw, *J. Chem. Soc.*, **1959**, 4020.
17. I. Collamati and A. Furlani, *J. Organomet. Chem.*, **1969**, *17*, 457.
18. R.A. Bell, M.H. Chisholm, D.A. Couch and L.A. Rankel, *Inorg. Chem.*, **1977**, *16*, 677.
19. R.A. Bell, M.H. Chisholm, *Inorg. Chem.*, **1977**, *16*, 687.
20. R.A. Bell, M.H. Chisholm, *Inorg. Chem.*, **1977**, *16*, 698.
21. D. Afzal, P.G. Lenhert and C.M. Lukehart, *J. Am. Chem. Soc.*, **1984**, *106*, 3050.

22. S.P. Deranlyagala and K.R. Grundy, *Organometallics,* **1985**, *4*, 424.

23. M. Cowie and S.J. Loeb, *Organometallics,* **1985**, *4*, 852.

24. P.O. Nubel and T.L. Brown, *Organometallics,* **1984**, *3*, 29.

25. A.J. Carty, in Advances in Chemistry Series, "Catalytic Aspects of Metal Phosphine Complexes", Eds. E.C. Alyea and D.W. Meek, *196*, p.163, American Chemical Society, **1982**.

26. H.A. Patel, R.G. Fischer, A.J. Carty, D.V. Naik and G.J. Palenik, *J. Organomet. Chem.,* **1973**, *60*, C49.

27. A.J. Carty, W.F. Smith and N.J. Taylor, *J. Organomet. Chem.,* **1978**, *146*, C1.

28. A.J. Carty, G.N. Mott and N.J. Taylor, *J. Organomet. Chem.,* **1981**, *212*, C54.

29. E. Sappa, O. Gambino, L. Milone and G. Cetini, *J. Organomet. Chem.,* **1972**, *39*, 169.

30. A.J. Deeming, S. Hasso and M. Underhill, *J. Chem. Soc., Dalton Trans.,* **1975**, 1614.

31. G. Gervasio and G. Ferraris, *Cryst. Struct. Comm.,* **1973**, *3*, 447.

32. M. Catti, G. Gervasio and S.A. Mason, *J. Chem. Soc., Dalton Trans.,* **1977**, 2260.

33. S. Aime, O. Gambino, L. Milone, E. Sappa and E. Rosenberg, *Inorg. Chim. Acta,* **1975**, *15*, 53.

34. C. Jangala, E. Rosenberg, D. Skinner, S. Aime, L. Milone and E. Sappa, *Inorg. Chem.,* **1980**, *19*, 1571.

35. E. Rosenberg, C.B. Thorsen, L. Milone and S. Aime, *Inorg. Chem.,* **1985**, *24*, 231.

36. S.A. MacLaughlin, J.P. Johnson, N.J. Taylor and A.J. Carty, *Organometallics,* **1983**, *2*, 352.

37. K. Henrick, M. McPartlin, A.J. Deeming, S. Hasso and P. Manning, *J. Chem. Soc., Dalton Trans.,* **1982**, 899.

38. S. Aime, D. Osella, A.J. Arce, A.J. Deeming, M.B. Hursthouse and A.M.R. Galas, *J. Chem. Soc., Dalton Trans.,* **1984**, 1981.

39. S. Aime and A.J. Deeming, *J. Chem. Soc., Dalton Trans.,* **1983**, 1807.

40. G. Granozzi, E. Tondello, R. Bertoncello, S. Aime and D. Osella, *Inorg. Chem.*, **1983**, *22*, 744.

41. C. Barner-Thorsen, K.I. Hardcastle, E. Rosenberg, J. Siegel, A.M. Manotti Landfredi, A. Tiripicchio and M. Tiripicchio Camellini, *Inorg. Chem.*, **1981**, *20*, 4306.

42. S. Ermer, K. King, K.I. Hardcastle, E. Rosenberg, A.M. Manotti Landfredi, A. Tiripicchio and M. Tiripicchio Camellini, *Inorg. Chem.*, **1983**, *22*, 1339.

43. A.J. Carty, N.J. Taylor and W.F. Smith, *J. Chem. Soc., Chem. Commun.*, **1979**, 750.

44. O.M. Abu Salah and M.I. Bruce, *J. Chem. Soc., Dalton Trans.*, **1974**, 2302.

45. K. Yasufuku, K. Aoki and H. Yamazaki, *Bull. Chem. Soc., Jpn.*, **1975**, *48*, 1616.

46. M. Green, K. Marsden, I.D. Salter, F.G.A. Stone and P. Woodward, *J. Chem. Soc., Chem. Commun.*, **1983**, 446.

47. D. de Montauzon and R. Mathieu, *J. Organomet. Chem.*, **1983**, *252*, C83.

48. J.A. Hriljac and D.F. Shriver, *Organometallics,* **1985**, *4*, 2225.

49. S.A. MacLaughlin, N.J. Taylor and A.J.Carty, *Organometallics,* **1983**, *2*, 1194.

50. O.M. Abu Salah and M.I. Bruce, *Aust. J. Chem.*, **1976**, *29*, 531.

51. M.R. Churchill and S.A. Bezman, *Inorg. Chem.*, **1974**, *13*, 1418.

52. O.M. Abu Salah, M.I. Bruce, M.R.Churchill and B.G. DeBoer, *J. Chem. Soc., Chem. Commun.*, **1974**, 688.

53. O.M. Abu Salah and M.I. Bruce, *Aust. J. Chem.*, **1977**, *30*, 2639.

54. W.A. Herrmann, *Angew. Chem., Int. Ed. Engl.*, **1982**, *21*, 117.

55. G.W. Parshall, D.L. Thorn and T.H. Tulip, *Chem. Tech.*, **1982**, 571.

56. R.J. Mercer, M. Green and A.G. Orpen, *J. Chem. Soc., Chem. Commun.*, **1986**, 567.

57. S.F.T. Froom, M. Green, R.J. Mercer, K.R. Nagle, A.G. Orpen and R.A. Rodrigues, *J. Chem. Soc., Dalton Trans.*, **1991**, 3171.

58. R.P. Durán, V.T. Amorebieta and A.J. Colussi, *J. Am. Chem. Soc.*, **1987**, *109*, 3154.

59. H.F. Schaefer III, *Acc. Chem. Res.*, **1979**, *12*, 288.

60. H. Ibach and S. Lehwald, *J. Vacuum Sci. Technol.*, **1978**, *15*, 407.

61. P.-K. Wang, C.P. Slichter and J.H. Sinfelt, *Phys. Rev. Lett.*, **1984**, *53*, 81.

62. W.T. Tysoe, G.L. Nyberg and R.M. Lambert, *Surf. Sci.*, **1983**, *135*, 128.

63. J.E. Demuth, H. Ibach and S. Lehwald, *Phys. Rev. Lett.*, **1978**, *40*, 1044.

64. R.J. Koestner, M.A. Van Hove and G.A. Somorjai, *J. Phys. Chem.*, **1983**, *87*, 203.

65. M. Salmeron and G.A. Somorjai, *J. Phys. Chem.*, **1982**, *86*, 341.

66. H. Ibach and S. Lehwald, *J. Vacuum Sci. Technol.*, **1981**, *18*, 625.

67. J. Evans and G.S. McNulty, *J. Chem. Soc., Dalton Trans.*, **1984**, 79.

68. J. Silvestre and R. Hoffmann, *Langmuir*, **1985**, *1*, 621.

69. E.L. Muetterties, *Angew. Chem., Int. Ed. Engl.*, **1978**, *17*, 545.

70. C. Zheng, Y. Apeloig and R. Hoffmann, *J. Am. Chem. Soc.*, **1988**, *110*, 749.

71. J.M. Bellerby and M.J. Mays, *J. Organomet. Chem.*, **1976**, *117*, C21.

72. A. Davison and J.P. Solar, *J. Organomet. Chem.*, **1978**, *155*, C8.

73. M.I. Bruce and R.C. Wallis, *J. Organomet. Chem.*, **1978**, *161*, C1.

74. G. Geoffroy and D.B. Pourreau, *Organometallics*, **1986**, *5*, 1337.

75. J.S. Adams, C. Bitcon, J.R. Brown, D. Collinson, M. Cunningham and M.W. Whiteley, *J. Chem. Soc., Dalton Trans.*, **1987**, 3049.

76. A.J.L. Pombeiro, S.S.P.R. Almeida, M.F.C.G. Silva, J.C. Jeffery and R.L. Richards, *J. Chem. Soc., Dalton Trans.*, **1989**, 2381.

77. A.B. Antonova, N.E. Kolobova, P.V. Petrovsky, B.V. Lokshin and N.S. Obezyuk, *J. Organomet. Chem.*, **1977**, *55*, 1937.

78. R.M. Bullock, *J. Chem. Soc., Chem. Commun.*, **1989**, 165.

79. D.H. Berry and R. Eisenberg, *Organometallics*, **1987**, *6*, 1796.

80. N.M. Doherty, C. Elschenbroich, H.-J. Kneuper and S.A.R. Knox, *J. Chem. Soc., Chem. Commun.*, **1985**, 170.

81. E. Roland and H. Vahrenkamp, *Chem. Ber.*, **1985**, *118*, 1133.

82. E. Roland, W. Bernhardt and H. Vahrenkamp, *Chem. Ber.*, **1985**, *118*, 2858.

83. R.D. Adams and S. Wang, *Organometallics*, **1985**, *4*, 1902.

84. M.I. Bruce and A.G. Swincer, *Adv. Organomet. Chem.*, **1983**, *22*, 60.

85. F.J.G. Alonso, A. Höhn, J. Wolf and H. Werner, *Angew. Chem., Int. Ed. Engl.*, **1985**, *24*, 406.

86. J. Silvestre and R. Hoffmann, *Helv. Chim. Acta.*, **1985**, *68*, 1461.

87. D.R. Senn, A. Wong, A.T. Patton, M. Marsi, C.E. Strouse and J.A. Gladysz, *J. Am. Chem. Soc.*, **1988**, *110*, 6096.

88. S.F.T. Froom, M. Green, R.J. Mercer, K.R. Nagle, A.G. Orpen and S. Schwiegk, *J. Chem. Soc., Chem. Commun.*, **1986**, 1666.

89. D. Seyferth, *Adv. Organomet. Chem.*, **1976**, *14*, 97.

90. R.T. Edidin, J.R. Norton and K. Mislow, *Organometallics*, **1982**, *1*, 561.

91. E. Boyar, A.J. Deeming, M.S.B. Felix, S.E. Kabir, T. Adatia, R. Bhusate, M. McPartlin and H.R. Powell, *J. Chem. Soc., Dalton Trans.*, **1989**, 5.

92. B.E.R. Schilling and R. Hoffmann, *J. Am. Chem. Soc.*, **1979**, *101*, 3456.

93. G. Maier, H.P. Reisenauer, W. Schwab, P. Cársky, B.A. Hess and L.J. Schaad, *J. Am. Chem. Soc.*, **1987**, *109*, 5183.

94. M.I. Bruce, *Chem. Rev.*, **1991**, *91*, 197.

95. E.O. Fischer, H.-J. Kalder, A. Frank, F. Köhler and G. Huttner, *Angew. Chem., Int. Ed. Engl.*, **1976**, *15*, 623.

96. J.P. Selegue, *Organometallics*, **1982**, *1*, 217.

97. H. Berke, G. Huttner, P. Härter and L. Zsolnai, *Chem. Ber.*, **1982**, *115*, 695.

98. H. Berke, *J. Organomet. Chem.*, **1980**, *185*, 75.

99. N.E. Kolobova, L.L. Ivanov, O.S. Zhvanko, G.G. Aleksandrov and Y.T. Struchkov, *J. Organomet. Chem.*, **1982**, *228*, 265.

100. B.E.R. Schilling, R. Hoffmann and D.L. Lichtenberger, *J. Am. Chem. Soc.*, **1979**, *101*, 585.

101. H. Berke, G. Huttner and J. von Seyerle, *Z. Naturforsch. B*, **1981**, *36*, 1277.

102. N.E. Kolobova, L.L. Ivanov, O.S. Zhvanko, I.N. Chechulina and V.V. Derunov, *Isvest. Akad. Nauk SSSR, Ser. Khim.*, **1982**, 2632.

103. S. Aime, A.J. Deeming, M.B. Hursthouse and J.D.J. Backer-Dirks, *J. Chem. Soc., Dalton Trans.*, **1982**, 1625.

104. H. Berke, U. Grössmann, G. Huttner and L. Zsolnai, *Chem. Ber.*, **1984**, *117*, 3432.

105. C.J. Tai and N.L. Allinger, *J. Am. Chem. Soc.*, **1976**, *98*, 7928.

106. M.E. Squillacote, R.S. Sheridan, O.L. Chapman and F.A. Anet, *J. Am. Chem. Soc.*, **1979**, *101*, 3657.

107. H. Reihlen, A. Grühl, G. von Hessling and O. Pfrengle, *Liebigs Ann. Chem.*, **1930**, *482*, 161.

108. H.E. Sasse and M.L. Ziegler, *Z. Anorg. Allg. Chem.*, **1972**, *392*, 167.

109. C.G. Pierpont, *Inorg. Chem.*, **1978**, *17*, 1976.

110. G. Erker, J. Wicher, K. Engel, F. Rosenfeldt, W. Dietrich and C. Krüger, *J. Am. Chem. Soc.*, **1980**, *102*, 6344.

111. G. Erker, C. Krüger and G. Muller, *Adv. Organomet. Chem.*, **1985**, *24*, 1.

112. T. Okamoto, H. Yasuda, A. Nakamura, Y. Kai, N. Kanehisa and N. Kasai, *J. Am. Chem. Soc.*, **1988**, *110*, 5008.

113. A. Nakamura and H Yasuda, *Angew. Chem., Int. Ed. Engl.*, **1987**, *26*, 723.

114. N. J. Christensen, A.D. Hunter and P. Legzdins, *Organometallics*, **1989**, *8*, 930.

115. S.A. Benyunes, A. Binelli, M. Green and M.J. Grimshire, *J. Chem. Soc., Dalton Trans.*, **1991**, 895.

116. S.A. Benyunes, J.P. Day, M. Green, A.W. Al-Saadoon and T.L. Waring, *Angew. Chem., Int. Ed. Engl.*, **1990**, *29*, 1416.

117. M. Bamber, PhD Thesis, Kings College, London, **1991**.

118. A. Meyer, D.J. McCabe and M.D. Curtis, *Organometallics*, **1987**, *6*, 1491.

119. P.W. Jolly and R. Mynott, *Adv. Organomet. Chem.*, **1981**, 257.

120. S.F.T. Froom, PhD Thesis, University of Bristol, **1990**.

121. A.W. Al-Saadoon, M. Green, R.J. Mercer and A.G. Orpen, *J. Organomet. Chem.*, **1990**, *384*, C12.

122. R.J. Mercer, PhD Thesis, University of Bristol, **1988**.

123. J.R. Morrow, T.L. Tonker and J.L. Templeton, *J. Am. Chem. Soc.*, **1985**, *107*, 6956.

124. J. Barrera, M. Sabat and W.D. Harman, *J. Am. Chem. Soc.*, **1991**, *113*, 8178.

125. J.L. Templeton and B.C. Ward, *J. Am. Chem. Soc.*, **1980**, *102*, 3288.

126. J.L. Templeton, *Advances in Organomet. Chem.*, **1989**, *29*, 1.

127. B. Olgemöler, H. Bauer, H. Löbermann, U. Nagel and W. Beck, *Chem. Ber.*, **1982**, *115*, 2271.

128. K. Isobe, K. Nanjo, Y. Nakamura and S. Kawaguchi, *Chem. Lett.*, **1979**, 1193.

129. R.V. Honeychuck and W.H. Hersh, *Inorg. Chem.*, **1989**, *28*, 2869.

130. E.W. Abel, M.A. Bennett and G. Wilkinson, *J. Chem. Soc.*, **1959**, 3178.

131. J.L. Herde, J.C. Lambert and C.V. Senoff, *Inorganic Syntheses*, **XV**, 18.

132. M. Green, T.A. Kuc and S.H. Taylor, *J. Chem. Soc. (A)*, **1971**, 2334.

133. D.A. Edwards and J. Marshalsea, *J. Organomet. Chem.*, **1977**, *131*, 73.

134. D.H. Gibson, W.-L. Hsu and D.-S. Lin, *J. Organomet. Chem.*, **1979**, *172*, C7.

135. B.F. Hallam and P.L. Pauson, *J. Chem. Soc.*, **1956**, 3030.

136. G.M. Sheldrick, SHELX76, a computer program for crystal structure determination, University of Cambridge, **1976**.

137. G.M. Sheldrick, SHELX86, a computer program for crystal structure determination, University of Gottingen, **1986**.

138. J. Barrera, M. Sabat and W.D. Harman, *Organometallics*, **1993**, *12*, 4381.

Appendix I

Crystallographic data for

$[Mo_2\{\mu_2\text{-}C(H)CCMe_2\}(CO)_4(\eta\text{-}C_5Me_5)_2]BF_4$ (3)

Note on $[Mo_2\{\mu_2\text{-}C(H)CCMe_2\}(CO)_4(\eta\text{-}C_5Me_5)_2]BF_4$ (3)

A crystal of approximate dimensions 0.2 x 0.2 x 0.25 mm was used for data collection.

Crystal data: $C_{29}H_{37}O_4BF_4Mo_2$, M = 728.3 orthorhombic, a = 8.832(4), b = 12.485(3), c = 27.654(6) Å, U = 3049.4 Å^3, space group $P2_12_12_1$, Z = 4, D_c = 1.58 gcm^{-3}, μ(Mo-K_α) = 8.1 cm^{-1}, F(000) = 1472. Data were measured at room temperature on the FAST system at Cardiff in the range $2\leq\theta\leq50.5°$. 6696 reflections were collected of which 1225 were unique with $I\geq2.5\sigma(I)$. Data were corrected for Lorentz and polarisation effects but not for absorption. The structure was solved by Patterson methods and refined using the SHELX[136, 137] suite of programs. In the final least squares cycles the molybdenum, fluorine and chlorine atoms were allowed to vibrate anisotropically. In addition, the charged moieties which compose the molecule were treated as separate blocks. All other atoms were treated isotropically. hydrogen atoms were not included.

Refinement was inhibited by several factors. Firstly, large significant residual maxima and minima were found in the difference Fourier (1.32, -1.16 eÅ^{-3}). The positive residual density peak was found to be at distances of 2.32, 1.87, 1.77 and 1.96 Å from Mo1, C3, C7 and C8 respectively. An effort to reduce the size of these peaks by raising the threshold on 'omitable' data served only to eliminate 80% of the data points and therefore was not feasible.

Secondly, the application of a weighting scheme failed to afford any improvement, and a DIFABS absorption correction was unsuccessful in providing a superior convergence to the initial data set. Subsequent to careful analysis of the data and the final difference map, it was reasonably clear that the above peaks were not chemically significant. In fact they are more likely to be a consequence of poor quality data and high mosaic spread within the crystal which was three times higher than the desired value of

0.8. Final residuals after 18 cycles of blocked-matrix least squares were $R = R_{\omega} = 0.0657$, for unit weights. Maximum final shift/esd values were 0.02 and 0.062 for the cation and anion respectively. Final fractional atomic coordinates and isotropic thermal parameters, anisotropic temperature factors, bond distances and angles are given in tables 1, 2, 3 and 4 respectively. Hydrogen atom positions are available as supplementary data. Some intramolecular distances are given in table 5. The asymmetric unit is shown in figure 79, along with the labelling scheme used.

Table 1 Fractional atomic coordinates and thermal parameters (Å) for $[Mo_2\{\mu_2\text{-}C(H)CCMe_2\}(CO)_4(\eta\text{-}C_5Me_5)_2]^+BF_4^-$

Atom	x	y	z	Uiso or Ueq	If Ueq ***
Mo1	0.8615 (3)	0.1970 (2)	0.8648 (1)	0.027 (1)	***
Mo2	0.9890 (3)	-0.0035 (2)	0.9102 (1)	0.024 (1)	***
O1	1.5398 (32)	0.2885 (18)	0.8923 (8)	0.081 (18)	***
O2	0.9755 (40)	0.3034 (21)	0.9620 (8)	0.106 (21)	***
O3	1.2558 (29)	0.1578 (18)	0.9207 (8)	0.064 (18)	***
O4	1.1213 (33)	-0.0796 (18)	0.8097 (9)	0.083 (19)	***
F1	0.1126 (35)	0.2917 (27)	0.3404 (7)	0.212 (32)	***
F2	0.0291 (40)	0.4183 (23)	0.3041 (10)	0.219 (37)	***
F3	-0.0001 (46)	0.4087 (26)	0.3764 (9)	0.300 (47)	***
F4	-0.1125 (37)	0.3088 (29)	0.3321 (15)	0.285 (51)	***
C1	0.6712 (41)	0.2503 (26)	0.8825 (12)	0.054 (10)	
C2	0.9354 (40)	0.2639 (28)	0.9291 (13)	0.060 (11)	
C3	1.1574 (38)	0.0990 (23)	0.9122 (11)	0.040 (8)	
C4	1.0621 (41)	-0.0460 (26)	0.8454 (12)	0.056 (11)	
C5	0.8160 (17)	0.2925 (17)	0.7942 (7)	0.038 (8)	
C6	0.9243 (17)	0.2144 (17)	0.7801 (7)	0.041 (8)	
C7	1.0605 (17)	0.2351 (17)	0.8057 (7)	0.041 (8)	
C8	1.0364 (17)	0.3260 (17)	0.8356 (7)	0.056 (9)	
C9	0.8853 (17)	0.3615 (17)	0.8285 (7)	0.035 (7)	
C10	0.6548 (46)	0.3161 (29)	0.7702 (12)	0.073 (11)	
C11	0.8952 (43)	0.1318 (27)	0.7394 (12)	0.067 (11)	

C12	1.2061 (39)	0.1867 (30)	0.7952 (13)	0.065 (11)
C13	1.1520 (27)	0.3969 (15)	0.8641 (9)	0.014 (5)
C14	0.8225 (37)	0.4717 (24)	0.8464 (11)	0.050 (10)
C15	0.9166 (25)	-0.0618 (14)	0.9882 (6)	0.028 (8)
C16	0.8707 (25)	-0.1393 (14)	0.9536 (6)	0.036 (8)
C17	1.0030 (25)	-0.1826 (14)	0.9319 (6)	0.028 (6)
C18	1.1306 (25)	-0.1318 (14)	0.9531 (6)	0.044 (8)
C19	1.0773 (25)	-0.0572 (14)	0.9879 (6)	0.044 (10)
C20	0.8191 (39)	0.0002 (34)	1.0260 (12)	0.060 (11)
C21	0.7152 (42)	-0.1704 (30)	0.9459 (13)	0.061 (12)
C22	1.0004 (48)	-0.2815 (25)	0.8994 (11)	0.067 (9)
C23	1.2996 (41)	-0.1598 (29)	0.9420 (13)	0.057 (12)
C24	1.1756 (35)	0.0080 (29)	1.0220 (11)	0.048 (9)
C25	0.7726 (35)	0.0850 (22)	0.9154 (11)	0.037 (8)
C26	0.7860 (28)	0.0177 (21)	0.8701 (9)	0.029 (7)
C27	0.6872 (30)	-0.0007 (29)	0.8323 (9)	0.040 (7)
C28	0.7318 (44)	-0.0797 (28)	0.7956 (13)	0.061 (10)
C29	0.5726 (37)	0.0356 (19)	0.8337 (9)	0.039 (8)
B1	0.0083 (31)	0.3572 (18)	0.3383 (8)	0.052 (9)

Table 2 Anisotropic thermal parameters (Å)

Atom	U11	U22	U33	U23	U13	U12
Mo1	0.026 (1)	0.029 (1)	0.026 (1)	0.000 (1)	0.002 (1)	0.001 (1)
Mo2	0.022 (1)	0.028 (1)	0.022 (1)	0.003 (1)	0.001 (1)	0.003 (1)
O1	0.115 (25)	0.054 (14)	0.072 (15)	-0.010 (12)	0.046 (15)	-0.007 (16)
O2	0.178 (31)	0.087 (18)	0.053 (14)	-0.034 (15)	-0.031 (19)	0.035 (25)
O3	0.082 (19)	0.058 (16)	0.052 (17)	0.018 (12)	0.001 (14)	-0.019 (14)
O4	0.103 (23)	0.071 (17)	0.075 (17)	-0.001 (14)	0.044 (18)	0.046 (17)
F1	0.142 (27)	0.435 (56)	0.058 (14)	0.014 (24)	0.013 (16)	0.177 (36)
F2	0.217 (41)	0.222 (33)	0.218 (36)	0.140 (30)	0.092 (34)	0.073 (32)
F3	0.398 (61)	0.338 (48)	0.165 (32)	-0.179 (34)	-0.028 (41)	0.199 (51)
F4	0.185 (40)	0.286 (49)	0.384 (65)	-0.090 (49)	0.068 (43)	-0.147 (42)

Table 3 Bond Lengths (Å)

Mo1-C1	1.87 (4)	Mo1-C2	2.07 (4)
Mo1-C5	2.324 (20)	Mo1-C6	2.417 (20)
Mo1-C7	2.446 (18)	Mo1-C8	2.373 (19)
Mo1-C9	2.296 (21)	Mo1-C25	2.13 (3)
Mo1-C26	2.34(3)	O1-C1	1.28 (4)
Mo2-C3	1.96 (3)	Mo2-C4	1.98(3)
Mo2-C15	2.365 (18)	Mo2-C16	2.325 (18)
Mo2-C17	2.319 (17)	Mo2-C18	2.354 (19)
Mo2-C19	2.382 (18)	Mo2-C25	2.21 (3)
Mo2-C26	2.126 (25)	O1-C1	1.28 (4)
O2-C2	1.09 (4)	O3-C3	1.16 (4)
O4-C4	1.19 (4)	C5-C6	1.42 (3)
C5-C9	1.42 (3)	C5-C10	1.60 (4)
C6-C7	1.420 (23)	C6-C11	1.55 (4)
C7-C8	1.42 (3)	C7-C12	1.45 (4)
C8-C9	1.420 (23)	C8-C13	1.56 (3)
C9-C14	1.56 (4)	C15-C16	1.420 (25)
C15-C19	1.42 (3)	C15-C20	1.56 (4)
C16-C17	1.42 (3)	C16-C21	1.44 (4)
C17-C18	1.42 (3)	C17-C22	1.53 (3)
C18-C19	1.420 (25)	C18-C23	1.56 (4)
C19-C24	1.52 (4)	C25-C26	1.52 (4)
C26-C27	1.38 (4)	C27-C28	1.47 (5)
C27-C29	1.48 (4)	B1-F1	1.23 (4)
B1-F2	1.23 (4)	B1-F3	1.24 (3)

B1-F4 1.24(4)

Table 4 Bond Angles (°)

C2-Mo1-C1	85 (1)	C5-Mo1-C1	83 (1)
C5-Mo1-C2	125 (1)	C6-Mo1-C1	115 (1)
C6-Mo1-C2	136 (1)	C6-Mo1-C5	34.8 (6)
C7-Mo1-C1	139 (1)	C7-Mo1-C2	106 (1)
C7-Mo1-C5	57.5 (6)	C7-Mo1-C6	33.9 (6)
C8-Mo1-C1	116 (1)	C8-Mo1-C2	79 (1)
C8-Mo1-C5	58.6 (6)	C8-Mo1-C6	57.3 (7)
C8-Mo1-C7	34.2 (7)	C9-Mo1-C1	83 (1)
C9-Mo1-C2	89 (1)	C9-Mo1-C5	35.8 (7)
C9-Mo1-C6	58.3 (7)	C9-Mo1-C7	57.9 (6)
C9-Mo1-C8	35.4 (6)	C25-Mo1-C1	74 (1)
C25-Mo1-C2	79 (1)	C25-Mo1-C5	145.7 (9)
C25-Mo1-C6	141.3 (9)	C25-Mo1-C7	146.3 (9)
C25-Mo1-C8	155 (1)	C25-Mo1-C9	155.4 (9)
C26-Mo1-C1	94 (1)	C26-Mo1-C2	115 (1)
C26-Mo1-C5	119.6 (8)	C26-Mo1-C6	102.2 (8)
C26-Mo1-C7	115.6 (8)	C26-Mo1-C8	148.8 (8)
C26-Mo1-C9	155.3 (8)	C26-Mo1-C25	39 (1)
O1-C1-Mo1	177 (3)	O2-C2-Mo1	177 (3)
C6-C5-Mo1	76 (1)	C9-C5-Mo1	71 (1)
C9-C5-C6	108 (1)	C10-C5-Mo1	127 (2)
C10-C5-C6	128 (2)	C10-C5-C9	123 (2)
C5-C6-Mo1	69 (1)	C7-C6-Mo1	74 (1)
C7-C6-C5	108 (2)	C11-C6-Mo1	127 (2)

C11-C6-C5	123 (2)	C11-C6-C7	129 (2)
C6-C7-Mo1	72 (1)	C8-C7-Mo1	70 (1)
C8-C7-C6	108 (1)	C12-C7-Mo1	134 (2)
C12-C7-C6	125 (2)	C12-C7-C8	126 (2)
C7-C8-Mo1	76 (1)	C9-C8-Mo1	69 (1)
C9-C8-C7	108 (2)	C13-C8-Mo1	130 (1)
C13-C8-C7	130 (1)	C13-C8-C9	120 (2)
C5-C9-Mo1	73 (1)	C8-C9-Mo1	75 (1)
C8-C9-C5	108 (2)	C14-C9-Mo1	128 (1)
C14-C9-C5	126 (2)	C14-C9-C8	124 (2)
C19-C15-C16	108 (2)	C20-C15-C16	129 (2)
C20-C15-C19	122 (2)	C17-C16-C15	108 (2)
C21-C16-C15	124 (2)	C21-C16-C17	128 (2)
C18-C17-C16	108 (2)	C22-C17-C16	123 (2)
C22-C17-C18	128 (2)	C19-C18-C17	108 (2)
C23-C18-C17	125 (2)	C23-C18-C19	127 (2)
C18-C19-C15	108 (2)	C24-C19-C15	126 (2)
C24-C19-C18	126 (2)	C26-C25-Mo1	78 (2)
C25-C26-Mo1	63 (1)	C27-C26-Mo1	107 (2)
C4-Mo2-C3	87 (1)	C15-Mo2-C3	112 (1)
C15-Mo2-C4	146 (1)	C16-Mo2-C3	143 (1)
C16-Mo2-C4	115 (1)	C16-Mo2-C15	35.2 (6)
C17-Mo2-C3	125 (1)	C17-Mo2-C4	88 (1)
C17-Mo2-C15	58.7 (6)	C17-Mo2-C16	35.6 (7)
C18-Mo2-C3	91 (1)	C18-Mo2-C4	96 (1)
C18-Mo2-C15	58.3 (7)	C18-Mo2-C16	58.8 (7)
C18-Mo2-C17	35.4 (7)	C19-Mo2-C3	85 (1)

C19-Mo2-C4	129 (1)	C19-Mo2-C15	34.8 (8)
C19-Mo2-C16	58.4 (7)	C19-Mo2-C17	58.5 (6)
C19-Mo2-C18	34.9 (6)	C25-Mo2-C3	109 (1)
C25-Mo2-C4	118 (1)	C25-Mo2-C15	82.0 (9)
C25-Mo2-C16	86.7 (9)	C25-Mo2-C17	120.7 (9)
C25-Mo2-C18	140.0 (9)	C25-Mo2-C19	111 (1)
C26-Mo2-C3	125 (1)	C26-Mo2-C4	80 (1)
C26-Mo2-C15	106.7 (9)	C26-Mo2-C16	88.9 (9)
C26-Mo2-C17	107.5 (9)	C26-Mo2-C18	142.8 (9)
C26-Mo2-C19	141.5 (9)	C26-Mo2-C25	41 (1)
O3-C3-Mo2	170 (3)	O4-C4-Mo2	171 (3)
C27-C26-C25	132 (2)	C28-C27-C26	118 (3)
C29-C27-C26	122 (2)	C29-C27-C28	119 (3)
F2-B1-F1	110 (3)	F3-B1-F1	110 (3)
F3-B1-F2	110 (3)	F4-B1-F1	109 (3)
F4-B1-F2	109 (3)	F4-B1-F3	109 (3)

Table 5 Intramolecular Distances (Å)

C1 ...C5	2.81	C1 ...C9	2.78
C1 ...C25	2.43	C2 ...C3	2.88
C2 ...C8	2.84	C2 ...C25	2.68
C3 ...C4	2.72	C3 ...C19	2.95
C4 ...C17	2.99	C4 ...C26	2.65
C5 ...C7	2.30	C5 ...C8	2.30
C5 ...C11	2.61	C5 ...C14	2.66
C6 ...C8	2.30	C6 ...C9	2.30
C6 ...C10	2.71	C6 ...C12	2.55
C7 ...C9	2.30	C7 ...C11	2.68
C7 ...C13	2.71	C8 ...C12	2.55
C8 ...C14	2.64	C9 ...C10	2.66
C9 ...C13	2.59	C15 ...C17	2.30
C15 ...C18	2.30	C15 ...C21	2.52
C15 ...C24	2.62	C16 ...C18	2.30
C16 ...C19	2.30	C16 ...C20	2.69
C16 ...C22	2.59	C17 ...C19	2.30
C17 ...C21	2.58	C17 ...C23	2.65
C18 ...C22	2.65	C18 ...C24	2.61
C19 ...C20	2.61	C19 ...C23	2.67
C25 ...C27	2.65	C26 ...C28	2.44
C26 ...C29	2.50	C28 ...C29	2.53
F1 ...F2	2.01	F1 ...F3	2.03
F1 ...F4	2.01	F2 ...F3	2.02
F2 ...F4	2.01	F3 ...F4	2.01

Appendix II

Crystallographic data for

$[Mo_2(\mu\text{-}HCCCH_2OCH_2CH_3)\ (CO)_4(\eta\text{-}C_5H_5)_2]$ (8)

Note on $[Mo_2(\mu\text{-}HCCCH_2OCH_2CH_3)(CO)_4(\eta\text{-}C_5H_5)_2]$ (8)

A crystal of approximate dimensions 0.25 x 0.25 x 0.2 mm was used for data collection.

Crystal data: $C_{19}H_{18}O_5Mo_2$, M = 518.2 triclinic, a = 9.034 (4), b = 10.320 (4), c = 11.422 (3) Å, α = 93.74 (3), β = 102.73 (3), γ = 110.69 (3), U = 960.0 Å^3, space group $P\bar{1}$, Z = 2, D_c = 1.79 gcm^{-3}, μ(Mo-$K\alpha$) = 11.96 cm^{-1}, F(000) = 512. Data were measured at room temperature on a Hilger and Watts Y290 four-circle diffractometer in the range 2 $\leq\theta\leq$24°. 4025 reflections were collected of which 3268 were unique with $I\geq3\sigma(I)$. Data were corrected for Lorentz and polarisation effects but not for absorption. The structure was solved by Patterson methods and refined using the SHELX[136, 137] suite of programs. In the final least squares cycles all atoms were allowed to vibrate anisotropically. Hydrogen atoms were included at calculated positions except in the cases of C15 and C17, where they were located in the penultimate difference Fourier and refined at fixed distances of 1.08 Å from the parent atoms. Final residuals after 10 cycles of least squares were R = 0.0333, R_w = 0.0347, for a weighting scheme of $w = 1.0000/[\sigma^2(F) + 0.006758(F)^2]$. Maximum final shift/esd was 0.009. The maximum and minimum residual densities were 0.28 and -1.29 eÅ^{-3} respectively. Final fractional atomic coordinates and isotropic thermal parameters, anisotropic temperature factors, bond distances, bond angles, fractional atomic coordinates for the hydrogen atoms, intermolecular distances and intramolecular distances are given in tables 6, 7, 8, 9, 10, 11 and 12, respectively. The asymmetric unit is shown in figure 84, along with the labelling scheme used.

Table 6 Fractional atomic coordinates and thermal parameters (Å) for [Mo_2(μ-$HCCCH_2OCH_2CH_3$) $(CO)_4$(η-$C_5H_5)_2$] (8)

Atom	x	y	z	Uiso or Ueq	If Ueq ***
Mo1	0.07630 (3)	0.37919 (2)	0.25931 (2)	0.0355 (2)	***
Mo2	0.24230 (2)	0.17632 (2)	0.29499 (2)	0.0334 (2)	***
O1	-0.2306 (4)	0.3214 (5)	0.0456 (3)	0.101 (2)	***
O2	-0.1838 (3)	0.1781 (3)	0.3737 (3)	0.070 (2)	***
O3	0.5660 (3)	0.4069 (3)	0.2761 (3)	0.073 (2)	***
O4	0.2451 (4)	0.3041 (3)	0.5497 (2)	0.071 (2)	***
C1	-0.1171 (5)	0.3410 (4)	0.1218 (3)	0.063 (2)	***
C2	-0.0883 (3)	0.2498 (3)	0.3322 (3)	0.042 (1)	***
C3	0.4449 (4)	0.3255 (3)	0.2868 (3)	0.047 (2)	***
C4	0.2392 (4)	0.2666 (3)	0.4504 (3)	0.048 (2)	***
C5	0.1365 (6)	0.6107 (4)	0.2290 (4)	0.080 (3)	***
C6	0.0629 (6)	0.5884 (3)	0.3283 (4)	0.072 (2)	***
C7	0.1694 (5)	0.5598 (3)	0.4228 (3)	0.057 (2)	***
C8	0.3087 (4)	0.5663 (3)	0.3848 (4)	0.056 (2)	***
C9	0.2892 (6)	0.5969 (3)	0.2656 (4)	0.074 (2)	***
C10	0.1113 (5)	-0.0663 (3)	0.2206 (4)	0.066 (2)	***
C11	0.2664 (6)	-0.0218 (4)	0.2006 (4)	0.075 (2)	***
C12	0.3801 (5)	0.0236 (4)	0.3154 (5)	0.082 (3)	***
C13	0.2935 (7)	0.0048 (5)	0.4032 (4)	0.084 (3)	***
C14	0.1263 (6)	-0.0502 (4)	0.3443 (5)	0.081 (3)	***
C15	0.0462 (3)	0.1798 (3)	0.1553 (2)	0.035 (1)	***

C16	0.1813 (3)	0.2835 (3)	0.1421 (2)	0.036 (1)	***
C17	0.2459 (4)	0.3289 (3)	0.0362 (3)	0.047 (1)	***
O5	0.2628 (3)	0.2151 (2)	-0.0270 (2)	0.050 (1)	***
C18	0.3489 (5)	0.2541 (4)	-0.1163 (4)	0.068 (2)	***
C19	0.3620 (6)	0.1308 (5)	-0.1769 (5)	0.095 (3)	***
H151	-0.0458 (31)	0.0924 (24)	0.1028 (25)	0.040 (8)	
H171	0.1621 (40)	0.3711 (40)	-0.0146 (31)	0.068 (11)	
H172	0.3671 (27)	0.4107 (30)	0.0652 (31)	0.050 (9)	

Table 7 Anisotropic thermal parameters (Å)

Atom	U11	U22	U33	U23	U13	U12
Mo1	0.0424 (2)	0.0256 (2)	0.0384 (2)	0.0062 (1)	0.0189 (1)	0.0159 (1)
Mo2	0.0349 (2)	0.0291 (2)	0.0362 (2)	0.0026 (1)	0.0077 (1)	0.0143 (1)
O1	0.083 (2)	0.143 (3)	0.076 (2)	0.022 (2)	-0.001 (2)	0.066 (2)
O2	0.075 (2)	0.052 (1)	0.082 (2)	0.010 (1)	0.048 (1)	0.008 (1)
O3	0.047 (1)	0.076 (2)	0.096 (2)	-0.005 (2)	0.020 (1)	-0.003 (1)
O4	0.095 (2)	0.083 (2)	0.034 (1)	-0.003 (1)	0.011 (1)	0.041 (2)
C1	0.066 (2)	0.074 (2)	0.051 (2)	0.013 (2)	0.013 (1)	0.044 (2)
C2	0.048 (1)	0.030 (1)	0.047 (1)	0.000 (1)	0.019 (1)	0.013 (1)
C3	0.042 (1)	0.047 (2)	0.053 (2)	-0.002 (1)	0.009 (1)	0.012 (1)
C4	0.051 (1)	0.047 (2)	0.046 (2)	0.004 (1)	0.007 (1)	0.020 (1)
C5	0.124 (4)	0.034 (2)	0.082 (3)	0.020 (2)	0.049 (3)	0.036 (2)
C6	0.093 (3)	0.032 (2)	0.090 (3)	0.005 (2)	0.045 (2)	0.033 (2)
C7	0.074 (2)	0.033 (1)	0.064 (2)	-0.006 (1)	0.032 (2)	0.013 (1)
C8	0.061 (2)	0.030 (1)	0.078 (2)	-0.013 (1)	0.022 (2)	0.003 (1)
C9	0.097 (3)	0.025 (1)	0.101 (3)	0.004 (2)	0.065 (2)	0.004 (2)
C10	0.068 (2)	0.028 (1)	0.103 (3)	0.000 (2)	0.005 (2)	0.022 (1)
C11	0.099 (3)	0.049 (2)	0.078 (2)	0.008 (2)	0.035 (2)	0.045 (2)
C12	0.058 (2)	0.056 (2)	0.130 (4)	0.018 (2)	0.020 (2)	0.039 (2)
C13	0.115 (3)	0.067 (2)	0.071 (2)	0.029 (2)	0.012 (2)	0.057 (2)
C14	0.083 (2)	0.042 (2)	0.119 (4)	0.038 (2)	0.052 (3)	0.031 (2)
C15	0.038 (1)	0.031 (1)	0.036 (1)	0.001 (1)	0.007 (1)	0.016 (1)
C16	0.042 (1)	0.031 (1)	0.036 (1)	0.003 (1)	0.014 (1)	0.016 (1)
C17	0.062 (2)	0.036 (1)	0.044 (1)	0.007 (1)	0.025 (1)	0.021 (1)

O5	0.060 (1)	0.040 (1)	0.051 (1)	0.000 (1)	0.029 (1)	0.015 (1)
C18	0.075 (2)	0.053 (2)	0.076 (2)	-0.005 (2)	0.050 (2)	0.011 (2)
C19	0.100 (3)	0.070 (3)	0.114 (4)	-0.016 (2)	0.072 (3)	0.021 (2)

Table 8 Bond Lengths (Å)

Mo1-Mo2	2.976 (1)	Mo1-C1	1.975 (4)
Mo1-C2	1.993 (3)	Mo1-C4	2.899 (3)
Mo1-C5	2.323 (3)	Mo1-C6	2.303 (3)
Mo1-C7	2.327 (3)	Mo1-C8	2.374 (3)
Mo1-C9	2.370 (3)	Mo1-C15	2.205 (3)
Mo1-C16	2.172 (2)	Mo2-C3	1.957 (3)
Mo2-C4	1.961 (3)	Mo2-C10	2.362 (3)
Mo2-C11	2.350 (4)	Mo2-C12	2.322 (4)
Mo2-C13	2.342 (4)	Mo2-C14	2.362 (3)
Mo2-C15	2.120 (3)	Mo2-C16	2.199 (3)
O1-C1	1.134 (4)	O2-C2	1.136 (3)
O3-C3	1.158 (4)	O4-C4	1.157 (4)
C5-C6	1.428 (5)	C5-C9	1.411 (7)
C6-C7	1.401 (6)	C7-C8	1.400 (5)
C8-C9	1.406 (6)	C10-C11	1.388 (6)
C10-C14	1.383 (6)	C11-C12	1.407 (6)
C12-C13	1.386 (7)	C13-C14	1.397 (7)
C15-C16	1.355 (4)	C15-H151	1.022 (17)
C16-C17	1.488 (4)	C17-O5	1.411 (3)
C17-H171	1.082 (18)	C17-H172	1.082 (17)
O5-C18	1.410 (4)	C18-C19	1.464 (5)

Table 9 Bond Angles (°)

C1-Mo1-Mo2	121.2 (1)	C2-Mo1-Mo2	85.0 (1)
C2-Mo1-C1	83.1 (1)	C4-Mo1-Mo2	39.0 (1)
C4-Mo1-C1	146.4 (1)	C4-Mo1-C2	70.2 (1)
C5-Mo1-Mo2	139.2 (1)	C5-Mo1-C1	83.8 (2)
C5-Mo1-C2	132.8 (1)	C5-Mo1-C4	129.3 (1)
C6-Mo1-Mo2	148.0 (1)	C6-Mo1-C1	90.7 (2)
C6-Mo1-C2	99.2 (1)	C6-Mo1-C4	112.8 (1)
C6-Mo1-C5	36.0 (1)	C7-Mo1-Mo2	113.2 (1)
C7-Mo1-C1	124.8 (1)	C7-Mo1-C2	93.6 (1)
C7-Mo1-C4	78.1 (1)	C7-Mo1-C5	59.0 (1)
C7-Mo1-C6	35.2 (2)	C8-Mo1-Mo2	92.4 (1)
C8-Mo1-C1	141.8 (2)	C8-Mo1-C2	120.4 (1)
C8-Mo1-C4	71.4 (1)	C8-Mo1-C5	58.0 (2)
C8-Mo1-C6	58.0 (1)	C8-Mo1-C7	34.6 (1)
C9-Mo1-Mo2	104.8 (1)	C9-Mo1-C1	112.3 (2)
C9-Mo1-C2	151.6 (1)	C9-Mo1-C4	100.6 (1)
C9-Mo1-C5	35.0 (2)	C9-Mo1-C6	58.6 (1)
C9-Mo1-C7	58.1 (1)	C9-Mo1-C8	34.5 (1)
C7-C5-C6	35.6 (2)	C8-C5-C6	71.3 (3)
C8-C5-C7	35.7 (1)	C9-C5-C6	107.3 (4)
C9-C5-C7	71.7 (3)	C9-C5-C8	36.0 (2)
C7-C6-C5	108.0 (4)	C8-C6-C5	72.1 (3)
C8-C6-C7	35.9 (2)	C9-C6-C5	36.1 (3)
C9-C6-C7	71.9 (3)	C9-C6-C8	36.0 (2)
C6-C7-C5	36.4 (2)	C8-C7-C5	71.7 (3)

C8-C7-C6	108.1 (3)	C9-C7-C5	36.0 (2)
C9-C7-C6	72.4 (3)	C9-C7-C8	35.7 (2)
C6-C8-C5	36.6 (2)	C7-C8-C5	72.6 (3)
C7-C8-C6	35.9 (2)	C9-C8-C5	36.1 (2)
C9-C8-C6	72.7 (3)	C9-C8-C7	108.7 (4)
C6-C9-C5	36.6 (2)	C7-C9-C5	72.4 (2)
C7-C9-C6	35.7 (2)	C8-C9-C5	107.9 (3)
C8-C9-C6	71.3 (2)	C8-C9-C7	35.6 (2)
C12-C10-C11	36.8 (3)	C13-C10-C11	72.7 (3)
C13-C10-C12	35.9 (2)	C14-C10-C11	109.1 (4)
C14-C10-C12	72.4 (3)	C14-C10-C13	36.4 (2)
C12-C11-C10	107.0 (4)	C13-C11-C10	71.4 (3)
C13-C11-C12	35.6 (3)	C14-C11-C10	35.4 (2)
C14-C11-C12	71.6 (3)	C14-C11-C13	36.0 (2)
C11-C12-C10	36.2 (2)	C13-C12-C10	71.9 (3)
C13-C12-C11	108.1 (4)	C14-C12-C10	35.8 (2)
C14-C12-C11	72.0 (3)	C14-C12-C13	36.1 (3)
C11-C13-C10	35.9 (2)	C12-C13-C10	72.2 (3)
C12-C13-C11	36.3 (2)	C14-C13-C10	36.0 (2)
C14-C13-C11	71.9 (3)	C14-C13-C12	108.2 (4)
C11-C14-C10	35.5 (2)	C12-C14-C10	71.9 (3)
C12-C14-C11	36.3 (2)	C13-C14-C10	107.6 (4)
C13-C14-C11	72.1 (3)	C13-C14-C12	35.8 (2)
H151-C15-C16	137 (2)	C17-C16-C15	134.3 (3)
O5-C17-C16	109.2 (2)	H171-C17-C16	105 (2)
H171-C17-O5	116 (2)	H172-C17-C16	111 (2)
H172-C17-O5	106 (2)	H172-C17-H171	109 (3)

C18-O5-C17	113.1 (2)	C19-C18-O5	109.8 (3)

Table 10 Fractional atomic coordinates for the hydrogen atoms

Atom	x	y	z
H51	0.0842	0.6317	0.1413
H61	-0.0533	0.5943	0.3310
H71	0.1470	0.5363	0.5096
H81	0.4141	0.5511	0.4384
H91	0.3763	0.6082	0.2119
H101	-0.0038	-0.1067	0.1515
H111	0.2952	-0.0228	0.1137
H121	0.5120	0.0677	0.3331
H131	0.3454	0.0284	0.5004
H141	0.0275	-0.0767	0.3882
H181	0.2843	0.2990	-0.1823
H182	0.4700	0.3310	-0.0732
H191	0.4283	0.1602	-0.2452
H192	0.2405	0.0543	-0.2194
H193	0.4263	0.0863	-0.1103

Table 11 Intermolecular distances (Å)

O1...H192	2.78	1	1.0	0.0	0.0
O1...H51	2.73	-1	0.0	1.0	0.0
O2...H121	2.49	1	1.0	0.0	0.0
O2...H131	2.81	-1	0.0	0.0	1.0
O2...H192	2.70	-1	0.0	0.0	0.0
O3...H71	3.00	-1	1.0	1.0	1.0
O4...H61	2.85	-1	0.0	1.0	1.0
O4...H81	2.87	-1	1.0	1.0	1.0
O4...H141	3.00	-1	0.0	0.0	1.0
C4...H81	2.95	-1	1.0	1.0	1.0
H51...H171	2.36	-1	0.0	1.0	0.0
C6...H71	2.97	-1	0.0	1.0	1.0
C7...H71	2.97	-1	0.0	1.0	1.0
C9...H191	2.94	-1	1.0	1.0	0.0
H91...C18	2.88	-1	1.0	1.0	0.0
H101...C17	2.90	-1	0.0	0.0	0.0
H101...O5	2.29	-1	0.0	0.0	0.0
H101...C18	2.86	-1	0.0	0.0	0.0
H192...H172	2.53	-1	1.0	1.0	0.0
H192...H151	2.56	-1	0.0	0.0	0.0

Table 12 Intramolecular distances (Å)

Mo1...H51	3.00	Mo1...H61	3.00
O3...H172	2.68	O4...H71	2.86
O4...H81	3.00	C1...C2	2.63
C1...C5	2.88	C1...H51	2.87
C1...C15	2.58	C1...C16	2.92
C1...H151	2.86	C2...C4	2.91
C2...C15	2.76	C3...C4	2.86
C3...H81	2.94	C3...H121	2.98
C3...C16	2.46	C3...H172	2.76
C4...H81	2.83	C4...C13	2.95
C4...H131	2.98	C5...H61	2.24
C5...H91	2.23	H51...C6	2.25
H51...C9	2.23	C6...H71	2.21
H61...C7	2.21	C7...H81	2.21
H71...C8	2.22	C8...H91	2.22
H81...C9	2.22	H91...H172	2.52
C10...H111	2.21	C10...H141	2.20
C10...C15	2.91	C10...H151	2.76
H101...C11	2.21	H101...C14	2.19
H101...C15	2.82	H101...H151	2.30
C11...H121	2.23	H111...C12	2.22
C12...H131	2.20	H121...C13	2.19
C13...H141	2.21	H131...C14	2.21
C15...C17	2.62	C15...H171	2.95
C16...O5	2.36	C16...H151	2.22

C16...H171	2.06	C16...H172	2.13
C17...C18	2.35	C17...H191	2.61
C17...H192	2.60	O5...H191	2.04
O5...H192	2.59	O5...C19	2.35
O5...H171	2.12	O5...H193	2.59
C18...H191	2.10	O5...H172	2.00
C18...H193	2.08	C18...H192	2.09
C18...H172	2.48	C18...H171	2.79
H191...H171	2.60	H191...C19	2.09
H192...H172	2.25	H192...C19	2.09
H171...H172	1.76		

Appendix III

Crystallographic data for

$[Mo_2Rh(\mu\text{-}C{\equiv}CPh)(CO)_6(\eta\text{-}C_5H_5)_2]$ (12)

Note on $[Mo_2Rh(\mu\text{-}C{\equiv}CPh)(CO)_6(\eta\text{-}C_5H_5)_2]$ (12)

A crystal of approximate dimensions 0.2 x 0.2 x 0.12 mm was used for data collection.

Crystal data: $C_{24}H_{15}O_6Mo_2Rh$, M = 694.3 monoclinic, a = 15.792 (4), b = 8.339 (2), c = 19.103 (3) Å, β = 112.00 (1), U = 2332.5 Å^3, space group $P2_1/a$, Z = 4, D_c = 1.98 gcm^{-3}, μ(Mo-$K\alpha$) = 16.24 cm^{-1}, $F(000)$ = 1344. Data were measured at room temperature on a CAD4 automatic four-circle diffractometer in the range $2 \leq \theta \leq 24°$. 4109 reflections were collected of which 2908 were unique with $I \geq 3\sigma(I)$. Data were corrected for Lorentz and polarisation effects but not for absorption. The structure was solved by Patterson methods and refined using the SHELX[136, 137] suite of programs. In the final least squares cycles all atoms were allowed to vibrate anisotropically. Hydrogen atoms were included at calculated positions. Final residuals after 8 cycles of least squares were R = 0.0232, R_w = 0.0269, for a weighting scheme of $w = 1.0000/[\sigma^2(F) + 0.0005754(F)^2]$. Maximum final shift/esd was 0.025. The maximum and minimum residual densities were 0.19 and -0.40 eÅ^{-3} respectively. Final fractional atomic coordinates and isotropic thermal parameters, anisotropic temperature factors, bond distances, bond angles, fractional atomic coordinates for the hydrogen atoms, intermolecular distances and intramolecular distances are given in tables 13, 14, 15, 16, 17, 18 and 19 respectively. The asymmetric unit is shown in figure 90, along with the labelling scheme used.

Table 13 Fractional atomic coordinates and thermal parameters (Å) for [$Mo_2Rh(\mu$-C≡CPh)$(CO)_6(\eta$-$C_5H_5)_2$] (12)

Atom	x	y	z	Uiso or Ueq	If Ueq ***
Mo1	0.47783 (2)	-0.09368 (4)	0.27050 (2)	0.0390 (2)	***
Mo2	0.44179 (2)	0.11500 (3)	0.12064 (2)	0.0351 (2)	***
Rh1	0.36033 (2)	0.15036 (4)	0.25220 (2)	0.0447 (2)	***
O1	0.4258 (2)	-0.2449 (3)	0.0700 (2)	0.075 (2)	***
O2	0.6420 (2)	0.0782 (4)	0.1308 (2)	0.079 (2)	***
O3	0.2913 (2)	-0.2612 (4)	0.1768 (2)	0.071 (2)	***
O4	0.4043 (3)	-0.0774 (5)	0.4005 (2)	0.105 (3)	***
O5	0.1635 (2)	0.0452 (5)	0.1789 (2)	0.090 (3)	***
O6	0.3240 (2)	0.4684 (5)	0.3089 (2)	0.098 (3)	***
C1	0.4313 (3)	-0.1159 (5)	0.0932 (3)	0.055 (2)	***
C2	0.5681 (3)	0.0889 (5)	0.1278 (2)	0.051 (2)	***
C3	0.3561 (3)	-0.1916 (5)	0.2091 (2)	0.051 (2)	***
C4	0.4236 (3)	-0.0686 (6)	0.3488 (3)	0.065 (3)	***
C5	0.2380 (3)	0.0841 (5)	0.2082 (3)	0.063 (3)	***
C6	0.3360 (3)	0.3511 (5)	0.2843 (3)	0.062 (3)	***
C7	0.4237 (4)	0.3549 (5)	0.0561 (3)	0.067 (3)	***
C8	0.3967 (3)	0.2358 (6)	0.0030 (2)	0.068 (3)	***
C9	0.3178 (3)	0.1668 (6)	0.0058 (3)	0.061 (3)	***
C10	0.2978 (3)	0.2488 (7)	0.0620 (3)	0.076 (3)	***
C11	0.3644 (4)	0.3634 (6)	0.0918 (3)	0.069 (3)	***
C12	0.6356 (3)	-0.1416 (6)	0.3170 (3)	0.071 (3)	***

C13	0.5991 (3)	-0.2260 (7)	0.2491 (3)	0.081 (3)	***
C14	0.5399 (4)	-0.3407 (6)	0.2579 (4)	0.073 (3)	***
C15	0.5399 (3)	-0.3276 (6)	0.3307 (3)	0.071 (3)	***
C16	0.5990 (3)	-0.2049 (6)	0.3667 (3)	0.069 (3)	***
C17	0.4929 (2)	0.1526 (4)	0.2305 (2)	0.038 (2)	***
C18	0.5052 (2)	0.1734 (4)	0.3024 (2)	0.040 (2)	***
C19	0.5690 (2)	0.2560 (4)	0.3688 (2)	0.043 (2)	***
C20	0.6511 (3)	0.3128 (5)	0.3674 (3)	0.059 (2)	***
C21	0.7098 (3)	0.4038 (6)	0.4268 (3)	0.072 (3)	***
C22	0.6875 (4)	0.4366 (6)	0.4881 (3)	0.074 (3)	***
C23	0.6082 (5)	0.3759 (7)	0.4909 (3)	0.086 (4)	***
C24	0.5480 (4)	0.2863 (6)	0.4325 (2)	0.069 (3)	***

Table 14 Anisotropic thermal parameters (Å)

Atom	U11	U22	U33	U23	U13	U12
Mo1	0.0387 (2)	0.0293 (2)	0.0489 (2)	0.0068 (1)	0.0115 (1)	0.0012 (1)
Mo2	0.0382 (2)	0.0286 (2)	0.0386 (2)	-0.0011 (1)	0.0124 (1)	-0.0010 (1)
Rh1	0.0399 (2)	0.0392 (2)	0.0549 (2)	0.0081 (1)	0.0198 (1)	0.0052 (1)
O1	0.102 (2)	0.036 (2)	0.087 (2)	-0.021 (1)	0.038 (2)	-0.010 (1)
O2	0.048 (2)	0.083 (2)	0.106 (3)	-0.020 (2)	0.038 (2)	-0.011 (2)
O3	0.060 (2)	0.064 (2)	0.088 (2)	0.000 (2)	0.013 (2)	-0.020 (2)
O4	0.131 (3)	0.095 (3)	0.089 (3)	0.037 (2)	0.072 (3)	0.025 (2)
O5	0.049 (2)	0.074 (2)	0.148 (3)	0.018 (2)	0.028 (2)	-0.007 (2)
O6	0.089 (2)	0.067 (2)	0.139 (3)	-0.024 (2)	0.056 (2)	0.015 (2)
C1	0.050 (2)	0.051 (3)	0.065 (3)	-0.002 (2)	0.025 (2)	0.000 (2)
C2	0.055 (2)	0.041 (2)	0.058 (2)	-0.008 (2)	0.023 (2)	-0.004 (2)
C3	0.050 (2)	0.044 (2)	0.059 (2)	0.009 (2)	0.014 (2)	-0.003 (2)
C4	0.070 (3)	0.054 (2)	0.071 (3)	0.018 (2)	0.031 (2)	0.004 (2)
C5	0.056 (3)	0.052 (2)	0.082 (3)	0.017 (2)	0.030 (2)	0.003 (2)
C6	0.052 (2)	0.054 (3)	0.079 (3)	0.006 (2)	0.032 (2)	0.008 (2)
C7	0.078 (3)	0.045 (2)	0.078 (3)	0.028 (2)	0.003 (3)	-0.009 (2)
C8	0.086 (3)	0.073 (3)	0.045 (2)	0.019 (2)	0.027 (2)	0.020 (3)
C9	0.067 (3)	0.055 (3)	0.060 (3)	0.008 (2)	-0.018 (2)	-0.003 (2)
C10	0.055 (2)	0.099 (4)	0.074 (3)	0.044 (3)	0.023 (2)	0.037 (3)
C11	0.103 (4)	0.050 (3)	0.055 (3)	0.004 (2)	0.011 (3)	0.033 (3)
C12	0.044 (2)	0.052 (3)	0.116 (4)	0.007 (3)	0.014 (3)	0.001 (2)
C13	0.073 (3)	0.076 (3)	0.096 (4)	0.030 (3)	0.039 (3)	0.047 (3)
C14	0.069 (3)	0.042 (3)	0.107 (4)	-0.007 (3)	0.006 (3)	0.020 (2)

C15	0.062 (3)	0.042 (2)	0.109 (4)	0.037 (3)	0.019 (3)	0.014 (2)
C16	0.055 (2)	0.075 (3)	0.075 (3)	0.020 (3)	0.003 (2)	0.013 (2)
C17	0.036 (2)	0.029 (2)	0.050 (2)	0.002 (1)	0.017 (1)	0.003 (1)
C18	0.045 (2)	0.030 (2)	0.044 (2)	0.005 (1)	0.016 (1)	0.002 (1)
C19	0.055 (2)	0.031 (2)	0.043 (2)	0.003 (1)	0.010 (2)	0.004 (1)
C20	0.054 (2)	0.050 (2)	0.072 (3)	-0.001 (2)	0.011 (2)	0.000 (2)
C21	0.055 (3)	0.067 (3)	0.094 (4)	0.004 (3)	-0.009 (3)	-0.007 (2)
C22	0.114 (4)	0.060 (3)	0.049 (3)	-0.003 (2)	-0.016 (3)	-0.001 (3)
C23	0.145 (6)	0.070 (3)	0.044 (2)	0.001 (2)	0.022 (3)	-0.003 (3)
C24	0.101 (3)	0.064 (3)	0.042 (2)	-0.002 (2)	0.026 (2)	-0.009 (3)

Table 15 Bond lengths (Å)

Mo1-Mo2	3.214 (1)	Mo1-Rh1	2.687 (1)
Mo1-C3	2.011 (4)	Mo1-C4	1.993 (5)
Mo1-C12	2.346 (4)	Mo1-C13	2.375 (4)
Mo1-C14	2.332 (4)	Mo1-C15	2.290 (4)
Mo1-C16	2.294 (4)	Mo1-C17	2.235 (3)
Mo1-C18	2.306 (3)	Mo2-Rh1	3.237 (1)
Mo2-C1	1.986 (4)	Mo2-C2	1.959 (4)
Mo2-C7	2.311 (4)	Mo2-C8	2.318 (4)
Mo2-C9	2.370 (4)	Mo2-C10	2.401 (4)
Mo2-C11	2.363 (4)	Mo2-C17	1.971 (4)
Rh1-C4	2.521 (4)	Rh1-C5	1.878 (5)
Rh1-C6	1.872 (5)	Rh1-C17	2.281 (3)
Rh1-C18	2.132 (3)	O1-C1	1.155 (5)
O2-C2	1.151 (5)	O3-C3	1.138 (5)
O4-C4	1.140 (5)	O5-C5	1.145 (5)
O6-C6	1.131 (5)	C7-C8	1.368 (7)
C7-C9	2.231 (7)	C7-C10	2.218 (7)
C7-C11	1.351 (8)	C8-C9	1.393 (7)
C8-C10	2.246 (6)	C8-C11	2.217 (7)
C9-C10	1.405 (7)	C9-C11	2.240 (7)
C10-C11	1.377 (8)	C12-C13	1.397 (8)
C12-C14	2.245 (7)	C12-C15	2.248 (7)
C12-C16	1.388 (8)	C13-C14	1.392 (8)
C13-C15	2.262 (8)	C13-C16	2.255 (8)
C14-C15	1.396 (8)	C14-C16	2.241 (8)

C15-C16	1.382 (7)	C17-C18	1.325 (5)
C18-C19	1.463 (5)	C19-C20	1.389 (6)
C19-C24	1.399 (6)	C20-C21	1.391 (7)
C21-C22	1.370 (8)	C22-C23	1.369 (9)
C23-C24	1.383 (7)		

Table 16 Bond angles (°)

Rh1-Mo1-Mo2	65.8 (1)	C3-Mo1-Mo2	83.6 (1)
C3-Mo1-Rh1	76.7 (1)	C4-Mo1-Mo2	129.0 (1)
C4-Mo1-Rh1	63.1 (1)	C4-Mo1-C3	84.0 (2)
C12-Mo1-Mo2	103.8 (1)	C12-Mo1-Rh1	139.7 (1)
C12-Mo1-C3	143.0 (2)	C12-Mo1-C4	115.3 (2)
C13-Mo1-Mo2	89.0 (1)	C13-Mo1-Rh1	153.1 (1)
C13-Mo1-C3	111.5 (2)	C13-Mo1-C4	141.2 (2)
C13-Mo1-C12	34.4 (2)	C14-Mo1-Mo2	109.1 (2)
C14-Mo1-Rh1	162.2 (1)	C14-Mo1-C3	85.9 (2)
C14-Mo1-C4	119.1 (2)	C14-Mo1-C12	57.4 (2)
C14-Mo1-C13	34.4 (2)	C15-Mo1-Mo2	143.9 (2)
C15-Mo1-Rh1	148.8 (1)	C15-Mo1-C3	94.8 (2)
C15-Mo1-C4	86.3 (2)	C15-Mo1-C12	58.0 (2)
C15-Mo1-C13	58.0 (2)	C15-Mo1-C14	35.1 (2)
C16-Mo1-Mo2	138.5 (1)	C16-Mo1-Rh1	137.6 (1)
C16-Mo1-C3	129.1 (2)	C16-Mo1-C4	84.6 (2)
C16-Mo1-C12	34.8 (2)	C16-Mo1-C13	57.7 (2)
C16-Mo1-C14	57.9 (2)	C16-Mo1-C15	35.1 (2)
C1-Mo2-Rh1	106.0 (1)	C2-Mo2-Rh1	130.2 (1)
C2-Mo2-C1	83.8 (2)	C7-Mo2-Rh1	109.3 (2)
C7-Mo2-C1	135.8 (2)	C7-Mo2-C2	93.0 (2)
C8-Mo2-Rh1	130.2 (1)	C8-Mo2-C1	101.6 (2)
C8-Mo2-C2	92.9 (2)	C8-Mo2-C7	34.4 (2)
C9-Mo2-Rh1	105.7 (2)	C9-Mo2-C1	88.5 (2)
C9-Mo2-C2	123.5 (2)	C9-Mo2-C7	56.9 (2)

C9-Mo2-C8	34.5 (2)	C10-Mo2-Rh1	74.8 (1)
C10-Mo2-C1	110.9 (2)	C10-Mo2-C2	147.8 (2)
C10-Mo2-C7	56.1 (2)	C10-Mo2-C8	56.8 (2)
C10-Mo2-C9	34.3 (2)	C11-Mo2-Rh1	77.3 (1)
C11-Mo2-C1	143.5 (2)	C11-Mo2-C2	122.5 (2)
C11-Mo2-C7	33.6 (2)	C11-Mo2-C8	56.5 (2)
C11-Mo2-C9	56.5 (2)	C11-Mo2-C10	33.6 (2)
C17-Mo2-Rh1	44.1 (1)	C17-Mo2-C1	113.3 (2)
C17-Mo2-C2	86.8 (2)	C17-Mo2-C7	110.5 (2)
C17-Mo2-C8	144.8 (2)	C17-Mo2-C9	145.4 (2)
C17-Mo2-C10	111.2 (2)	C17-Mo2-C11	94.5 (1)
C4-Rh1-Mo2	109.8 (1)	C5-Rh1-Mo2	105.5 (1)
C5-Rh1-C4	100.0 (2)	C6-Rh1-Mo2	121.8 (1)
C6-Rh1-C4	118.8 (2)	C6-Rh1-C5	96.1 (2)
C17-Rh1-Mo2	37.0 (1)	C17-Rh1-C4	90.0 (1)
C17-Rh1-C5	141.4 (2)	C17-Rh1-C6	111.6 (2)
C18-Rh1-Mo2	71.7 (1)	C18-Rh1-C4	70.8 (1)
C18-Rh1-C5	168.0 (2)	C18-Rh1-C6	95.1 (2)
C18-Rh1-C17	34.7 (1)	O1-C1-Mo2	172.7 (4)
O2-C2-Mo2	177.7 (4)	O4-C4-Rh1	121.3 (4)
O5-C5-Rh1	177.5 (4)	O6-C6-Rh1	175.1 (5)
C8-C7-Mo2	73.1 (2)	C9-C7-Mo2	62.9 (2)
C9-C7-C8	36.5 (3)	C10-C7-Mo2	64.0 (2)
C10-C7-C8	73.3 (3)	C10-C7-CC9	36.8 (2)
C11-C7-Mo2	75.3 (3)	C11-C7-C8	109.3 (4)
C11-C7-C9	72.8 (3)	C11-C7-C10	36.0 (3)
C7-C8-Mo2	72.5 (2)	C9-C8-Mo2	74.7 (2)

C9-C8-C7	107.8 (4)	C10-C8-Mo2	63.4 (1)
C10-C8-C7	71.0 (3)	C10-C8-C9	36.8 (3)
C11-C8-Mo2	62.8 (2)	C11-C8-C7	35.1 (3)
C11-C8-C9	72.7 (3)	C11-C8-C10	35.9 (2)
C7-C9-Mo2	60.2 (2)	C8-C9-Mo2	70.7 (2)
C8-C9-C7	35.7 (3)	C10-C9-Mo2	74.1 (2)
C10-C9-C7	71.1 (3)	C10-C9-C8	106.8 (4)
C11-C9-Mo2	61.6 (2)	C11-C9-C7	35.2 (2)
C11-C9-C8	70.9 (3)	C11-C9-C10	35.9 (3)
C7-C10-Mo2	59.9 (2)	C8-C10-Mo2	59.7 (1)
C8-C10-C7	35.7 (2)	C9-C10-Mo2	71.7 (2)
C9-C10-C7	72.1 (3)	C9-C10-C8	36.4 (3)
C11-C10-Mo2	71.7 (2)	C11-C10-C7	35.2 (3)
C11-C10-C8	70.9 (3)	C11-C10-C9	107.3 (4)
C7-C11-Mo2	71.1 (3)	C8-C11-Mo2	60.7 (2)
C8-C11-C7	35.6 (3)	C9-C11-Mo2	61.9 (2)
C9-C11-C7	72.0 (3)	C9-C11-C8	36.4 (2)
C10-C11-Mo2	74.7 (3)	C10-C11-C7	108.8 (4)
C10-C11-C8	73.2 (3)	C10-C11-C9	36.8 (3)
C14-C12-C13	36.3 (3)	C15-C12-C13	72.5 (4)
C15-C12-C14	36.2 (2)	C16-C12-C13	108.1 (5)
C16-C12-C14	71.8 (3)	C16-C12-C15	35.6 (3)
C14-C13-C12	107.2 (5)	C15-C13-C12	71.4 (3)
C15-C13-C14	35.8 (3)	C16-C13-C12	35.8 (3)
C16-C13-C14	71.4 (4)	C16-C13-C15	35.6 (2)
C13-C14-C12	36.5 (3)	C15-C14-C12	72.0 (3)
C15-C14-C13	108.5 (5)	C16-C14-C12	36.0 (2)

C16-C14-C13	72.5 (4)	C16-C14-C15	36.0 (3)
C13-C15-C12	36.1 (2)	C14-C15-C12	71.8 (3)
C14-C15-C13	35.7 (3)	C16-C15-C12	35.8 (3)
C16-C15-C13	71.9 (3)	C16-C15-C14	107.6 (5)
C13-C16-C12	36.1 (3)	C14-C16-C12	72.1 (4)
C14-C16-C13	36.1 (2)	C15-C16-C12	108.6 (5)
C15-C16-C13	72.5 (4)	C15-C16-C14	36.4 (3)
Rh1-C17-Mo2	98.9 (1)	C18-C17-Mo2	165.4 (3)
C18-C17-Rh1	66.5 (2)	C17-C18-Rh1	78.8 (2)
C19-C18-Rh1	135.0 (3)	C19-C18-C17	138.3 (3)
C20-C19-C18	119.3 (4)	C24-C19-C18	121.9 (4)
C24-C19-C20	118.7 (4)	C21-C20-C19	120.8 (5)
C22-C21-C20	120.0 (5)	C23-C22-C21	119.4 (5)
C24-C23-C22	122.0 (5)	C23-C24-C19	119.0 (5)

Table 17 Fractional atomic coordinates for the hydrogen atoms

Atom	x	y	z
H71	0.4830	0.4297	0.0667
H81	0.4294	0.2007	-0.0352
H91	0.2800	0.0678	-0.0281
H101	0.2404	0.2256	0.0783
H111	0.3687	0.4462	0.1364
H121	0.6837	-0.0437	0.3280
H131	0.6146	-0.2050	0.1993
H141	0.5007	-0.4248	0.2150
H151	0.5010	-0.4006	0.3546
H161	0.6150	-0.1638	0.4238
H201	0.6692	0.2879	0.3193
H211	0.7735	0.4472	0.4254
H221	0.7315	0.5110	0.5334
H231	0.5927	0.3980	0.5405
H241	0.4855	0.2412	0.4358

Table 18 Intermolecular distances (Å)

O1...H71	2.87	1	0.0	1.0	0.0
O1...H81	2.64	-1	1.0	0.0	0.0
O2...H81	2.91	-1	1.0	0.0	0.0
O2...H91	2.94	-1	1.0	0.0	0.0
O2...H101	2.69	-2	0.0	1.0	0.0
O3...H111	2.96	1	0.0	1.0	0.0
O3...H91	3.00	2	0.0	0.0	0.0
O3...H131	2.99	-2	1.0	0.0	0.0
O4...H231	2.90	-1	1.0	0.0	1.0
O4...H211	2.53	-2	1.0	1.0	0.0
O5...H71	2.86	-2	1.0	1.0	0.0
O5...H201	2.99	-2	1.0	1.0	0.0
O6...H151	2.82	1	0.0	-1.0	0.0
O6...H231	2.90	-1	1.0	1.0	1.0
O6...H121	2.46	-2	1.0	1.0	0.0
C1...H81	2.90	-1	1.0	0.0	0.0
C5...H201	2.92	-2	1.0	1.0	0.0
H91...C10	2.90	2	0.0	0.0	0.0
H91...C11	2.74	2	0.0	0.0	0.0
H151...C24	2.96	1	0.0	1.0	0.0

Table 19 Intramolecular distances (Å)

Mo1...H151	2.97	Mo1...H161	2.98
Mo2...H71	2.98	Mo2...H81	3.00
Rh1...O6	3.00	Rh1...C3	2.96
O1...H141	2.98	O2...H131	2.81
O4...H241	2.92	C1...C2	2.64
C1...C3	2.95	C1...H131	2.94
C2...H131	2.77	C2...C17	2.70
C3...C4	2.68	C3...C5	2.96
C3...C14	2.97	C3...H141	2.97
C4...C15	2.94	C4...C16	2.89
C4...H161	2.93	C4...C18	2.72
C5...C6	2.79	C5...H101	2.76
C6...C18	2.96	C6...H81	2.20
C7...H111	2.17	H71...C8	2.17
H71...C11	2.17	C8...H91	2.21
H81...C9	2.20	C9...H101	2.22
H91...C10	2.23	C10...H111	2.19
H101...C11	2.20	C12...H131	2.21
C12...H161	2.19	H121...C13	2.20
H121...C16	2.21	C13...H141	2.20
H131...C14	2.22	C14...H151	2.21
H141...C15	2.21	C15...H161	2.20
H151...C16	2.20	C17...C19	2.60
C17...H201	2.89	C18...C20	2.46
C18...H201	2.66	C18...C24	2.50

C18...H241	2.74	C19...H201	2.14
C19...C21	2.42	C19...C22	2.79
C19...C23	2.40	C19...H241	2.16
C20...H211	2.15	C20...C22	2.39
C20...C23	2.74	C20...C24	2.40
H201...C21	2.14	C21...H221	2.13
C21...C23	2.36	C21...C24	2.77
H211...C22	2.12	C22...H231	2.11
C22...C24	2.41	H221...C23	2.13
C23...H241	2.15	H231...C24	2.13

Appendix IV

Crystallographic data for

$[Mo_2Mn(\mu\text{-}C{\equiv}C^tBu)(CO)_7(\eta\text{-}C_5H_5)_2]$ (24)

Note on $[Mo_2Mn(\mu\text{-}C{\equiv}C^tBu)(CO)_7(\eta\text{-}C_5H_5)_2]$ (24)

A crystal of approximate dimensions 0.2 x 0.2 x 0.15 mm was used for data collection.

Crystal data: $C_{23}H_{19}O_7MnMo_2$, M = 654.2 monoclinic, a = 9.502 (1), b = 16.503 (2), c = 15.382 (2) Å, β = 99.638 (1), U = 2378.1 Å^3, space group $P2_1/n$, Z = 4, D_c = 1.83 gcm^{-3}, μ(Mo-$K\alpha$) = 15.6 cm^{-1}, $F(000)$ = 1288. Data were measured at room temperature on a CAD4 automatic four-circle diffractometer in the range $2{\leq}\theta{\leq}24°$. 4125 reflections were collected of which 3080 were unique with $I{\geq}3\sigma(I)$. Data were corrected for Lorentz and polarisation effects but not for absorption. The structure was solved by Patterson methods and refined using the SHELX[136, 137] suite of programs. In the final least squares cycles all atoms were allowed to vibrate anisotropically. Hydrogen atoms were included at calculated positions. Final residuals after 5 cycles of least squares were R = 0.0258, R_w = 0.0281, for a weighting scheme of $w = 3.5622/[\sigma^2(F) + 0.000226(F)^2]$. Maximum final shift/esd was 0.108. The maximum and minimum residual densities were 0.34 and -0.21 eÅ^{-3} respectively. Final fractional atomic coordinates and isotropic thermal parameters, anisotropic temperature factors, bond distances, bond angles, fractional atomic coordinates for the hydrogen atoms, intermolecular distances and intramolecular distances are given in tables 20, 21, 22, 23, 24, 25 and 26 respectively. The asymmetric unit is shown in figure 94, along with the labelling scheme used.

Table 20 Fractional atomic coordinates and thermal parameters (Å) for [$Mo_2Mn(\mu$-$C{\equiv}C^tBu)(CO)_7(\eta$-$C_5H_5)_2$] (24)

Atom	x	y	z	Uiso or Ueq	*** if Ueq
Mo1	0.22844 (3)	0.11820 (2)	0.37834 (2)	0.0387 (2)	***
Mo2	0.23610 (3)	0.09599 (2)	0.17821 (2)	0.0380 (2)	***
Mn1	-0.00449 (6)	0.05127 (3)	0.26628 (3)	0.0422 (3)	***
O1	0.0218 (4)	0.0975 (3)	0.5155 (2)	0.103 (3)	***
O2	0.2629 (4)	-0.0694 (2)	0.3997 (3)	0.088 (2)	***
O3	0.0958 (4)	-0.0607 (2)	0.0935 (2)	0.086 (2)	***
O4	0.4874 (4)	-0.0078 (3)	0.2780 (3)	0.109 (3)	***
O5	-0.0007 (4)	-0.1277 (2)	0.2618 (3)	0.093 (3)	***
O6	-0.2301 (4)	0.0599 (3)	0.1108 (2)	0.105 (3)	***
O7	-0.2280 (4)	0.0329 (3)	0.3766 (2)	0.099 (3)	***
C1	0.0909 (5)	0.1021 (3)	0.4621 (3)	0.067 (3)	***
C2	0.2386 (4)	-0.0016 (3)	0.3859 (3)	0.060 (3)	***
C3	0.1376 (5)	-0.0044 (2)	0.1347 (3)	0.057 (2)	***
C4	0.3898 (5)	0.0292 (3)	0.2470 (3)	0.066 (3)	***
C5	0.0016 (4)	-0.0584 (3)	0.2640 (3)	0.061 (3)	***
C6	-0.1410 (5)	0.0565 (3)	0.1711 (3)	0.065 (3)	***
C7	-0.1397 (5)	0.0418 (3)	0.3344 (3)	0.065 (3)	***
C8	0.1077 (4)	0.1542 (2)	0.2468 (2)	0.037 (2)	***
C9	0.0238 (4)	0.1787 (2)	0.3007 (2)	0.042 (2)	***
C10	-0.0736 (5)	0.2491 (3)	0.3118 (3)	0.066 (3)	***
C11	-0.1628 (8)	0.2367 (4)	0.3832 (5)	0.144 (6)	***

C12	0.0111 (8)	0.3243 (3)	0.3363 (7)	0.184 (8)	***
C13	-0.1672 (11)	0.2612 (7)	0.2266 (4)	0.241 (10)	***
C14	0.4710 (5)	0.1199 (3)	0.4407 (3)	0.068 (3)	***
C15	0.3898 (5)	0.1426 (3)	0.5045 (3)	0.067 (3)	***
C16	0.3199 (6)	0.2166 (3)	0.4779 (3)	0.074 (3)	***
C17	0.3623 (6)	0.2395 (3)	0.3968 (3)	0.073 (3)	***
C18	0.4544 (5)	0.1799 (3)	0.3746 (3)	0.072 (3)	***
C19	0.3447 (12)	0.2095 (4)	0.1274 (4)	0.110 (5)	***
C20	0.2109 (10)	0.2060 (5)	0.0832 (6)	0.120 (6)	***
C21	0.1987 (10)	0.1372 (7)	0.0331 (4)	0.114 (6)	***
C22	0.3234 (15)	0.1006 (4)	0.0476 (6)	0.130 (6)	***
C23	0.4131 (6)	0.1422 (7)	0.1044 (6)	0.122 (6)	***

Table 21 Anisotropic thermal parameters (Å)

Atom	U11	U22	U33	U23	U13	U12
Mo1	0.0437 (2)	0.0396 (2)	0.0329 (2)	0.0033 (1)	-0.0010 (1)	-0.0056 (1)
Mo2	0.0392 (2)	0.0382 (2)	0.0368 (2)	-0.0048 (1)	0.0072 (1)	0.0001 (1)
Mn1	0.0376 (3)	0.0464 (3)	0.0425 (3)	0.0039 (2)	0.0012 (2)	-0.0060 (2)
O1	0.093 (3)	0.158 (4)	0.057 (2)	0.034 (2)	0.027 (2)	-0.016 (3)
O2	0.099 (3)	0.048 (2)	0.118 (3)	0.031 (2)	-0.024 (2)	0.002 (2)
O3	0.124 (3)	0.057 (2)	0.077 (2)	-0.029 (2)	0.018 (2)	-0.027 (2)
O4	0.098 (3)	0.128 (3)	0.102 (3)	-0.037 (2)	-0.029 (2)	0.070 (3)
O5	0.117 (3)	0.046 (2)	0.117 (3)	0.005 (2)	0.008 (2)	-0.026 (2)
O6	0.072 (2)	0.163 (4)	0.080 (2)	-0.018 (2)	-0.031 (2)	0.014 (2)
O7	0.067 (2)	0.135 (4)	0.094 (3)	0.011 (2)	0.036 (2)	-0.024 (2)
C1	0.071 (3)	0.085 (3)	0.043 (2)	0.022 (2)	0.000 (2)	-0.010 (2)
C2	0.060 (3)	0.059 (3)	0.062 (3)	0.015 (2)	-0.013 (2)	-0.006 (2)
C3	0.071 (3)	0.048 (2)	0.051 (2)	-0.001 (2)	0.008 (2)	-0.006 (2)
C4	0.060 (3)	0.072 (3)	0.065 (3)	-0.017 (2)	0.000 (2)	0.019 (2)
C5	0.058 (3)	0.061 (3)	0.065 (3)	0.003 (2)	0.001 (2)	-0.017 (2)
C6	0.055 (3)	0.083 (3)	0.057 (2)	-0.009 (2)	-0.002 (2)	0.001 (2)
C7	0.056 (3)	0.077 (3)	0.061 (3)	0.004 (2)	0.005 (2)	-0.013 (2)
C8	0.045 (2)	0.034 (2)	0.032 (2)	0.006 (1)	0.005 (1)	0.002 (1)
C9	0.052 (2)	0.042 (2)	0.033 (2)	0.007 (1)	0.007 (2)	0.007 (2)
C10	0.077 (3)	0.068 (3)	0.052 (2)	0.005 (2)	0.026 (2)	0.027 (2)
C11	0.166 (7)	0.099 (5)	0.167 (7)	-0.010 (4)	0.124 (6)	0.031 (4)
C12	0.141 (6)	0.044 (3)	0.368 (14)	0.004 (5)	0.105 (8)	0.030 (4)
C13	0.297 (12)	0.338 (14)	0.088 (5)	-0.038 (6)	-0.035 (6)	0.283 (12)

C14	0.055 (3)	0.086 (3)	0.063 (3)	-0.015 (2)	-0.011 (2)	-0.013 (2)
C15	0.069 (3)	0.083 (3)	0.049 (2)	-0.006 (2)	-0.015 (2)	-0.014 (3)
C16	0.086 (3)	0.074 (3)	0.063 (3)	-0.030 (2)	0.004 (2)	-0.018 (3)
C17	0.087 (4)	0.060 (3)	0.072 (3)	-0.007 (2)	-0.007 (3)	-0.034 (3)
C18	0.056 (3)	0.093 (4)	0.067 (3)	-0.018 (3)	0.004 (2)	-0.032 (3)
C19	0.187 (8)	0.083 (4)	0.061 (3)	-0.009 (3)	0.043 (4)	-0.076 (5)
C20	0.132 (6)	0.111 (5)	0.118 (6)	0.080 (5)	0.086 (5)	0.054 (5)
C21	0.127 (6)	0.171 (8)	0.044 (3)	0.035 (4)	-0.009 (3)	-0.083 (6)
C22	0.216 (10)	0.080 (4)	0.095 (5)	-0.021 (4)	0.106 (7)	-0.015 (6)
C23	0.058 (4)	0.181 (9)	0.125 (6)	0.064 (6)	0.045 (4)	0.007 (4)

Table 22 Bond lengths (Å)

Mo1-Mo2	3.113 (1)	Mo1-Mn1	2.795 (1)
Mo1-C1	2.000 (5)	Mo1-C2	1.981 (5)
Mo1-C8	2.233 (3)	Mo1-C9	2.330 (3)
Mo1-C14	2.343 (4)	Mo1-C15	2.299 (4)
Mo1-C16	2.301 (4)	Mo1-C17	2.363 (4)
Mo1-C18	2.385 (4)	Mo2-Mn1	2.940 (1)
Mo2-C3	1.965 (4)	Mo2-C4	1.988 (5)
Mo2-C8	2.989 (3)	Mo2-C19	2.336 (5)
Mo2-C20	2.318 (5)	Mo2-C21	2.303 (5)
Mo2-C22	2.299 (6)	Mo2-C23	2.310 (5)
Mn1-C5	1.812 (5)	Mn1-C6	1.788 (4)
Mn1-C7	1.796 (5)	Mn1-C8	2.054 (3)
Mn1-C9	2.175 (4)	O1-C1	1.137 (6)
O2-C2	1.155 (5)	O3-C3	1.157 (5)
O4-C4	1.146 (5)	O5-C5	1.143 (5)
O6-C6	1.149 (5)	O7-C7	1.152 (5)
C8-C9	1.307 (5)	C9-C10	1.513 (5)
C10-C11	1.510 (6)	C10-C12	1.492 (8)
C10-C13	1.468 (8)	C14-C15	1.398 (7)
C14-C18	1.409 (7)	C15-C16	1.417 (7)
C16-C17	1.425 (7)	C17-C18	1.396 (7)
C19-C20	1.340 (10)	C19-C23	1.364 (10)
C20-C21	1.365 (10)	C21-C22	1.315 (10)
C22-C23	1.309 (11)		

Table 23 Bond angles (°)

Mn1-Mo1-Mo2	59.4 (1)	C1-Mo1-Mo2	138.3 (1)
C1-Mo1-Mn1	79.0 (1)	C2-Mo1-Mo2	86.1 (1)
C2-Mo1-Mn1	70.6 (1)	C2-Mo1-C1	82.0 (2)
C8-Mo1-Mo2	39.5 (1)	C8-Mo1-Mn1	46.6 (1)
C8-Mo1-C1	109.1 (2)	C8-Mo1-C2	109.3 (1)
C9-Mo1-Mo2	72.5 (1)	C9-Mo1-Mn1	49.2 (1)
C9-Mo1-C1	78.9 (2)	C9-Mo1-C2	119.1 (1)
C9-Mo1-C8	33.2 (1)	C14-Mo1-Mo2	102.8 (1)
C14-Mo1-Mn1	151.6 (1)	C14-Mo1-C1	116.2 (2)
C14-Mo1-C2	87.3 (2)	C14-Mo1-C8	133.5 (2)
C14-Mo1-C9	152.1 (2)	C15-Mo1-Mo2	137.1 (1)
C15-Mo1-Mo2	159.6 (1)	C15-Mo1-C1	84.0 (2)
C15-Mo1-C2	96.1 (2)	C15-Mo1-C8	152.6 (2)
C15-Mo1-C9	137.6 (2)	C15-Mo1-C14	35.0 (2)
C16-Mo1-Mo2	132.3 (1)	C16-Mo1-Mn1	149.5 (1)
C16-Mo1-C1	83.1 (2)	C16-Mo1-C2	131.0 (2)
C16-Mo1-C8	119.7 (2)	C16-Mo1-C9	103.2 (2)
C16-Mo1-C14	58.9 (2)	C16-Mo1-C15	35.9 (2)
C3-Mo2-Mn1	65.3 (1)	C4-Mo2-Mn1	100.0 (1)
C4-Mo2-C3	88.8 (2)	C8-Mo2-Mn1	44.2 (1)
C8-Mo2-C3	106.7 (2)	C8-Mo2-C4	116.5 (2)
C19-Mo2-Mn1	141.0 (3)	C19-Mo2-C3	140.8 (2)
C19-Mo2-C4	107.3 (3)	C19-Mo2-C8	97.7 (3)
C20-Mo2-Mn1	118.7 (2)	C20-Mo2-C3	116.9 (3)
C20-Mo2-C4	139.4 (3	C20-Mo2-C8	87.1 (2)

C20-Mo2-C19	33.5 (2)	C21-Mo2-Mn1	121.0 (2)
C21-Mo2-C3	86.1 (2)	C21-Mo2-C4	131.3 (3)
C21-Mo2-C8	111.3 (4)	C21-Mo2-C19	56.2 (2)
C21-Mo2-C20	34.4 (3)	C22-Mo2-Mn1	146.4 (3)
C22-Mo2-C3	87.2 (3)	C22-Mo2-C4	98.2 (4)
C22-Mo2-C8	142.2 (3)	C22-Mo2-C19	55.7 (2)
C22-Mo2-C20	55.8 (2)	C22-Mo2-C21	33.2 (3)
C23-Mo2-Mn1	174.5 (2)	C23-Mo2-C3	117.1 (3)
C23-Mo2-C4	85.1 (2)	C23-Mo2-C8	131.5 (3)
C23-Mo2-C19	34.1 (2)	C23-Mo2-C20	55.8 (2)
C23-Mo2-C21	55.5 (2)	C23-Mo2-C22	33.0 (3)
C5-Mn1-Mo2	102.3 (1)	C6-Mn1-Mo2	97.1 (2)
C6-Mn1-C5	93.1 (2)	C7-Mn1-Mo2	168.0 (1)
C7-Mn1-C5	87.3 (2)	C7-Mn1-C6	89.4 (2)
C8-Mn1-Mo2	42.5 (1)	C8-Mn1-C5	143.6 (2)
C8-Mn1-C6	99.4 (2)	C8-Mn1-C7	126.6 (2)
C9-Mn1-Mo2	78.2 (1)	C9-Mn1-C5	165.5 (2)
C9-Mn1-C6	101.3 (2)	C9-Mn1-C7	90.8 (2)
C9-Mn1-C8	35.9 (1)	O3-C3-Mo2	164.5 (4)
O4-C4-Mo2	171.4 (5)	O5-C5-Mn1	177.1 (4)
O6-C6-Mn1	179.0 (5)	O7-C7-Mn1	177.3 (4)
Mn1-C8-Mo2	93.3 (1)	C9-C8-Mo2	168.4 (3)
C9-C8-Mn1	77.1 (2)	C8-C9-Mn1	67.0 (2)
C10-C9-Mn1	135.8 (3)	C10-C9-C8	139.4 (3)
C11-C10-C9	114.0 (4)	C12-C10-C9	110.6 (4)
C12-C10-C11	105.9 (5)	C13-C10-C9	107.1 (4)
C13-C10-C11	109.8 (7)	C13-C10-C12	109.5 (7)

C18-C14-C15	108.0 (5)	C16-C15-C14	108.4 (4)
C17-C16-C15	107.1 (5)	C18-C17-C16	107.9 (5)
C17-C18-C14	108.5 (4)	C20-C19-Mo2	72.5 (3)
C23-C19-Mo2	71.9 (3)	C23-C19-C20	106.6 (6)
C19-C20-Mo2	74.0 (3)	C21-C20-Mo2	72.2 (3)
C21-C20-C19	107.9 (6)	C20-C21-Mo2	73.4 (3)
C22-C21-Mo2	73.2 (4)	C22-C21-C20	107.3 (6)
C21-C22-Mo2	73.5 (3)	C23-C22-Mo2	74.0 (4)
C23-C22-C21	109.9 (7)	C19-C23-Mo2	74.0 (3)
C22-C23-Mo2	73.1 (4)	C22-C23-C19	108.4 (7)

Table 24 Fractional atomic coordinates for the hydrogen atoms

Atom	x	y	z
H111	-0.2270	0.1828	0.3690
H112	-0.2317	0.2885	0.3854
H113	-0.0939	0.2300	0.4462
H121	0.0779	0.3365	0.2875
H122	0.0772	0.3161	0.4000
H123	-0.0606	0.3746	0.3392
H131	-0.2387	0.3111	0.2317
H132	-0.2284	0.2068	0.2088
H133	-0.1031	0.2745	0.1766
H141	0.5351	0.0657	0.4418
H151	0.3817	0.1095	0.5641
H161	0.2480	0.2494	0.5125
H171	0.3292	0.2934	0.3592
H181	0.5044	0.1797	0.3165
H191	0.3898	0.2565	0.1725
H201	0.1274	0.2497	0.0865
H211	0.1043	0.1166	-0.0104
H221	0.3480	0.0445	0.0172
H231	0.5227	0.1259	0.1288

Table 25 Intermolecular distances (Å)

O2...H141	2.84	-1	1.0	0.0	1.0
O3...H211	2.30	-1	0.0	0.0	0.0
O3...H171	2.58	2	0.0	0.0	0.0
O4...O7	2.95	1	-1.0	0.0	0.0
O4...H121	2.79	2	0.0	0.0	0.0
O4...H123	2.81	2	0.0	0.0	0.0
O5...H131	2.69	2	-1.0	0.0	0.0
O5...H171	2.97	2	0.0	0.0	0.0
O5...H191	2.33	2	0.0	0.0	0.0
O6...H231	2.65	1	1.0	0.0	0.0
O6...H221	2.71	-1	0.0	0.0	0.0
O7...H141	2.67	1	1.0	0.0	0.0
O7...H151	2.99	-1	0.0	0.0	1.0
H112...C21	2.76	-2	1.0	1.0	0.0
H133...C15	2.97	-2	1.0	1.0	1.0
C15...H201	2.98	-2	0.0	1.0	0.0

Table 26 Intramolecular distances (Å)

Mo1...H151	2.98	Mo1...H161	2.98
Mo2...H231	2.99	Mn1...O6	2.94
Mn1...O7	2.95	Mn1...C2	2.84
O1...H113	2.60	O2...C5	2.97
O3...C5	2.91	O4...H141	2.77
O6...H132	2.85	O7...H111	2.48
C1...C2	2.61	C1...C7	2.86
C1...C9	2.76	C1...H113	2.73
C1...C15	2.88	C1...H151	2.94
C1...C16	2.86	C1...H161	2.89
C2...C4	2.81	C2...C5	2.84
C2...C14	3.00	C3...C4	2.77
C3...C5	2.70	C3...C6	2.97
C3...C21	2.92	C3...H211	2.97
C3...C22	2.95	C4...H181	2.85
C4...C23	2.92	C4...H231	2.87
C5...C5	2.61	C5...C7	2.49
C6...C7	2.52	C6...C8	2.94
C6...H132	2.71	C7...C9	2.84
C7...H111	2.56	C8...C10	2.65
C8...H133	2.90	C8...C20	2.98
C8...H201	2.96	C9...C11	2.53
C9...H111	2.76	C9...H113	2.80
C9...C12	2.47	C9...H121	2.67
C9...H122	2.73	C9...C13	2.40

C9...H132	2.61	C9...H133	2.61
C10...H111	2.13	C10...H112	2.13
C10...H113	2.13	C10...H121	2.11
C10...H122	2.11	C10...H123	2.11
C10...H131	2.09	C10...H132	2.09
C10...H133	2.09	C11...C12	2.40
C11...H122	2.61	C11...H123	2.61
C11...C13	2.44	C11...H131	2.63
C11...H132	2.70	H111...C13	2.69
H112...C12	2.61	H112...C13	2.65
H113...C12	2.61	C12...C13	2.42
C12...H131	2.65	C12...H133	2.65
H121...C13	2.67	H122...C16	2.92
H122...C17	3.00	H123...C13	2.64
C14...H151	2.21	C14...C16	2.28
C14...C17	2.28	C14...H181	2.22
H141...C15	2.21	H141...C18	2.22
C15...H161	2.23	C15...C17	2.29
C15...C18	2.27	H151...C16	2.23
C16...H171	2.24	C16...C18	2.28
H161...C17	2.24	C17...H181	2.21
H171...C18	2.21	C19...H201	2.16
C19...C21	2.19	C19...C22	2.17
C19...H231	2.18	H191...C20	2.17
H191...C23	2.19	C20...H211	2.19
C20...C22	2.16	C20...C23	2.17
H201...C21	2.18	C21...H221	2.13

C21...C23	2.15	H211...C22	2.14
C22...H231	2.13	H221...C23	2.12